UNIVERSITY OF
LIVERPOOL

An interdisciplinary analysis of physical and functional interactions between the NF-kappaB and E2F systems

Thesis submitted in accordance with the requirements of
the University of Liverpool
for the degree of Doctor in Philosophy by

John-Mark Ankers

March 2009

Declaration

This thesis is the result of my own work, unless otherwise stated, and is based upon results from experimental and theoretical work performed as a PhD student between October 2005 and September 2008 in the department of Biological Sciences within the University of Liverpool.

Neither this thesis nor any part of it has been submitted in support of an application for another degree or qualification at this or any other University or other institute of learning.

John Ankers

March 2009

Abstract

In the post-genomic era of biological research, integrative studies, examining how low-level biological components "re-assemble" into organised systems are becoming increasingly common. Integrative approaches of the past have often been limited by the complexity of systems of interest and by the techniques available to visualise and quantify biological events. Recently there have been significant advances in techniques to measure dynamic and complex intra-cellular phenomena. Importantly, these have included higher-throughput, quantitative experimental approaches using fluorescent protein fusions. It is now possible to take advantage of such quantitative data to construct mathematical models that are capable of simulating the complexities found in many dynamical systems. The success of future systems-level studies lies in the strength of such interdisciplinary approaches.

The data presented here represent an application of interdisciplinary Systems Biology to characterise interactions between two intra-cellular signalling systems; E2F-1 involved in cell cycle regulation, and NF-κB, involved in inflammatory responses and cancer. These two systems are both "oscillatory", as one or more of their components changes regularly over time in their predominant localisation within an individual cell (eg. NF-κB, with a time scale of minutes) or concentration and stability (eg. E2F-1, with a time scale of hours).

Evidence is presented for both physical and functional interactions between components of the NF-κB and E2F-1 systems. Physical binding between NF-κB proteins and E2F-1 was determined by Förster Resonance Energy Transfer (FRET) and Co-Immunoprecipitation. This supported concurrent live cell imaging data suggesting ectopically expressed E2F-1 was able to sequester NF-κB in the nucleus, altering its dynamics in response to TNFα stimulation. Due to the complex nature of these dynamics, it was necessary to develop a predicative mathematical model for the interactions between the NF-κB system and E2F-1. The model was fitted to quantified live cell imaging data, and subsequently used to make non-intuitive predictions for system behaviour, including the suspension of nucleo-cytoplasmic oscillations in response to TNFα in the presence of E2F-1, and a difference in degradation rate of E2F-1 between cellular compartments. Validation of model predictions involved investigations into the functional effects of these interactions. Quantitative PCR and Luciferase Reporter Assays were used to examine transcriptional activity associated with exogenous expression of NF-κB and E2F-1. These data suggested that certain target genes (IκBα and IκBε for NF-κB and Cyclin E for E2F-1) are repressed. Concurrently, ectopic expression of NF-κB was able to rescue ~40% of cells from apoptosis associated with ectopic expression of E2F-1. The relationship between endogenous NF-κB and E2F-1 was investigated by addition of TNFα at different times after release from a cell cycle block. Both live cell imaging and Immuno-cytochemistry showed different NF-κB dynamics in response to stimulus at G1/S (when E2F-1 reaches peak levels) in synchronised cells compared to normally cycling cells.

Considered together, these data suggested that the signalling dynamics of NF-κB regulated in a cell cycle-dependant manner. The integration of such oscillatory systems over different time-scales presents a paradigm for the coupling of similar systems in general. The physiological implications of cell cycle control in the dynamics of responses are also considered, through the development of a hypothetical "balance" model based on the presented data and the emergent view from current literature.

Contents

Declaration ii
Abstract iii
Contents iv
List of Figures, Tables and Supplementary Materials vii
Figures vii
Tables x
Supplementary materials x
Movies xi
Commonly Used Abbreviations xii
Acknowledgements xiv
Chapter 1 – Introduction 1
1.1 Introduction I - Systems approaches to biological research 2
1.1.1 What is Systems Biology? 2
1.1.2 Integration in the Systems Biology approach 3
1.1.3 Requirements of Mathematics in Systems Biology 4
1.1.3.1 Biological context 4
1.1.3.2 Predictive ability 6
1.1.3.3 Resolution 6
1.1.4 Experimental model system – Protein dynamics in single living cells 6
1.1.5 Biological model system - Oscillatory behaviour in cell signalling 7
1.1.6 Integration of linked processes across scales 9
1.1.7 Interdisciplinary Systems Biology in practice 9
1.1.8 The application of Mathematics in Systems Biology 11
1.1.9 Mathematical Systems Biology applied to oscillatory systems 14
1.1.10 Discussion - Systems Biology applied to this project 15
1.2 Introduction II – E2F and G1/S cell cycle progression 16
1.2.1 Summary 16
1.2.2 The E2F family of proteins 17
1.2.3 The G1/S checkpoint 19
1.2.4 Robustness in G1/S progression 21
1.2.4.1 Functional robustness 21
1.2.4.2 Robustness arising from feedback 22
1.2.5 Sensitivity of G1/S progression 23
1.2.5.1 p53 DNA damage response at G1/S – The importance of context 24
1.2.5.2 Introducing the G1/S "balance" model 25
1.3 Introduction III – The NF-κB signalling system 27
1.3.1 NF-κB - A key oscillatory system 27
1.3.2 Structure of NF-κB proteins 29
1.3.3 Characterisation of NF-κB dynamics 30
1.3.4 Thesis context: Crosstalk between NF-κB and G1/S of the cell cycle 32
1.4 Project Aims – A Systems Biology framework 34
Chapter 2 - Materials & Methods 35
2.1 Materials 36
2.1.1 Reagents 36
2.1.2 Plasmids 36
2.2 Methods 37

2.2.1 Molecular Biology 37
2.2.1.1 Transformation of competent cells 37
2.2.1.2 Amplification of plasmid DNA (Maxiprep) 37
2.2.1.3 Agarose gel electrophoresis and gel extraction 37
2.2.1.4 Restriction endonuclease digestion 38
2.2.1.5 Blunting 5'- and 3'- DNA overhangs 38
2.2.1.6 5'-Phosphate removal 39
2.2.1.7 DNA ligation 39
2.2.1.8 DNA sequencing 40
2.2.2 Cell culture 40
2.2.2.1 Subculturing cells 40
2.2.2.2 Transient transfection 41
2.2.2.3 Cell cycle synchronisation 41
2.2.2.4 TNFα stimulation 42
2.2.3 Single cell techniques 43
2.2.3.1 Live cell fluorescence imaging 43
2.2.3.2 Förster (Fluorescence) Resonance Energy Transfer (FRET) imaging 44
2.2.4 Bulk cell techniques 45
2.2.4.1 Flow cytometric DNA analysis 45
2.2.4.2 Luciferase reporter assays 45
2.2.4.3 Immuno-blotting 46
2.2.4.4 Co-ImmunoPrecipitation (Co-IP) 47
2.2.4.5 Immuno-cytochemistry (ICC) 48
2.2.4.6 Quantitative RT-PCR 48
2.2.5 Analytical tools and databases 49
2.3 Theoretical work 50
2.3.1 Mathematical modelling 50
Chapter 3 - Generation & Characterisation of Tools 52
3.1 Generation of E2F fluorescent fusion constructs 53
3.2 Characterisation of EGFP-E2F-1 and endogenous controls 56
Chapter 4 - E2F-1 and The NF-κB System: Towards a model foundation 60
4.1 Introduction – Shuttling and Translocation 61
4.2 The effects of exogenous E2F-1 on NF-κB localisation 62
4.3 The effect of transiently expressed E2F-1 on NF-κB localisation 64
4.4 Binding between ectopically expressed E2F-1, p65 and p50 and IκBα 67
4.5 The NF-κB:E2F-1 conceptual model and its assumptions 70
4.6 NF-κB affects E2F-1 related Apoptosis 73
4.7 Discussion 74
Chapter 5 - The NF-κB:E2F-1 Model: Extension, Prediction, and Verification 75
5.1 Introduction and rationale 76
5.2 Revision and extension of the NF-κB model 76
5.3 Experimental and mathematical reproduction of past NF-κB work 81
5.4 Implementation of the NF-κB:E2F-1 module 83
5.5 Model predictions (1): The effect of TNFα on localisation, stability and short-term dynamics 86
5.6 Predictions (2) - Long time course dynamics after TNFα stimulation 94
5.7 Discussion – How can we explain these dynamics? 97

Chapter 6 - NF-κB:E2F-1 Model Evolution 99
6.1 Introduction and rationale 100
6.2 Re-assessment of transcriptional assumptions 100
6.3 Model evolution 110
6.4 Suspended oscillations revisited 114
6.5 Discussion – Variability in NF-κB dynamics 117
Chapter 7 – NF-κB:E2F-1 - The Cell Cycle Context 119
7.1 Introduction and rationale 120
7.2 Conceptual and experimental models for cell cycle studies 121
7.3 Endogenous localisation and binding of E2F-1 and NF-κB 125
7.4 Transcriptional studies revisited 129
7.5 Apoptosis revisited 133
7.6 Variability in NF-κB dynamics revisited 134
7.7 Discussion 138
Chapter 8 - General Discussion 139
8.1 Overall reflection on project 140
8.1.1 General comments 140
8.1.2 Reflection on Thesis aims 140
8.2 The NF-κB context 141
8.2.1 Results in perspective 141
8.2.2 Future work 144
8.3 The cell cycle context 146
8.3.1 Results in perspective 146
8.3.2 Future work 147
8.3.3 The Systems Biology of the cell cycle 149
8.5 G1/S Response context – Physiological perspective 150
8.6 Final Comment – The importance of metaphor 157
Chapter 9 - References 158
Appendix 1 171
A1.1 Complete plots for NF-κB:E2F-1 model Mk.I 172
A1.2 Complete plots for NF-κB:E2F-1 model Mk.II 174

List of Figures, Tables and Supplementary Materials

Figures

Figure 1.1 Stepwise approach to coupling linked systems in Systems Biology

Figure 1.2 A typical Interdisciplinary research cycle

Figure 1.3 An example of a Deterministic ODE system

Figure 1.4 Comparing Deterministic and Stochastic processes

Figure 1.5 Simple negative feedback

Figure 1.6 Phases of the Mammalian Cell Cycle

Figure 1.7 Characterisation of the E2F family of proteins

Figure 1.8 G1/S phase: Regulation of S-phase transition by E2F-1

Figure 1.9 Relative levels of Cell Cycle proteins at G1/S phase

Figure 1.10 The p53:G1/S Balance model

Figure 1.11 Conceptual model of the NF-κB System

Figure 1.12 Structure of members of the classical NF-κB System

Figure 1.13 Dynamics of p65-dsRedXP - a quantifiable output of the NF-κB System

Figure 1.14 The NF-κB:G1/S Balance model

Figure 2.1 A typical model simulation protocol

Figure 3.1 Gateway Cloning Steps for EGFP-E2F-1

Figure 3.2 Localisation of exogenous and endogenous E2F-1

Figure 3.3 Degradation of EGFP-E2F-1

Figure 3.4 Transcriptional functionality of EGFP-E2F-1

Figure 4.1 Localisation of transiently transfected NF-κB and E2F-1 fluorescent reporter proteins

Figure 4.2 The effect of E2F-1 level on NF-κB nuclear occupancy in unstimulated conditions

Figure 4.3 Proportional relationship between p65-dsRedXP nuclear occupancy and EGFP-E2F-1 degradation

Figure 4.4 FRET between E2F-1, p65 and p50 fusion proteins

Figure 4.5 Assessment of endogenous binding between E2F-1, p65 and p50 via Co-Immunoprecipitation in SK-N-AS cells

Figure 4.6	The NF-κB:E2F-1 Conceptual model Mk.1
Figure 4.7	NF-κB transcriptional activity in transient transfection conditions
Figure 4.8	NF-κB affects the level of E2F-1 mediated Apoptosis
Figure 5.1	Ordinary Differential Equation for nNFkB
Figure 5.2	Experimental and Mathematical reproduction of NF-κB dynamics
Figure 5.3	Network "wiring" diagram for major species in E2F:NFkB model
Figure 5.4	Modelling proportional sequestration of E2F-1 on NF-κB
Figure 5.5	NFkB:E2F-1 Model Prediction(1): Short time-course TNFα
Figure 5.6	Short time-course dynamics following TNFα stimulation
Figure 5.7	Modelling short time-course dynamics following TNFα stimulation
Figure 5.8	Experimental verification of effect of E2F-1:p65 ratio
Figure 5.9	Proportional analysis of E2F-1:p65 ratio on p65 dynamics
Figure 5.10	Model Prediction: Long time-course dynamics following TNFα stimulation
Figure 5.11	Experimental Verification: Long time-course dynamics following TNFα stimulation
Figure 5.12	Examining long time course dynamics following TNFα stimulation
Figure 6.1	Assessment of IκBα protein levels in transfected cells
Figure 6.2	Assessment of IκB transcription levels in transfected cells
Figure 6.3	Assessment of IκBα stability in transfected cells stimulated with TNFα
Figure 6.4	The effect of exogenous E2F-1 on TNFα stimulated NF-κB transcription
Figure 6.5	Dynamics of p65-dsRedXP with IκBα-AmCyan after TNFα stimulation
Figure 6.6	Dynamics of p65-dsRedXP with EGFP-E2F-1 and exogenous IκBα after TNFα stimulation
Figure 6.7	Estimated half-life of EGFP-E2F-1 in nucleus and cytoplasm
Figure 6.8	Proportional relationship between E2F-1 degradation and suspension of nucleo-cytoplasmic oscillations in p65-dsRedXP
Figure 6.9	The NF-κB:E2F-1 mathematical model Mk.II
Figure 6.10	Variability in p65-dsRedXP dynamics in SK-N-AS cells
Figure 7.1	Imaging parent and daughter cells

Figure 7.2 Flow Cytometric DNA Analysis of Thymidine synchronisation model

Figure 7.3 Conceptual "catch" model: NF-κB response at different cell cycle stages

Figure 7.4 E2F profiles achieved through Thymidine synchronisation

Figure 7.5 Experimental Model: NF-κB response at different cell cycle stages

Figure 7.6 Immuno-CytoChemistry to assess p65 and E2F-1 co-localisation in HeLa cells

Figure 7.7 Co-ImmunoPrecipitation in synchronised HeLa cells

Figure 7.8 Assessment of p65 cleavage in synchronised, stimulated cells

Figure 7.9 IκB Levels associated with NF-κB response at different cell cycle stages

Figure 7.10 Transcriptional Studies on Cell Cycle genes in exogenous system

Figure 7.11 E2F-1 related Apoptosis (II)

Figure 7.12 Variability in NF-κB dynamics in non-synchronised HeLa cells

Figure 7.13 NF-κB dynamics in synchronised HeLa cells stimulated prior to G1/S

Figure 7.14 Variability in NF-κB dynamics in synchronised and non-synchronised HeLa cells

Figure 8.1 Conceptual "Catch" model Mk.II for NF-κB:E2F-1 interaction

Figure 8.2 Review of steps taken towards coupling the NF-κB and G1/S linked systems

Figure 8.3 Localisation of transiently transfected p65 with E2F-2 and E2F-3 fluorescent reporter proteins

Figure 8.4 Localisation of transiently transfected E2F-1 and Cyclin E fluorescent reporter proteins

Figure 8.5 Localisation of transiently transfected E2F-1 and p105 fluorescent reporter proteins

Figure 8.6 G1/S Balance Model

Figure 8.7 G1/S Balance Model – Cell Cycle Suspension mechanisms for p53 and NF-κB

Figure 8.8 G1/S Balance Model – G1/S mediated co-ordination of p53 and NF-κB signalling

Figure 8.9 G1/S Balance Model – Cell Cycle Resumption mechanisms for p53 and NF-κB

Figure A.1 Model plots for species in the NF-κB:E2F-1 model Mk.I

Figure A.2 Model plots for species in the NF-κB:E2F-1 model Mk.II

Tables

Table 2.1 Number of HeLa and SK-N-AS cells seeded for different applications

Table 2.2 Details of primary anti-bodies used in this study

Table 3.1 Initial conditions for NF-κB:E2F-1 mathematical model

Table 5.1 New or amended species introduced to the E2F-1:NF-κB model

Table 5.2 Considering reactions in the NF-κB:E2F-1 model

Table 5.3 Ordinary Differential Equations in the NF-κB:E2F-1 Model

Table 6.1 NF-κB:E2F-1 mathematical model Mk.II evolutionary steps

Table 6.2 Reactions affected by the evolution of the NF-κB:E2F-1 model MkII

Supplementary materials

(accompanying DVD)

S1. Dynamic Model - NFKBE2F model Mk.1

S2. Dynamic Model - NFKBE2F model Mk.2

S3. Movies (detailed below)

S4. Various Sketches (models and diagrams)

Movies

(accompanying DVD)

All movies show live cell imaging of SK-N-AS and HeLa cells (as indicated); culture and transfection proceeded in accordance with Materials & Methods. Frame rates adjusted so that 1 s ≈ 1 h in each case. See text for experimental details.

Movie M1.13	SK-N-AS p65-dsRedXP +TNF.avi
Movie M3.3	SK-N-AS EGFP-E2F-1 non-stim.avi
Movie M4.2	SK-N-AS p65-dsRedXP EGFP-E2F-1 non-stim.avi
Movie M4.4	SK-N-AS p65-EYFP ECFP-E2F-1 FRET.avi
Movie M5.6	SK-N-AS p65-dsRedXP EGFP-E2F-1 +TNF short time-course.avi
Movie M5.11	SK-N-AS p65-dsRedXP EGFP-E2F-1 +TNF long time-course.avi
Movie M6.5	SK-N-AS p65-dsRedXP AmCyan-IkBa +TNF.avi
Movie M6.6	SK-N-AS p65-dsRedXP EGFP-E2F-1 cmv-IkBa.avi
Movie M7.12	HeLa p65-dsRedXP non-synch +TNF.avi
Movie M7.13	HeLa p65-dsRedXP synch +TNF T90.avi
Movie M8.4	SK-N-AS p105-dsRedXP EGFP-E2F-1 non-stim.avi

Commonly Used Abbreviations

Abbreviations used as per SI unit conventions, with the following additions:-

AA (aa)	Amino Acid
cDNA	Complementary DNA
CDK	Cyclin Dependent Kinase
CDKI	Cyclin Dependent Kinase Inhibitor
ChIP	Chromatin Immuno-Precipitation
CMV	Cytomegalovirus
Co-IP	Co-Immuno-Precipitation
dCTP	Deoxycytidine-5'-diphosphate
DMEM	Dulbecco's Modified Eagle's Medium
DNA	Deoxyribonucleic Acid
DP	DRTF Polypeptide
dsRed-XP	*Discosoma* Red-Express Fluorescent Protein
E2F	E2-Factor
ECFP	Enhanced Cyan Fluorescent Protein
EGFP	Enhanced Green Fluorescent Protein
EYFP	Enhanced Yellow Fluorescent Protein
FCS	Fluorescence Correlation Spectroscopy
FRET	Fluorescence (Förster) Resonance Energy Transfer
G1,G2 phase	Gap phases
HCl	Hydrochloric acid
ICC	Immuno-cytochemistry
IκBα,ε	Inhibitor κB (α,ε)
IKK	IκB Kinase (α)
ka	association rate coefficient
kd	dissociation rate coefficient
ke	export rate coefficient
kg	degradation rate coefficient
ki	import rate coefficient
Luc	Luciferase
NF-κB	Nuclear Factor κB

M-Phase	Mitosis phase
MDM2	Murine (Mouse) Double Minute protein 2
MEM	Minimal Essential Medium
MNL	Maximum Nuclear Localisation
mRNA	Messenger RNA
NES	Nuclear Export Sequence (Signal)
NLS	Nuclear Localisation Sequence (Signal)
NR	Nuclear Retention
PBS	Phosphate-Buffered Saline
PCR	Polymerase Chain Reaction
pRB	Retino-blastoma protein
Q-PCR	Quantitative PCR
RHD	Rel-Homology Domain
RNA	Ribonucleic Acid
S-Phase	DNA Synthesis phase
SD	Standard Deviation
SDS	Sodium Dodecyl Sulphate
SEM	Standard Error Mean
TNFα	Tumour Necrosis Factor (α)
Tris	Tris(hydroxymethyl)methylamine

Acknowledgements

his is hardly the time for pretention, but there are some people I really need to thank. Firstly; Mike, for taking a risk in turning a dry scientist a little bit wet. Likewise to Violaine and Dave for not once turning me away when I had a (silly) question. Next, delving into the past, I'd like to thank Glyn for taking me to the pub roughly 10 seconds after I'd joined the group, and for teaching me how to open almost any door with either foot; Caroline for the spirit of solidarity (CompSci '02, woohoo!); and James for being the funniest and campest person I've ever met. Next, bang up to date, I'd like to thank "the girls"; Dhanya for the wry smiles at "office goings-on"; Kate and Louise for being a pleasure to sit next to for 3 and a bit years; Denise and Anne for bringing the Scouse count up; Rachel for leaving her email open one too many times; and Steph for all the coffee. Sheila is of course a real-life lady and should be thanked in those terms. Nearly there... it's fun this... middle-class Pete for being spotted; Cath and Carol for their big smiles; *il bello eccentrico* Marco; and Daniel for being the nicest man in existence. Speaking of nice people, Pawel is one of those (with the paperwork to prove it). I'd like to thank him for his sense of humour and his single-minded determination not to suffer fools gladly. I'd like to thank "Baggers" and Nick for letting David know his place; Kate and the Awaises for a warm welcome upstairs; and Luke for the good times. Next... to Antony, "Debone" remains a worthy adversary, a friend, and one of the most devious minds ever to be left in charge of a spiced sausage. I've said largely positive things so far haven't I? Which brings me to David. What can I say about this pre-pubescent, big-faced, slightly insane train enthusiast, that I haven't said before? Well I can say that he's equal parts annoying and adorable and I wish I had a little brother just like him. So I could kick him. And finally, to Claire. Some might say a worthy subject for a thesis herself. The inspiration for a future series of children's books in the 'Noddy' vein, and orator of such notable musings as "Public transport is for the poor", "I'd breast-feed a puppy for 500 quid" and "That was my idea"; she has contributed a great deal to my PhD experience and I am eternally grateful. All of the above should be applauded for their super-human patience with me; in return you will all have a part to play when the sitcom is written. In the real world, I'd like to thank Richy and George for convincing me to do the PhD in the first place and my Dad, Katie and Nan for asking questions when the answers didn't matter... and my mum, for her "genes". Which are apparently quite important. Whatever they are. Finally, I'd like to thank Sammy, for turning everything upside down, so it was the right way up. Random thanks go to Angus Young, Dufton Mwaengo, David Hasselhoff, and Jonny Sparrow. I could go on forever, but I have a cup of tea to drink, and you have a thesis to read! ... Wadda 'ya say? Let's Boogie! ... David, make the tea.


PASZEK
APPROVED

Chapter 1 –
Introduction

1.1 Introduction I - Systems approaches to biological research

1.1.1 What is Systems Biology?

Definitions of Systems Biology vary, albeit with common principles. The Biotechnology and Biological Sciences Research Council (BBSRC) characterises a Systems Biology approach broadly as *"...placing a greater emphasis on the interactions between components, and the consequences of such interactions, than on the components themselves* (BBSRC Website 2008). Put simplistically, there is a need to appreciate the context of biological phenomena. As such, "integration" of biological processes has now become favourable to "reduction" of systems to their components, which, in a post-genomic era, may be largely known. The Systems Biology approach may be considered "integrative" in a number of further ways, most obviously by bringing together scientists from different disciplines, The Institute for Systems Biology (ISB) characterise Systems Biology as *"...the study of an organism, viewed as an integrated and interacting network of genes, proteins and biochemical reactions which give rise to life... aided by the infusion of scientists from other disciplines..."* (SystemsBiology.org 2008). However, interdisciplinary approaches are by no means novel in Biology (Lotka 1925; Volterra 1926; Hodgkin *et al.* 1952). Denis Noble, pioneer of arguably the longest-standing Systems Biology approach, modelling Ion channels in the human heart (Noble 2006) argues that their increasing popularity in recent times is symptomatic of a change in thinking: *"[Systems Biology]...is about putting together rather than taking apart, integration rather than reduction. It requires that we develop ways of thinking about integration that are as rigorous as our reductionist programmes, but different....It means changing our philosophy, in the full sense of the term"* (Noble 2006). One might argue that in order to deal with the rise in complexity brought about by systems-level approaches, mathematical models are becoming essential, interdisciplinary collaboration is now a necessity.

Systems Biology applied to the study of intra-cellular signalling is best illustrated with an example. Consider two proteins 'X' and 'Y' which display evidence of physical interaction when examined. Many characteristics of the X:Y interaction, such as quantification of relative protein levels, analysis of their dynamics over time, and response to stimuli may be investigated in isolation from networks of proteins that may

also interact with X and Y. The picture of X:Y has in effect been simplified, or reduced. This reductionist approach may take us a long way towards quantifying the observed behaviour of X and Y in terms of space and time and with the mathematical tools it may even be possible to build a computer model which mimics an interaction between X and Y.

However, the reductionist approach is not enough to fully characterise such an interaction because it lacks an appreciation for context. It has emerged over a number of years that single genes cannot usually be attributed to single phenomena, and that proteins do not act in isolation but rather in collaborative networks or systems (Noble 2006). As such, a study of X and Y may give interesting results, but this is arguably less important from a physiological viewpoint, than the behaviour of the system or systems in which they act, their context. Investigating the behaviour of single biological entities whilst maintaining an appreciation for their role as components in larger systems is the essence of Systems Biology.

1.1.2 Integration in the Systems Biology approach

Despite presenting an alternative to reductionist approaches, systems-level approaches are able to incorporate data from such studies. Such approaches applied to intra-cellular signalling may draw upon quantitative data gathered from bulk cell and single cell based experimental work, as well as from high-throughput proteomic, transcriptomic and bioinformatic techniques. Integration of data from a variety of sources helps to form a central conceptual picture or "model", allowing entire systems to be mapped out (Kohn 1999; Kohn *et al.* 2006). Conceptual models are key to assessing the roles of individual components and therefore provide the basis of a Systems Biology approach. However, as the complexity of these systems increases (if for example protein X regulates the transcription of an inhibitor protein, generating negative feedback), holistic appreciation of system dynamics may prove difficult from a conceptual model alone.

However, with a conceptual model at its foundation, the Systems Biology approach can be taken a step further, turning conceptual models into mathematical *in-silico* models. For a mathematical Systems Biology approach, Mathematics, Computer Science and Biology may overlap, combining advanced techniques to both measure and quantify

experimental data with predictive modelling techniques to provide a dynamic view of an entire system, that is able to test (and hence make predictions for) the effect of changes to individual systems components (such as protein X) to the overall systemic context. As such, integration of techniques from different disciplines provides a further strength of the Systems Biology approach.

It is important to note that in addition to being integrative in terms of approach, Systems Biology often aims to be integrative in terms of results, resolving linked processes across different time scales (such as stress signalling and the cell cycle) or physiological scales (such and cellular and tissue). This is considered in greater detail below (Section 1.1.6)

1.1.3 Requirements of Mathematics in Systems Biology

Interdisciplinary Systems Biology approaches are becoming increasingly popular (Sauer *et al.* 2007), to the extent that "Systems Biology" itself is often synonymous with "mathematical modelling". This may be misleading as mathematical modelling may equally be applied to reductionist studies as much as to Systems Biology. As such, care must be taken to apply mathematical approaches appropriately. A well-formed mathematical Systems Biology approach requires three elements; a biological *context* on which the current conceptual view of a system is based, the ability to make a hypothetical *prediction* for system behaviour and the experimental means with which to provide an *answer* which resolves the prediction. We shall now consider each of these requirements in greater detail.

1.1.3.1 Biological context

There is a calculated risk to defining biological systems as models. Model boundaries must be defined to include processes driving systemic behaviour, whilst simplifying less important processes, hence reducing complexity and allowing a conceptual model to be clearer, or a mathematical model to be more easily fitted. Definition of the context for a model is therefore highly subjective. Indeed, defining the boundary or "level of abstraction" of a system has principles deeply rooted in Applied Mathematics and Computer Science and is arguably best approached from a philosophical stand-point (Wright 1983; Colburn *et al.* 2007; Floridi 2008)

Figure 1.1 shows a step-wise approach to coupling intracellular signalling systems linked by interacting proteins 'X' and 'Y'. Firstly, models are defined for each system (A1 and A2 in Figure 1.1). Once the separate models are fitted, the interaction between X and Y may be modelled through boundary expansion encompassing either "the effect of Y on system 1" or "the effect of X on system 2", as an intermediate step (A#). An A#-type model may be expanded further to define a model for both "linked" systems (B).

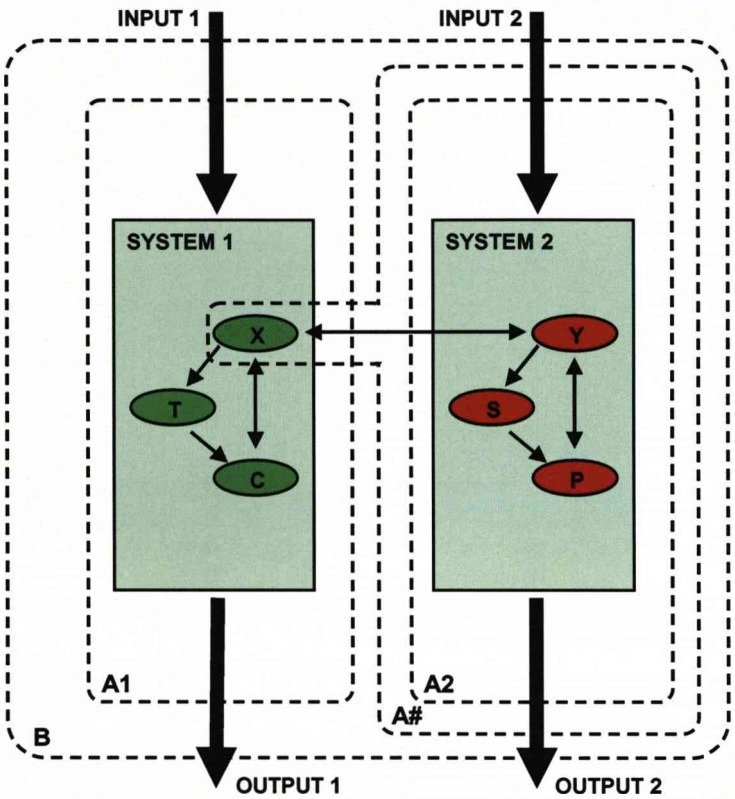

Figure 1.1 Stepwise approach to coupling linked systems in Systems Biology: A1 and **A2** Showing models defined for system 1 and system 2 respectively involving processes which may occur over different temporal or physiological scales. Systems 1 and 2 have unique, or separable, inputs and outputs with respect to each other. **A#** Model A2 is expanded to include interaction between protein 'Y' (system 2) and protein 'X' (system 1). Interaction between X and Y may now be considered within the context of system 2. **B** Once characterised, model A# may be expanded further to encompass system 1 and fitting proceeds. Solid lines represent physiological boundaries for Systems 1 and 2, dotted lines represent models that can conceivably be defined. Black arrows represent system inputs and outputs.

1.1.3.2 Predictive ability

A mathematical model should be able to make non-intuitive predictions regarding the behaviour of a given system. Strictly, mathematical models should only be created when the complexity of a system exceeds the ability of a conceptual model to make intuitive predictions. Cross-talk between linked signalling systems is an example of such a situation, allowing us to make predictions regarding the effect of protein X from system 1 on system 2 behaviour through cross-talk with Protein Y (Figure 1.1 A#). The ability of a model to make predications depends heavily on the ability of the experimental model system to supply a strong experimental foundation.

1.1.3.3 Resolution

In order to be functional, a model of a system requires at least one quantifiable input and output. These should be system specific, for example, in the case of model B in Figure 1.1 Input 1 should not be able to elicit a response through Output 2 independently of interaction between systems 1 and 2. This is a common issue when investigating linked signalling systems involving transcription factors, where care must be taken to ensure stimuli used as inputs and target genes used as outputs are system specific. Choice of both biological and experimental model systems is therefore important, firstly to provide the correct context in which model predictions can be made, and secondly to be able to test these predictions experimentally, in a quantifiable manner.

1.1.4 Experimental model system – Protein dynamics in single living cells

Within all complex biological systems, cells must communicate to produce co-ordinated temporal, local or global responses. Cells regulate these responses by alterations in complex intra-cellular signalling cascades. Proteins undergo changes in their interactions, stability and location within and between cell compartments. Dynamic modifications, such as the phosphorylation state of proteins that typically transduce a signal into a response, are usually measured using techniques that necessarily give a population average. These and other measures are often from a population of cells over time, or single cells at a given time point; and any temporal heterogeneity is lost

as a result. The onset of fluorescent fusion protein technology and time-lapse fluorescence microscopy has provided the ability to perform non-invasive measurement of protein dynamics in the same cell over time. Transient exogenous expression, stable integration or the generation of transgenic animals provide tools for studying the localisation, translocation and stability of specific proteins of interest at the single cell level and ultimately in living tissues. Where single cell time-lapse data is available, such as in NF-κB signalling (Nelson *et al.* 2004), or circadian rhythms (Welsh *et al.* 2004), single cell heterogeneity is shown to be masked by population averaging. An *in silico* model derived from population data may miss crucial dynamic and functional details. However, single cell studies unmask stochastic events that lead to cell to cell variation. Incorporation of the stochastic non-linear dynamics of the system into a model allows a better understanding and appreciation of the kinetics and function of mechanisms within signalling networks.

1.1.5 Biological model system - Oscillatory behaviour in cell signalling

Although complex when taken as a whole, intra-cellular networks are often made up of a common set of simple motifs (for example feedback loops; (Milo *et al.* 2002)), which generate a wide range of dynamic behaviours, including oscillations. The negative feedback loop (e.g. when a protein inhibits its own transcription, considered further in Section 1.1.9) is one example which can lead to oscillatory behaviour, such as cycles in protein concentration or translocation between cellular compartments. Although a single delayed negative feedback loop is all that may be required to drive oscillatory behaviour, many systems have multiple feedback loops, leading to much more complex dynamic behaviour (Tsai *et al.* 2008). It can be argued that this level of complexity can only be fully understood with a mathematical Systems Biology approach.

The involvement of a core negative feedback loop to generate sequential cycles of nuclear to cytoplasmic (nucleo-cytoplasmic) protein translocation are particularly well documented in the transcription factor Nuclear Factor kappa B (NF-κB) signalling system (Nelson *et al.* 2004) and thus this provides a good model system for evaluating complex and non-linear protein dynamics (Chapter 2). Oscillations in other signalling systems have been discovered using fluorescence techniques and imaging at a single cell resolution. Variation in oscillatory kinetics between single cells was first

characterised in acute responses such as cytoplasmic calcium concentration (Berridge 1990), where the response to stimuli was transduced by changes in the frequency of oscillations in intracellular calcium concentration that can occur from fractions of a second (Nelson *et al.* 1995) to minutes (Cuthbertson *et al.* 1985). Although changes in intracellular calcium concentration were detected many years ago with the calcium-specific photoprotein, Aequorin (Ridgway *et al.* 1976); (Woods *et al.* 1986) the onset of highly selective fluorescent calcium indicators enabled the visualisation of small, high frequency changes in ion concentration within individual live cells (Grynkiewicz *et al.* 1985), and thus first made the connection between oscillatory behaviour and target gene expression (Dolmetsch *et al.* 1997) (Dolmetsch *et al.* 1998) (Li *et al.* 1998).

Oscillatory movement between nuclear and cytoplasmic compartments shown by the tumour suppressor protein p53 result from a negative feedback loop, involving the relationship between p53 and its inhibitor MDM2 (Lahav *et al.* 2004). In contrast to the timing of calcium oscillations, these changes occur in the order of hours (Lahav *et al.* 2004). Regulation of MDM2-independent nuclear export depends on the exposure of the p53 NES, contained within a leucine-rich tetramerisation domain. Upon import as a monomer species, p53 tetramerises to become transcriptionally active (Friedman *et al.* 1993), masking its intrinsic NES from exportins and maintaining its active, nuclear localisation. It is only upon fragmentation of the p53 tetramer to dimers that its NES becomes accessible and subsequently targetable for nuclear export. Not only have oscillations in p53/MDM2 been shown at the single cell level (Geva-Zatorsky *et al.* 2006) but also from an MDM2-luciferase reporter *in vivo* from living irradiated transgenic mice (Hamstra *et al.* 2006). The emergence of molecular oscillators have been documented in recent studies for example Notch/Hes1 and Wnt (Shimojo *et al.* 2008). These genes have been shown to have significant roles in the somitic segmentation clock, most notably in showing oscillations within cell populations in whole embryos independent of β-Catenin levels (Aulehla *et al.* 2008). Similar oscillations have also been suggested in the Smad and Stat1 (Yoshiura *et al.* 2007) signalling systems.

Molecular oscillations have also been visualised on much longer time-scales, for example in the mammalian and plant circadian clocks (reviewed in (Ko *et al.* 2006) and (Schultz *et al.* 2003) respectively). Here, the discovery that circadian rhythms could be

induced in mammalian culture cells (Balsalobre *et al.* 1998) has allowed new and detailed single cell investigations of the mammalian circadian clock (Welsh *et al.* 2004). Single cell studies have also given new insights into the mammalian cell cycle oscillator. Live cell imaging has been used to show dynamic shuttling of both Cyclin E and Cyclin A (associated with G1/S and S phase progression respectively) (Jackman *et al.* 2002). Recently, non-invasive "markers" of cell cycle transition have been developed to track particular phases of specific proteolysis (Sakaue-Sawano *et al.* 2008), and destabilised GFP constructs used to investigate fail-safe mechanisms to maximise cell cycle synchrony between single budding yeast (Bean *et al.* 2006).

1.1.6 Integration of linked processes across scales

A key challenge in Systems Biology is to integrate the behaviour of systems across both physiological scales, ranging from single molecules to whole organisms and time scales ranging from seconds to hours. A classic example linking ion channel function to organ physiology comes from the model of the virtual heart (DiFrancesco *et al.* 1985). Other modelling projects have encompassed biochemical (Novak *et al.* 2004), cellular (Turner *et al.* 2002), organ (Noble 2006), and population (Spencer *et al.* 2008) level based approaches. Cell signalling networks are integral to organism adaptation and survival and underlie normal cell function, communication and disease. The observation that key systems may oscillate suggests a possibility that this may be one important feature of many signalling networks. Such oscillatory processes may span periods of time from fractions of a second/minutes (calcium) to minutes/hours (NF-κB, p53, segmentation clock) to hours/days (circadian clock and cell cycle) suggests an intriguing possibility that interactions between these dynamical processes may well intermesh like the cogs in a clock to provide error-free interpretation of signalling information in normal cells. These ideas are developed further in Chapter 8.

1.1.7 Interdisciplinary Systems Biology in practice

The interdisciplinary step between conceptual Systems Biology and mathematical Systems Biology requires close collaboration between experimentalists and theoreticians. Where possible, the transfer of skills between disciplines is desirable, not only to help researchers to be more flexible, but to foster an appreciation and

understanding for the critical timescales involved in both approaches. Figure 1.2 shows a typical cycle for interdisciplinary research. An important observation about the cycle is that the experimental path (pink) drives the resolution of prediction to result and is therefore critical. The blue theoretical paths, whilst not critical, aim to speed up the cycle by making it shorter (conceptualised here by the sub-cycle of "Model > Prediction > Answer > Model"). A model abstracted carefully from a context (conceptual model) should be able to make non-intuitive predictions about a given system as complexity increases past the point of intuitive prediction. In addition to predictive experimental design, a mathematical model may be used to assess system sensitivity to quantitative changes in model parameters.

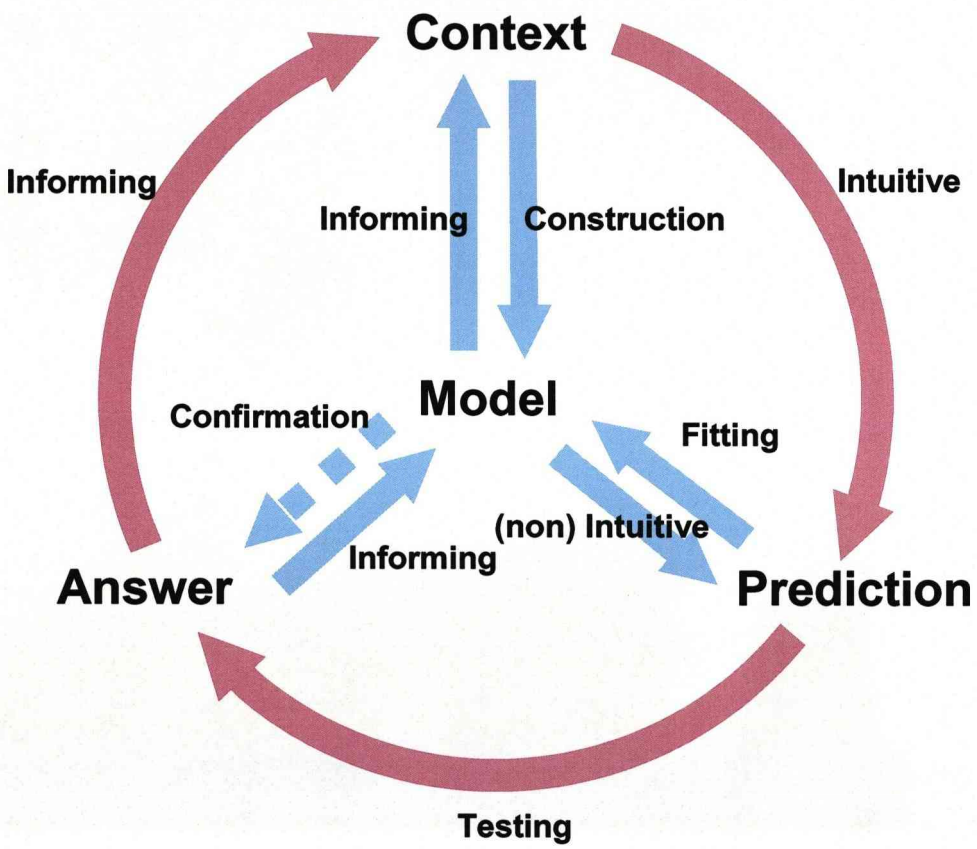

Figure 1.2 A typical interdisciplinary research cycle: Showing three requirements of a Systems Biology approach; Context (from which a conceptual model is derived), predictive ability and answer. Critical path of experimental research (pink), and paths made possible by the interdisciplinary approaches to Systems Biology (blue), including non-intuitive prediction and a faster cycle of research between prediction, answer and model abstracted from a conceptual model.

1.1.8 The application of Mathematics in Systems Biology

Although the application of mathematical models to the study of biological systems is not a new approach (Lotka 1925; Volterra 1926; Hodgkin *et al.* 1952), in recent years the field has enjoyed a resurgence in popularity. This is due in part to increased awareness and appreciation for systems-level approaches to biological investigation (building on reductionist studies of the past), but also the concurrent development of high throughput techniques, driving an increase in both the complexity of systems under investigation and the volume of data available for analysis.

As we have discussed (Section 1.1.3.1), the process of abstracting a model from physiology requires careful consideration. This usually involves a compromise since "*no single model can simultaneously optimise generality, realism and precision*" (Levins 1966), so care must be taken to assess which processes are critical to adequately represent the behaviour of a system (Ting *et al.* 2002). When considering modelling approximations to intra-cellular signalling systems, mechanical processes are often grouped into several categories; 'physical binding' involving association and dissociation between proteins, 'transport' involving import or export of proteins between cellular compartments, 'protein modification' involving processes such as phosphorylation and acetylation, and 'protein stability' involving processes such as synthesis and degradation. These processes are mathematically modelled as biochemical reactions, involving the transition of molecular species between specific states in combination with kinetic parameters defining the rate of a given process. Using these conventions, biochemical reactions can be converted into systems of Ordinary Differential Equations (ODEs) with each reaction expressed as one such equation, as shown in Figure 1.3. Systems of linked ODEs allow changes in concentration of given molecular species to be quantitatively assessed over time with respect to other interacting species.

A

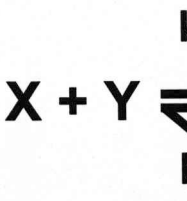

B

$$d[xy]/dt = ka[x][y] - kd[xy]$$
$$d[x]/dt = kd[xy] - ka[x][y]$$
$$d[y]/dt = kd[xy] - ka[x][y]$$

Figure 1.3 An example of a Deterministic ODE system: A Showing a reversible biochemical reaction representing the association and dissociation of two species 'X' and 'Y' and a complex species 'XY'. The forwards reaction, association, is driven by the kinetic parameter '*ka*', the reverse reaction, dissociation is driven by '*kd*'. **B** A system of ODEs describing the dynamics of the reaction in A.

There are certain implicit assumptions taken into account by the ODE approach; firstly, that reaction probability is proportional to the (product of the) concentration of molecular species involved in a given process (Fall 2002) and that reaction times are small. Secondly, that reaction space is homogenous. The latter of these assumptions is increasingly important when considering modelling systems which involve movement of species between cellular compartments, for example oscillatory systems such as NF-κB, p53 or the cell cycle, as discussed in Section 1.1.9.

ODE based models constitute the conventional approach to modelling dynamical systems (Phair *et al.* 2001) and assume each value of a given species is determined uniquely by given parameters and by previous values of model species, such models are therefore termed "Deterministic". A deterministic approximation to a biochemical reaction assumes that the discrete movement of reactant molecules (moving from one space to another) is adequately approximated as a continuous process (molecules occupy all space at all times). This is acceptable when numbers of molecules of reactant species are high. However, for processes involving low numbers of molecules of reactant species (such as transcription involving a small gene copy number or cytokine signalling involving a low number of receptors) fluctuation in species concentration becomes increasingly significant, leading to randomness or "Stochasticity" in given reactions and discrete kinetics cannot be approximated as continuous (Figure 1.4). Stochasticity in key processes may have concomitant effect on

the overall system behaviour. Stochastic models, can be used to simulate randomness in system processes, accounting for the probabilistic occurrence of collisions of reactant molecules (Elowitz *et al.* 2002; Kerszberg 2004; Cai *et al.* 2008) and have been recently applied to extend deterministic models involving linked ODEs of the NF-κB system (Lipniacki *et al.* 2007; Ashall *et al.* 2009)

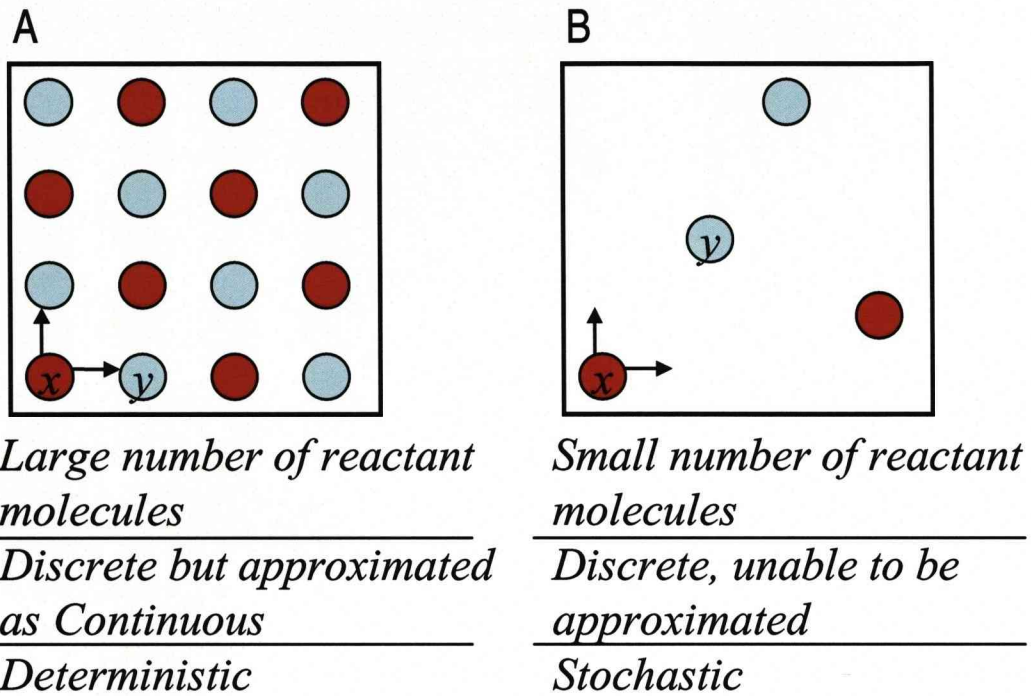

Figure 1.4 Comparing Deterministic and Stochastic processes: A Showing a large number of reactant molecules, the discrete kinetics of which can approximated as continuous by a Deterministic approach. **B** Showing a small number of reactant molecules, the discrete kinetics of which cannot be approximated as continuous. The randomness in this situation calls for a Stochastic modelling approach.

1.1.9 Mathematical Systems Biology applied to oscillatory systems

As introduced in (Section 1.1.5), oscillatory behaviour in intra-cellular signalling systems stems from feedback. The simplest form of negative feedback is outlined in Figure 1.5 and can be modelled with ODEs.

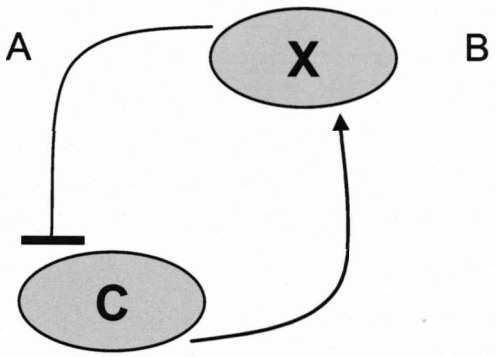

$$d[x]/dt = +\delta[c]$$
$$d[c]/dt = -\psi[x]$$

Figure 1.5 Simple negative feedback: A Showing negative feedback between C which positively regulates X, and X which negatively regulates C. **B** Showing ODE system describing negative feedback between X and C, where δ and ψ are arbitrary kinetic parameters.

In this example, species 'X' is positively regulated by species 'C', so the level of X at time t+1 is equal to the sum of X_{t0} and C multiplied by a positive kinetic parameter, $+\delta$. Species C is negatively regulated by protein X, so that the level of C at time t+1 is equal to the sum of C_{t0} and X multiplied by a negative kinetic parameter, $-\psi$. As such the depletion of C over time is proportional to the rise of X which is regulated by C, leading to negative feedback.

This core oscillatory motif is at the heart of deterministic approaches to modelling both NF-κB (Hoffmann *et al.* 2002), p53 (Lahav *et al.* 2004) and cell cycle (Novak *et al.* 2004). Subsequent development of modelling approaches to the NF-κB system provide a suitable example for the discussion of model development in general. As has been highlighted in Section 1.1.4 and (Ting *et al.* 2002) model development is highly influenced by the data in which it takes foundation. Consequently, there has been some disparity between subsequent development of NF-κB models based on data derived from single cell (Nelson *et al.* 2004) and bulk cell techniques (Hoffmann *et al.* 2002). Groups have sought to extend existing NF-κB models through provision for additional feedback mechanisms (Lipniacki *et al.* 2005; Basak *et al.* 2007; Ashall *et al.* 2009) and stochastic representation of processes involving randomness, such as gene expression ((Lipniacki *et al.* 2006; Ashall *et al.* 2009). Extension of models to consider "upstream"

activation of the system in greater detail has allowed emergent experimental data to be fitted (Lipniacki *et al.* 2007; Werner *et al.* 2008). Models have also been used to quantifiably predict the effects of drugs on the NF-κB system (Sung *et al.* 2004). Further examples of modelling approaches to oscillatory systems are discussed in Chapter 8, including the Systems Biology of the cell cycle, which is discussed in detail in Section 8.6.

1.1.10 Discussion - Systems Biology applied to this project

In this chapter we have presented a view of Systems Biology. Systems Biology is presented as an integrative approach as the antithesis of Reductionism, but capable of adsorbing data from such studies, highlighting the importance of integration. We then considered the requirements for a mathematical Systems Biology approach in terms of context, predictive ability and experimental resolution, which were used to define the step-wise process for model expansion (Figure 1.1). We went on to discuss the importance of biological and experimental model systems in resolving model predications experimentally, and proposed a research cycle linking context, prediction and answer (Figure 1.2).

The work described in this thesis applies a mathematical Systems Biology approach to the coupling of oscillatory systems operating over different time scales; the cell cycle (outlined in Section 1.2) and the NF-κB signalling system (outlined in Section 1.3) through interaction between NF-κB and the G1/S phase cell cycle regulator E2F-1. It involves both bulk and single cell based biological studies characterising the effects of E2F-1 on NF-κB signalling, and the expansion of a deterministic mathematical model for the NF-κB system. As such, the study has focused on the NF-κB system, with the model extended to include interaction with cell cycle regulator E2F-1 in a similar manner to model A# in Figure 1.1. However, work outlined in Chapter 7 is aimed to provide significant scope for future work characterising the reciprocal relationship within the context of the G1/S progression of the mammalian cell cycle.

1.2 Introduction II – E2F and G1/S cell cycle progression

1.2.1 Summary

The life cycle of the mammalian cell is heavily regulated, with transition from apparent resting states ("gap" phases) to the critical activities of DNA Synthesis (S-phase) and Mitosis (M-phase) subject to passage through checkpoints (Figure 1.6). Normal transition from early growth in the first gap phase through to S-phase (G1/S) is mediated by interactions between members of protein families including the E2-factor (E2F) family, Cyclins, Cyclin Dependent Kinases and CDK Inhibitors. These mechanisms are robust, ensuring healthy cells are able to repeatedly cycle through the G1/S checkpoint towards the point of senescence. However, the multiple levels of regulation also provide many molecular targets sensitive to stress response systems such as those controlled by p53 and NF-κB. The well characterised mechanisms for interaction between the p53 and G1/S systems allow us to introduce a conceptual model for DNA damage response prior to S-phase. The principles behind this model may be used to consider in detail the data presented on E2F-1 interaction with NF-κB (Chapters 5-7) within the context of a TNFα-mediated inflammatory response at G1/S (Chapter 8).

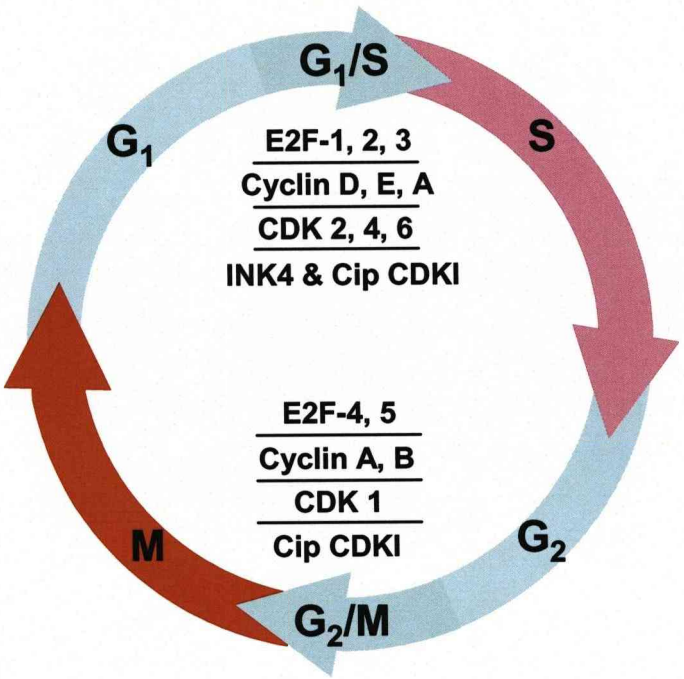

Figure 1.6 Phases of the mammalian cell cycle: Showing Gap phases G1 and G2 prior to "S-phase" DNA Synthesis and "M-phase" Mitosis, respectively. Transition from Gap phase into S or M phase is subject to passage through checkpoints (G1/S and G2/M). Cell cycle progression is regulated by the E2F family of transcription factors, Cyclins, CDKs and CDKIs, explained in detail in Section 1.2.3.

1.2.2 The E2F family of proteins

E2F-1 was originally discovered as a transcriptional activator of the viral E2 promoter (Kovesdi *et al.* 1986) predominantly bound by a protein later characterised as the retinoblastoma protein (pRB) (Bagchi *et al.* 1990). E2F-1 was subsequently found to regulate the transcription of genes essential for cell division (Bracken *et al.* 2004) many of which are outlined below. The E2F family currently consists of 9 members, although only the first 7 (E2F1, 2, 3a, 3b, 4, 5, 6) share any sequence homology (Figure 1.7). All E2F proteins form heterodimeric complexes with members of the DRTF-1 Polypeptide (DP) family, which are essential to E2F transcriptional activity (Trimarchi *et al.* 2002). E2F-1-3a are known as the "activating E2Fs" due to their transcription role governing entry into S-phase (Johnson *et al.* 1993; DeGregori *et al.* 1997), and are thought to be predominantly nuclear (characterised in Section 3.2). Over-expression of the activating E2Fs has been shown to drive progression into S-phase (Johnson *et al.* 1993), consequently leading to higher levels of apoptosis in mammalian cells (Qin *et al.* 1994).

Excluding the lesser characterised E2F-7 and E2F-8, the latter half of the E2F family (including E2F3b, a splice variant of E2F3a) are predominantly associated with transcriptional repression. E2F-4 and E2F-5 lack the Nuclear Localisation Sequence (NLS) present in E2F-1-3a, and possess a Nuclear Export Sequence (NES), yielding a predominant cytoplasmic localisation (Muller *et al.* 1997). However, it has been shown that E2F-4 and E2F-5 may take a nuclear localisation when bound in an inactive state to pocket proteins (possessing their own NLS), and bind to E2F promoters in competition with the activating E2Fs (Verona *et al.* 1997; Takahashi *et al.* 2000). As such, E2F-4 and E2F-5 are considered repressive, although it is possible that they may be able to activate certain genes (Wells *et al.* 2000). E2F proteins have a well characterised degradation pathway involving ubiquitination by the Skp2-SCF E3 Ubiquitin ligase (Campanero *et al.* 1997) and subsequent destruction in the nucleolar proteosome (Martelli *et al.* 2001).

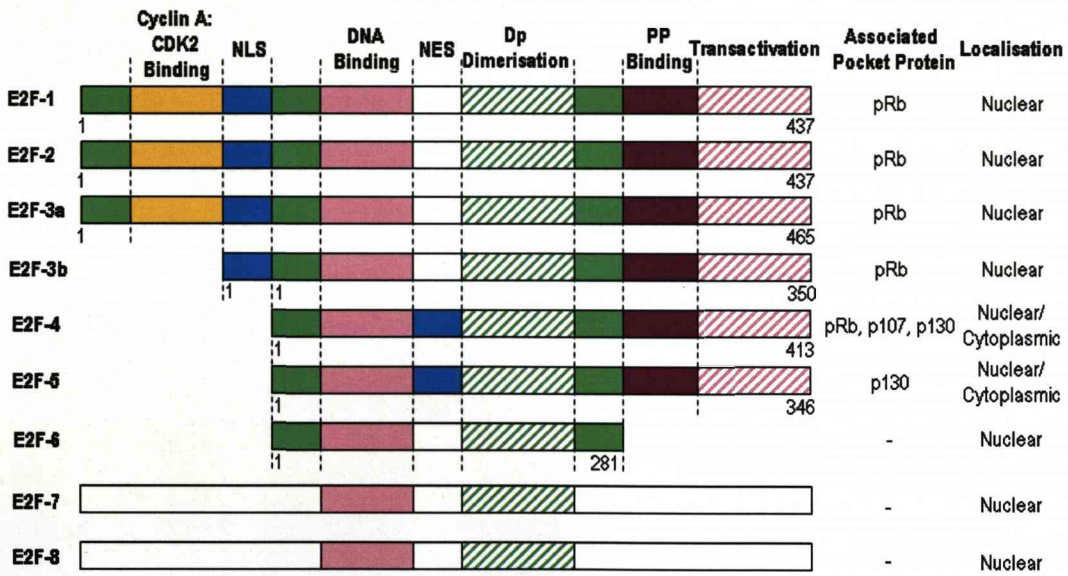

Figure 1.7 Characteristics of the E2F family of proteins. Showing strong sequence homology between the activating E2Fs (E2F-1,2,3a) and E2F-3b, which have a NLS. E2F-4 and E2F-5 contain a NES but not a NLS leading to a predominantly cytoplasmic localisation. Adapted from (Tsantoulis *et al.* 2005).

1.2.3 The G1/S checkpoint

Cell cycle progression from early growth in G1 to the onset of S-phase DNA synthesis is strictly controlled (Pardee 1974; Hartwell *et al.* 1989). As previously highlighted, transcription factors from the E2F family of proteins, namely E2F-1, E2F-2 and E2F-1-3a (in complexes with members of the DP family) have functional and physical roles in preparing the cell for S phase transition and the irreversible commitment to division (Dyson 1998) (Figure 1.8). Progression from G1 requires the activation of these E2F/Dp complexes via hyper-phosphorylation of inhibitor "pocket" protein, pRB by Cyclin:CDK complexes CyclinD:CDK4/6 and Cyclin E:CDK2 (Dyson 1998) enabling E2F-mediated transcription of a regulon containing over 200 cell cycle genes (Bracken *et al.* 2004), including Cyclins D, E and A which are essential for normal S-phase progression (Sherr *et al.* 1997; Ohtsubo *et al.* 1995; Assoian 1997). Concurrently, a loss of the activating E2Fs is attributed to cell cycle arrest and quiescence (Attwooll *et al.* 2004). Progressive activation of E2F-1-3a is reinforced through E2F auto-transcription, and generates a ramping level of active E2F throughout G1 which peaks at G1/S. This level falls during early S-phase as Cyclin A builds to a threshold (Schulze *et al.* 1995) (Figure 1.9), enabling the CyclinA:CDK2 complex to change the phosphorylation states of pRB and E2F-1-3a thus increasing binding affinity for the pRB/E2F/DP complex and effectively ending E2F related transcription (Peeper *et al.* 1995).

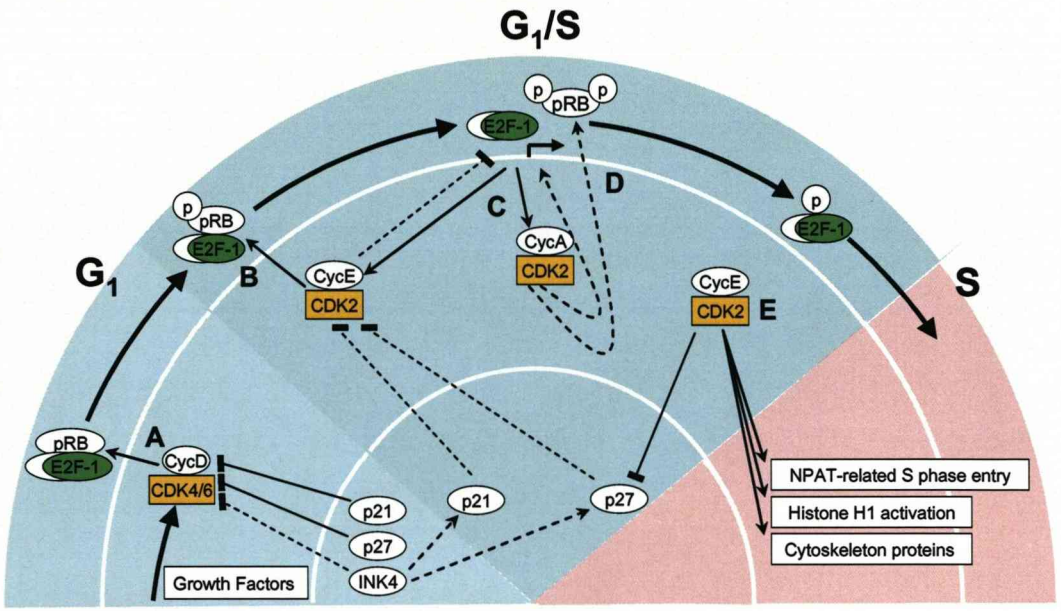

Figure 1.8 G1/S phase: Regulation of S-phase transition by E2F-1. A G1 phase - growth factors promote a rise in active CyclinD:CDK4/6, phosphorylating pRB, leading to a rise in active E2F-1. **B** Late G1 phase – hyper-phosphorylation of pRB occurs through CyclinE:CDK2 complex, levels of Cyclin D, E, A and E2F-1-3a rise due to E2F related transcription. **C** G1/S phase – Cyclin E:CDK2-mediated phosphorylation leads to degradation of E2F-1, Cyclin A may also phosphorylate E2F-1 increasing affinity for rebinding to pRB. **D** E2F-1-3a related transcription ends **E** Early S-phase Cyclin E and A complexes chaperone S-phase related processes (see text for details). Solid black lines represent direct processes, dotted lines represent indirect and delayed processes. An arrowhead represents positive regulation, a flat-head line represents repression. Large arrows mark the transition between cell cycle stages.

A further "off switch" to E2F-related transcription is the concurrent activation of predominantly repressive E2F complexes (E2Fs 4 and 5 together with their pocket protein binding partners p107 and p130, respectively) which compete for the same genetic loci as E2F-1-3a whilst bound in an inactive state to their pocket proteins (Verona *et al.* 1997; Takahashi *et al.* 2000) (Figure 1.9).

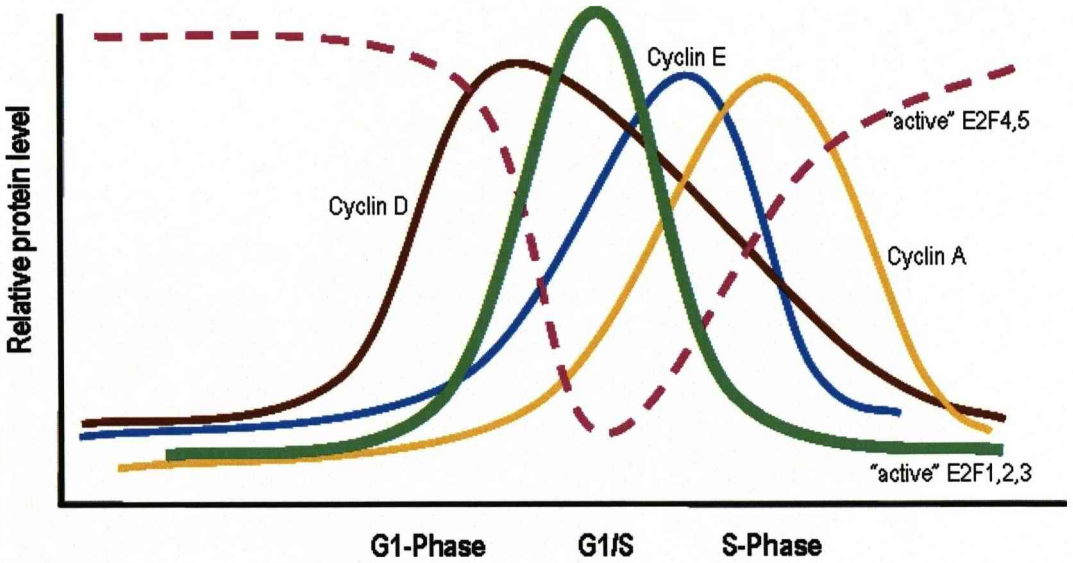

Figure 1.9 Relative levels of cell cycle proteins at G1/S phase. Showing a peak of E2F-1-3a at G1/S and the progressive decrease in active levels corresponding with a rise in E2F-4 and 5 which are transcriptionally repressive.

1.2.4 Robustness in G1/S progression

To reach the point of replicative senescence, cells must complete their life cycle many times (Mathon *et al.* 2001). As previously highlighted, the commitment to critical activities such as DNA replication is irreversible and requires well-timed transcription of large sets of genes (Bracken *et al.* 2004; Carey *et al.* 2008). The mechanisms governing this progression must therefore be accurate (i.e. timely) and repeatable. The picture of "normal" G1/S cell cycle progression outlined in Figure 1.8, although already complex, encompasses further subtle mechanisms which add to the robustness of S-phase progression.

1.2.4.1 Functional robustness

As described in Figure 1.7 E2F1, 2 and 3a share a high degree of structural and functional similarity. This allows for functional redundancy and robustness in transcriptional activity (Wu *et al.* 2001). All combinations of E2F1 E2F2 and E2F3a with transcriptional binding partners DP-1 and DP-2 have been discovered *in vivo* (Wu *et al.* 1995). Indeed, only a complete loss of all of the "activating" E2Fs is attributed to cell cycle arrest and quiescence (Attwooll *et al.* 2004). Redundancy also extends to the Cyclin:CDK complexes with three known functional proteins comprising Cyclin D (Bartkova *et al.* 1998) and two each of cyclins A and E (Murphy *et al.* 1997; Lauper *et*

al. 1998). Indeed it can be argued that the mechanisms governing G1/S progression are evolutionarily robust with many G1/S proteins highly conserved across species (Skotheim *et al.* 2008; van den Heuvel *et al.* 2008; Doonan *et al.* 2009).

1.2.4.2 Robustness arising from feedback

The cell cycle is an oscillatory system. The cycle oscillates between two checkpoints, one governing transition into DNA Replication phase (G1/S) and one into Mitosis (G2/M). Progression through these checkpoints is controlled by families of proteins which themselves oscillate in level with a period of several hours (see Figure 1.9). Individual cell cycle controlling components may also oscillate in terms of their localisation, phosphorylation status, stability and activity.

Feedback in oscillatory systems, involving direct and indirect auto-regulation of protein activity (previously introduced in Sections 1.1.5 and 1.1.9), has been shown as a source of robustness, allowing the adjustment of frequency in oscillatory systems involving coupled positive and negative feedback (Tsai *et al.* 2008). Transition from G1 to S-phase (Figure 1.8) involves multiple coupled feedback mechanisms. Progressive activation of E2F1-3a throughout late G1 requires hyper-phosphorylation of inhibitor "pocket" protein, pRB by Cyclin:Cyclin dependent kinase (CDK) complexes CyclinD:CDK4/6 and Cyclin E:CDK2 (Stanelle *et al.* 2002), both of which are under the transcriptional control of E2F1-3a (Young *et al.* 2003) and are essential for S-phase progression (Sherr *et al.* 1997) (Ohtsubo *et al.* 1995). Indeed, Cyclin E itself has been theorised to drive oscillations in E2F-1 transcriptional activity through coupled positive and negative feedback (Baguley *et al.* 2005; Yao *et al.* 2008), both contributing to hyper-phosphorylation of pRB at G1/S freeing E2F-1 (Dyson 1998) and the CDK2-mediated phosphorylation of E2F-1, marking it for proteolytic degradation (Reis *et al.* 2004). Cyclin A is also part of the E2F regulome (Assoian 1997) and builds to a threshold during early S-phase (Schulze *et al.* 1995), enabling the CyclinA:CDK2 complex to contribute to the decrease in E2F related transcription in S-phase, as outlined above (Peeper *et al.* 1995).

In addition to indirect feedback through the Cyclins, E2F is subject to direct positive and negative self-regulation. The progressive activation of E2F-1-3a is reinforced through E2F auto-transcription, with E2F-1 regulating the gene products of E2F-1,2 and 3

(Hsiao *et al.* 1994) However, E2F-1 also regulates the gene product of its inhibitor, pRB (Ishida *et al.* 2001).

In summary, the robust mechanisms at G1/S contribute to flexibility in the expression profile of the active E2F complexes, both in the rising level of E2F1-3a though multiple positive feedbacks (Cyclin:CDK activity, auto-transcription) leading up to S-phase - and hence the correct timing of target genes - but also to the abrupt termination of E2F-related transcription through multiple negative feedbacks (inhibitory E2Fs, pocket proteins, S-phase Cyclins) (profiles summarised in Figure 1.9). These coupled positive and negative feedbacks have been suggested to contribute to the role of E2F as a bi-stable switch at G1/S (Yao *et al.* 2008).

1.2.5 Sensitivity of G1/S progression

A caveat to the robust nature of cell cycle progression is that arrest is inevitable (Hayflick 1965), meaning mechanisms controlling cell cycle progression must be sensitive to arrest. At G1/S, arrest is commonly mediated by specific Cyclin:CDK inhibitors (CDIs). CDIs are predominantly grouped into two families:- INK – p15, p18, p19 and principal member p16INK4, and CIP/KIP – p21, p27 and p57 (Collins *et al.* 2003).These CDIs inactivate G1 CDK:Cyclin complexes (the INK family being specific to CDKs 4 and 6) by stably binding to the CDK in direct competition with the Cyclins (Carnero *et al.* 1998), or (in the case of the CIP family) by direct inactivation of CDK complexes (Polyak *et al.* 1994; Harper *et al.* 1995). Prior to permanent senescent arrest the cell cycle may be temporarily arrested ("delayed") at G1/S in the event of DNA damage (Pellegata *et al.* 1996; Galbiati *et al.* 2005). The regulatory mechanisms involved in normal G1/S progression (Figure 1.8) provide multiple molecular targets for stress response systems such as p53 and NF-κB.

1.2.5.1 p53 DNA damage response at G1/S – The importance of context

E2F-1 plays a crucial role in DNA damage response at G1/S via interaction with the p53 system (reviewed in (Tsantoulis *et al.* 2005; Braithwaite *et al.* 2006)). Normally the p53 tetrameric complex is bound to MDM2 and sequestered in the cytoplasm (Chen *et al.* 1995). Upon phosphorylation by p14ARF, MDM2/p53 binding is disrupted, leading to exposure of the p53 Nuclear Localisation Sequence (NLS), leaving p53 free to translocate and begin transcription of target genes, including that for MDM2 (considered in greater detail in (Prives *et al.* 1999)). The feedback between p53 and MDM2 has been shown to lead to nucleo-cytoplasmic and concentration based oscillations of the active p53 complex (Lahav *et al.* 2004).

Crosstalk between the G1/S and p53 systems may involve p53-mediated cell cycle arrest through up-regulation of target gene p21 (waf-1/cip-1) (el-Deiry *et al.* 1993), E2F-1 reinforcement of p53 through up-regulation of E2F-1 target gene p14 (Dimri *et al.* 2000) and direct binding of E2F-1 to p53 at a region which blocks the intrinsic nuclear export sequence of p53 (Sakaguchi *et al.* 1997). p53 mediation of cell cycle progression may occur through up-regulation of MDM2, ending p53-mediated transcription of p21, and releasing E2F-1 to bind to Cyclin A in a manner consistent with S-phase progression (Price *et al.* 1995).

Considered simultaneously, these interactions may appear to be contradictory as factors associated with both cell cycle arrest and proliferation are up regulated. Similar situations occur in inflammatory responses through the NF-κB system (Guttridge *et al.* 1999; Hinata *et al.* 2003). This reinforces both the importance of context to cell fate decisions and a potential flaw in reductionist approaches as confirming transcriptional control of a gene or set of genes might not be enough to determine or predict specific outcome(s). Interaction and collaboration between networks of proteins must therefore be considered in context, which may change over time. As an example a model may be constructed to describe the response to DNA damage at G1/S, describing both the p53 signalling network and G1/S checkpoint control systems.

1.2.5.2 Introducing the G1/S "balance" model

In senescent cells, DNA damage signals transduced through the RB/E2F and p53 systems result in permanent withdrawal from the cell cycle (Shay *et al.* 1991). However, in dividing cells DNA damage may require only provisional arrest of passage through the G1/S checkpoint, (Galbiati *et al.* 2005) i.e. successful resumption of the cell cycle once the damage has been repaired or, alternatively the invocation of apoptotic cascades should the damage be irreparable (considered in greater detail in (Iaquinta *et al.* 2007)). In cells with reparable DNA damage, the interactions involving E2F-1-3a and the p53 system at G1/S can be separated into those which contribute to temporary arrest, to the coordination of the p53 response to DNA damage, and to successful resumption of the cell cycle.

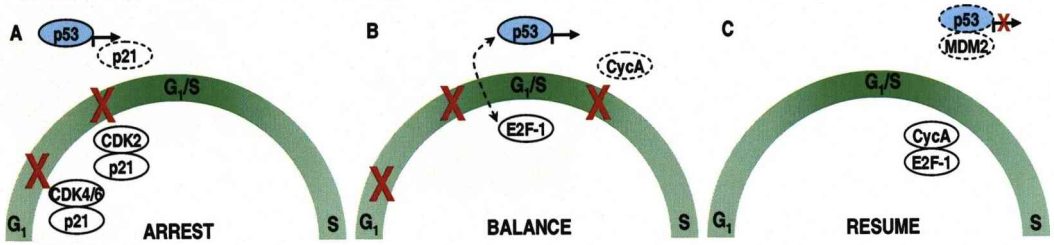

Figure 1.10 The p53:G1/S balance model: A p53-mediated cell cycle arrest through transcriptional up-regulation of CDI p21. **B** Interaction of G1/S proteins with p53 coordinating the p53 response (see text for details) **C** p53-mediated resumption of the cell cycle through up-regulation of MDM2 which ends transcription of p21 and stabilises E2F-1, and the release of Cyclin A from p53 binding to bind to E2F-1. The intensity of the green line represents the level of E2F-1 which reaches its peak at the G1/S transition. Red crosses represent cell cycle arrest at different stages.

The model in Figure 1.10 presents a scenario for p53-mediated DNA damage responses at G1/S assuming this involves temporary arrest of the cell cycle. As such, the interaction between the G1/S and p53 systems logically must provide mechanisms for both prompt cell cycle exit (to ensure genomic stability) and re-entry at the appropriate phase, hence resolving the apparent contradiction presented by both proliferative and anti-proliferative behaviour. Successful re-entry of the cell cycle prior to S-phase depends on the outcome of a period of "balance" in which G1/S proteins may coordinate p53-mediated invocation of further mechanisms associated with repair,

or indeed with apoptosis, senescence or differentiation (Tanaka *et al.* 2000), considered in greater detail in (Gatz *et al.* 2006) and (Braithwaite *et al.* 2006).

The balance model is considered in greater detail in Chapter 8, but is introduced here to provide a context for the major focus of this thesis which is to investigate a similar scenario connecting G1/S with stress responses and the NF-κB system. Interactions between NF-κB and G1/S proteins such as E2F-1 are less well characterised than those between the G1/S and p53 systems, but share common proliferative/anti-proliferative function. In order to consider interactions between E2F-1 and NF-κB in context, it is now necessary to introduce the NF-κB system in detail.

1.3 Introduction III – The NF-κB signalling system

1.3.1 NF-κB - A key oscillatory system

The NF-κB signalling system describes one of the most important stress and inflammatory response networks in mammalian cells. Activation of the system leads to down-stream expression of genes involved in a range of critical activities such as inflammation (Shakhov *et al.* 1990), and apoptosis (Schauvliege *et al.* 2002), as well as proliferation and the cell cycle (Guttridge *et al.* 1999), the latter is discussed in detail in Section 1.3.4.

The NF-κB system acts to convey an extracellular signal through cell surface receptor(s), through the cytoplasm to the nucleus via protein interactions centred around members of the Reticuloendotheliosis (Rel) and Inhibitor kappa B (IκB) families, including p65 (RelA), p50/p105, RelB, p52/p100, cRel (and its retroviral homologue vRel), IκBα, IκBβ and IκBε. The architecture of the system involves interactions between different Rel and IκB family members, several of which are under the transcriptional control of NF-κB, leading to regulatory feedbacks.

In resting, unstimulated conditions the prototypical transcriptionally active NF-κB complex, a heterodimer of p65 and p50 (often referred to simply as NF-κB) is held in a dormant cytoplasmic state by the IκB proteins. Inflammatory stimuli, for example the cytokine TNFα, induce rapid phosphorylation (within 5 minutes), ubiquitination, and proteasomal degradation of IκBα, via activation of the IκB kinase IKK (Miyamoto *et al.* 1994). The degradation of inhibitor IκBα enables free NF-κB to move to the nucleus where it can activate transcription of target genes, which include IκBα. Following protein maturation, newly synthesised IκBα binds to nuclear NF-κB removing it from the nucleus via IκBα nuclear export sequence (NES) to be sequestered in the cytoplasm, exemplifying negative feedback. In addition to IκBα, NF-κB regulates the transcription of genes coding for further inhibitory proteins, such as the IκBα homologue IκBε (Kearns *et al.* 2006) and IKK regulator A20 (Lee *et al.* 2000) (Figure 1.11).

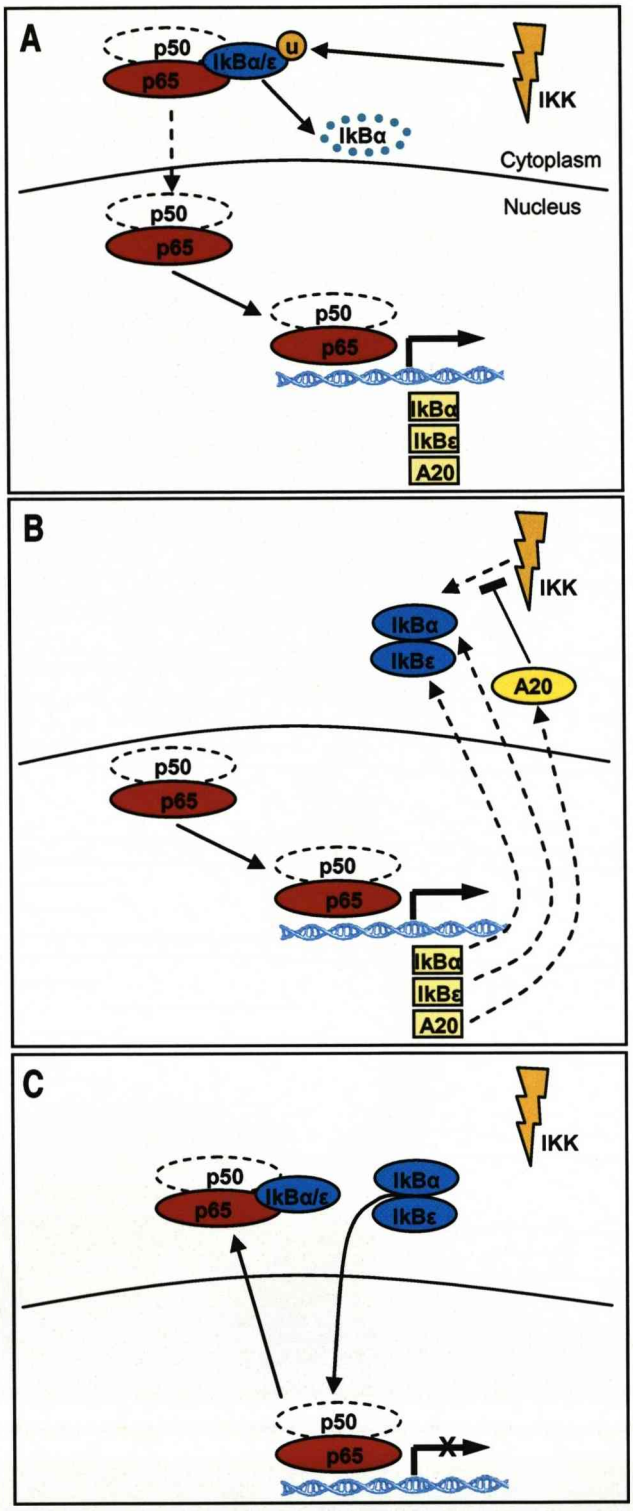

Figure 1.11 Conceptual model of the NF-κB system. A Stimulation by TNFα induces a rise in levels of IKK, which phosphorylates IκBα marking it for ubiquitination, freeing the NF-κB heterodimer and allowing it to translocate into the nucleus **B** NF-κB activates the transcription of IκB proteins and A20 which blocks their phosphorylation by IKK **C** *De-novo* IκB proteins translocate into the nucleus and "pull" NF-κB back into a dormant cytoplasmic state. The system exemplifies negative feedback.

1.3.2 Structure of NF-κB proteins

This project is primarily focussed on interaction between cell cycle regulator E2F-1, and the canonical NF-κB system, involving p65, p50 (the cleavage product of p105) and IκBα. Structures for these classical NF-κB family members are shown below (Figure 1.12). NF-κB oscillatory behaviour is driven by Nuclear Localisation and Nuclear Export Sequences (NLS and NES). Combinations of these structural motifs in proteins and protein complexes lead to a steady state localisation. This may change as the make-up of a complex changes. Crystallographic studies of the p65:p50 complex bound to IκBα revealed that IκBα binds to NF-κB in such a way that the p65 NLS is masked but the p50 NLS is left exposed leading to nucleo-cytoplasmic shuttling of the complex (Huxford *et al.* 1998; Jacobs *et al.* 1998; Malek *et al.* 2001; Malek *et al.* 2003) but a predominant "steady state" in the cytoplasm due to the combined effect of the p65 and IκBα NES (Harhaj *et al.* 1999; Johnson *et al.* 1999; Huang *et al.* 2000). TNFα-mediated degradation of IκBα is enough to alter the steady state as it both removes the contribution of the IκB NES to the complex and leads to the exposure of the p65 NLS. Re-synthesis of IκBα restores the cytoplasmic localisation, leading to nucleo-cytoplasmic oscillations in the presence of continuous TNFα stimulation. Homodimers of p50 lack transactivation domains but have a strong combined NLS leading to a largely repressive role (Zhong *et al.* 2002) p65 homodimers however, may be transcriptionally active (Chen *et al.* 2000).

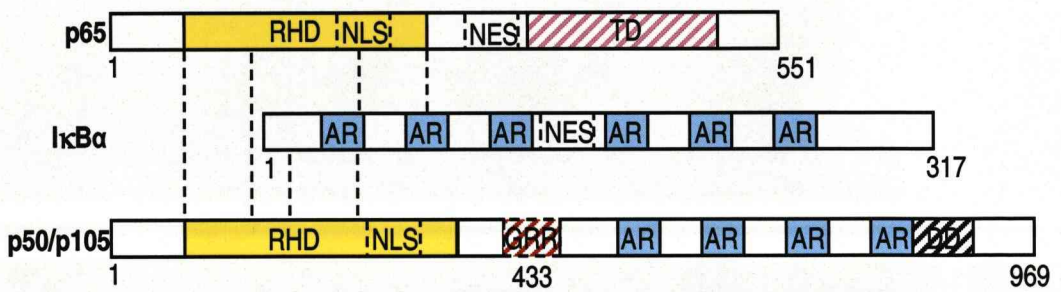

Figure 1.12 Structure of members of the classical NF-κB system. Showing p65 able to bind to both p50 (the cleavage product of p105) and IκBα leading to a predominant cytoplasmic localisation for the p65:p50:IκBα complex. Degradation of IκBα leads to removal of the IκBα NES from the complex and unmasking of the p65 NLS, leading to predominant nuclear localisation of the p65:p50 complex. TD= Transactivation Domain, AR= Ankyrin Repeats, GRR= Glycine Rich Region, DD= Death Domain.

1.3.3 Characterisation of NF-κB dynamics

Original bulk-cell studies suggested that stimulus-induced movement of NF-κB occurred as a biphasic response (Baeuerle *et al.* 1988; Hoffmann *et al.* 2002), resulting from degradation and subsequent re-synthesis of IκBα. However, recent theoretical and experimental studies focussing on single cell protein dynamics have suggested that this negative feedback leads to asynchronous nucleo-cytoplasmic oscillations in NF-κB protein localisation among single cells (Nelson *et al.* 2004). These oscillations are observed to persist for several hours, with a period of 100minutes (Nelson *et al.* 2004). Asynchrony in the timing of the oscillations, makes them undetectable at the population level even though they are readily observable in single cells subject to time lapse imaging, discussed in Chapter 5 and (Ankers *et al.* 2008).

In single cell studies, time-lapse imaging of p65-dsRedXP has been used as a quantifiable output of the NF-κB system, representative of the dynamics of the p65:p50 NF-κB complex (Nelson *et al.* 2004). The effects of different experimental conditions on TNFα-mediated dynamics of the NF-κB system for the work presented in Chapters 4-7, were assessed by analysing p65-dsRedXP dynamic traces in detail (Figure 1.13, movie M1.13 on accompanying DVD). The Maximum Nuclear Localisation (MNL) Time of NF-κB was defined as the time taken to reach the peak of nuclear occupancy from a predominant cytoplasmic state. The Nuclear Retention (NR) time of NF-κB was defined as the time taken to reach a predominant cytoplasmic state following MNL. Correspondingly, peak width is equal to MNL+NR. In experiments involving persistent oscillations, the second Maximum Nuclear Localisation time (MNL2) is defined as the time taken to reach a steady oscillatory state from the point of post-peak1 predominant cytoplasmic localisation. Throughout this thesis these calculations are made from Nuclear:Cytoplasmic ratio or nuclear fluorescence trajectories, over time.

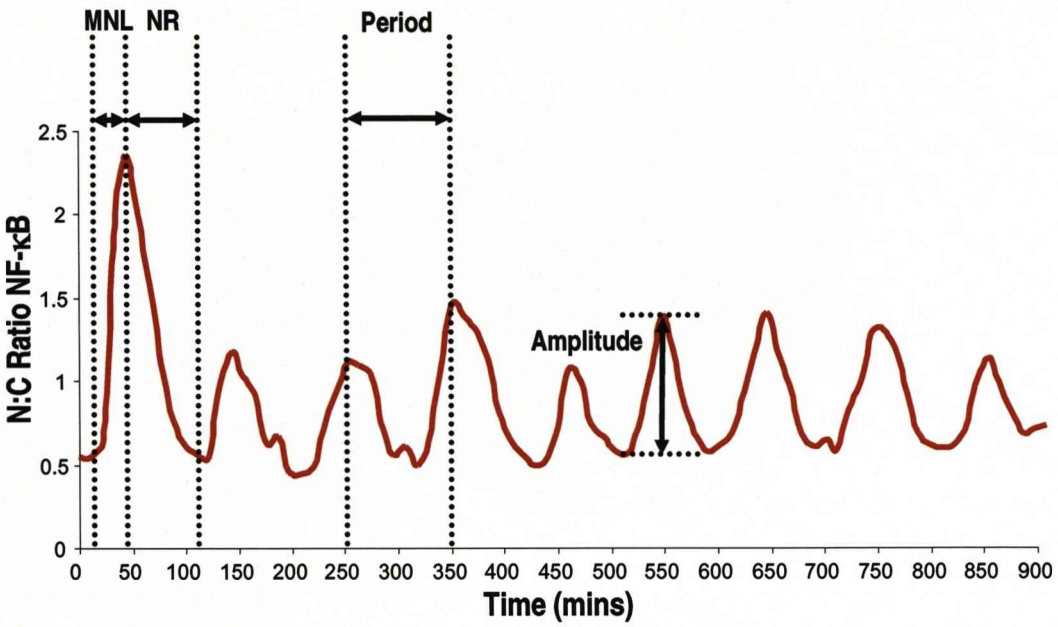

Figure 1.13 Dynamics of p65-dsRedXP - a quantifiable output of the NF-κB system. N:C ratio is taken from a time lapse image series images every 3 minutes analysed by Cell Tracker software (Section 2.2.5) Showing a Maximum Nuclear Localisation (MNL) time of 30 minutes after TNFα stimulation. A nuclear retention (NR) time of 50 minutes follows. The steady state oscillatory period is roughly 100 minutes from peak to peak. This figure shows a representative SK-N-AS cell stimulated at t=10 minutes with 10ng/ml TNFα.

1.3.4 Thesis context: Crosstalk between NF-κB and G1/S of the cell cycle

As previously highlighted, NF-κB may interact with a large number of other signalling systems, such as the Glucocorticoid Receptor system (Nelson *et al.* 2003) and the p53 system (Webster *et al.* 1999) to give rise to markedly different physiological events. Such prevalence again highlights the importance of context when considering the influence of NF-κB on cell fate. Similarly to p53, NF-κB has also been shown to have both proliferative and anti-proliferative roles at G1/S phase of the cell cycle, (Guttridge *et al.* 1999; Hinata *et al.* 2003).

Throughout G1, cell cycle arrest may be mediated by the NF-κB system in several ways. Cyclin D may be targeted for degradation as a result of phosphorylation by IKK (Kwak *et al.* 2005) with IκBα shown to inhibit Cyclin D substrate CDK4 in certain contexts (Li *et al.* 2003). Activity of the Cyclin D:CDK4 complex may be further inhibited by NF-κB-mediated transcription of CDK inhibitor p21 (Hinata *et al.* 2003). Through transcription of p21, NF-κB also plays a role in cell cycle arrest from late G1 through to early S-phase through inhibition of Cyclin E:CDK2 activity, which is further targeted by direct binding between Cyclin E and NF-κB family member c-Rel (Eying Chen 1998).

Proliferative activity attributed to NF-κB is also contextually linked to G1/S. Interestingly, given the relationships described above, Cyclin D is a well characterised NF-κB target gene (Guttridge *et al.* 1999). Furthermore, IKK, previously described as an inhibitor of Cyclin D, has been attributed to promotion of Cyclin D activity in certain contexts (Lamberti *et al.* 2001; Albanese *et al.* 2003). In addition, the expression of IκBα which has been shown to stabilise G1 progression through stabilisation of E2F-1 in breast cancer (Tu *et al.* 2006).

Similar to relationships between the p53 and G1/S systems, the interactions between NF-κB and G1/S proteins present apparent contradiction when considered simultaneously. However, considering an inflammatory response within the scenario of progression from G1 into S-phase, we may suggest a model similar to that for DNA damage response at G1/S (Figure 1.10), which takes into account all of the relationships outlined above. The NF-κB:G1/S balance model (Figure 1.14) assumes an NF-κB response at G1/S involves temporary cell cycle arrest, allowing a response

to occur prior to S-phase entry. Logically, this model requires mechanisms for cell cycle resumption, to allow the cell to resume its S-phase related activity at a later stage. Successful re-entry of the cell cycle prior to S-phase depends on the outcome of a period of "balance" which involves the coordination of the NF-κB response by G1/S proteins. Previous work has suggested the promotion of certain genes requires both E2F-1 and p65 to be bound to promoter regions (Lim *et al.* 2007), but intriguingly also to suggest that E2F-1 and p50 (the binding partner of p65) interact to repress certain target genes (Kundu *et al.* 1997). An exemplary recent study has also suggested cell cycle phase-dependant regulation of NF-κB subunits, concomitantly controlling the expression of NF-κB related cell cycle genes (Barre *et al.* 2007), complimenting the presented model for an NF-κB response at G1/S.

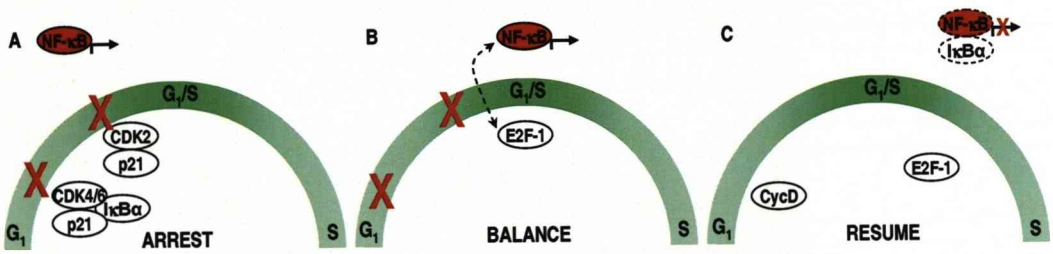

Figure 1.14 The NF-κB:G1/S "balance" model: A NF-κB-mediated cell cycle arrest through transcriptional up-regulation of p21. **B** Balance phase involving coordination of the NF-κB response by G1/S proteins. **C** Cell cycle resumption through transcription of IκBα which terminates transcription of p21, and Cyclin D which is required for G1/S progression.

1.4 Project Aims – A Systems Biology framework

This project aims to take a Systems Biology approach towards characterising an NF-κB response at G1/S phase of the mammalian cell cycle. The central hypothesis of this work is that E2F-1 takes a temporal role in the control of NF-κB signalling dynamics in a similar manner to its role in p53 signalling.

Towards resolving this hypothesis, it is first intended to characterise interaction between E2F-1, and the NF-κB dimer (p65:p50) experimentally, within the context of the NF-κB system. Subsequently, it is intended to extend a mathematical model for the NF-κB system to include a module for interaction with E2F-1, in a manner consistent with the step-wise model expansion detailed in Figure 1.1 A#, and to use this model to make experimentally resolvable predictions for the behaviour of the NF-κB system in the presence of E2F-1.This approach will be reviewed at intermediate stages to consider the significance of any data both in terms of Systems Biology and physiological context.

Work contributing to this thesis is considered in four stages:

1. Experimental work designed to provide a foundation for both conceptual and mathematical models depicting interaction between E2F-1 and the NF-κB system.
2. Theoretical work implementing a mathematical model for NF-κB:E2F-1 that is able to make non-intuitive predictions for the role of the interaction within the context of the NF-κB system.
3. Subsequent experimental resolution of dynamic model predications.
4. Work towards extending this model to the context of G1/S and cell cycle progression (Figure 1.1 B), and to consider the reciprocal relationship of NF-κB on E2F-1 signalling.

Recalling the requirements of dynamic Systems Biology (Section 1.1.3), the biological *context* to this approach is provided by the NF-κB system in the first instance. The *predictive* ability stems from a mathematical model of the NF-κB extended to include E2F-1 and experimental *resolution* may proceed via biological and experimental model systems outlined in Sections 1.1.4 and 1.1.5. With these aims defined, we begin by providing an experimental foundation for the NF-κB:E2F-1 model.

Chapter 2 -
Materials & Methods

2.1 Materials

2.1.1 Reagents

Tissue culture medium and non-essential amino acids were purchased from Gibco Life Technologies (UK) and Foetal Bovine Serum (FBS) from Harlan Seralab (UK). Human recombinant TNFα was supplied by Calbiochem (UK). All other chemicals were supplied by Sigma-Aldrich (UK) unless stated otherwise. Oligodeoxynucleotides were purchased from Invitrogen (UK).

2.1.2 Plasmids

The expression vectors pCMV-E2F-1, pCMV-E2F-2 and pCMV-E2F-3 were kindly supplied by Emmanuelle Trinh (BRIC, Copenhagen), and genes excised for use with Invitrogen's Gateway cloning system (see Section 3.1). Luciferase reporter vector CyclinE-luc was obtained from Peggy Farnham (University of Wisconsin-Madison,USA) p65-DsRed-XP, IκBα-EGFP, IκBα-AmCyan, NF-luc (Clontech), have been described previously (Nelson *et al.* 2002).

2.2 Methods

2.2.1 Molecular Biology

2.2.1.1 Transformation of competent cells

Employed to integrate "foreign" plasmid DNA into competent bacterial cells as a purcusor step to large-scale DNA preperation.

Competent cells were previously produced in the laboratory using the DH5α or Db3.1 Escherichia coli (E.coli) strain. 1 μg of plasmid was incubated on ice for 45 min with 50 μl of cells and subsequently heat shocked at 42˚C for 1 min. Heat-shocked cells were then returned to ice for a further 2 min, before being rescued by addition of 800 μl of "Rescue media" (LB Broth, 20 mM glucose). The cells were then incubated at 37˚C with shaking (~250 rpm) for 1 h. Cells were then pelleted by centrifugation at 4000rpm for 2 min and resuspended in 40μl of media. This was then plated onto selective LB agar (100 g/ml kanamycin or Ampicilin) and incubated overnight at 37˚C.

2.2.1.2 Amplification of plasmid DNA (Maxiprep)

Employed to provide a good quality working stock of plasmid DNA. Typically yielding up to 300μl of DNA at a concentration >1μg/μl.

Plasmid DNA was amplified from transformed *E.coli* DH5α or DB3.1 cells that were cultured overnight in 250ml of selective LB broth using the QIAfilter Plasmid Maxi Kit (Qiagen, Germany) according to manufacturer's instructions. Plasmid DNA was quantified using a UV-1601 UV-Visible spectrophotometer (Shimadzu, Japan). The absorbance was measured at 260 and 280 nm using monochromatic light. All expression vectors were of sufficient purity with a A_{260}/A_{280} ratio between 1.8-1.9 for transfection into cells.

2.2.1.3 Agarose gel electrophoresis and gel extraction

Employed to separate DNA fragments from reaction mixtures post-restriction digest, both in order to extract an purify specific bands or carry out diagnostic restriction tests on DNA samples.

DNA fragments were separated by 1% (w/v) Agarose gel electrophoresis using 1x TAE buffer (Tris-acetate-EDTA: For a 50x solution – 242g Tris base, 57.1ml glacial acetic acid, 100ml 0.5M EDTA (pH 8.0)). Restriction-digested DNA samples were combined

with 1/5 volume 6x Orange G loading dye solution (0.35% (w/v) Orange G; 30% (w/v) sucrose) and ran alongside a 1kb Plus DNA Ladder (Invitrogen) at 80mA for 1.5 h.
Gels were visualised under 302nm (UV) light using a trans-illuminator and imaged using the Syngene G-Box gel imaging system (Syngene, UK). Selected DNA fragments were cut from the gel with a scalpel blade and purified using the QIAquick Gel Extraction Kit (Qiagen). In this protocol, Agarose is dissolved to release the DNA, which is then bound to an anion-exchange membrane as used in plasmid preparation kits. Purified DNA fragment is then eluted in 30µl TE.

2.2.1.4 Restriction endonuclease digestion

Employed to cut DNA samples (usually from plasmid DNA for this work) into pieces of desired size, for either diagnostic checks or as part of molecular cloning procedures.
For complete digestion, in a 20µl reaction volume, 5µg of DNA was incubated with the appropriate restriction enzyme (RE) (3U/µg DNA) in 1x RE buffer (supplied) for 3h at the appropriate temperature (usually 37°C). If two REs were used simultaneously (double digest), 3U of each RE was used per µg DNA. DNA from the reaction was then purified with the QIAquick Gel Extraction Kit (Qiagen) or modified further as below. For diagnostic digestion of 0.5-1.0µg of plasmid DNA where partial digestion was preferred, less RE was used per reaction(<1U/µg DNA) and the incubation time was reduced to 1-1.5 h.

2.2.1.5 Blunting 5'- and 3'- DNA overhangs

Employed to allow greater flexibility in RE digestion and subsequent cloning steps.
At the end of the 3h RE digest, polishing of 5'-overhangs and filling-in of 3'-overhangs was performed by adding T4 DNA Polymerase (1U/µg) and 100µM dNTPs (final concentration) to the reaction mixture and incubating for a further 15min at room temperature. T4 DNA Polymerase works in any RE buffer when supplemented with dNTPs. The DNA in this reaction was then cleaned up with the QIAquick Gel Extraction Kit (Qiagen) or separated by electrophoresis on an agarose gel

2.2.1.6 5'-Phosphate removal

Employed to prevent self-ligation in post-digest cloning reactions.

5'-phosphates were removed from RE-digested vector backbones. This was achieved by incubation with 1U/µg DNA of Shrimp Alkaline Phosphatase (SAP) (Promega, UK) for the final 15min of the RE digest. SAP is also active in RE buffers. Alternatively, SAP was incubated for 15min at 37°C in a 1x concentration of its own reaction buffer along with target DNA at 1U SAP per µg DNA. DNA was then purified by QIAquick Gel Extraction Kit (Qiagen) or separated on an agarose gel and used in ligation reactions.

2.2.1.7 DNA ligation

Employed to join together DNA fragments, usually involving a plasmid vector "backbone" and an insert purified after RE digest.

T4 DNA ligase (Invitrogen) was used to promote the formation of circular plasmids from two complementary pieces of linear DNA formed through some or all of the reactions described above. For the ligation of two fragments of DNA, an appropriate amount of insert and vector DNA was used. A 3:1 molar ratio of insert:vector gave efficient ligation. To calculate the amount of each, the following equation was used:

Vec/Ins (ng/µl) X Ins/Vec (kb) = µl Insert per µl Vector that gives a 1:1 ratio.

The final figure was multiplied by 3 to achieve the 3:1 ratio. (In practice a range of ratios were chosen typically 3:1, 5:1 and 10:2). Depending on whether the DNA fragments had cohesive or blunt ends, the reaction conditions were altered but the volume of reaction mixture was kept constant. Cohesive "Sticky"-ended ligations were performed with a maximum of 0.1µg DNA, 0.5U T4 DNA ligase and incubated at 25°C for 3h. Non-cohesive "blunt"-ended ligations were found to work best with a maximum of 1.0µg total DNA, 1U T4 DNA ligase and were incubated at 14°C for 20h. 2-4µl of the ligation reaction was then transformed into competent *E. coli* cells. Transformants were selected by their antibiotic resistance, plasmid DNA was purified, prior to diagnostic restriction digests and agarose gel electrophoresis.

2.2.1.8 DNA sequencing

Employed to compare desired DNA sequences to actual physical samples.

Automated DNA sequencing was carried out by The Sequencing Service, University of Dundee, UK (www.DNASEQ.co.uk). Sufficient DNA for two sequencing reactions were prepared for each sample, which consisted of the following: 500ng template DNA, 6.4µM sequencing primer, made up to 32µl with TE. The theoretical melting temperature (Tm) of the sequencing primers were all designed to be approximately 55°C and their Guanine/Cytosine content was constrained within a range of 40-60%. Sequence analysis was performed with MegAlign software (DNA Star) along with NCBI BLAST searches.

2.2.2 Cell culture

2.2.2.1 Subculturing cells

SK-N-AS (ECACC No. 94092302) and HeLa cells were cultured as a monolayer and grown in Minimal Essential Medium (MEM) with Earle's salts, supplemented with 10% (v/v) Foetal Bovine Serum (FBS) and maintained at 37ºC with 5% CO_2 in a humidified incubator (Sanyo, Japan). Cells (~10-25%) were passaged when the monolayer reached 80% confluency in a 75 cm^3 tissue culture flask (Corning, UK) in a final volume of 20 ml. Cells were washed with Mg^{2+}/Ca^{2+} free Phosphate Buffered Saline (PBS) then incubated with 1 ml of 0.05% (w/v) trypsin in 0.53 mM EDTA / PBS (Gibco,UK) to detach the monolayer from the flask. Cells were resuspended in 9 ml of medium and centrifuged in an Eppendorf Centrifuge 5804 (Eppendorf, UK) at 1000 rpm for 5 min to remove the trypsin and cell debris. The supernatant was discarded and the cell pellet resuspended in 10 ml of fresh gassed medium. A sample from the cell suspension was counted using a Z2 Coulter counter (Coulter, UK), and the remaining cells were diluted in medium and seeded as required. Different seeding densities were used for each type of experiment as shown in Table 2.1. For most applications, seeding was optimised to give a 60% confluency 24 h post-transfection.

Dish size	Cell no. SK-N-AS	Cell no. HeLa	Example Application
16mm	6 x10^4	-	Luciferase Reporter As.
35mm	16x10^4	6x10^4	Live cell imaging
60mm	50x10^4	20x10^4	Immuno-blot, Q-PCR
100mm	200x10^4	80x10^4	Co-IP

Table 2.1 Numbers of HeLa and SK-N-AS cells seeded for different applications: The number of cells seeded depended on the size of the dish, the cell type, the duration of the experiment and the number of cells required to perform the assay.

2.2.2.2 Transient transfection

Employed to introduce plasmid DNA into host cells for the purpose of exogenous expression.

Cells were transfected at 60% confluency (usually 24 h after seeding) with the appropriate plasmid(s) using Fugene 6 (Roche Diagnostics, Germany) according to the manufacturer's protocol. The optimum Fugene 6:DNA ratio was 2:1 and 4:2 for SK-N-AS and HeLa cells respectively. For all experiments involving transient transfection, cells were seeded to ensure a 60-70% confluency at time of transfection.

2.2.2.3 Cell cycle synchronisation

Employed to synchronise populations of HeLa cells in early S-phase (G1/S)

Thymidine was used to block cells at the G1/S boundary. It acts primarily through altering the balance of the deoxy-triphosphate base building blocks, which inhibits DNA replication. Growth inhibition by the addition Thymidine to the culture medium was also shown to involve feedback involving several other Pyrimidine biosynthetic enzymes (Bjursell *et al.* 1973; Kufe *et al.* 1980; Whitfield *et al.* 2000). The Double Thymidine Block protocol (adapted from (Whitfield *et al.* 2000)) was found to be most suitable for synchronising HeLa cell cultures. HeLa cells were seeded on Day 1 according to densities described in Figure 2.1. Following a 24 hour incubation period, Thymidine (Sigma,UK) was added to the culture medium to a final concentration of 2mM. 19 h later the Thymidine was removed from the cells using 3 PBS sequental washing steps and fresh MEM was added to the cells. Cells were transfected at thistime as required using the methods described above (2.2.2.2.). Following a 9 h incubation, Thymidine

was again added to the culture medium to a final concentration of 2mM, Following a further 16 h incubation, the cells were successfully synchronised at G1/S as confirmed by flow cytometric DNA analysis (Chapter 7). Cells were then washed 3 times with PBS, and fresh medium was added to release the cell cycle block. The cells were subsequently analysed by live cell imaging (Section 2.2.3.1), immuno-blot (Section 2.2.4.3) or Q-PCR (section 2.2.4.6) at the appropriate time after release from the cell cycle block. The time at which the majority of cells were at each stage of the cell cycle was estimated using flow cytyometic DNA analysis. (see Chapter 7)

2.2.2.4 TNFα stimulation

Employed to stimulate the NF-κB pathway through induction of IKK activity. Stimulation with human inflammatory cytokine TNFα proceeded as a saturated dose of 10ng/ml. Stimulation timing varies between experimental techniques as indicated. Cells were stimulated with a saturating dose of 10ng/ml human recombinant TNFα (Sigma, UK) at the indicated times prior to analysis.

2.2.3 Single cell techniques

2.2.3.1 Live cell fluorescence imaging

Employed to measure levels of transiently transfected fluorescent fusion proteins over time in single living cells, giving quantifiable data relating to localisation and stability.

Imaging of transfection cells (as indicated) proceeded 24 h post-transfection with a Zeiss LSM510 confocal microscope using AIM version 3.2 software. Prior to imaging, cells were incubated on the microscope stage for 30 min at 37°C, 5% CO_2. EGFP fusion proteins were excited using the minimum amount of 488nm light from an Argon ion laser. Fluorescent signals were collected with a 545nm dichroic mirror through a 505-550nm band-pass filter. Similarly, dsRedXP fluorescence was excited with a 543nm Helium Neon laser and collected with a 545nm dichroic mirror and a 560nm long-pass filter. In all cases a transmission image was collected at the same time as the fluorescent image(s). Stimulation with TNFα, where applicable, normally occurred after an initial period of time lapse imaging. For imaging experiments involving synchronised cells (double Thymidine block method, as above) TNFα stimulation proceeded after release from Thymidine, prior to desired cell cycle time points (as indicated).

2.2.3.2 Förster (Fluorescence) Resonance Energy Transfer (FRET) imaging

Employed to provide evidence of a physical interaction between two proteins in-vivo

FRET involves the transfer of non-radiant energy between two fluorophores with overlapping donor emission and acceptor excitation spectra (typically Cyan and Yellow Fluorescent proteins; ECFP and EYFP (Karpova *et al.* 2003)) each "tagged" to one terminus of a protein of interest. Using the Acceptor Photo-bleaching method, increases in the levels of donor protein fluorescence are observed if the two proteins are close enough (~8nm) together to cause FRET and energy is no longer transferred to the acceptor and is therefore emitted as light (at the donor emission wavelengths).

FRET was carried out using a Zeiss LSM510 with "META" spectral detector mounted on a Axiovert 100S microscope with a Plan-Apochromat 63x, 1.4 NA oil-immersion objective (Zeiss). ECFP and EYFP were excited with 458nm laser light, emitted fluorescence was collected in 8 images each separated by 10nm between 467nm and 638nm in lambda scanning mode. Separation of ECFP and EYFP fluorescence was carried out using the linear unmixing algorithms of the Zeiss LSM510 software (Zeiss). using reference spectra taken from cells expressing the ECFP or EYFP fusion proteins alone or nothing (background reference). The fluorescence spectrum was separated into ECFP, EYFP and background signals. FRET was assayed by acceptor (EYFP) photo-bleaching. Bleaching was accomplished using 50 iterations of 514nm laser light with no attenuation from the acousto-optical tuneable filter (AOTF).

2.2.4 Bulk cell techniques

2.2.4.1 Flow cytometric DNA analysis

Employed to determine the subsets of populations of HeLa cells at different cell cycle phases.

Following synchronisation, HeLa cells cultured in 100mm^2 dishes were detached as a single cell suspension with 900µl trypsin. The cells were stained by addition of 250µl of 50 µg/ml propidium iodide, 0.15% TritonX-100, and 150 µg/ml RNase A before analysis in an Altra flow cytometer (Beckman Coulter).

2.2.4.2 *Luciferase reporter assays*

Employed to determine the relative transcriptional activity for a given condition by assaying an enzymatic reaction between luciferin and the luciferase protein product from a transiently transfected luciferase reporter construct with a specific promoter.

Cells (as indicated) were seeded into 16mm wells of 24-well plates and transfected after 24 h with an appropriate luciferase reporter construct, with or without additional expression vectors. After an appropriate period of incubation, media was poured off, cells were rinsed with Ca^{2+}-free PBS, and 250µl of lysis buffer added (0.025% (w/v) dithiothreitol (DTT), 1% (w/v) bovine serum albumin (BSA), 25mM Tris-phosphate, 1% Triton X-100, 15% (v/v) glycerol, 0.1mM EDTA, 8mM $MgCl_2$) (White *et al.* 1990). Lysis was aided by agitation at room temperature and supplemented with 1mM ATP (final concentration). 100µl lysate was transferred in duplicate to an opaque 96-well plate (Greiner ,UK). Luminescence was measured using a LUMIstar plate reading luminometer (BMG, Germany). 100µl 2mM D-luciferin (Biosynth AG, Switzerland) was added to each well and photons counted and integrated over 5 sec. Luminescence from each lysate duplicate was averaged and exported to Excel for data analysis.

2.2.4.3 Immuno-blotting

Employed as a semi-quantitative measure of protein levels across a cell population.

SK-N-AS and HeLa cells were seeded into 60mm dishes (Iwaki, Japan), incubated for 24 h and subjected to experimental conditions (transfection, TNFα stimulation etc.). Cells were lysed in 200µl of a lysis buffer consisting of 40mM Tris-HCl, pH6.8, 1% w/v SDS, 1%v/v glycerol, 1% v/v β-mercaptoethanol and 0.01% w/v bromophenol blue. Samples were boiled for 10 min to reduce viscosity and eliminate protease activity and 20µl of each was loaded onto a 10% SDS-PAGE gel. Electrophoresis and blotting was carried out using the Bio-Rad Protean II apparatus (Bio-Rad, UK) according to the manufacturer's instructions. Detection of the proteins was carried out using the appropriate primary and secondary antibodies as per manufacturer's instructions (Cell Signalling, USA, Santa Cruz, USA, UpState, USA, see below). Nitrocellulose membranes were incubated in ECL reagent, (100mM Tris HCl pH8.5, 0.001% H_2O_2, 1.25mM luminol, 0.2mM para-coumaric acid made up to 10ml per membrane with H_20) for 1 minute. Membranes were then either exposed to photographic film (Pierce CL-Xposure, England) or imaged in real time with the Syngene G-Box gel imaging system (Syngene UK) to visualize protein bands on the membranes. Primary antibodies used for this study are described in Table 2.2.

Probe	Source	Typical dilution	Species/ Type	Application
p65 (65kDa)	Cell Signalling, Cat no. 3034	1:1000	Rabbit Polyclonal	Immuno-blot
p50 (50kDa)	Cell Signalling, 3035	1:1000	Rabbit Polyclonal	Immuno-blot
IκBα (38kDa)	Cell Signalling, 9242	1:1000	Rabbit Polyclonal	Immuno-blot
E2F-1 (55kDa)	Upstate, KH95	1:1000	Mouse Monoclonal	Co-IP, Immuno
CycloA (18kDa)	Cell Signalling, 2175	1:1000	Rabbit Polyclonal	Immuno-blot

Table 2.2 Details of primary anti-bodies used in this study.

2.2.4.4 Co-ImmunoPrecipitation (Co-IP)

Employed to assess physical binding between proteins across a cell population.

The general principle of Co-IP is that it is possible to indentify unknown or predicted species in a protein complex by specific antibody targeting of a known member of a complex. Firstly, an antibody against a target protein is coupled to Sepharose beads through protein A or G, then the complexes containing the target protein are immunoprecipitated ("pulled-down") with the antibody-coupled beads. Protein species in the complexes are subsequently investigated by immuno-blotting using specific antibodies.

SK-N-AS and HeLa Cell lysates were prepared using combinations of the above techniques, typically involving either synchronisation or transfection of cells seeded at appropriate density into 100mm dishes. After 3 PBS washes, lysis proceeded using 500µl of specific buffer (20mM Tris-HCl, 250mM NaCl, 3mM EDTA, 2mM EGTA, 0.5% Triton (x100)) to which was added a 1:100 dilution of Protease Inhibitor cocktail (Roche, UK). Lysates were then scraped into 1.5ml microfuge tubes and placed onto an orbital rocker for 15 min at 4 °C, samples were then centrifuged at 14,000 rpm for 15 min, maintaining the 4 °C temperature. In between lysate preparatory steps, quantities of Agarose A/G beads were prepared (Pierce,UK) for each lysate. This involved washing 30-50µl of beads in 5x 1ml PBS, pulsing the bead samples at 8,000 rpm for 30 sec after each wash. After removal of as much supernatant as possible from the beads, the supernatant from the Co-IP lysates were added to bead samples and placed on an orbital rocker for 1 hour at 4 °C. The supernatant from these samples were then incubated with specific antibodies overnight on an orbital rocker at 4 °C. The following day, similar amounts of A/G beads were prepared, and added to the lystate/antibody samples. After a further 2 hour incubation on an orbital rocker at 4 °C, the beads should in theory be bound to protein complexes in which a target protein is bound. These samples were subjected to a 5x PBS wash and then resuspended in an equal volume of 2x immuno-blot lysis buffer (see Section 2.2.4.3). Samples were then boiled to detach proteins from beads and probed for proteins of interest via immuno-blot.

2.2.4.5 Immuno-cytochemistry (ICC)

Employed to visualise the localisation of endogenous protein or proteins

SK-N-AS and HeLa Cells were prepared using combinations of the above techniques, typically involving synchronisation and/or TNFα stimulation of cells seeded at appropriate density into 35mm glass-bottomed dishes (see Table 2.1). Dishes were subsequently washed three times with PBS and fixed with 1ml 4% Paraformaldehyde for 15 min. Dishes were then washed three times with PBS, and "blocked" to prevent non-specific antibody binding with the addition of 1-2ml of 1% BSA, 0.1% Triton X-100 (in PBS) from 20 min up to overnight.

The primary antibody (or antibodies for dual-staining) dissolved in 1% BSA,0.1% Triton X-100 -PBS were added to the dishes for 60/90 min at a 1:2000 dilution. Dishes were then subjected to 3 1ml washes of 1% BSA,0.1% Triton X-100 -PBS of 10 min length. Secondary Antibody(s) were subsequently added to dishes (Cy3-anti-mouse, 1:200 dilution (Sigma), FITC Rabbit, 1:200 (AbCam)) for 30/45 min, prior to 3 sequential washes of PBS blocking buffer (described above). Subsequent to the addition of light-sensitive secondary antibodies, dishes were covered in aluminium foil and left in 2ml PBS prior to imaging.

2.2.4.6 Quantitative RT-PCR

Employed to quantify transcript levels for specific genes upon conversion of mRNA to cDNA.

The RNeasy Mini Kit (Qiagen, Germany) was used to extract mRNA from SK-N-AS and HeLa cells previously seeded into 60mm dishes. Cells were washed with ice cold PBS prior to lysis, then 600µl of buffer RLT containing β-Mercaptoethanol (1 % (v/v)) was added. The lysed cells were scraped and the lysate homogenised by passing through a 20-gauge needle (0.9 mm diameter) approximately 10 times to mechanically cleave long strands of genomic DNA that may reduce the efficiency of mRNA extraction. The 'Spin Protocol' was then used to extract the mRNA, which was eluted into 30 µl of RNase free water and stored at -80°C. The mRNA concentration and purity was quantified using a UV-1601 UV-Visible spectrophotometer (Shimadzu, Japan). The absorbance was measured at 260 and 280 nm monochromatic light. All mRNA were of

sufficient purity with a A_{260}/A_{280} ratio between 1.9-2.1 used in the reverse transcriptase reaction.

The VILO reverse transcription kit (Invitrogen, UK) was used for the production of cDNA. For each sample, 1 µg of mRNA was used. The cDNA was diluted 1:1 with RNase free H_2O. In each reaction 1 µl of cDNA was incubated with 300 nM of each primer: IκBα left TGGTGTCCTTGGGTGCTGAT right GGCAGTCCGGCCATTACA, IκBε left GGACCCTGAAACACCGTTGT right CCCCAGTGGCTCAGTTCAGA, E2F-1 left TGCAGAGCAGATGGTTATGG right TATGGTGGCAGAGTCAGTGG, cyclophilin A left GCTTTGGGTCCAGGAATG right GTTGTCCACAGTCAGCAATGGT, 1 x Power SYBR Green PCR mastermix (Applied Biosystems) with RNase free H_2O added to a total volume of 20 µl. The cycling parameters are as follows: initial denaturation at 95 °C for 20 sec, followed by 95 °C for 3 sec (45 cycles) followed by 95 °C for 15 sec, 60 °C (2 cycles), carried out on an ABI7500 Fast thermocycler. The efficiency of the primers was tested, which gave a slope value of ~ -3.13 and R^2 value of 0.99. Relative quantification was used to calculate the fold difference based on the threshold cycle (CT) value for each PCR reaction using $2^{-\Delta\Delta CT}$ method. The target gene was normalised to the reference gene cyclophilin A, with calibrator as indicated.

2.2.5 Analytical tools and databases

The live-cell time lapse imaging data sets were analysed using Cell Tracker, a program specifically developed for use with such data (Shen *et al.* 2006). Analysed data was then exported to Excel (Microsoft, USA) for further analysis. Imaging and experimental Meta data and tags to high-throughput imaging data (typical imaging files are between 4-6Gb in size) were managed using a custom database designed for the purpose (Jameson *et al.* 2008).

2.3 Theoretical work

2.3.1 Mathematical modelling

All modelling work was implemented using MatLab Release 14 (MathsWorks,USA), and solved using MATLAB function ODE15s. Analysis of simulated time course data was performed in both Microsoft Excel and MATLAB. Model ODEs are described in Chapters 5 and 6, and all MatLab code is included on the accompanying DVD.

Model simulation protocols were designed to approximate transient transfection experiments. Typical modelling experiments involved two concurrent simulations (Figure 2.1). The first involved initialisation of model species representing IKK and cytoplasmic IκBα:NF-κB (model species *IkBaNFkB*), to 0.1 μM, in order to achieve a "steady-state" equilibrium for the NF-κB system. The model was then recapitulated using the initial conditions provided by the steady-state to provide a stage on which to simulate "transfection". This involved a Heaviside function "step" in the levels of cytoplasmic NF-κB (*NFkB*) and/or E2F-1 (*E2F*), as desired. Concentrations of involved species were supplemented with an additional 0.1μM (at T=1000 in Figure 2.1). Stimulation of the NF-κB system was simulated by activation of TNFα signal (*TR*), represented as a binary switch.

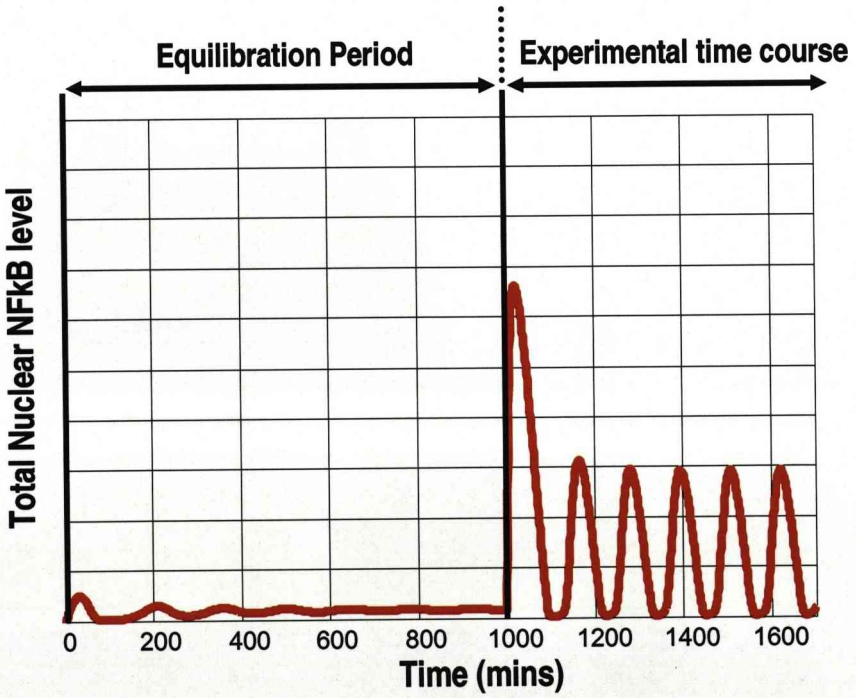

Figure 2.1 A typical model simulation protocol: Involving transfection and stimulation (at T=1000) simulated from a steady state (see text for details).

Specific strategies for modelling are discussed at length in Chapters 5 and 6. Full lists of initial conditions for pre- and post- equilibration are shown in Table 3.1.

Species	Initial Conditions pre- Equilibration (μM)	Initial Conditions post- Equilibration (μM)
NFkB	*0*	*0.004 (+0.1)*
nNFkB	*0*	*0.015*
E2F	*0*	*0 (+0.1)*
nE2F	*0*	*0*
tIkBa	*0*	*1x e-005*
IkBa	*0*	*0.017 (+0.1)*
nIkBa	*0*	*0.004*
IKKn	*0.1*	*0.1*
IKK	*0*	*0*
IKKi	*0*	*0*
tA20	*0*	*1x e-005*
A20	*0*	*0.001*
pIkBa	*0*	*0*
pIkBaNFkB	*0*	*0*
NFkBE2F	*0*	*0*
nNFkBE2F	*0*	*0*
IkBaNFkB	*0.1*	*0.091*
nIkBaNFkB	*0*	*0.001*

Table 3.1 Initial conditions for NF-κB:E2F-1 mathematical model: Involving transfection (typically transfected species indicted in red) and stimulation modelled from a steady state (see text for details).

Chapter 3 -
Generation & Characterisation of Tools

3.1 Generation of E2F fluorescent fusion constructs

E2F expression vectors were created using the Invitrogen Gateway® system. The Gateway system allows the creation of multiple expression vectors via site-specific, bacteriophage lambda recombination of preparatory "Entry" or "Donor" vectors with "Destination" vectors for a variety of expression types. For this project, the majority of the work will focus on live cell fluorescence microscopy as an experimental model system. It was therefore decided to develop fluorescent expression vectors for E2F-1, E2F-2 and E2F-3 for transfection into cells. Destination vectors for Enhanced Green Fluorescent Protein (EGFP) were initially chosen in the knowledge that co-transfection would proceed with a p65 *Discosoma*-Red-Express (dsRedXP) vector, which has excitation and emission spectra easily separable from EGFP. These experiments were designed to compliment previous work characterising the dynamics of p65-dsRedXP alone.

Recombination between Entry and Destination vectors was the product of a straight-forward, hour-long Clonase reaction. Correspondingly, the majority of the work in Gateway cloning involves manipulating the gene of interest into the preparatory Entry vector. Invitrogen provide a PCR method for engineering backbone DNA specific for producing peptide sequences onto the N- and -C termini of the gene to allow easy recombination from a starting vector into a "pDonr" vector and then into a choice of destination vector. However, for the creation of the E2F vectors, a more traditional approach was chosen, involving restriction enzyme digest of starting vector and ligation into Entry vector.

E2F gene fragments were excised from pCMVHA-E2F using a *Bam*HI restriction enzyme (NEB) and inserted via sticky ligation into Gateway Entry vector p-ENTR-2A at the *Bam*HI site, then subsequently transformed into Db3.1 bacteria. The ccdb "placeholder" gene present in p-ENTR-2A was then removed via *Eco*RI digest and the new entry vector "pENTR-2A-E2F-1" transformed in Dh5α cells. The Entry Vectors for E2F-1,E2F-2 and E2F-3 were then sequenced to ascertain the correct reading frame(s) for subsequent recombination (to ensure consistency of reading frame between fluorescent tag and protein of interest). Using an N-Terminus, C1-frame destination vector, Gateway LR-Clonase reactions were performed to produce EGFP-E2F-1

(Figure 3.1), EGFP-E2F-2 and EGFP-E2F-3. These vectors were then sequenced prior to use.

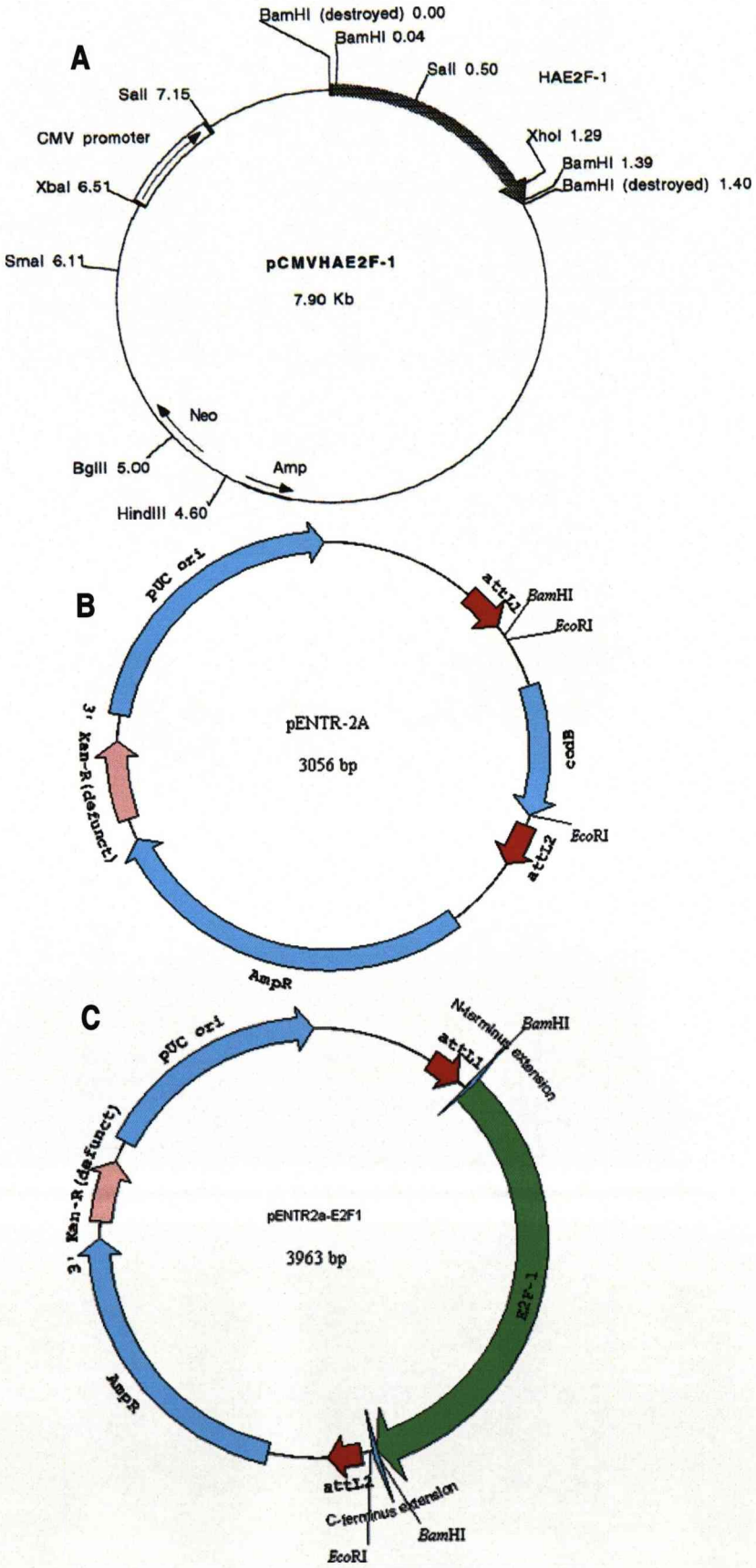

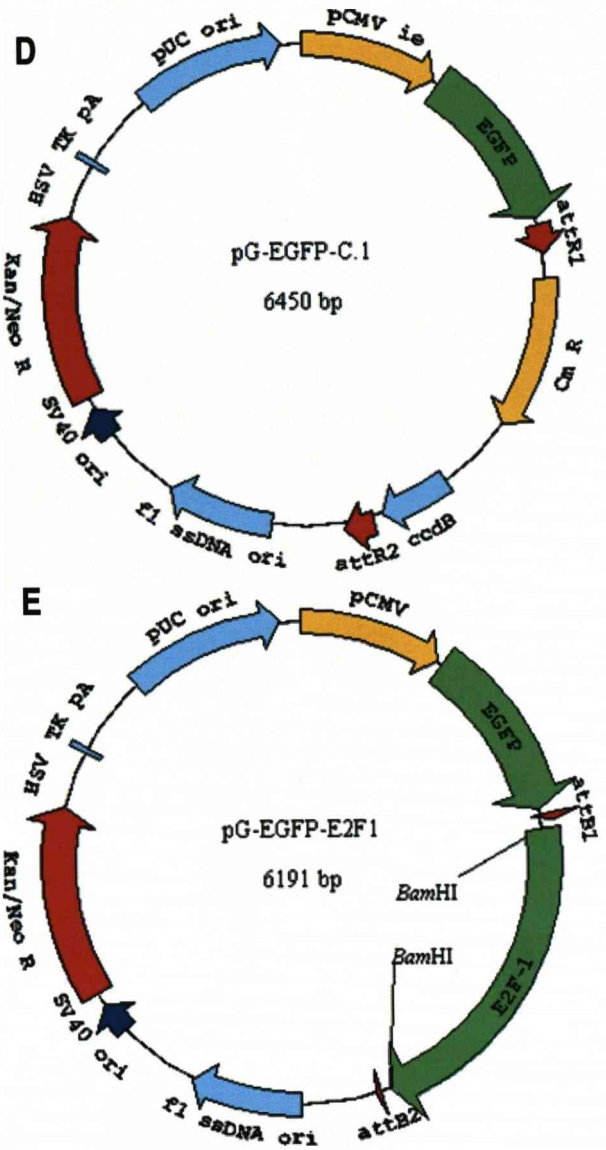

Figure 3.1 Gateway cloning steps for EGFP-E2F-1: A Showing pCMVHAE2F-1 from which the human E2F-1 gene was excised using BamHI digest. **B** Showing pENTR2A, modified Gateway Entry vector, into which the E2F-1 gene is inserted (see text for details). **C** Final map for pENTRA2A-E2F-1. **D** pG-EGFP-C1, EGFP destination vector with EGFP in reading frame C. **E** Final map for EGFP-E2F-1, produced after clonase reaction between pG-EGFP-C1 and pENTRa2A-E2F-1.

3.2 Characterisation of EGFP-E2F-1 and endogenous controls

GFP variants of E2F-1 have been previously used for studies in the context of the G1/S cell cycle system (Angus *et al.* 2003; Yao *et al.* 2008). Expression of the newly generated EGFP-E2F-1 in SK-N-AS human neuroblastoma cells was used to characterise the exogenous E2F-1 protein and to draw comparisons with previously published work characterising the endogenous E2F-1 protein. Firstly, the sub-cellular localisation of EGFP-E2F-1 was observed via live cell imaging and compared to that of endogenous E2F-1, determined via Immuno-cytochemistry. Figure 3.2 shows representative SK-N-AS cells showing a predominantly nuclear localisation for both exogenous and endogenous E2F-1, with roughly 10% of the protein localised in the cytoplasm at equilibrium.

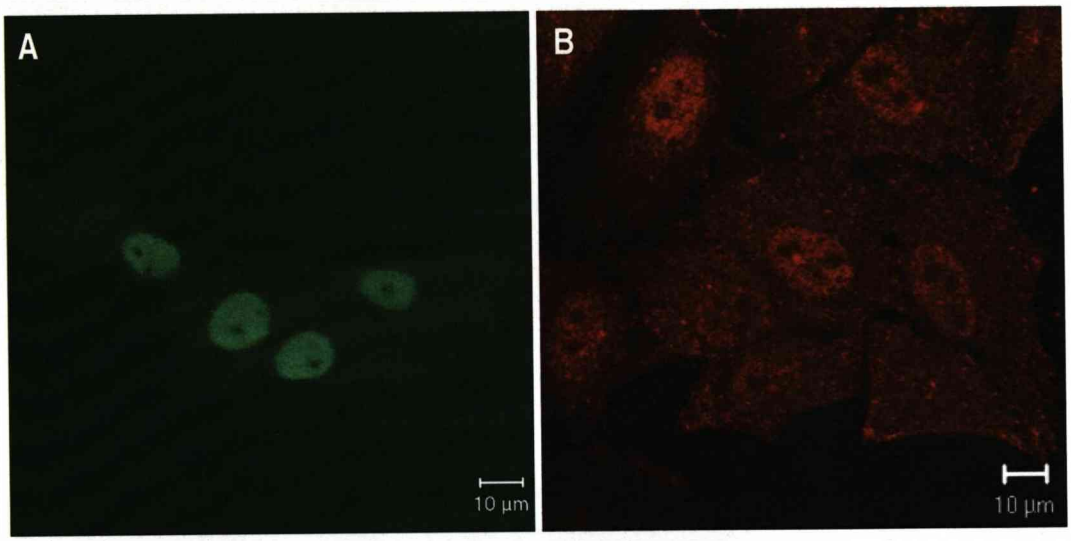

Figure 3.2 Localisation of exogenous and endogenous E2F-1: A Showing EGFP-E2F-1 predominantly localised to the nucleus with ~10% cytoplasmic in SK-N-AS cells. **B** Showing immuno-staining for E2F-1 in SK-N-AS cells showing a similar pattern of localisation.

This is consistent with previously published work suggesting a dynamic balance between nuclear and cytoplasm shuttling producing a steady-state predominantly nuclear localisation that is subject to dynamic changes (Magae *et al.* 1996; Verona *et al.* 1997), subsequently likened to the NF-κB system (Cartwright *et al.* 2000; Baguley *et al.* 2005). The observation of dynamic equilibria in live cell imaging is introduced in Chapter 4.

The degradation half-life of endogenous E2F-1 was reported to be between 2 and 3 hours, although this may be extended by up to 3 fold through stabilisation by pRB

(Hofmann *et al.* 1996; Campanero *et al.* 1997). As discussed in Section 1.2.3, pRB was found to be a transcriptional target gene of E2F-1 (Ishida *et al.* 2001). Assuming the fusion construct was transcriptionally active, exogenous expression of the fusion protein may have changed its own half life through transcription of pRB. Figure 3.3 (movie M3.3 on accompanying DVD) shows SK-N-AS cell expressing EGFP-E2F-1 at an appropriate level, i.e. across a population of cells expressing EGFP-E2F-1, cells were selected based on a level of fluorescence that would allow non-saturated images to be recorded and analysed, whilst allowing the cytoplasmic fraction of EGFP-E2F-1 to be observed (see below). Analysis of EGFP-E2F-1 fluorescence levels over time revealed an average degradation time of between 3 and 4 hours, with certain cells showing a EGFP-E2F-1 half-life of up to 7 hours. The half-life of EGFP-E2F-1 is considered further in Chapter 7.

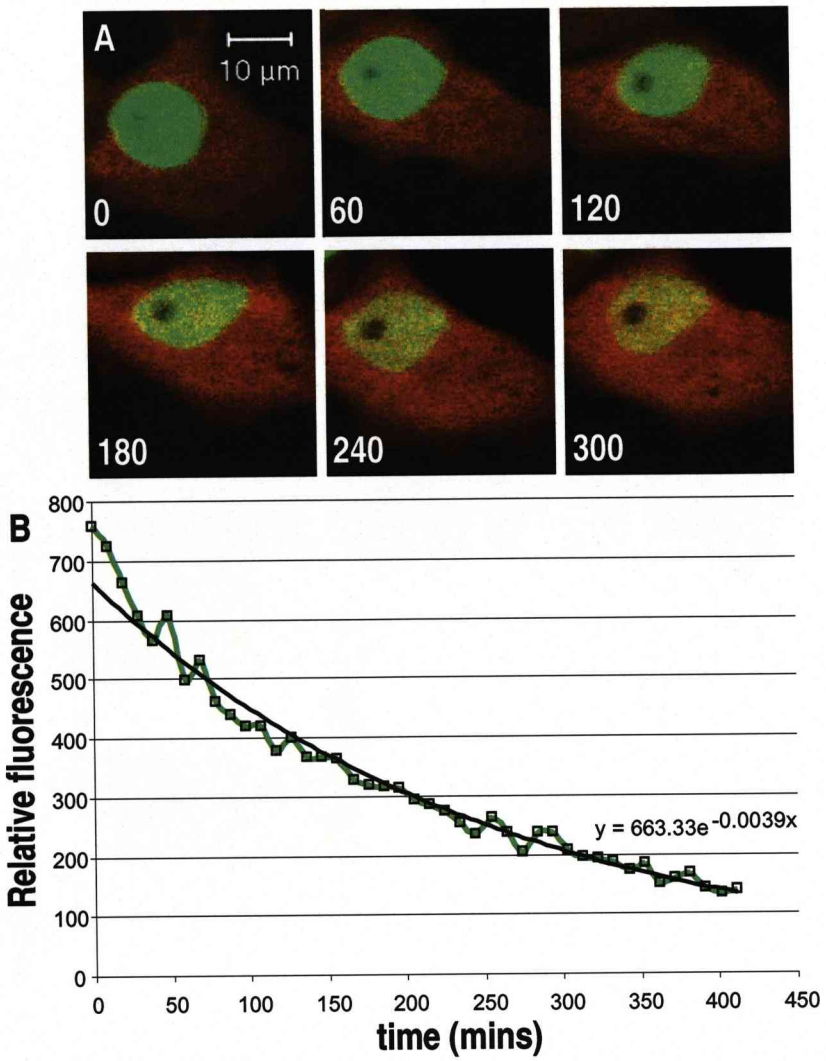

Figure 3.3 Degradation of EGFP-E2F-1: A Showing a typical SK-N-AS cell expressing EGFP-E2F-1 with an empty-Red control plasmid. **B** Quantification of EGFP levels over time. Fitted to an exponential curve giving a degradation half-life of ~180 min. Data set considered further in Chapter 6.

These data suggest that the E2F-1-EGFP construct has a similar degradation time to the endogenous protein. Direct evidence supporting a transcriptional role for EGFP-E2F-1 was gathered from luciferase reporter assays, considering the effect of EGFP-E2F-1 expression on an E2F-luc luciferase reporter construct (Figure 3.4).

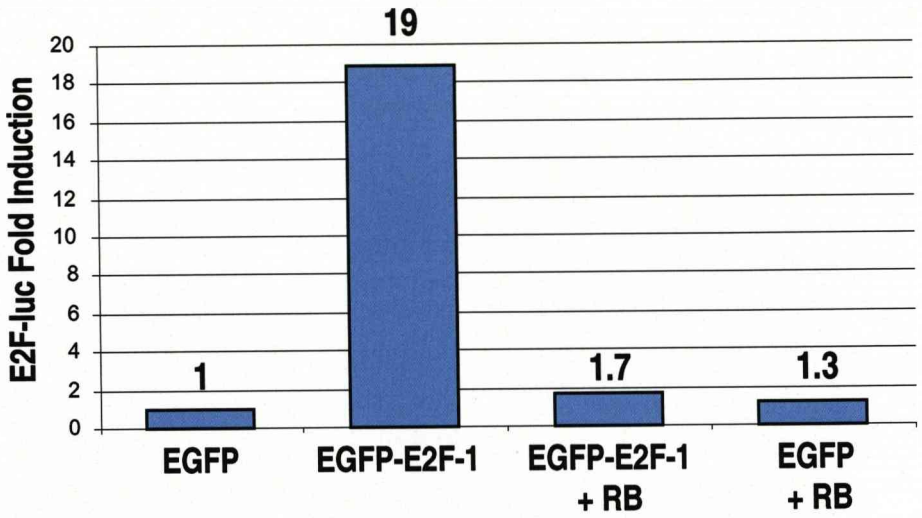

Figure 3.4 Transcriptional functionality of EGFP-E2F-1: Showing data from luciferase reporter assays using an E2F-luc construct to report on relative levels of E2F associated transcription in unstimulated SK-N-AS cells. Transient transfection with EGFP-E2F-1 alone gives a ~19 fold rise above an empty transfection. Co-transfection with a non fluorescent RB vector inhibited the transcriptional activity associated with EGFP-E2F-1 transient transfection.

Further evidence for the functionality of EGFP-E2F-1 is referred to throughout this work as appropriate, such as the link between exogenous expression of E2F-1 and apoptosis (Sections 4.6 and 7.5) and the endogenous E2F-1 profile generated by successful synchronisation with double-Thymidine block (Section 7.4). As EGFP-E2F-1 was shown to be transcriptionally active and show a similar intracellular localisation to that of endogenous E2F-1, further E2F-1 vectors were created from pENTR-2A-E2F-1. These included Enhanced Cyan and Yellow Fluorescent Proteins, ECFP-E2F-1 and EYFP-E2F-1 used for FRET studies (Section 4.4) and DsRedXP-E2F-1, to provide flexibility for live cell imaging studies involving co-transfection with different combinations of expression vectors.

Chapter 4 -

E2F-1 and The NF-κB System:

Towards a model foundation

4.1 Introduction – Shuttling and Translocation

Protein localisation is a dynamic process. Protein molecules move constantly around the cell, shuttling between nuclear and cytoplasmic compartments. The dynamic balance between nuclear and cytoplasmic protein concentration is influenced, at least in part, by the relative strength of nuclear import and export sequences contained in the structure of some proteins and protein complexes, resulting in an apparent predominant "steady-state" localisation. Rather than proteins being fixed in one place, an image of a live cell at a particular point in time gives a relative indication of how long molecules spend in a particular localisation by their abundance.

Perturbations to intracellular protein networks may result in bulk movement of protein molecules between compartments and a shift in their predominant localisation. As such there is an important difference between "shuttling" which is a constitutive process where molecules exchange places at equilibrium and "translocation", a process involving bulk movement from one equilibrium to another.

This is an important distinction to make when considering patterns of translocation or "oscillations", as mechanistically distinct from protein shuttling. The bulk dynamics of transcription factor NF-κB (where stochastic events such as gene transcription depend heavily on its nuclear protein concentration) involve oscillations driven by negative feedback and shifts in the suitability of the NF-κB complex for nuclear import (due to the exposure of the NLS of p65 and p50) or export (due to the binding of IκBα to p65 which masks the p65 NLS and exposes the IκBα NES) as highlighted in Section 1.3.2.

The dynamics of the NF-κB system in response to TNFα have been well defined ((Nelson *et al.* 2004) and Section1.3.3) and provide a model "system output" for quantitative or semi-quantitative assessment of the effect of perturbations to the system. One may assess the role of an external factor, for example cell cycle regulator E2F-1, on p65 and p50 within the context of the NF-κB system simply by looking for changes in predicted localisation and dynamics.

4.2 The effects of exogenous E2F-1 on NF-κB localisation

As previously stated, NF-κB family members p65 and p50 form the prototypical NF-κB transcriptional complex, and remain predominantly sequestered in the cytoplasm by IκB proteins in non-stimulated conditions. Initial work investigated the potential changes to the localisation of fluorescently labelled, transiently expressed NF-κB and E2F family members in order to determine relationships between E2F-1 and NF-κB. Combinations of expression vectors were transiently transfected into SK-N-AS human neuroblastoma cells and imaged at least 24 h later (Figure 4.1). When expressed alone, p65-dsRedXP had a predominantly cytoplasmic localisation whereas EGFP-E2F-1 was mainly nuclear. However, when expressed together, both p65-dsRedXP and EGFP-E2F-1 were predominantly nuclear. Interestingly, a triple-transfection of plasmids expressing p65-dsRedXP, EGFP-E2F-1 and a CMV-IκBα construct (that expressed a non-fluorescently tagged IκBα protein) yielded a cytoplasmic localisation of p65-dsRedXP (protein) which was consistent with the localisation observed when the same protein was expressed alone or in combination with IκBα-EGFP. These results suggest that EGFP-E2F-1 sequestered p65-dsRedXP to the nucleus and that this effect is reversed by IκBα co-expression. The cytoplasmic localisation of p65-dsRedXP when expressed alone implied that the endogenous levels of IκBα were higher than that of E2F-1 in SK-N-AS cells, requiring exogenous expression of E2F-1-EGFP to over-turn the balance. Furthermore, cells emitting lower levels of E2F-1-EGFP fluorescence showed a predominantly cytoplasmic localisation of p65-dsRedXP whilst E2F-1-EGFP remained predominantly nuclear.

When p50-dsRedXP and EGFP-E2F-1 fluorescent proteins were expressed alone both showed a predominant nuclear localisation (Figure 4.1). The observed localisation of p50-dsRedXP was expected as p50 contains an intrinsic NLS (Huxford *et al.* 1998). When p50-dsRedXP and EGFP-E2F-1 fluorescent proteins were expressed in combination they co-localised in the nucleus. This observation was consistent with (but not evidence for) physical interaction between p50 and E2F-1.

Similarly to cells expressing p65-dsRedXP, a triple transfection of plasmids expressing p50-dsRedXP, EGFP-E2F-1 and IκBα yielded a predominant cytoplasmic localisation for p50-dsRedXP consistent with co-expression of p50-dsRedXP and EGFP-IκBα.

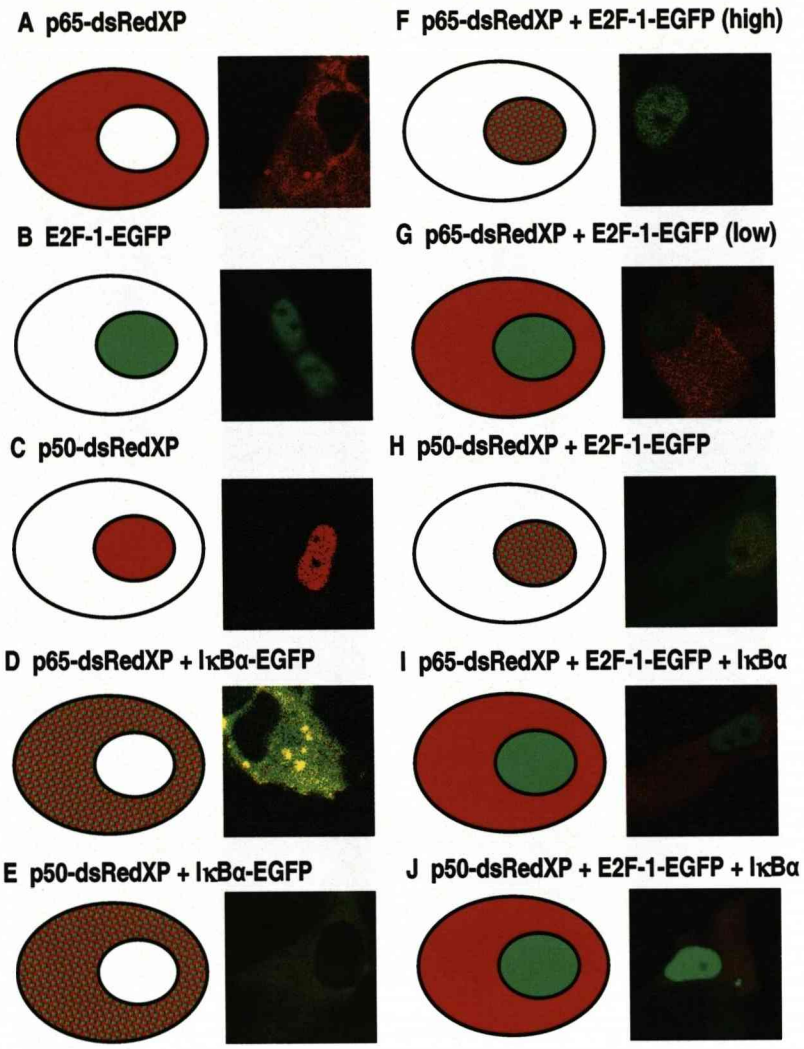

Figure 4.1 Localisation of transiently expressed NF-κB and E2F-1 fluorescent reporter proteins: Showing SK-N-AS cells transfected with combinations of plasmids expressing fluorescent fusion proteins. **A**, **B** and **C** Showing the predominant localisation taken by p65-dsRedXP (cytoplasmic), EGFP-E2F-1 (nuclear) and p50-dsRedXP (nuclear), respectively, when expressed alone. **D** and **E** The effect of co-expression of IκBα-EGFP on the predominant localisation of p65-dsRedXP (no change; remaining cytoplasmic) and p50-dsRedXP (changed; cytoplasmic). **F** and **G** The different effects of high and low levels of E2F-1 on p65-dsRedXP localisation. **H** The expected co-localisation of EGFP-E2F-1 and p50-dsRedXP in the nucleus upon co-expression. **I** and **J** The restored cytoplasmic localisation for p65-dsRedXP and p50-dsRedXP respectively when co-expressed with non fluorescent IκBα in addition to EGFP-E2F-1, suggesting a competition between E2F-1 and IκBα.

4.3 The effect of transiently expressed E2F-1 on NF-κB localisation

The observed relationship between high E2F-1-EGFP level and predominantly nuclear p65-dsRedXP and low E2F-1-EGFP level and predominantly cytoplasmic p65-dsRedXP suggested a possible physical relationship. This was investigated by imaging SK-N-AS cells expressing p65-dsRedXP and EGFP-E2F-1 for up to 12 hours. The time-lapse imaging data represented by the selected images and graph in Figure 4.2 (movie M4.2 on accompanying DVD) showed that when p65-dsRedXP and EGFP-E2F-1 were expressed simultaneously p65-dsRedXP resumed a predominant cytoplasmic localisation upon degradation of EGFP-E2F-1. These data were consistent with a nuclear sequestration effect of E2F-1 on p65 that is proportional to the level of E2F-1 in the cell, and supported the hypothesis that there is competition between E2F-1 and IκBα for NF-κB binding.

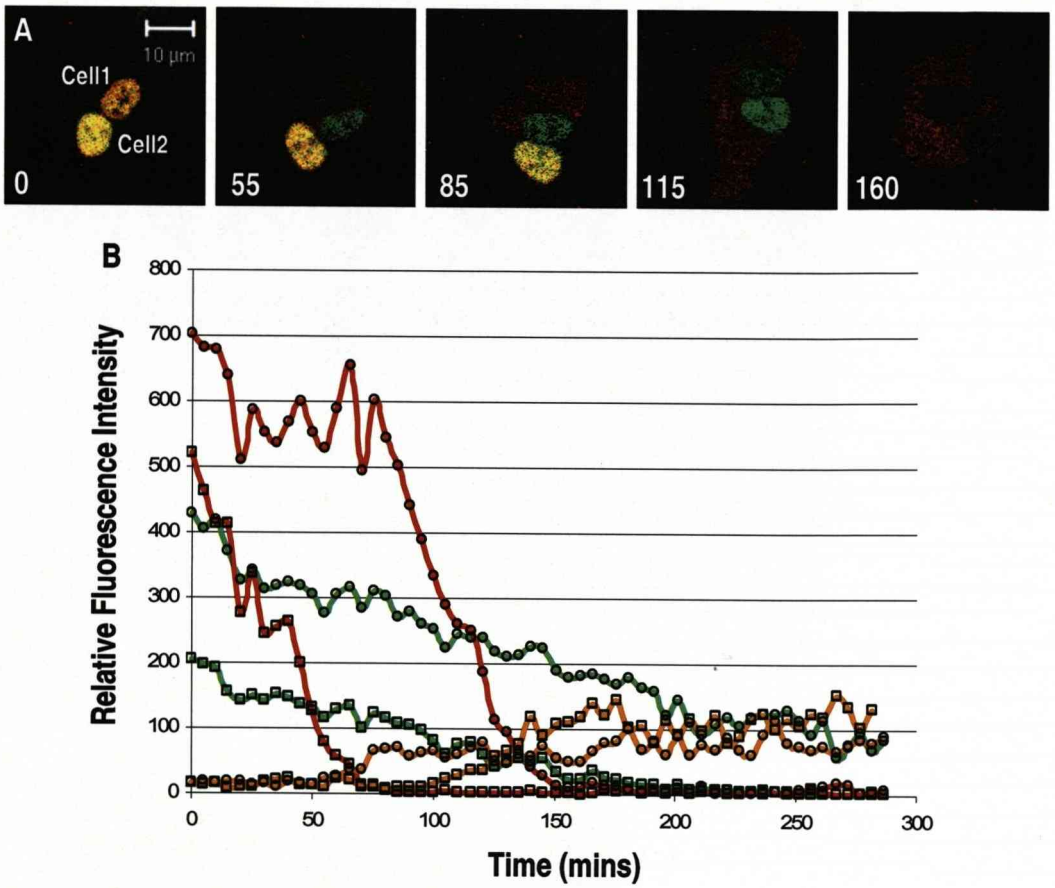

Figure 4.2 The effect of E2F-1 level on NF-κB nuclear occupancy in unstimulated conditions: **A** SK-N-AS cells imaged over time by fluorescence microscopy. Both cells show a predominant nuclear localisation for both EGFP-E2F-1 and p65-dsRedXP at 0, but show a movement of p65-dsRedXP to take a predominant cytoplasmic localisation coincident with the degradation of EGFP-E2F-1. **B** Quantification of nuclear fluorescence levels in the two cells shown in Panel A, showing a difference in levels of EGFP-E2F-1 (green lines) at 0. The cell with a lower level of EGFP-E2F-1 at 0 shows an earlier drop in nuclear p65-dsRedXP fluorescence (red lines), suggesting a proportional nuclear sequestration effect of E2F-1 on p65 in the nucleus. Red lines show p65-dsRedXP nuclear relative fluorescence intensity, orange lines show p65-dsRedXP cytoplasmic relative fluorescence intensity, green lines show EGFP-E2F-1 nuclear relative fluorescence intensity, for two different cells labelled by □ and ○. Fluorescence intensity is measured as average intensity per pixel. Time series images post-processed for clarity.

Co-localisation of EGFP-E2F-1 and p65-dsRedXP was measured over time in cells showing varied expression levels of both fluorescent proteins. Longitudinal imaging of cells expressing high EGFP-E2F-1 levels shows a much longer nuclear retention (NR) time of p65-dsRedXP than observed in cells expressing low levels of EGFP-E2F-1 or p65-dsRedXP alone. The resultant data set shows high correlation (R^2=0.8592)

between level of EGFP-E2F-1 nuclear fluorescence and the duration of p65 nuclear retention (Figure 4.3).

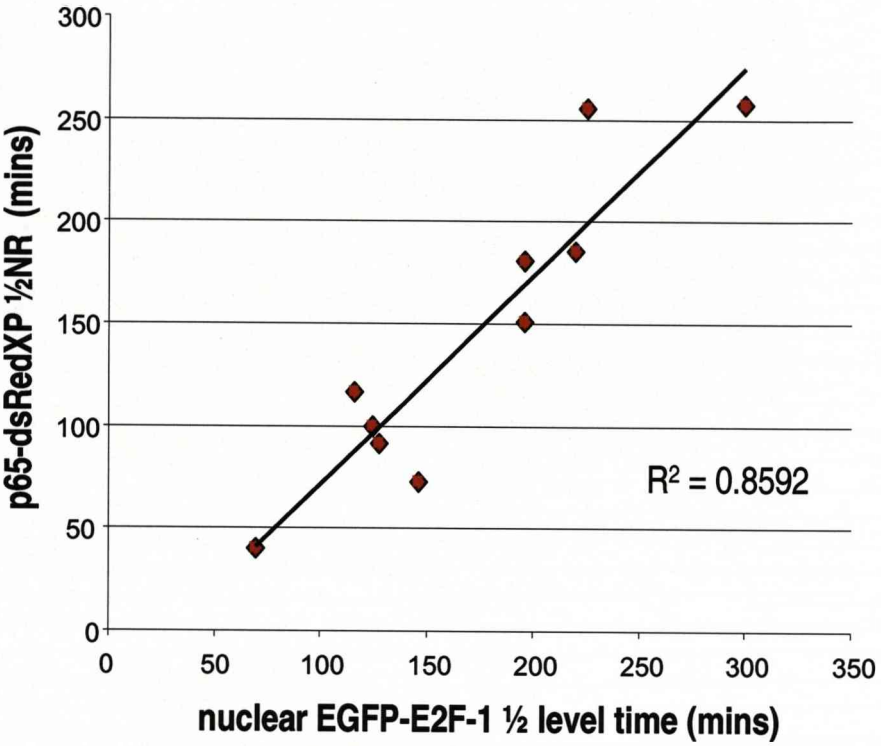

Figure 4.3 Proportional relationship between p65-dsRedXP nuclear occupancy and EGFP-E2F-1 degradation: Showing a high degree of correlation between p65-dsRedXP translocation from nucleus to cytoplasm, and the loss of nuclear EGFP-E2F-1 fluorescence in SK-N-AS expressing both fluorescent proteins. Chart representative of 10 SK-N-AS cells.

4.4 Binding between ectopically expressed E2F-1, p65 and p50 and IκBα

It might be assumed that in the studies above the p65-dsRedXP dynamics represent the dynamics of both the p65:p65 homodimer and the p65:p50 heterodimer. As can be seen from Figure 4.1, p50 takes a nuclear localisation in un-stimulated conditions, making the co-localisation of E2F-1-EGFP and p50-dsRedXP consistent with, but not evidence for, physical interaction. Similarly, the proportional relationship between EGFP-E2F-1 degradation and p65-dsRedXP nuclear retention time could be explained by indirect interaction between the NF-κB and E2F systems.

To investigate direct protein-protein interaction between NF-κB proteins and E2F-1 *in vivo*, binding between E2F-1, p65 and p50 was assessed using Förster Resonance Electron Transfer (FRET) (Figure 4.4). Although there are many FRET-based techniques, the approach is not straightforward due to overlaps between the excitation and emission spectra of both the donor and acceptor fluorophores. For example, when using the 458 and the 514 laser lines in confocal microscopy the emission spectrum of ECFP fusions have an emission peak at the same wavelength as EYFP which itself is excited with the 458 laser line used to excite ECFP. To alleviate these problems, acceptor photobleaching is commonly used as a control. SK-N-AS cells were transiently transfected with plasmid vectors expressing pairs of ECFP and EYFP fusion variants of NF-κB and E2F-1 proteins and assessed for FRET. The results yielded positive results for p65 and p50 (components of the predominant NF-κB heterodimer) but also for p65 and E2F-1 and p50 and E2F-1 (Figure 4.4, example shown in movie M4.4) in both nuclear and cytoplasmic compartments. No FRET was detected between IκBα and E2F-1 fusion proteins.

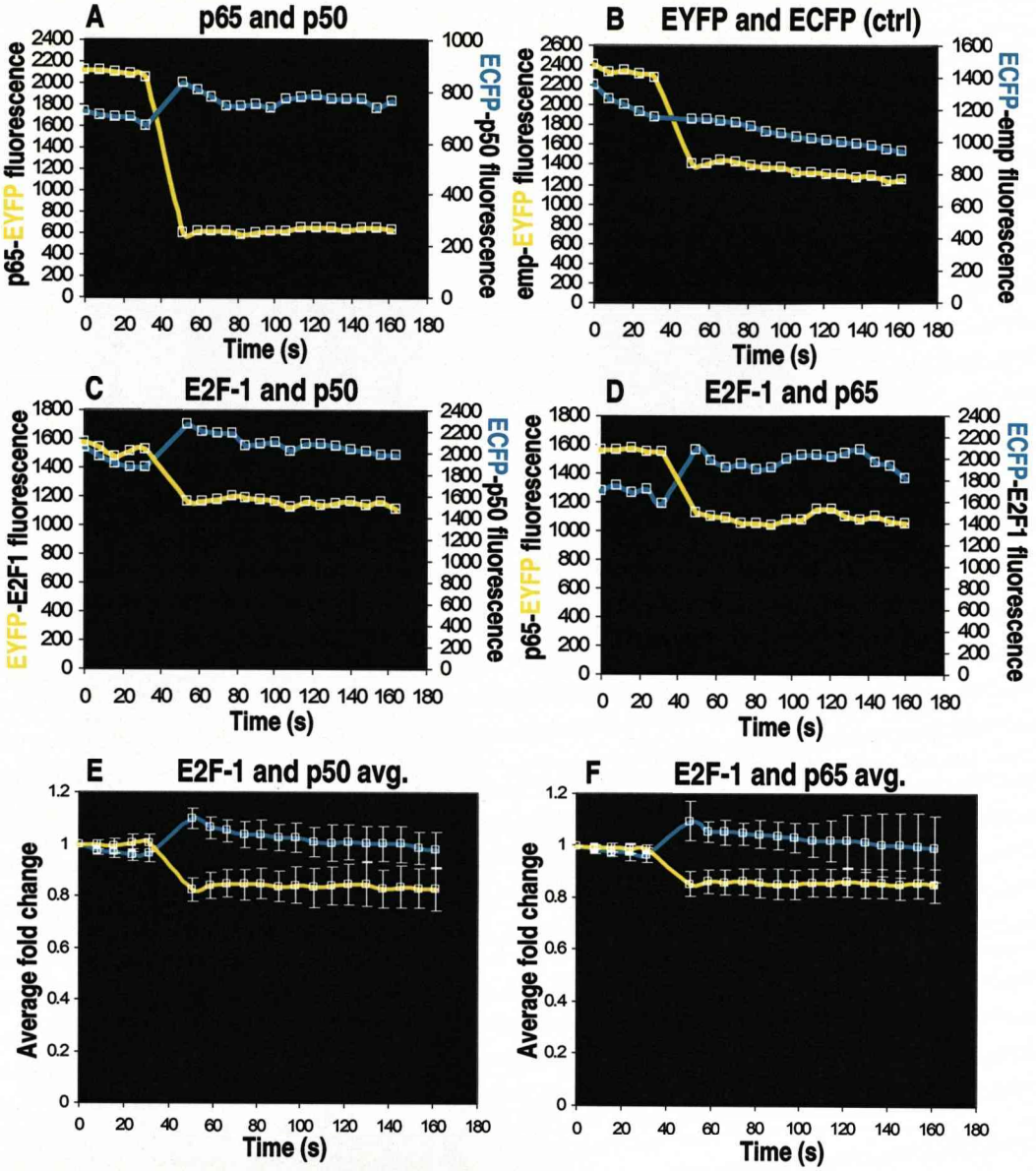

Figure 4.4 FRET between E2F-1, p65 and p50 fusion proteins: **A** Typical cell showing a decrease in p65-EYFP fluorescent signal following bleaching coincident with a rise in ECFP-p50 fluorescent signal, indicating positive FRET. **B** Loss of signal from CMV-EYFP does not lead to a rise in CMV-ECFP signal, no FRET produced **C** FRET between EYFP-E2F-1 and ECFP-p50 **D** FRET between p65-EYFP and ECFP-E2F-1 **E** and **F** show the respective average fold changes in fluorescent signal for the EYFP-E2F-1 / ECFP-p50 and p65-EYFP / ECFP-E2F-1 FRET pairs. Averages are taken from a data set of at least 25 cells and displayed +/- 1 std. deviation.

Physical binding of E2F-1 and NF-κB proteins was confirmed *in vivo* via Co-Immuno-Precipitation. Populations of SK-N-AS cells were subject to protein pull-down with an E2F-1 antibody, and yielded bands representative of p65 and p50 when probed (Figure 4.5). No positive Co-IP results were found between E2F-1 and IκBα.

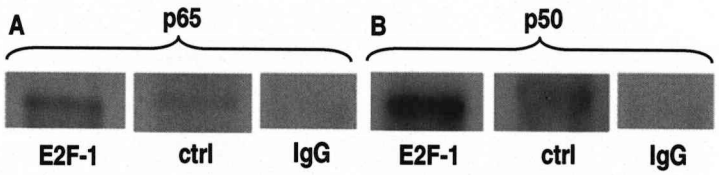

Figure 4.5 Assessment of endogenous binding between E2F-1, p65 and p50 via Co-Immunoprecipitation in SK-N-AS cells: A Showing a band representative of p65 in E2F-1 protein pull-down that is not present in the rabbit IgG lane. **B** Showing a band representative of p50 in E2F-1 protein pull-down that is not present in the rabbit IgG lane. Positive control 'ctrl' was SK-N-AS cells immuno-blotted for specific antibody against p65.

4.5 The NF-κB:E2F-1 conceptual model and its assumptions

Binding between E2F-1 and both members of the prototypical NF-κB complex, together with nuclear sequestration of p65 by E2F-1 observed in unstimulated conditions, allowed a conceptual model to be drawn up (Figure 4.6). The nuclear occupancy of p65-dsRedXP in the presence of ectopic levels of EGFP-E2F-1 is consistent with binding between the predominant NF-κB complex p65:p50 and E2F-1, in competition with endogenous levels of IκBα. This competition concurs with the observed translocation of p65-dsRedXP into the cytoplasm following EGFP-E2F-1 degradation. In order to explain the bulk cytoplasmic movement of NF-κB, it is necessary that levels of IκBα are high enough to remove free NF-κB from the nucleus. The most obvious mechanism to offer in explanation is that the NF-κB is transcriptionally active whilst bound to E2F-1 in the nucleus allowing the induction of the expression of IκBα.

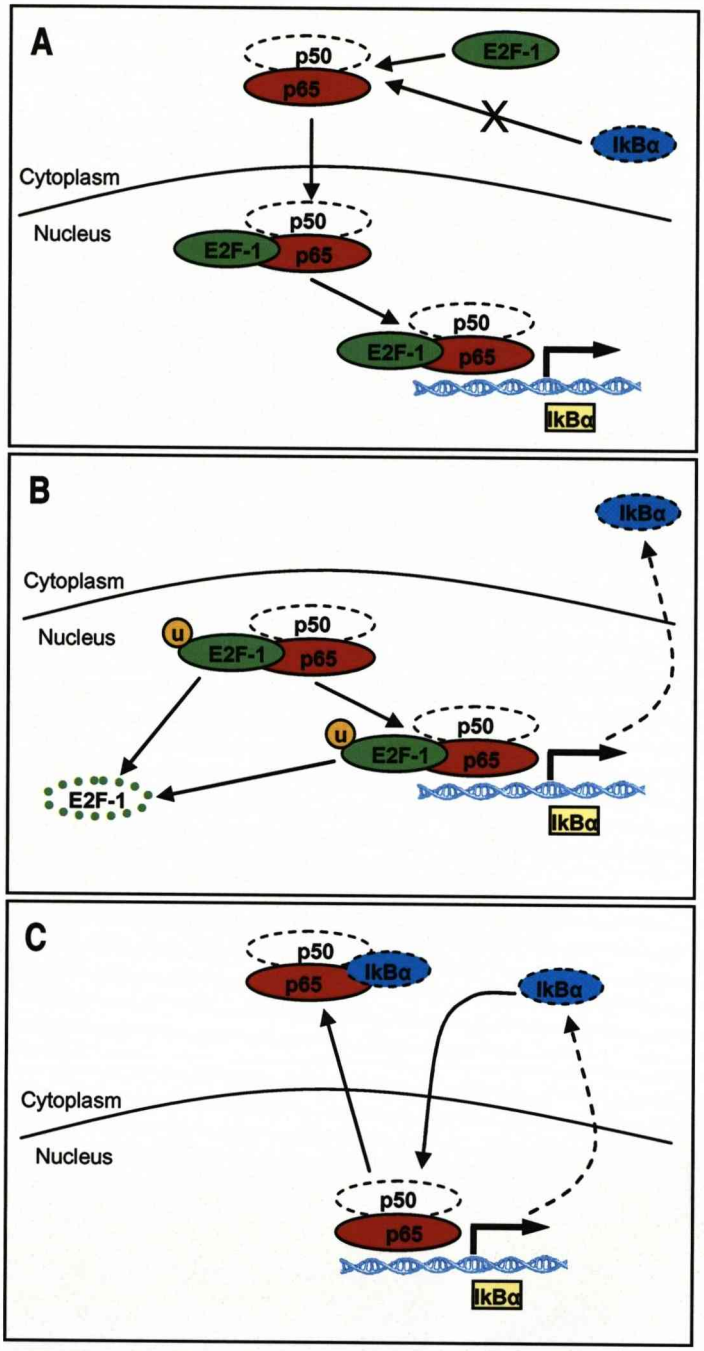

Figure 4.6 The NF-κB:E2F-1 conceptual model Mk.I: A Competition for binding to "free" NF-κB between IκBα and E2F-1 is mutually exclusive. In transient transfection conditions ectopic levels of E2F-1 are higher than endogenous IκBα leading to a balance turned in favour of the formation of the NF-κB:E2F-1 complex, which translocates to the nucleus and initiates transcription of target genes including IκBα. **B** E2F-1 degrades over time, leading to dissociation of the NF-κB:E2F-1 complex and an increased amount of free NF-κB in the nucleus. **C** *De-novo* IκBα translocates to the nucleus, binds to free NF-κB and pulls it back to a predominantly cytoplasmic localisation.

To test this assumption, luciferase reporter assays were carried out, examining the effects of combinations of transiently transfected plasmids expressing EGFP-E2F-1 and p65-dsRedXP proteins on NF-κB-related transcription. Luciferase activity was measured from an NF-κB reporter construct (NF-luc) composed of five NF consensus sequences fused to luciferase (Figure 4.7). It can be clearly seen that the combination of EGFP-E2F-1 and p65-dsRedXP produced a reduced level of NF-κB transcription compared to that measured in cells expressing p65-dsRedXP alone. However, this level was still significantly higher than the NF-luc signal measured in cells transfected with empty plasmids. These data may suggest that the nuclear NF-κB:E2F-1 complex is less active (2.5-fold) at this promoter compared to the "free" NF-κB complex.

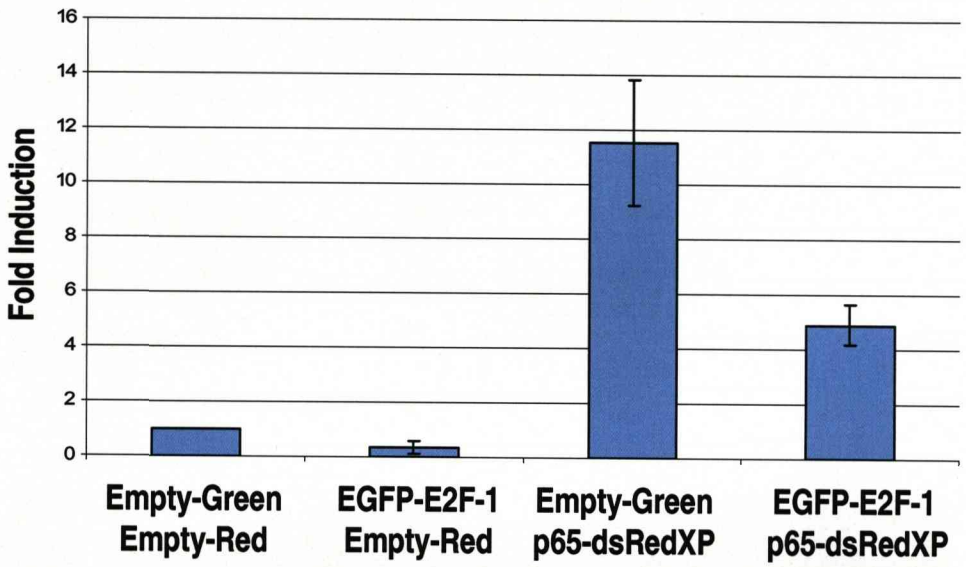

Figure 4.7 NF-κB transcriptional activity in transient transfection conditions: Showing data from luciferase reporter assays. NF-luc construct used to report on NF-κB associated transcription in SK-N-AS cells in unstimulated conditions, 24-hours post transfection. Expression of p65-dsRedXP alone gives a ~10 fold rise above an empty transfection. EGFP-E2F-1 does not cause an increase in NF-luc activity when expressed alone and significantly inhibits the level of transcription derived from p65-dsRedXP when co-expressed. Chart representative of 3 biological replicates. Error bars indicate +/- Standard Error Mean (SEM) values.

4.6 NF-κB affects E2F-1 related Apoptosis

As highlighted in Section 1.2.2, over-expression of E2F-1 habitually leads to apoptosis due to premature "entry" into S-Phase (Johnson *et al.* 1993; Qin *et al.* 1994). One striking observation made from time-lapse imaging experiments was that SK-N-AS cells expressing p65-dsRedXP and EGFP-E2F-1 show low levels of cell death compared to cells expressing EGFP-E2F-1 alone (Figure 4.8). The number of cells expressing EGFP-E2F-1 at the start of imaging was calculated, and compared to the number of these cells that remained alive after a 12-hour period. The percentage of cell death was compared to a similar calculation for cells expressing p65-dsRedXP alongside EGFP-E2F-1. From data sets of at least 50 cells per condition, 68% of cells expressing EGFP-E2F-1 were dead after 12 hours. However, cells co-expressing p65-dsRedXP showed a ~36% decrease in cell death with 32% of transfected cells dead after 12 hours. From these data it was concluded that the interaction between NF-κB and E2F-1 may block E2F-related apoptosis. This work is extended in Chapter 7.

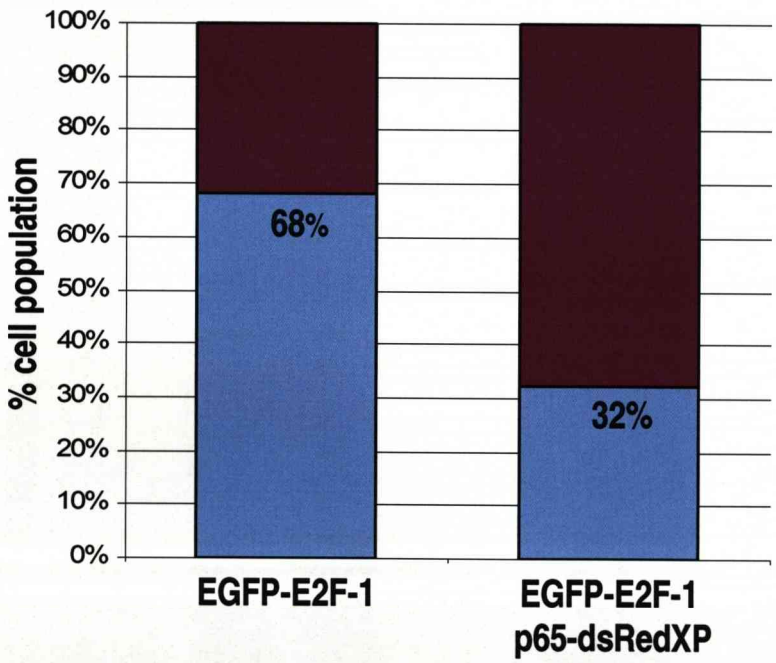

Figure 4.8 NF-κB affects the level of E2F-1-mediated Apoptosis: Levels of cell death were measured in cells expressing EGFP-E2F-1 alone and EGFP-E2F-1 together with p65-dsRedXP in a 12 hour period, 24-hours post-transfection. Expression of EGFP-E2F-1 alone resulting in 68% cell death whereas co-expression of p65-dsRedXP resulted in only 32% cell death. Data sets representative of at least 50 cells per condition.

4.7 Discussion

In the work described in this chapter, we have presented evidence of physical interaction between E2F-1 and the NF-κB system. E2F-1 affects a change in NF-κB protein localisation in unstimulated conditions (Figure 4.1). Time-lapse imaging reveals this effect to be proportional to the level of EGFP-E2F-1 in the cell, and is therefore variable from cell to cell (Figures 4.2 and 4.3). This relationship was found to be a result of direct physical interaction between E2F-1, p65 and p50 (Figures 4.4 and 4.5). The proportional sequestration of NF-κB through direct binding to E2F-1 raised a question over the transcriptional efficiency of NF-κB whilst bound to E2F-1, which was subsequently found to be less than that of "free" NF-κB (Figure 4.7). The relationship between E2F-1 and NF-κB was shown to be functional as well as physical due firstly to the effect of E2F-1 on NF-κB transcription, but also due to the ability of NF-κB to decrease the apoptotic effect of E2F-1 ectopic expression.

A conceptual model of the NF-κB system, extended to include E2F-1 is the simplest way to explain observed dynamics (Figure 4.6). This conceptual model provides an ideal foundation for a Mathematical Systems Biology approach. Recalling the criteria defined for the application of Mathematical Systems Biology, there is now a choice of *context* (either NF-κB at G1/S of the cell cycle or E2F-1 interaction in the NF-κB system); *predictions* to resolve (characterisation of the effects of E2F-1 on the NF-κB system and it's dynamics); and an experimental system with which to provide an *answer* (An NF-κB response to stimulus, with TNFα as system input and p65-dsRedXP dynamics as system output). The next step in this study was to create a testable mathematical model from the conceptual model.

Chapter 5 -

The NF-κB:E2F-1 Model:

Extension, Prediction, and Verification

5.1 Introduction and rationale

In this chapter the conceptual model created in chapter 4 will be implemented using mathematical description. As highlighted in Section 4.7, there is a choice of biological context for this model; either NF-κB at G1/S of the cell cycle or E2F-1 interaction in the NF-κB system. Although the cell cycle context presented the opportunity to obtain novel data, it was decided to apply the model to the context of the NF-κB system. This was due to the presence of well characterised experimental systems to allow some experimental work to proceed immediately, and the availability of an existing deterministic mathematical model for the NF-κB system providing a foundation for subsequent extension. This strategy was also intended to provide the opportunity to gather data comparable to previous and current studies (Nelson *et al.* 2004; Ashall *et al.* 2009)

5.2 Revision and extension of the NF-κB model

To mathematically describe the NF-κB:E2F-1 conceptual model as a deterministic mathematical model, the existing deterministic model of the NF-κB system fitted to single cell SK-N-AS cells (Ashall *et al.* 2009) was extended to include a "module" for interaction with E2F-1.

Inclusion of the E2F-1 module required revision of the existing NF-κB model to ensure consistent nomenclature between original and new species. The convention chosen was to name complexes in a hierarchical manner, i.e. with the order of IκBα (denoted by *IkBa*) in front of NF-κB (*NFkB*) in front of E2F-1 (*E2F*). Although the experimental work outlined in Chapter 4 confirms binding between E2F-1 and the active NF-κB complex (p65 and p50 are modelled as a single complex in the NF-κB model), hypothetical complexes involving E2F-1 and IκBα were included in the design, giving 8 new species, 4 of which involve complexes of E2F-1 and IκBα which were left unpopulated in the first version of the model (Table 5.1).

There are several reasons for including complexes involving IκBα and E2F-1 in the model structure. Firstly, lack of positive FRET or Co-Immunoprecipitation does not discount direct interaction between two protein species, if for example, the bound

complex is unstable or the binding occurs in such a way that fluorescent fluorophores are too far away from each other for FRET to occur (this situation becomes increasingly likely if a protein complex is composed of multiple protein species). Secondly, it is much easier to make provision for all potential interacting species during the early stages of model creation (and leave some species inactive during implementation) than it is to include a new species to all related ODEs of a working model. Thirdly, should it be required, any network species may be renamed and still retain its effect on other model species, allowing redundancy to be built into the model for easier expansion of the network in the future.

Cytoplasmic Species			
	Species	***Represents***	***Associates with***
1	*NFkB*	NF-κB	*2,3*
2	*E2F*	E2F-1	*1,3*
3	*IkBa*	IκBα	*1,2*
4	*NFkBE2F*	NF-κB:E2F-1	*3*
5	*IkBaNFkB*	IκBα:NF-κB	*2*
6	*IkBaE2F*	IκBα:E2F-1	*1*
7	*IkBaNFkBE2F*	IκBα:NF-κB :E2F-1	-
Nuclear Species			
	Species	***Represents***	***Associates with***
8	*nNFkB*	nNF-κB	*9,10*
9	*nE2F*	nE2F-1	*8,10*
10	*nIkBa*	nIκBα	*8,9*
11	*nNFkBE2F*	nNF-κB:E2F-1	*10*
12	*nIkBaNFkB*	nIκBα:NF-κB	*9*
13	*nIkBaE2F*	nIκBα:E2F-1	*10*
14	*nIkBaNFkBE2F*	nIκBα:NF-κB :E2F-1	-

Table 5.1 New or amended species introduced to the NF-κB:E2F-1 model: Populated species, shown in red, represent cytoplasmic and nuclear species for *E2F* and the *NFkBE2F* complex species. Unpopulated species, shown in blue, represent hypothetical complexes involving *E2F* and *IkBa* allowing redundancy to be built into the network.

Network parameters were also given a coherent nomenclature; Association *ka*, Dissociation *kd*, Import *ki*, Export *ke*, Constitutive degradation *kg*, Inducible (phospho) degradation *kgp*, catalysis *kc*, constitutive transcription *kcscpt*, inducible transcription *kiscpt*, translation *trl*. A full list of model parameters for the NF-κB:E2F-1 model, together with listings of initial conditions can be found in Section 2.3.1 or in the full model code (see attached DVD).

With the aim of ensuring a sound network structure of correctly linked ODEs prior to implementation, a network wiring diagram of the system was drawn for both nuclear and cytoplasmic species in the NF-κB:E2F-1 model (Figure 5.3) Taking the *nNFkB* species as an example, reactions affecting the concentration of *nNFkB* as shown in Table 5.2.

Reaction	*Type*	*Parameters*
NF-κB ↔ nNF-κB	*Import/Export*	*i1,e1*
nNF-κB + nE2F → nNF-κB:E2F	*Association/ Dissociation*	*a7,d7*
nNF-κB + nIκBα → nIκBα:NF-κB	*Association/ Dissociation*	*a6,d6*
nIκBα:NF-κB → Sink + nNF-κB	*Degradation*	*g2*
nNF-κB:E2F → Sink + nNF-κB	*Degradation*	*g14*

Table 5.2 Considering reactions in the NF-κB:E2F-1 model: Showing reactions contributing to the overall value of *nNFkB*, showing association/dissociation (parameter prefix "a" and "d"), import/export (parameter prefix "i" and "e"), and degradation (parameter prefix "g").

The reactions in Table 5.2 can be converted into an ODE describing the change of *nNFkB* concentration over time (Figure 5.1).

$$\frac{d}{dt}nNF\kappa B(t) =$$

$$\overbrace{kd6\times(nNF\kappa B:nI\kappa B\alpha)(t)-ka6\times nI\kappa B\alpha(t)\times nNF\kappa B(t)}^{\mathbf{A}}$$

$$+\overbrace{kd7\times(nNF\kappa B:nE2F)(t)-ka7\times nE2F(t)\times nNF\kappa B(t)}^{\mathbf{B}}$$

$$+\overbrace{ki1\times kv\times NF\kappa B(t)-ke1\times kv\times nNF\kappa B(t)}^{\mathbf{C}}$$

$$+\overbrace{kg2\times(I\kappa B\alpha:NF\kappa B)(t)}^{\mathbf{D}}+\overbrace{kg14\times(nNF\kappa B:nE2F)(t)}^{\mathbf{E}}$$

Figure 5.1 Ordinary Differential Equation for *nNFkB*: A Association/Dissociation equilibrium of the *nIkBaNFkB* complex **B** Association/Dissociation of the *nNFkBE2F* complex **C** Import/Export of *nNFkB* normalised by '*kv*' to allow for change of cellular compartment **D** Degradation of the *nIkBaNFkB* complex contributes to the level of *nNFKB* complex **E** Degradation of the *nIkBaNFkB* complex contributes to the level of uncomplexed *nNFKB*. **A**, **C** and **D** re-formulated from original model. **B** and **E** added as part of E2F module. Equation shown that for *nNFkB* in initial NF-κB:E2F-1 model.

The full set of populated ODEs for the NF-κB:E2F model is shown in Table 5.3, with new or amended ODEs added to the original NF-κB model marked in red.

$$\frac{d}{dt}NF\kappa B(t) = kd1\times(I\kappa B\alpha : NF\kappa B)(t) - ka1\times I\kappa B\alpha(t)\times NF\kappa B(t) - ki1\times NF\kappa B(t) + ke1\times nNF\kappa B(t) + kgp2\times(pI\kappa B\alpha : NF\kappa B)(t) + kg1\times(I\kappa B\alpha : NF\kappa B)(t) + kd3\times(NF\kappa B : E2F)(t) - ka3\times E2F(t)\times NF\kappa B(t) + kg13\times(NF\kappa B : E2F)(t) \quad (1)$$

$$\frac{d}{dt}nNF\kappa B(t) = kd6\times(nNF\kappa B : nI\kappa B\alpha)(t) - ka6\times nI\kappa B\alpha(t)\times nNF\kappa B(t) + ki1\times kv\times NF\kappa B(t) - ke1\times kv\times nNF\kappa B(t) + kg2\times(I\kappa B\alpha : NF\kappa B)(t) + kd7\times(nNF\kappa B : nE2F)(t) - ka7\times nE2F(t)\times nNF\kappa B(t) + kg14\times(nNF\kappa B : nE2F)(t) \quad (2)$$

$$\frac{d}{dt}E2F(t) = -ki2\times E2F(t) + ke2\times nE2F(t) - kg3\times E2F(t) + kd3\times(NF\kappa B : E2F)(t) - ka3\times E2F(t)\times NF\kappa B(t) \quad (3)$$

$$\frac{d}{dt}nE2F(t) = +ki2\times kv\times E2F(t) - ke2\times kv\times nE2F(t) - kg4\times nE2F(t) + kd7\times(nNF\kappa B : nE2F)(t) - ka7\times nE2F(t)\times nNF\kappa B(t) \quad (4)$$

$$\frac{d}{dt}tI\kappa B\alpha(t) = kiscpt1\times 0.6\times\frac{nNF\kappa B:nE2F^h(t)}{nNF\kappa B:nE2F^h(t)+k^h} + kiscpt1\times\frac{nNF\kappa B^h(t)}{nNF\kappa B^h(t)+k^h} - kg5\times tI\kappa B\alpha(t) \quad (5)$$

$$\frac{d}{dt}I\kappa B\alpha(t) = kd1\times(I\kappa B\alpha : NF\kappa B)(t) - ka1\times I\kappa B\alpha(t)\times NF\kappa B(t) + ktrl1\times tI\kappa B\alpha(t) - kg6\times I\kappa B\alpha(t) - ki3\times I\kappa B\alpha(t) + ke3\times nI\kappa B\alpha(t) - kc1\times IKK(t)\times I\kappa B\alpha(t) \quad (6)$$

$$\frac{d}{dt}nI\kappa B\alpha(t) = kd6\times(nI\kappa B\alpha : nNF\kappa B)(t) - ka6\times nI\kappa B\alpha(t)\times nNF\kappa B(t) - kg7\times nI\kappa B\alpha(t) + ki3\times kv\times I\kappa B\alpha(t) + ke3\times kv\times nI\kappa B\alpha(t) \quad (7)$$

$$\frac{d}{dt}IKKn(t) = kpd\times\frac{kiA20}{kiA20+TR\times A20(t)}\times IKKi(t) - TR\times kact1\times IKKn(t) \quad (8)$$

$$\frac{d}{dt}IKK(t) = TR\times kact1\times IKKn(t) - kinact1\times IKK(t) \quad (9)$$

$$\frac{d}{dt}IKKi(t) = kinact1\times IKK(t) - kpd\times\frac{kiA20}{kiA20+TR\times A20(t)}\times IKKi(t) \quad (10)$$

$$\frac{d}{dt}tA20(t) = kiscpt2\times 0.6\times\frac{nNF\kappa B:nE2F^h(t)}{nNF\kappa B:nE2F^h(t)+k^h} + kiscpt2\times\frac{nNF\kappa B^h(t)}{nNF\kappa B^h(t)+k^h} - kg11\times tA20(t) \quad (11)$$

$$\frac{d}{dt}A20(t) = ktrl2\times tA20(t) - kg12\times A20(t) \quad (12)$$

$$\frac{d}{dt}pI\kappa B\alpha(t) = kc1\times IKK(t)\times I\kappa B\alpha(t) - kgp1\times pI\kappa B\alpha(t) \quad (13)$$

$$\frac{d}{dt}(pI\kappa B\alpha : NF\kappa B)(t) = kc2\times IKK(t)\times(I\kappa B\alpha : NF\kappa B)(t) - kgp2\times(pI\kappa B\alpha\circ NF\kappa B)(t) \quad (14)$$

$$\frac{d}{dt}(NF\kappa B : E2F)(t) = ka3\times E2F(t)\times NF\kappa B(t) - kd3\times(NF\kappa B : E2F)(t) - ki4\times(NF\kappa B : E2F)(t) + ke4\times(nNF\kappa B : nE2F)(t) - kg13\times(NF\kappa B : E2F)(t) \quad (17)$$

$$\frac{d}{dt}(nNF\kappa B : nE2F)(t) = ka7\times nE2F(t)\times nNF\kappa B(t) - kd7\times(nNF\kappa B : nE2F)(t) + ki4\times kv\times(NF\kappa B : E2F)(t) - ke4\times kv\times(nNF\kappa B : nE2F)(t) - kg14\times(nNF\kappa B : nE2F)(t) \quad (18)$$

$$\frac{d}{dt}(I\kappa B\alpha : NF\kappa B)(t) = ka1\times I\kappa B\alpha(t)\times NF\kappa B(t) - kd1\times(I\kappa B\alpha : NF\kappa B)(t) - kg1\times(I\kappa B\alpha : NF\kappa B)(t) + ke6\times(nI\kappa B\alpha : nNF\kappa B)(t) - kc2\times IKK(t)\times(I\kappa B\alpha : NF\kappa B)(t) \quad (21)$$

$$\frac{d}{dt}(nI\kappa B\alpha : nNF\kappa B)(t) = ka6\times nI\kappa B\alpha(t)\times nNF\kappa B(t) - kd6\times(nI\kappa B\alpha\circ nNF\kappa B)(t) - ke6\times kv\times(nI\kappa B\alpha\circ nNF\kappa B)(t) - kg2\times(nI\kappa B\alpha : nNF\kappa B)(t) \quad (22)$$

Table 5.3 Ordinary Differential Equations in the NF-κB:E2F-1 Model: Showing ODEs representing all model species. Symbol '*n*' denotes nuclear variables, '*t*' denotes mRNA transcript, while '*p*' denotes phosphorylated form of *IkBa*. Symbols denoting cytoplasmic localization were omitted. Transport rates for nuclear variables (Equations. (2), (4), (7), (18) and (22)) were adjusted by 'k_v' (ratio of cytoplasmic and nuclear volume) to reflect smaller nuclear volume; hence increasing molecular concentrations within this compartment. Initial Concentrations for these species can be found in Appendix 1.

5.3 Experimental and mathematical reproduction of past NF-κB work

In order to experimentally reproduce TNFα-mediated NF-κB dynamics observed via time-lapse fluorescence microscopy (Nelson *et al.* 2004), SK-N-AS cells were transfected with a plasmid vector expressing p65-dsRedXP and stimulated with 10ng/ml TNFα. Resultant oscillatory dynamics display an average MNL time of 30 minutes, an average NR time of 60 minutes and an oscillatory period of 100 minutes in cells with similar p65-dsRedXP expression levels (Figure 5.2, movie M1.13). As highlighted in Section 1.3.3, the average dynamic trace masks asynchronous oscillations displayed in the population of single cells. Variability in peak1 MNL and NR times is addressed in Section 6.5. Concurrently to experimental work, implementation of the NF-κB:E2F-1 model proceeded, with the E2F-1 module set to zero, to test the ability of the new NF-κB:E2F-1 model to recapitulate *NFkB* dynamics in response to TNFα (Ashall *et al.* 2009). In the model, stimulation with TNFα is assumed to be a saturated dose of 10ng/ml and is modelled as a binary switch, i.e. the TNF signal (*TR*) may be on ("1") or off ("0"). Figure 5.2 shows that the extended mathematical model is able to faithfully model the average MNL, NR and oscillatory period times of p65-dsRedXP in response to TNFα.

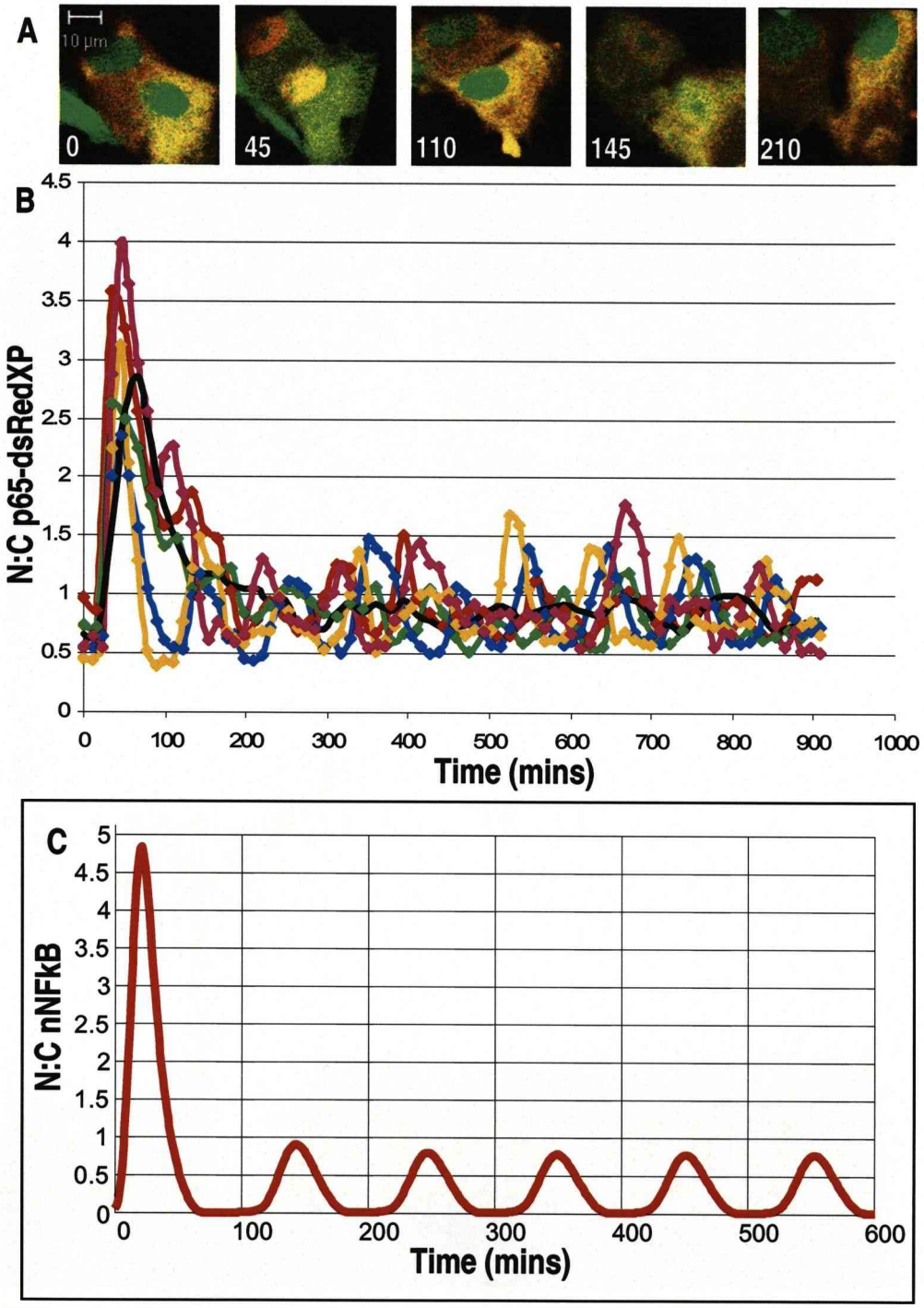

Figure 5.2 Experimental and Mathematical reproduction of NF-κB dynamics: A Time series showing nucleo-cytoplasmic oscillations in p65-dsRedXP (co-transfected with a plasmid vector expressing untagged GFP) in response to TNFα stimulus in SK-N-AS cells **B** Quantification of p65-dsRedXP oscillations in multiple cells, giving an average MNL of 30 minutes, an average NR of 60 minutes and an oscillatory period of 100 minutes for the first peak of nuclear occupancy. Subsequent asynchronous oscillations are masked by the population average (shown in black) **C** Predictive model plot of extended NF-κB model with E2F-1 module set to Ø. Model plot concurs with experimental data.

5.4 Implementation of the NF-κB:E2F-1 module

A network diagram of the NF-κB:E2F-1 module is shown in Figure 5.3, which is sufficient to reproduce the simple conceptual model outlined in Section 4.5. The ODEs forming the basis of the initial version of NF-κB:E2F-1 model can be found in Table 5.2.

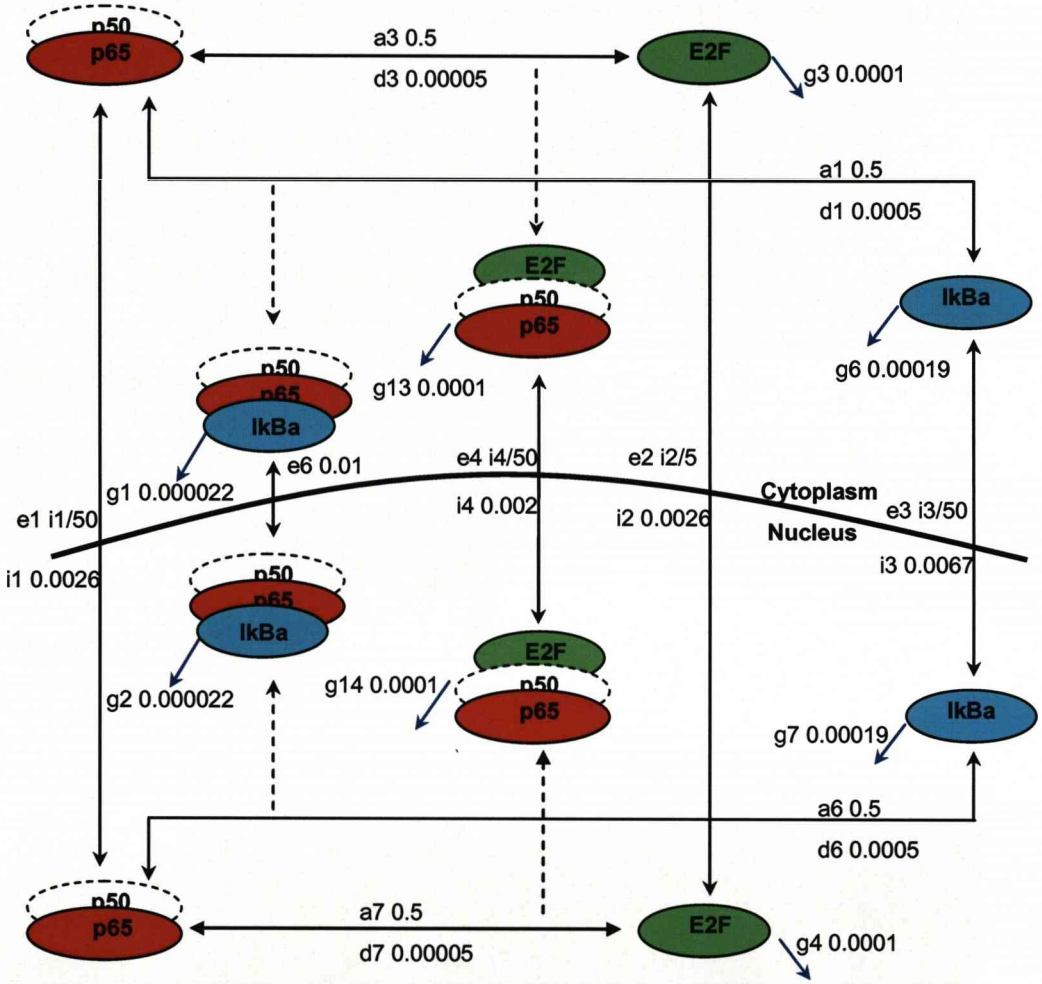

Figure 5.3 Network "wiring" diagram for major species in NF-κB:E2F-1 model Mk. I: Lines connecting related species represent biochemical equations. As such, for any given time the concentration of a particular species is the sum of outward and inward reactions. Reactions and parameters shown represent the initial NF-κB:E2F-1 model (in s^{-1}).

Competition between IκBα and E2F-1 is modelled in the simplest fashion by fitting the association rate between *NFkB* and *E2F* in both cellular compartments (parameters *a3* and *a7*, respectively) equivalent to *IkBa* and *NFkB*. The resting steady state localisation of EGFP-E2F-1 (Section 3.2) was fitted by inhibiting degradation (setting degradation

rates of *E2F* and *nE2F* to zero) whilst fitting import and export rates (parameters *ke2*= *ki1*/5) to give a 9:1 ratio between nuclear and cytoplasmic localisation.

Simulation protocols (described in detail in Section 2.3) were designed to mimic transient transfection experiments. Expression of exogenous levels of E2F-1, NF-κB or IκBα (or combinations thereof) are modelled as Heaviside Functions involving a "step" in level from a steady-state in the case of *NFkB* and 0 in the case of *E2F*. As such the model operates on the assumption that the level of E2F-1 prior to transfection is minimal (approximate to its basal level for ~80% of the cell cycle), or at least sufficiently low that the level of exogenous E2F-1 introduced during transfection is significant. The model assumes transfected species are initiated to the cytoplasm (*E2F*, *NFkB*, *IkBa*) corresponding to translation. The high nuclear import rate of *E2F* (similar to free *NFkB* species) and comparable association rates between *E2F* and *NFkB* to *IkBa* and *NFkB* allow the level of *E2F* to dramatically effect the localisation of *NFKB*.

In non-stimulated conditions, the NFκB:E2F-1 model successfully reproduces the nuclear co-localisation of p65-dsRedXP and EGFP-E2F-1 (Figure 5.4) shown experimentally in transfected SK-N-AS cells (section 4.1). By running the model with different initial levels of EGFP-E2F-1, the model is also able to faithfully reproduce the proportional relationship between p65-dsRedXP NR time and level of EGFP-E2F-1 (Figure 5.4). The export of *NFkB* is intuitively associated with the binding of *de-novo IkBa* to *NFkB* as it unbinds from *E2F* in the conceptual model (Section 4.5). In the mathematical model, the level of *de-novo IkBa* present at this point is the result of transcription from "free, active" nuclear NF-κB ("*nNFKB*") and the *NFkBE2F* complex. Transcription associated with the *nNFKBE2F* complex is fitted to roughly 0.6 of that of the *NFKB* complex, as suggested by transcriptional studies (Figure 4.7).

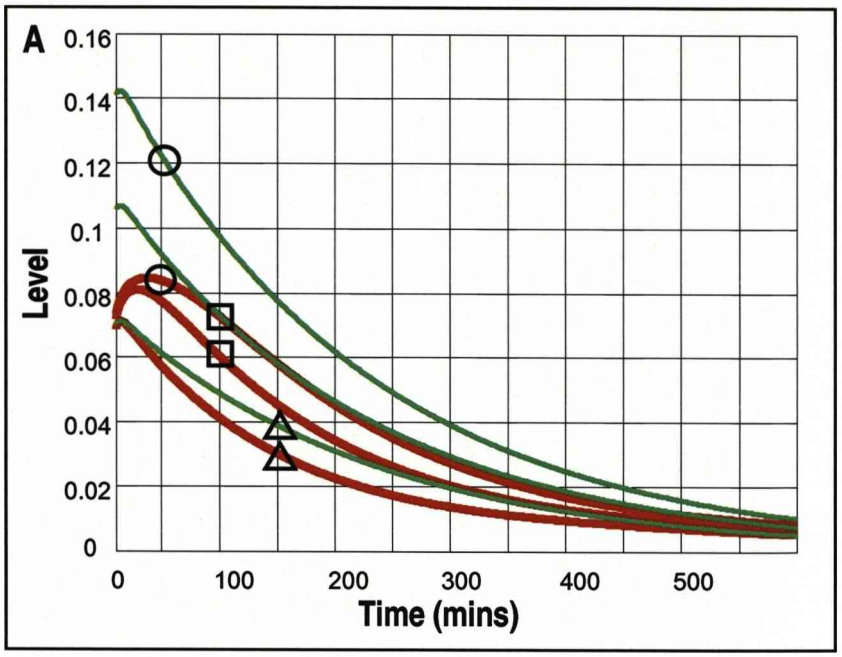
A
0.16
0.14
0.12
0.1
0.08
0.06
0.04
0.02
0
Level
0
100
200
300
400
500
Time (mins)

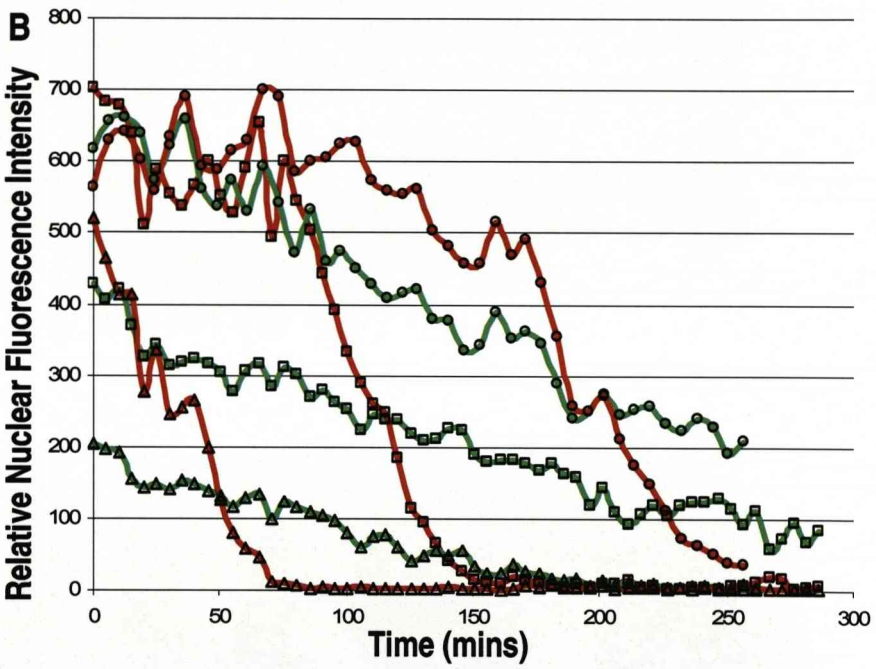
B
800
700
600
500
400
300
200
100
0
Relative Nuclear Fluorescence Intensity
0
50
100
150
200
250
300
Time (mins)

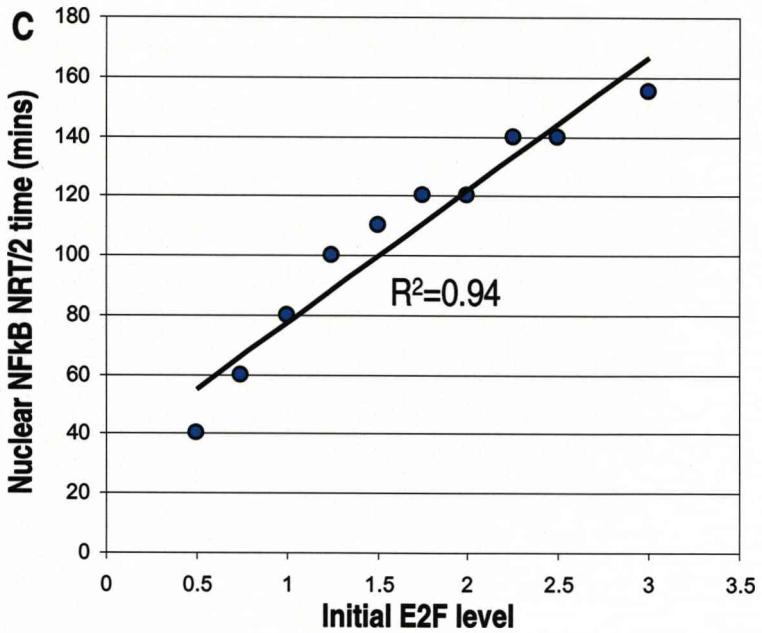

Figure 5.4 Modelling proportional sequestration of E2F-1 on NF-κB: A The NF-κB:E2F-1 model is able to reproduce a proportionally higher NFkB NR time with increase in initial levels of E2F **B** Experimental data from SK-N-AS cells expressing similar levels of p65-dsRedXP but different levels of EGFP-E2F-1. Data shows the proportional effect of EGFP-E2F-1 level of p65-dsRedXP NR time. Cells shown are representative of data set of 25+ cells. Green lines represent EGFP-E2F-1 fluorescence and are marked to correspond with red lines representing p65-dsRedXP fluorescence in the same cell. In each panel, lines with similar shapes are grouped. **C** The model is able to reproduce high correlation (R^2=0.94) between initial level of *E2F* and corresponding Nuclear Retention time of *NFkB*. See Section 6.3 for the second generation (Mk II) model.

5.5 Model predictions (1): The effect of TNFα on localisation, stability and short-term dynamics

With the NFkB:E2F-1 model able to reproduce observed dynamics in un-stimulated conditions, TNFα stimulation of the NF-κB system was used to test the model. This was a logical choice, as the scientific "questions" were straightforward to both ask of the model and to answer experimentally.

The effect of TNFα on the system was simulated over a 200 minute timescale to capture the relative dynamics of the first peak of NF-κB nuclear occupancy (Figure 5.5). The model was simulated for three different conditions; transfection with a plasmid vector expressing p65-dsRedXP alone with TNFα stimulation (*NFkB* initialised at 0.1, *TR*=1), co-expression of p65-dsRedXP and EGFP-E2F-1 with TNFα stimulation (*NFkB*

and *E2F* initialised at 0.1, *TR*=1) and, for comparison, co-expression of p65-dsRedXP and EGFP-E2F-1 in unstimulated conditions (*NFkB* and *E2F* initialised at 0.1, *TR*=0).

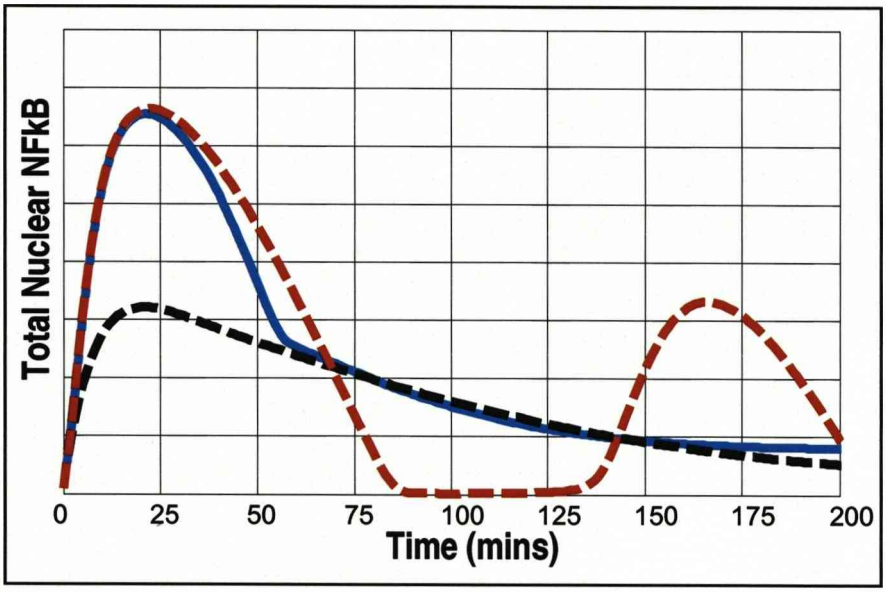

Figure 5.5 NF-κB:E2F-1 Model Prediction(1): Short time-course TNFα: The NF-κB:E2F-1 model predicts a 30 minute MNL time for *NFkB* and *E2F* co-expression (initialised at 0.1 from a steady state for the NF-κB system) with TNFα stimulation (blue line) similar to unstimulated conditions (black dotted line), and a stimulated expression of *NFkB* alone (red dotted line) although through distinct mechanisms (see text).

The model predicts that TNFα would have little effect on p65-dsRedXP MNL timing when co-expressed with EGFP-E2F-1. Intuitively this is due to TNFα not being required to cause nuclear translocation when free, cytoplasmic *E2F* coincides with free, cytoplasmic *NFkB*. However, peak amplitudes vary between stimulated and non-stimulated co-transfection conditions due to the TNFα-mediated disruption of the steady state ("endogenous") *IkBaNFkB* complex and the translocation of a second pool of free, cytoplasmic *NFkB* to the nucleus. The MNL time of p65-dsRedXP co-expressed with EGFP-E2F-1 is 30 minutes, similar to that of p65-dsRedXP expressed alone. However, the model predicts a clear difference in NR time between a single transfection of a plasmid vector expressing p65-dsRedXP and co-transfection with a vector expressing EGFP-E2F-1.

Experimental data validated these predictions (Figure 5.6, movie M5.6). The NR times of p65-dsRedXP co-expressed with EGFP-E2F-1 were similar, irrespective of TNFα stimulation and both stimulated and unstimulated cells had longer NR times than

stimulated cells expressing p65-dsRedXP alone. Due to co-expression of EGFP-E2F-1 causing a predominant nuclear localisation on p65-dsRedXP, it was difficult to measure the translocation rate of the NF-κB:E2F-1 complex as the localisation of the protein is altered from the time of cytoplasmic translation. The question of how to observe the MNL time of this association is further raised in the introduction to Chapter 7.

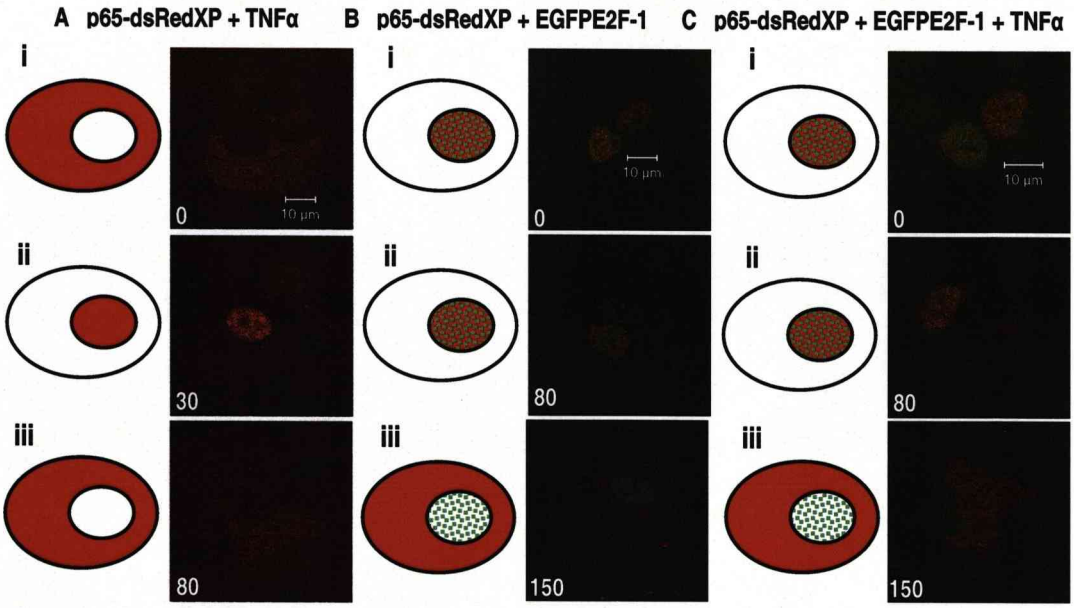

Figure 5.6 Short time-course dynamics following TNFα stimulation: A SK-N-AS cells transfected with a plasmid vector expressing p65-dsRedXP alone i) at time of stimulation showing predominant cytoplasmic localisation ii) showing predominant nuclear localisation with a MNL time of 30 minutes iii) showing predominant cytoplasmic localisation with a NR time of 50 minutes. **B** Unstimulated cells co-expressing EGFP-E2F-1 and p65-dsRedXP. Showing a ½NR time of the fluorescent p65-dsRedXP of 80 minutes and an NR of 150 minutes **C** Stimulated cells co-expressing EGFP-E2F-1 and p65-dsRedXP showing similar dynamics to unstimulated cells over a 200 minute time course.

For the purpose of explaining differences in TNFα-associated dynamics between the NF-κB model with and without active NF-κB:E2F-1 module (as well as corresponding transfection experiments), cell trajectories could be split in terms of their Maximum Nuclear Localisation (MNL) timing and Nuclear Retention (NR) timing (recalling definitions introduced in Section 1.3.3). For short time-course TNFα experiments (Figure 5.7) one may consider; the initial Maximum Nuclear Localisation time, (MNL_{NFkB} for the NF-κB model and $MNL_{NFkB:E2F}$ for the NF-κB:E2F-1 model), the post-peak 1 Nuclear Retention Time and ½ Nuclear Retention Times (NR_{NFkB}, $NR_{NFkB:E2F}$, $½NR_{NFkB}$, $½NR_{NFkB:E2F}$) and, in the case of the NF-κB model, the timing from post-peak 1 cytoplasmic localisation to the second oscillatory peak ($MNL2_{NFkB}$).

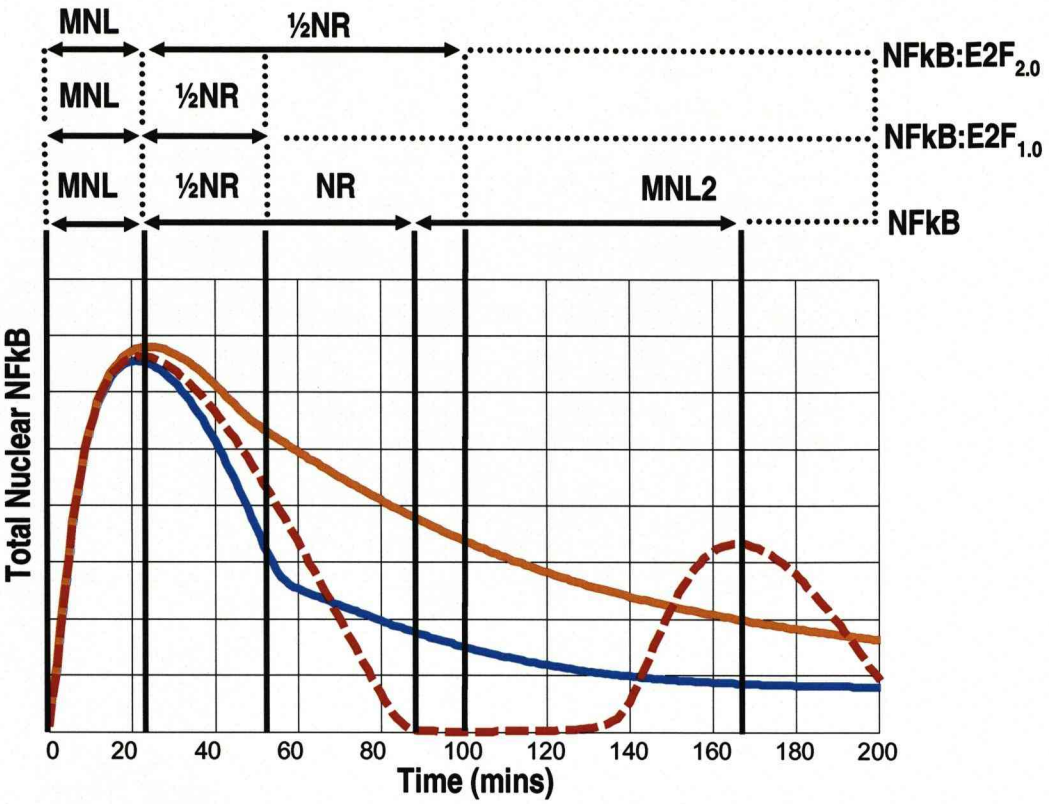

Figure 5.7 Modelling short time-course dynamics following TNFα stimulation: Showing model trajectories for total Nuclear *NFkB* with three different initial levels of *E2F*; 0, (representing single transfection of plasmid expressing p65-dsRedXP, red line), 0.1 (matched to *NFkB*, blue line) and 0.2 (giving an initial *E2F*:*NFkB* ratio of 2:1, orange line), The NF-κB:E2F-1 model is able to predict a longer p65-dsRedXP NR time with increase in initial levels of E2F-1. A higher ratio of *E2F*:*NFkB* is predicted to lead to nuclear retention which is more dependant on the degradation of the *NFkBE2F* complex than a 1:1 ratio, giving different dynamics.

As has been highlighted above, MNL_{NFkB} and $MNL_{NFkB:E2F}$ with TNFα are similar, but have differing underlying mechanisms; TNFα-mediated degradation of IκBα in the former case and binding between exogenous levels of E2F-1 and p65 in the later case. However, NR_{NFkB} and $NR_{NFkB:E2F}$ are significantly different, with NR_{NFkB} = 50 minutes (as introduced experimentally in Section 1.3.3) and $NR_{NFkB:E2F}$ seen experimentally to vary from 40 minutes to 300 minutes dependant on level of E2F-1 (see Section 4.3).

Varying the initial level of the *E2F* species in the NF-κB:E2F-1 model leads to an interesting prediction. An initial *E2F* level greater than *NFkB* (*NFkB* initialised at 0.1, *E2F* initialised at 0.2, Figure 5.7 orange line) generates a different dynamic profile to that derived from matched levels (Figure 5.7 blue line) giving a longer NR time. These

dynamics may be explained by considering how the proportional sequestration effect of E2F-1 varies with E2F-1 level, and the stimulation state of the cell. In stimulated conditions with matched transfected levels of p65 and E2F-1, there is only sufficient E2F-1 to bind to the exogenous pool of p65, leaving endogenous p65 able to translocate to the nucleus, transcribe IκBα and be "pulled" out of the nucleus by *de-novo* IκBα. However, with a level of E2F-1 equal to the total level (exogenous+ endogenous) of p65, E2F-1 is able to bind to both pools of NF-κB in the nucleus and hence NR time is slowed to the degradation rate of the NF-κB:E2F-1 complex. This can be summarised as a prediction: Co-expression of p65-dsRedXP and EGFP-E2F-1 and subsequent stimulation with TNFα should generate a split in a population of single cells based on their NR times. Cells with equal expression levels of p65-dsRedXP and EGFP-E2F-1 should have short NR times due to semi independence from sequestration by E2F-1 whereas cells with a larger ratio of E2F-1:p65 should show longer NR times due to greater dependence on the stability of the NFkB:E2F-1 complex.

Experimental evidence supported this prediction with stimulated cells expressing EGFP-E2F-1 and p65-dsRedXP at a ratio ≤ 1 showing shorter NR times than those for which the ratio of expression was > 1. The NR dynamics of these two subsets are similar to the blue and orange lines (respectively) in the model plot in Figure 5.7. Figure 5.8 shows two typical cells displaying these different dynamics. Although the two cells show similar levels of EGFP-E2F-1, their p65-dsRedXP dynamics are different due to the difference in ratio between peak level of EGFP-E2F-1 and p65-dsRedXP.

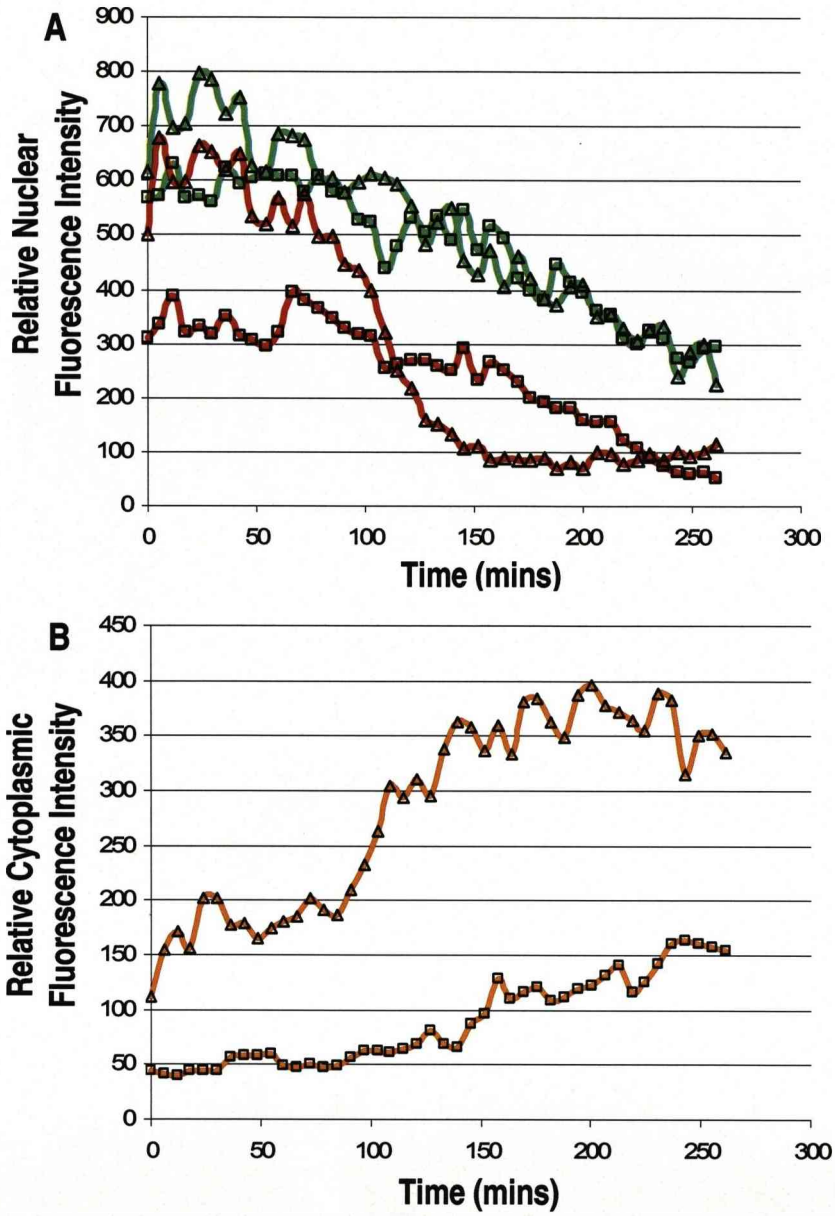

Figure 5.8 Experimental verification of effect of E2F-1:p65 ratio: A Showing SK-N-AS cells transfected with plasmids expressing p65-dsRedXP and EGFP-E2F-1. Despite similar levels of EGFP-E2F-1 the cells have different EGFP-E2F-1:p65-dsRedXP ratios. Lines marked Δ (ratio close to 1:1) show partial p65-dsRedXP independence of EGFP-E2F-1 in nuclear retention. Lines marked □ (ratio 2:1) show stronger dependence of p65-dsRedXP on EGFP-E2F-1 degradation. **B** Showing increase in relative cytoplasmic p65-dsRedXP fluoresecne levels as nuclear levels decrease due to translocation. Fluorescence intensity is measured as average intensity per pixel.

The data set of stimulated co-transfected cells show a proportional relationship between EGFP-E2F-1 ½ degradation time and $NR_{NFkB:E2F}$ (Figure 5.9) similar to unstimulated cells considered in Section 4.3. However in the case of cells in which the

initial ratio of EGFP-E2F-1 to p65-dsRedXP is >1 (green dots Figure 5.9 R^2= 0.92) there is a slower cytoplasmic translocation than in cells in which this ratio is ≤1 (pink dots Figure 5.9 R^2= 0.86).

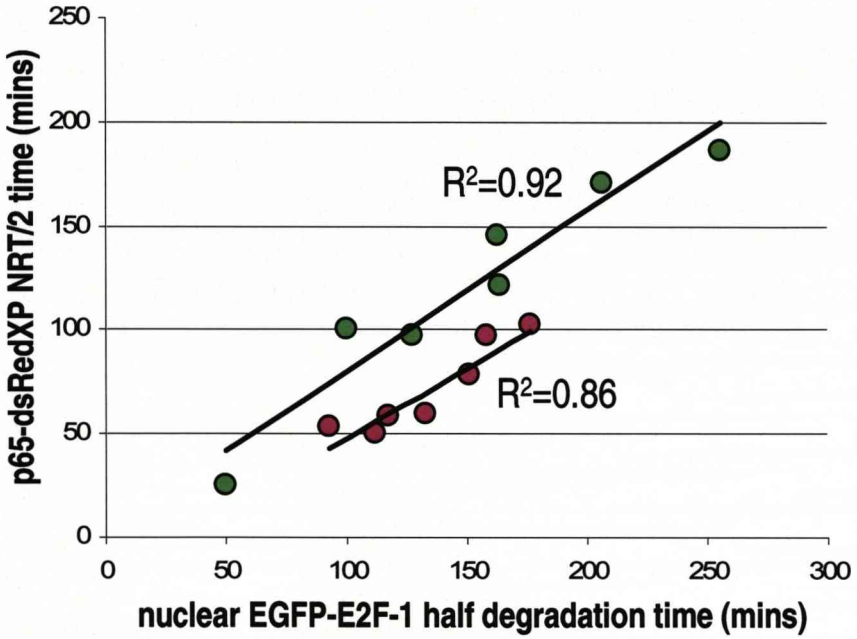

Figure 5.9 Proportional analysis of E2F-1:p65 ratio on p65 dynamics: Showing high degree of correlation between EGFP-E2F-1 degradation and p65-dsRedXP translocation into the cytoplasm. In the case of cells in which the initial ratio of EGFP-E2F-1 to p65-dsRedXP is >1 (green dots R^2= 0.92) there is a slower cytoplasmic translocation than in cells in which this ratio is ≤1 (pink dots, R^2= 0.86). Figure representative of ~20 cells.

5.6 Predictions (2) - Long time course dynamics after TNFα stimulation

Under constant TNFα stimulation, the original NF-κB model (without NF-κB:E2F-1 module) predicts experimentally observed persistent oscillations in p65-dsRedXP nuclear occupancy with MNL_{NFkB} = 20 minutes, NR_{NFkB} = 50 minutes (due to synthesis of *de-novo* IκBα), $MNL2_{NFkB}$ = 80 minutes (due to continuous activation IKK in the presence of continuous TNFα) and a subsequent peak-to-peak oscillatory period (from peak 2 onwards) of ~100 minutes as the system reaches a steady state of oscillations (Sections 1.3.3 and 5.3). The model and experimental data concur that these oscillations persist for several hours. (Section 5.3 shows NF-κB oscillations used to "test" model)

The NF-κB:E2F-1 model, however, predicts the silencing of these oscillations whilst E2F degrades. Simulating the dynamics over a long time-course (up to 12 hours), yields an interesting prediction; the resumption of steady-state NF-κB oscillatory behaviour at such a time when E2F has degraded (Figure 5.10)

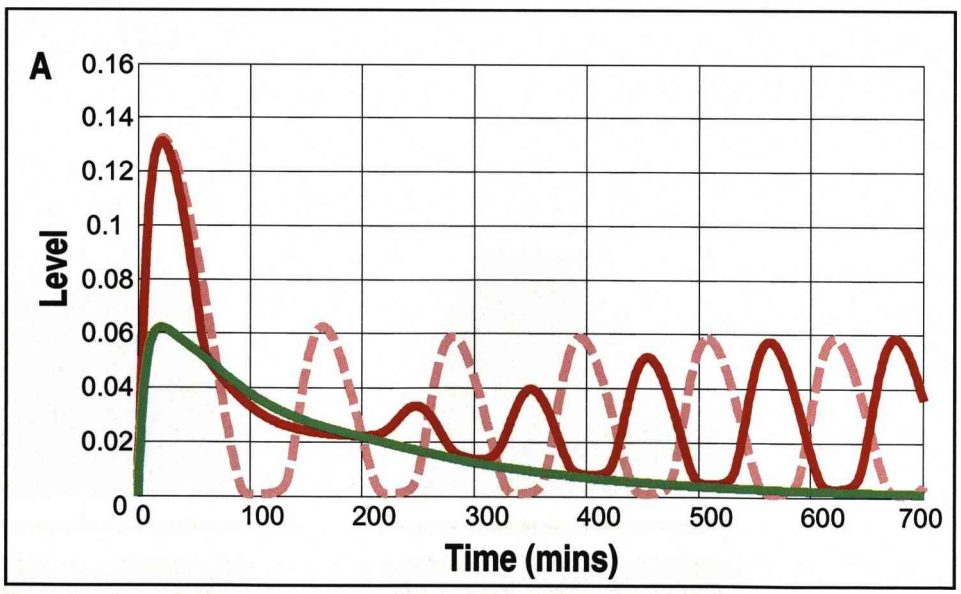

Figure 5.10 Model prediction: Long time-course dynamics following TNFα stimulation: Showing *NFkB* dynamics with *E2F* initialised at 0 (dashed pink line) and 0.1 (red line). Model predicts suspension of nucleo-cytoplasmic oscillations, to resume to a steady state upon degradation of nuclear *E2F* (green line).

Experimentally, it was observed that this was indeed the case (Figure 5.11, M5.11). In the presence of TNFα, oscillations were seen to be suspended coincident with EGFP-E2F-1 degradation, and then began several hours after the point of post-peak1 predominant cytoplasmic localisation. The suspension time (synonymous with $MNL2_{NFkB:E2F}$) is defined as the time to reach the first peak of nuclear occupancy once a steady-state has been achieved. This data set is considered further in Section 6.4.

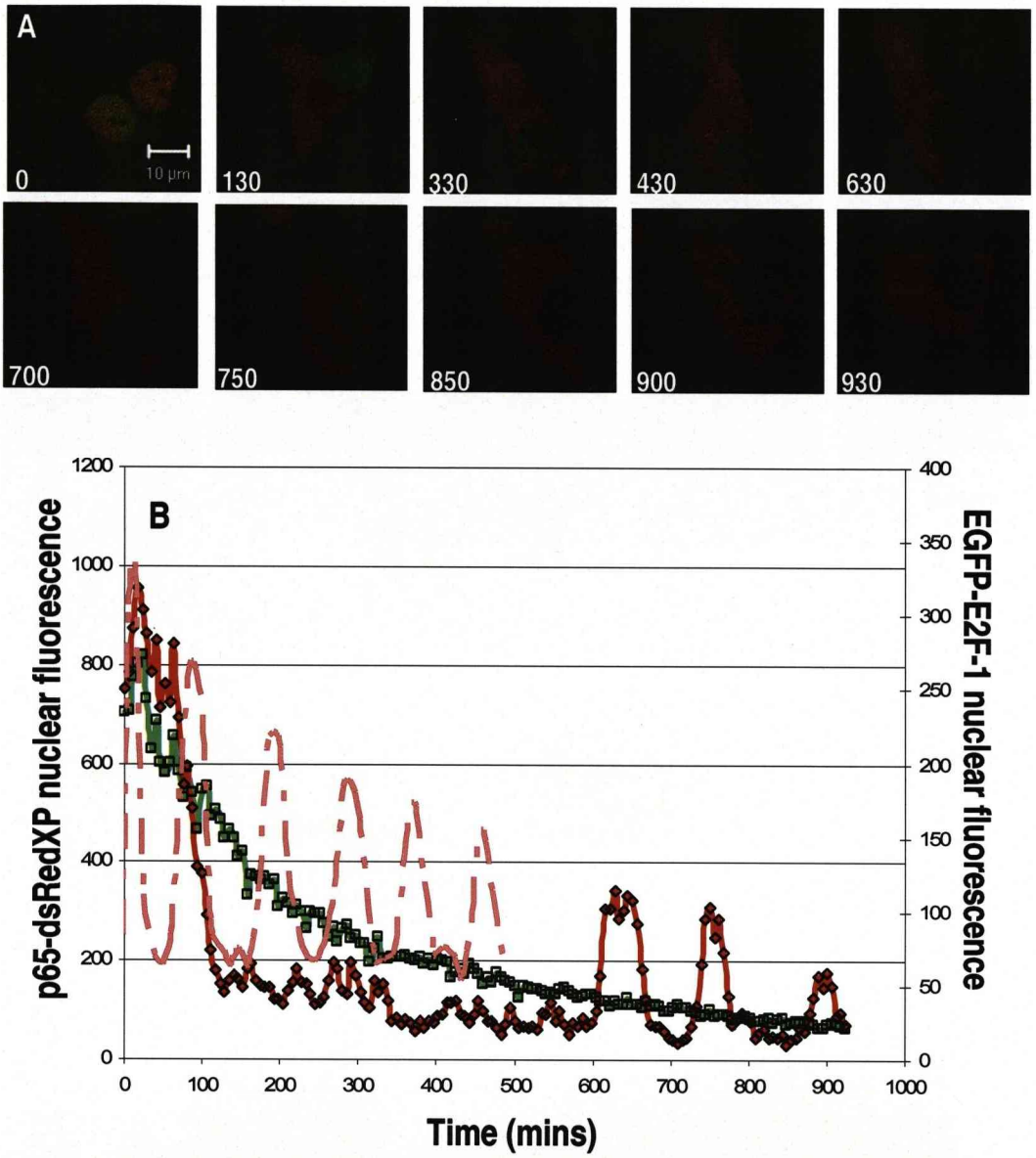

Figure 5.11 Experimental verification: Long time-course dynamics following TNFα stimulation: A Time course showing SK-N-AS cells co-expressing p65-dsRedXP and EGFP-E2F-1 stimulated with TNFα at T0. **B** Showing nuclear p65-dsRedXP dynamics (red line) and degradation of nuclear EGFP-E2F-1 (green line). Nucleo-cytoplasmic oscillations are suspended and resume coincident with the degradation of nuclear EGFP-E2F-1. Pink dashed line shows "normal" nucleo-cytoplasmic oscillations in p65-dsRedXP in a cell from the same experiment with negligible detectable levels of EGFP-E2F-1.

5.7 Discussion – How can we explain these dynamics?

In the work described in this chapter we have seen that a simple module representing interaction between E2F-1 and NF-κB is enough to reproduce experimentally observed un-stimulated dynamics of p65-dsRedXP and EGFP-E2F-1 in single SK-N-AS cells (Figure 5.4). This achieved, we have a suitable context for testing the effects of E2F-1 on the stimulated NF-κB system allowing predictions to be made (Figure 5.7). These predictions have then been experimentally verified using the same experimental model from which the original conceptual model was drawn (Figure 5.11).

We shall now consider a biological explanation for these dynamics over a long time course, to try to suggest a mechanism for the suspension of nucleo-cytoplasmic oscillations. To this end we shall analyse the NF-κB system in response to TNFα using multiple read-outs from the NF-κB:E2F-1 mathematical model to assess any insight from their relative dynamics.

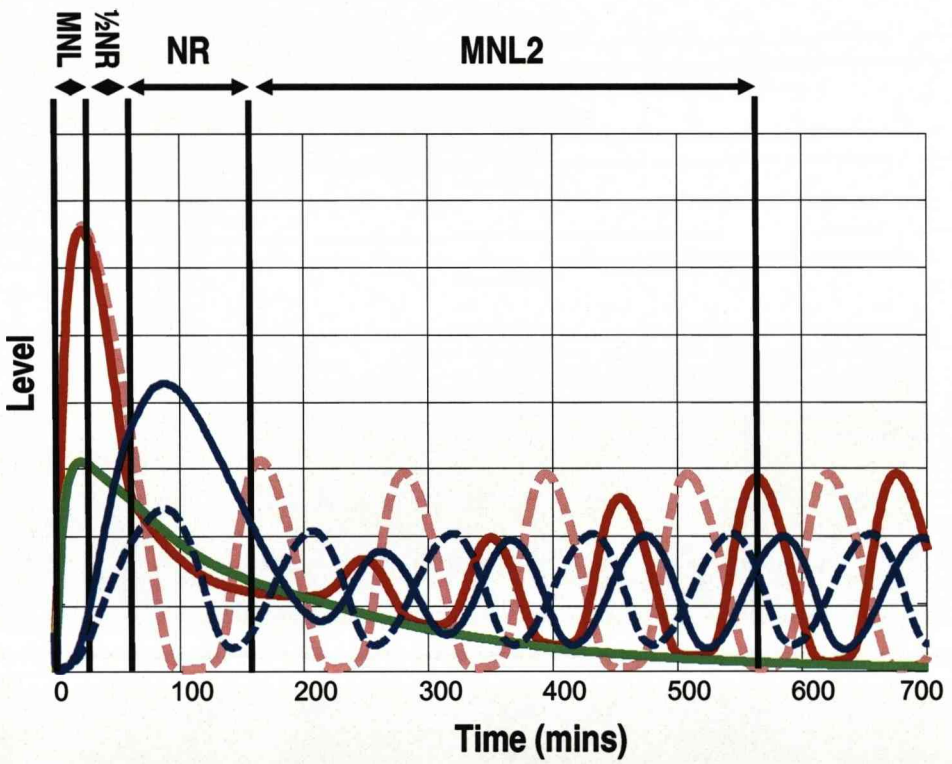

Figure 5.12 Examining long time course dynamics following TNFα stimulation: Showing identical plot to Figure 5.10 with additional species, cytoplasmic *IkBa* with *E2F* set to 0 (dashed blue line), and cytoplasmic *IkBa* with *E2F* set to 1 (blue line). Model suggests suspension in nucleo-cytoplasmic oscillations is due to increased transcription of *IkBα*.

Over a long stimulated time-course, the model predicts nucleo-cytoplasmic oscillations are suspended as both a direct and indirect result of the NFkB:E2F-1 interaction (Figure 5.12). Direct binding of *E2F* to *NFkB* gives nuclear sequestration irrespective of the presence of active TNFα (*TR*=0/1) and a higher period of nuclear retention (longer NR time with initial *E2F* set to 0.1 than 0). The interaction between *E2F* and *NFkB* leads to indirect suspension of nucleo-cytoplasmic oscillations due to the increased "pool" of cytoplasmic IκBα resulting from the prolonged nuclear occupancy of the active NF-κB complex. Intuitively, this pool of IκBa is able to sequester NF-κB in the cytoplasm for a longer period following E2F-1 degradation, as there is more to degrade leading to a suspension of steady-state oscillations ($MNL2_{NFkB:E2F} > MNL2_{NFkB}$). Although the mathematical prediction has been verified experimentally, the predicted underlying mechanism, involving the level of IκBα, has yet to be examined. In the next chapter we will examine this prediction, and begin to consider coupling the context of the model of the NF-κB system to the role of E2F-1 in the cell cycle.

Chapter 6 -

NF-κB:E2F-1 Model Evolution

6.1 Introduction and rationale

At this stage, there is a mathematical model for E2F-1 interaction with the NF-κB system, which adequately represents experimentally observed p65-dsRedXP dynamics and is able to make verifiable predictions for suspension of nucleo-cytoplasmic oscillations in p65-dsRedXP upon co-expression of EGFP-E2F-1. The model also makes accurate predictions regarding variation in ½NR time derived from different populations of transfected cells; those with a low ratio of E2F-1 to p65 having a shorter ½NR time than those in which levels are matched or higher, i.e. a proportional relationship between E2F degradation and p65 nuclear retention.

However, this initial model is not without fault. At this point it is unable to recapitulate the total cytoplasmic localisation of p65-dsRedXP in cells co-expressing EGFP-E2F-1 following the point of maximum nuclear occupancy. In such cells, p65-dsRedXP resides in a predominantly cytoplasmic state for several hours following translocation from the nucleus (Section 5.6). As the mechanism controlling re-localisation of p65-dsRedXP to the cytoplasm concerns IκBα, it was decided to investigate in greater detail how IκBα levels vary with co-expression of p65-dsRedXP and EGFP-E2F-1.

6.2 Re-assessment of transcriptional assumptions

The level of IκBα protein was measured in a population of SK-N-AS cells co-expressing EGFP-E2F-1 and p65-dsRedXP by immuno-blotting, and compared to cells transfected with a plasmid expressing p65-dsRedXP alone (Figure 6.1). Surprisingly, blots showed a lower level of IκBα protein present in cells co-expressing with E2F-1-EGFP and p65-dsRedXP compared to p65-dsRedXP single transfection or non transfected cells. This trend was common to both SK-N-AS and HeLa cell lines.

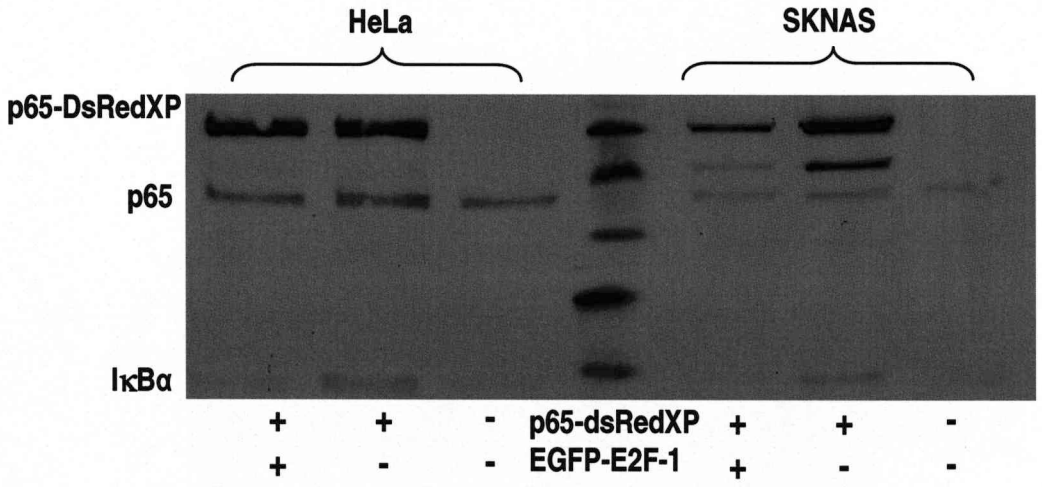

Figure 6.1 Assessment of IκBα protein levels in transfected cells: Showing populations of SK-N-AS and HeLa cells assessed for IκBα protein levels via Immunoblot. Cell samples are either untransfected, or involve co-expression of p65-dsRedXP or p65-dsRedXP and EGFP-E2F-1. Cells expressing p65-dsRedXP show higher levels of IκBα than untransfected cells. Co-expression of EGFP-E2F-1 leads to knock-down in IκBα levels in both SK-N-AS and HeLa cells. Samples were run together then the blot was cut for separate probing. A composite image was later taken of the entire blot.

Quantitative PCR was performed to assess if this result was due to E2F-1 inhibition of IκBα mRNA production rather than on the stability of the IκBα protein (Figure 6.2). It is clear that both IκBα and IκBε mRNA levels were knocked down in samples transfected with plasmids expressing p65-dsRedXP and E2F-1-EGFP. These results are interesting since they appear to contradict luciferase reporter assay data (Figure 4.7), which suggested that the effect of exogenous E2F-1 expression is to partially inhibit NF-κB-related transcription. Considered together, these data imply that although NF-κB may be transcriptionally active whilst associated with E2F-1 in the nucleus (Lim *et al.* 2007), it may not be active at either IκBα or IκBε promoters.

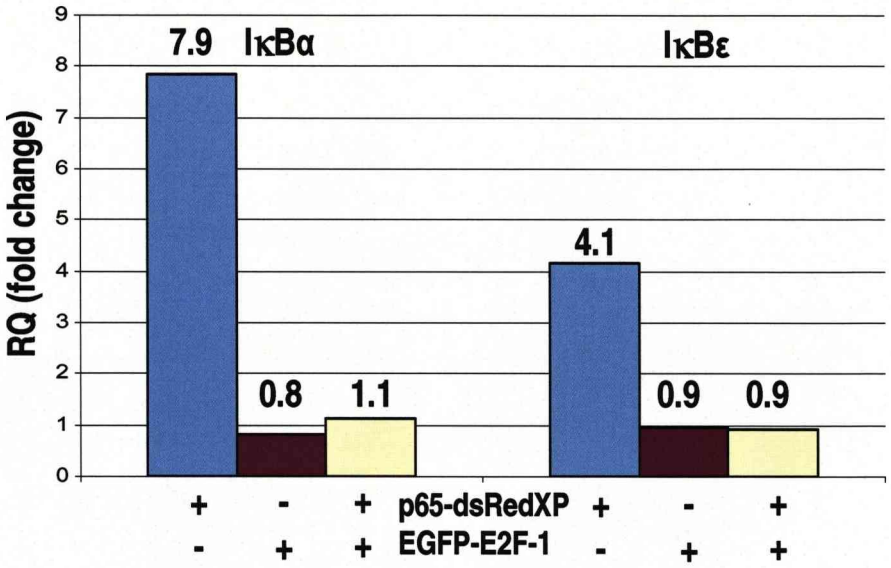

Figure 6.2 Assessment of IκB transcription levels in transfected cells: Showing populations of HeLa cells assessed for IκBα and IκBε transcription via Quantitative PCR. Samples are either transfected with plasmids expressing p65-dsRedXP, EGFP-E2F-1 or p65-dsRedXP and EGFP-E2F-1 and assessed 24 hours post-transfection. Data shown as fold induction relative to untransfected cells. Cells expressing p65-dsRedXP show induction of IκBα and IκBε transcript levels (7.9 and 4.1 fold respectively, over untransfected cells). Cells expressing EGFP-E2F-1 show no increase in IκBα or IκBε transcription levels. Cells co-expressing p65-dsRedXP and EGFP-E2F-1 show no increase IκBα or IκBε transcription levels. Single replicate.

It could be commented that E2F-1-mediated disruption of IκBα and ε transcription is inconsistent with the view of the system thus far, as IκB protein is required in the model to account for the suspension of nucleo-cytoplasmic oscillations (Figure 5.10). Having shown that ectopic E2F-1 co-expression does not lead to a larger pool of IκBα protein, the next logical hypothesis to explain sustained IκBα activity (implied by the initial model) is that IκBα stability is somehow affected by the relationship between E2F-1 and the NF-κB system.

To investigate this hypothesis, cellular lysates were made from cells transfected with plasmid vectors expressing p65-dsRedXP and E2F-1-EGFP, p65-dsRedXP alone (as positive control) and non transfected cells over a TNFα stimulation time course (Figure 6.3). Concurrent with results in Figure 6.2 the "T0" samples (non-stimulated) show lower levels of IκBα protein in p65-dsRedXP + E2F1-EGFP co-expressing cells, than in either of the controls. After 15 minutes exposure to TNFα, IκBα levels are seen to be

depleted in both cells expressing p65-dsRedXP (~10% of "0" time point) and the untransfected cells (~5% of "0" time point). However, the p65-dsRedXP + E2F1-EGFP samples show much higher levels of IκBα protein (~70% of "0" time point). A further experiment, examining a similar situation in HeLa cells, showed that after 15 minutes exposure to TNFα, IκBα levels were depleted in both cells expressing p65-dsRedXP (~40% of "0" time point) and the untransfected cells (~30% of "0" time point) with the p65-dsRedXP + E2F1-EGFP samples showing higher levels of IκBα protein (~90% of "0" time point), consistent with SK-N-AS data Having already assessed that this increased level cannot be due to increased transcription associated with ectopic EGFP-E2F-1 co-expression (Figure 6.1), this effect was assumed to occur through stabilisation of IκBα.

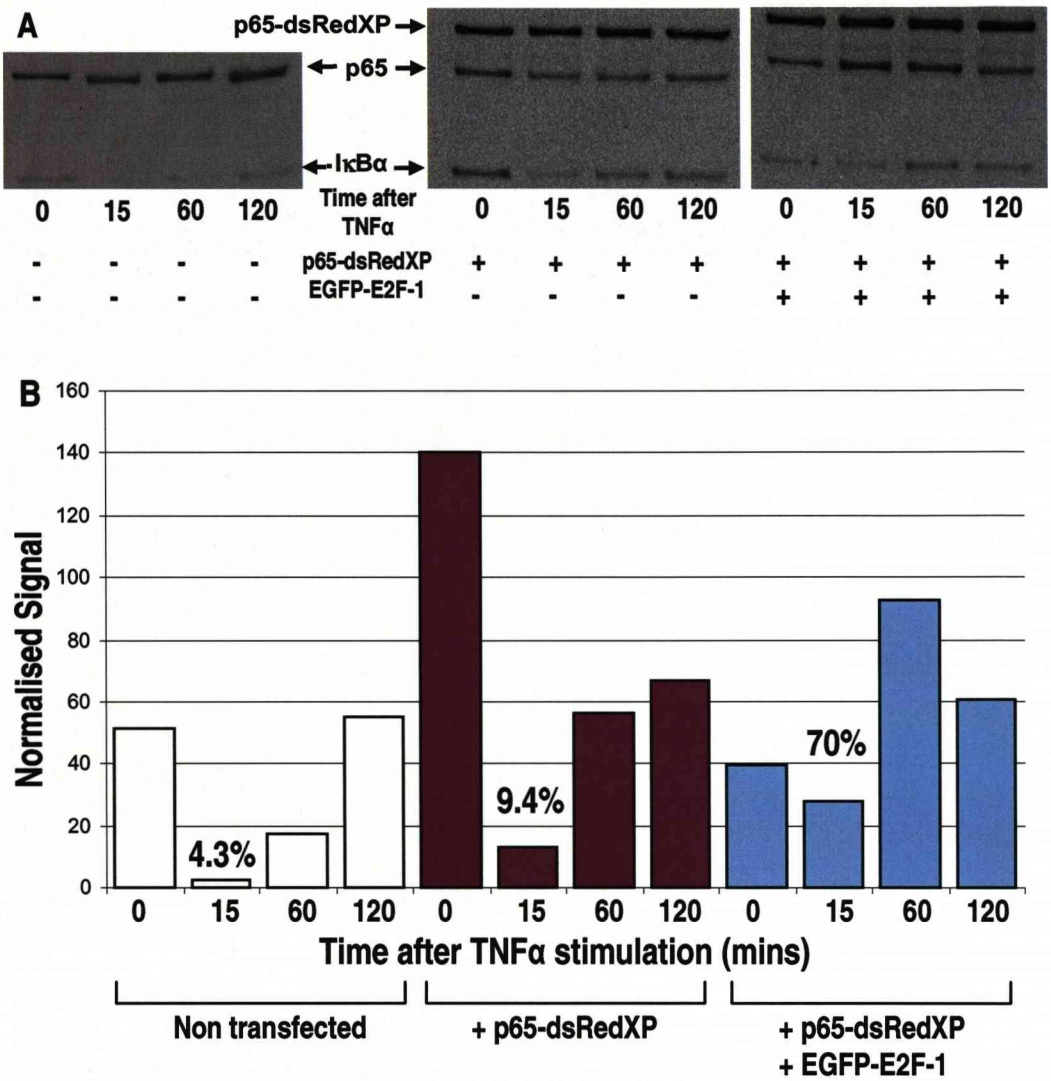

Figure 6.3 Assessment of IκBα stability in transfected cells stimulated with TNFα: Showing populations of HeLa cells either untransfected, transfected with plasmid vectors expressing p65-dsRedXP or p65-dsRedXP and EGFP-E2F-1. Samples stimulated with TNFα as indicated. **A** Western blot showing IκBα levels in transfected and untransfected samples **B** Quantification of western blot is shown in A, showing a higher level of IκBα protein after 15 minutes TNFα stimulation in cells expressing EGFP-E2F-1 and p65-dsRedXP than in untransfected cells or cells expressing p65-dsRedXP alone. Quanitfication normalised to cyclophilin A levels for each sample. Samples were run together then the blot was cut for separate probing. A composite image was later taken of the entire blot.

The apparent effect of E2F-1 on the stability of IκBα raises the question of a possible explanatory mechanism. The literature suggests a role for E2F-1 in regulating the activity of the IκB kinase, IKK (Phillips *et al.* 1999). Such regulation could explain the lack of IKK-mediated degradation of IκBα and an increase in IκBα stability despite the presence of TNFα. Supporting this theory, further work was carried out to investigate the effect of exogenous E2F-1 expression on TNFα-mediated NF-κB related transcription. Figure 6.4 shows the clear effect of TNFα stimulation on NF-κB related transcription in cells transfected with empty vectors, due to the concomitant rise in IKK activity, IκBα degradation and release of active NF-κB to translocate into the nucleus and begin transcription. As such, the dramatic effect TNFα has on the equilibrium of the NF-κB system may be observed. However, expression of EGFP-E2F-1 is seen to inhibit this process, consistent with inhibition of IKK activity.

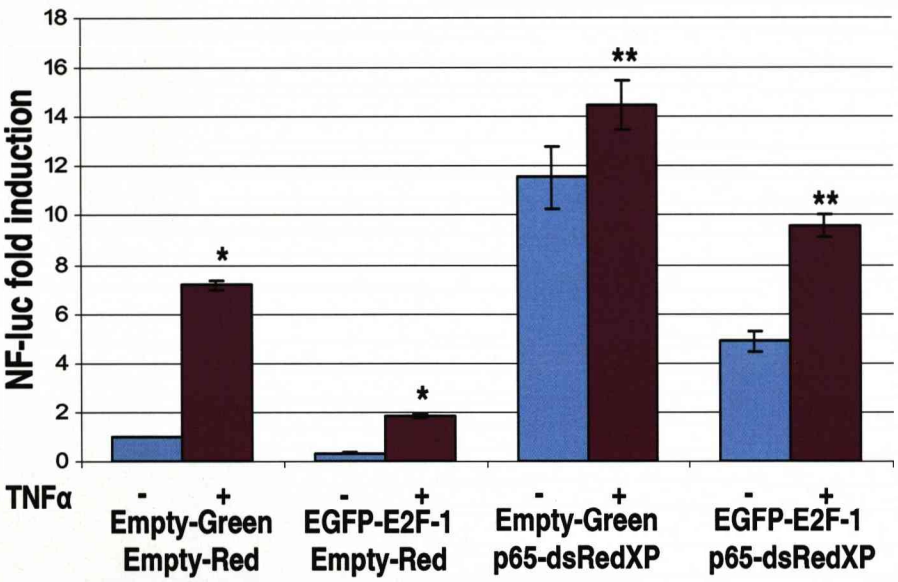

Figure 6.4 The effect of exogenous E2F-1 on TNFα stimulated NF-κB transcription: Showing luciferase reporter assay using NF-luciferase reporter. Expression of EGFP-E2F-1 causes significant fold decrease in NF-κB related transcription (*) under populations of cells stimulated for 6 hours with TNFα (red bars). This effect is consistent to similar populations of cells co-expressing with p65-dsRedXP (**). Unstimulated samples represented by blue bars. Representative of 3 biological replicates +/- SEM in each case.

To investigate the effect of E2F-1 on IKK-mediated degradation of exogenous IκBα and the dynamics of p65-dsRedXP (the model system output characterised in Chapter 3) time-lapse microscopy experiments were carried out in the presence of exogenous IκBα (Figures 6.5 and 6.6). SK-N-AS cells transfected with plasmid vectors expressing p65-dsRedXP and IκBα-AmCyan, show a steady-state predominant cytoplasmic localisation for p65-dsRedXP. TNFα stimulation gives a p65-dsRedXP MNL which varies dependent on the level of exogenous IκBα in the cell (Figure 6.5, movie M6.5 as shown in (Nelson *et al.* 2002)).

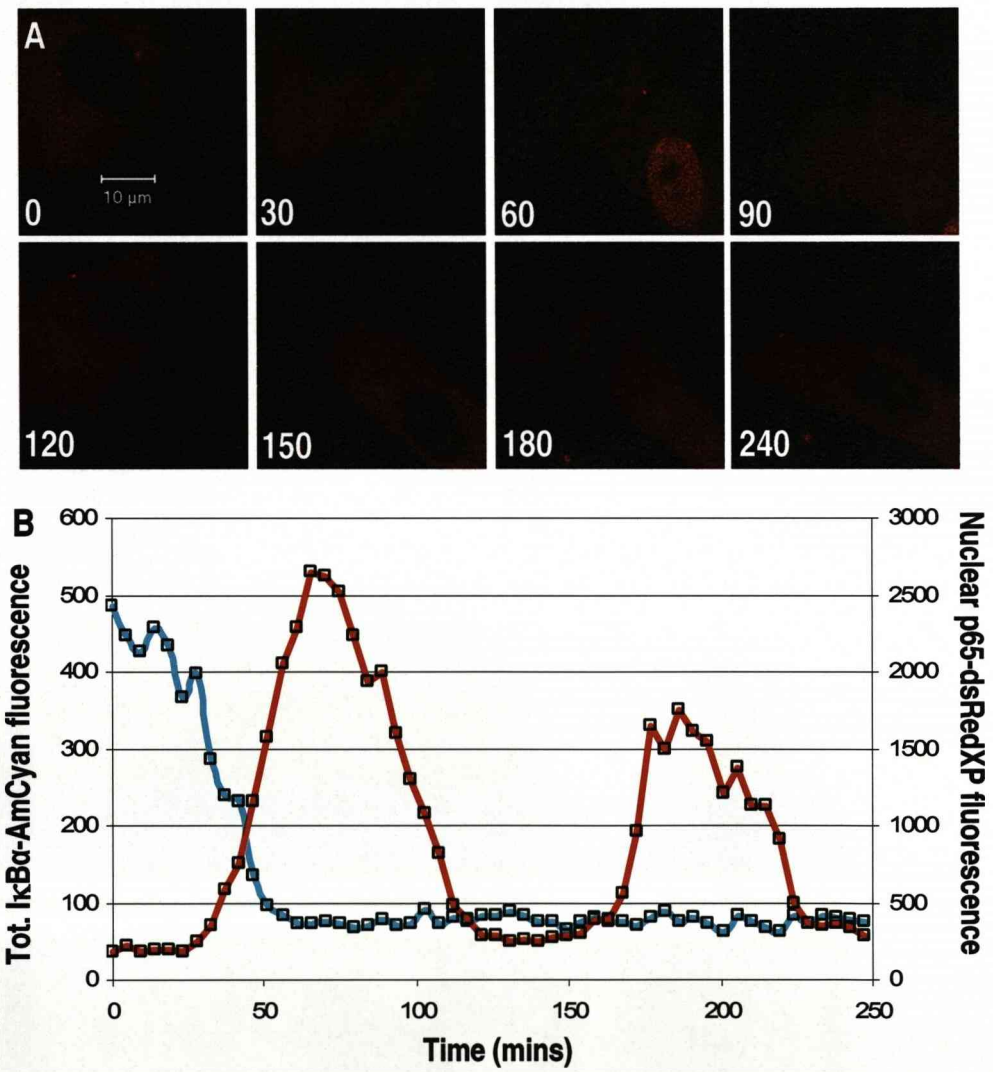

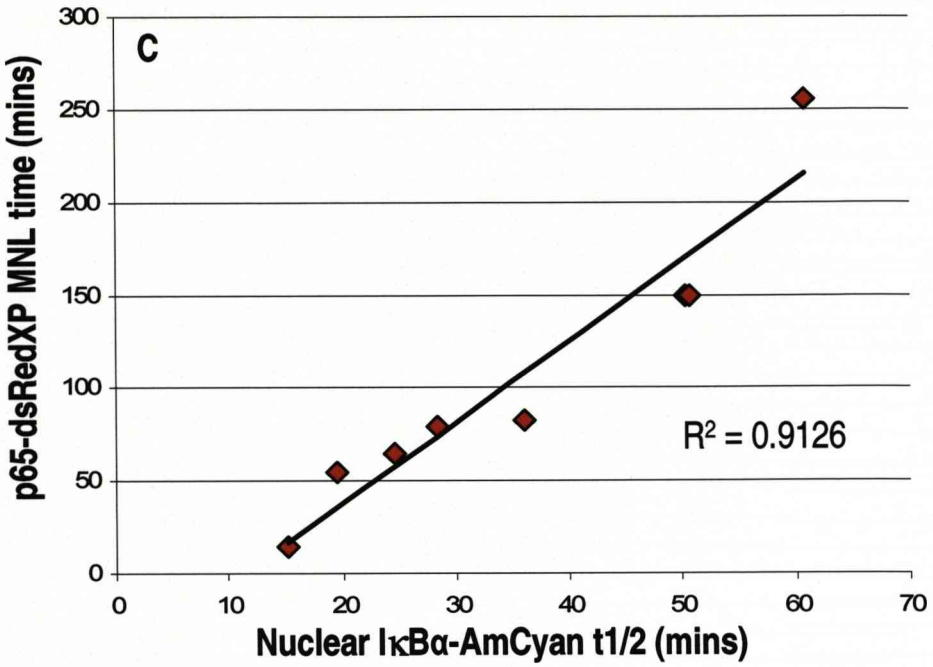

Figure 6.5 Dynamics of p65-dsRedXP with IκBα-AmCyan after TNFα stimulation: A Time-course for p65-dsRedXP in SK-N-As cells, showing MNL time of 60 minutes and NR time of 90 minutes when ectopically expressing IκBα. **B** Analysis of IκBα-AmCyan degradation (blue line) and p65-dsRedXP dynamics (red line) from cell shown in A. **C** Strong correlation (R2=0.9126) between fitted half-life of IκBα-AmCyan and MNL time of p65-dsRedXP in population of single SK-N-AS cells. Chart representative of 10 cells.

To assess the effect of exogenous expression of EGFP-E2F-1 on these dynamics, triple transfection experiments were planned. However, the overlapping emission spectra of the Enhanced Green and AmCyan fluorescent proteins made simultaneous detection of exogenous p65-dsRedXP, EGFP-E2F-1 and IκBα-AmCyan difficult. To circumvent this problem a plasmid vector expressing an IκBα-AmCyan fusion protein was transfected into cells but not observed, which is an acceptable alteration to experimental conditions as the output from the system, p65-dsRedXP translocation, remains visible and is itself dependant on the degradation of IκBα.

SK-N-AS cells transfected with plasmid vectors expressing p65-dsRedXP, a non-fluorescent IκBα fusion protein and EGFP-E2F-1, also showed a steady-state predominant cytoplasmic localisation for p65-dsRedXP. However, TNFα stimulation yielded a greatly increased p65-dsRedXP MNL time, which was seen to vary

dependent on the degradation time of cytoplasmic EGFP-E2F-1 in the cell (Figure 6.6, movie M6.6).

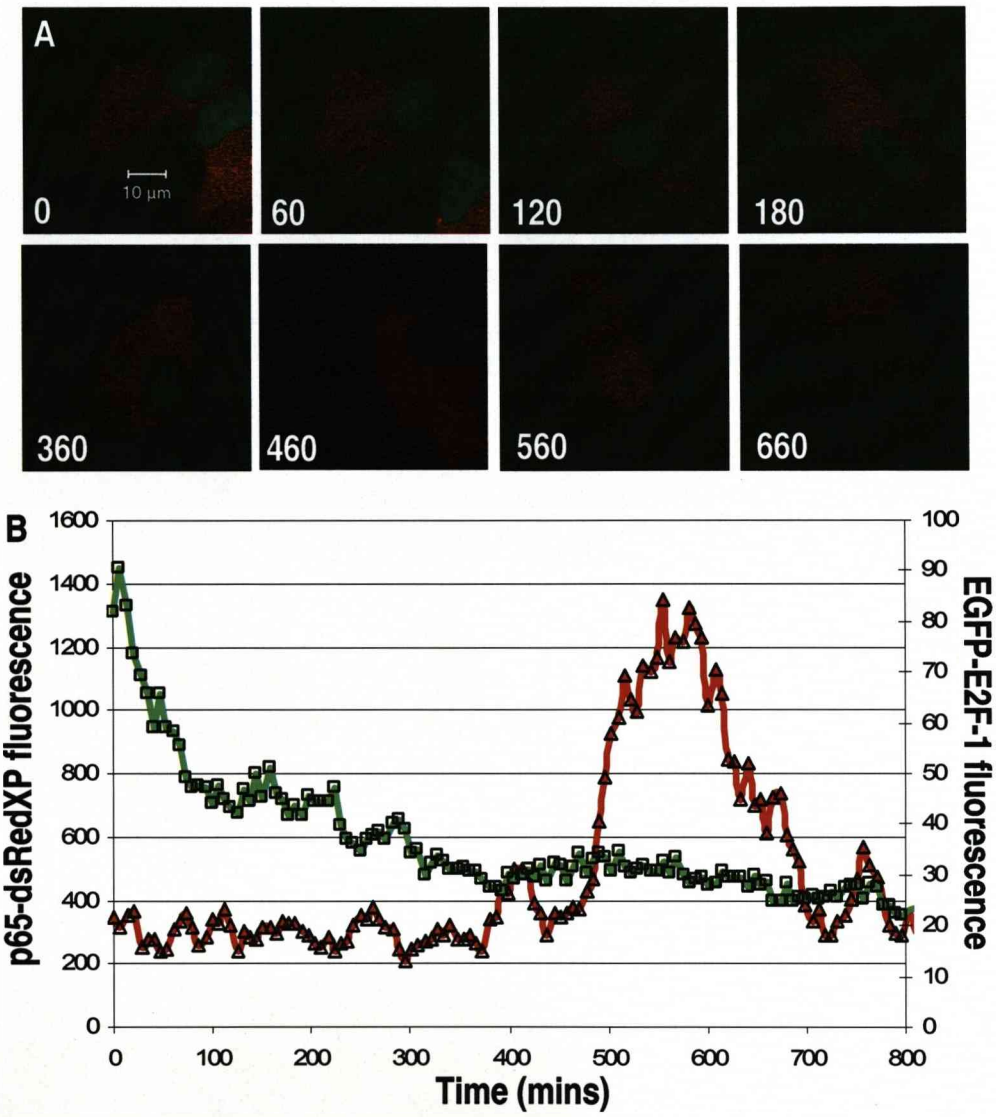

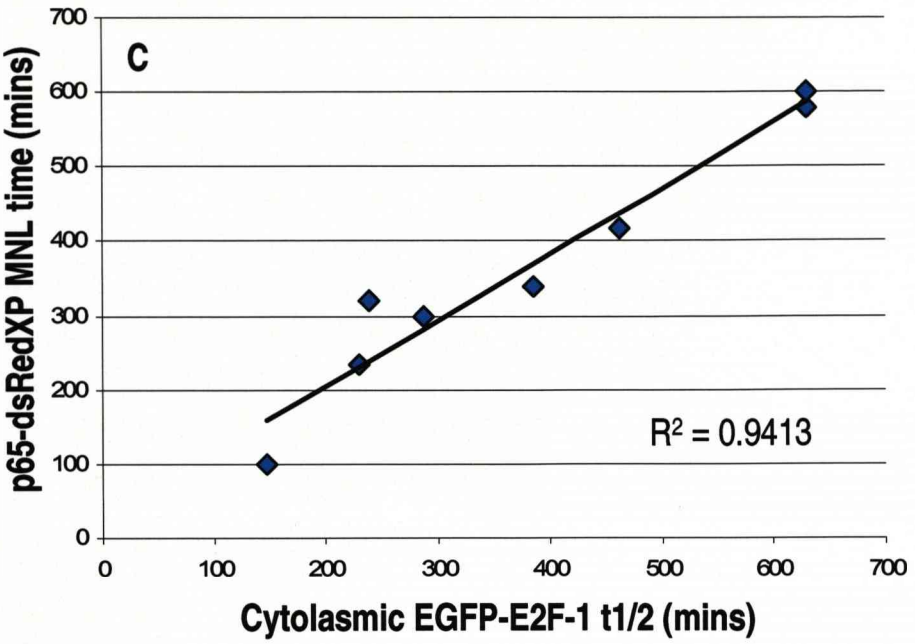

Figure 6.6 Dynamics of p65-dsRedXP with EGFP-E2F-1 and exogenous IκBα after TNFα stimulation: A Time-course for p65-dsRedXP in SK-N-AS cells, showing MNL time of ~500 minutes following stimulation when co-transfected with plasmid vectors expressing EGFP-E2F-1 and exogenous IκBα-AmCyan. Nuclear translocation coincides with the loss of cytoplasmic EGFP-E2F-1 fluorescence **B** Analysis of cytoplasmic EGFP-E2F-1 degradation and p65-dsRedXP dynamics from cell shown in A. **C** Strong correlation (R^2=0.9413) between fitted half-life of cytoplasmic EGFP-E2F-1 and MNL time of p65-dsRedXP in population of single SK-N-AS cells. Chart representative of 10 cells.

6.3 Model evolution

The first adjustment to the NF-κB:E2F-1 mathematical model involved IκBα transcription. Although initial transcriptional studies and previously published work (Lim *et al.* 2007) show a positive effect of E2F-1 on the regulation of certain NF-κB target genes, it has been subsequently suggested that exogenous expression of E2F-1 causes a knock-down in transcription of both IκBα and IκBε (Figures 6.2 and 6.3). Within the model, it was subsequently assumed that the nuclear NF-κB:E2F-1 species (*nNFkBE2F*) does not contribute to the production of the IκBα transcript (*tIkBa*). As such, levels of *tIkBa* rise only as the level of free nuclear NF-κB (*nNFkB*) rises, proportional to the disruption of the *nNFkBE2F* complex. For the model, this effect is assumed to be common to A20, based on previous studies showing similar regulatory mechanisms between IκBα and A20 promoters (Ainbinder *et al.* 2002).

Secondly, the model was extended to consider inhibition of IKK activity by the cytoplasmic fraction of E2F-1. Interestingly, the model made a prediction at this stage. As the cytoplasmic fraction of EGFP-E2F-1 accounts for only 10% of total E2F-1 (Figure 3.2), cytoplasmic E2F-1 (model species *E2F*) was seen to degrade quickly in the initial model, so that inhibition of IKK had little effect on the timing of nucleo-cytoplasmic oscillations. In short, the model predicts that in order to fit the suspension of oscillations with a mechanism involving cytoplasmic E2F-1 inhibition of IKK, cytoplasmic E2F-1 must have a longer half-life than nuclear E2F-1.

Experimentally it was observed that is indeed the case (Figure 6.7) Pooling data from all time-lapse imaging experiments involving EGFP-E2F-1, protein degradation curves were fitted to exponential functions from which degradation rates were taken. These values were then used to calculate the half-life of the EGFP-E2F-1 in nuclear and cytoplasmic compartments for each cell in a data set of 40+ cells, using the expression $\mathrm{Ln}(2)/\lambda$. The resultant data set shows an average half-life for nuclear EGFP-E2F-1 of 240 minutes compared to 440 minutes for cytoplasmic EGFP-E2F-1. Performing a paired t-test a clear statistical significance may be seen ($p\text{-value}=1.8\times10^{-8}$).

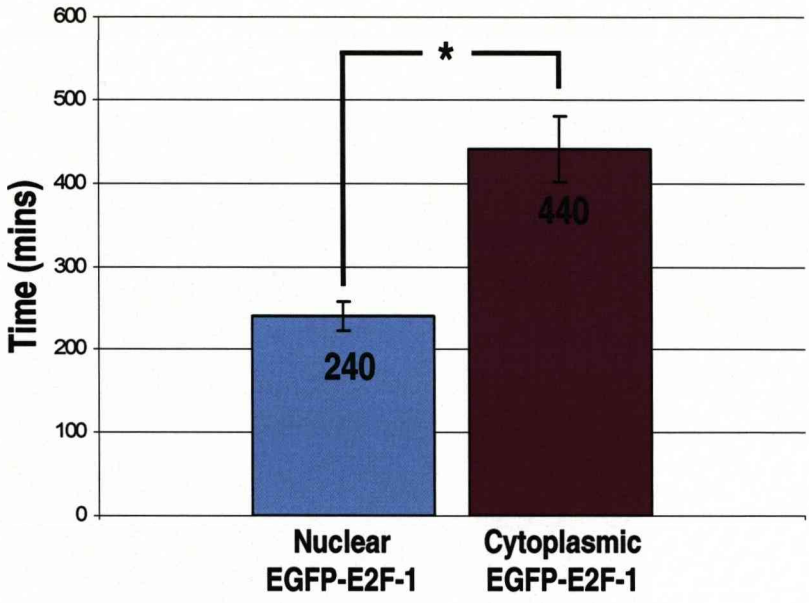

Figure 6.7 Estimated half-life of EGFP-E2F-1 in nucleus and cytoplasm: A The half-life of nuclear and cytoplasmic EGFP-E2F-1 was calculated by fitting an exponential function to degradation curves generated by time lapse imaging experiments. The λ value for these lines were then used to calculate to estimated half-life of EGFP-E2F-1 in a cell specific manner, using Ln(2)/λ. The resultant data set shows an average half-life of nuclear EGFP-E2F-1 of 240 minutes compared to 440 minutes for cytoplasmic EGFP-E2F-1. A paired T-test revealed this difference to be significant (* $P=1.8x10^{-8}$). Data taken from 40+ SK-N-AS cells.

The degradation coefficient of *E2F* (*g3*) was adjusted with respect to *nE2F* (*g4*) fitting to experimental data (Table 6.1). Inhibition of IKK was modelled as a reinforcement of the IKK inactivation (Table 6.1) and was best fitted as a 2nd order term proportional to the total amount of cytoplasmic E2F-1 (*E2F* + *NFkBE2F*).

To improve the fitting of the new model, competition between E2F-1 and IκBα for binding to NF-κB was re-addressed. Dissociation of *NFkBE2F* and *nNFkBE2F* is not enough to drive total cytoplasmic localisation in the new model as the level of de-novo IκBα is not high enough to compete with free nuclear *E2F*, leading to rebinding between *nE2F* and free nuclear *NFkB*. To overcome this issue, it was assumed that IκBα is capable of disrupting nuclear and cytoplasmic complexes of NF-κB and E2F-1 (Table 6.1).

original model term	latest model	designed to affect	experimental rationale
A *kg3 = 0.0005/3, kg4 = 0.0005/3, kg3 = 0.0005/5, kg4 = 0.0005/3*	*kg3 = 0.0005/5, kg4 = 0.0005/3, kg13 = 0.0005/5, kg14 = 0.0005/3*	*E2F,nE2F NFkBE2F, nNFkBE2F*	half-life of cyto E2F-1 longer than nuclear E2F-1 (Figure 6.7)
B *0.6*kiscpt1* (nNFkBE2F^h/(nNFkBE2F^h + k^h))*	*0*kiscpt1* (nNFkBE2F^h/(nNFkBE2F^h + k^h))*	*tIkba, tA20*	null transcription from NF-κB whilst bound to E2F-1 (Figure 6.2)
C *kinact1*IKK*	*kinact1*((kact2+E2F^2+NFkBE2F^2)/kact2)*IKK*	*IKKi, IKK*	IKK inactivation by E2F-1 (assumed from Figure 6.3)
D -	*kd7b*NFkBE2F* IkBa*	*NFkBE2F, nNFkBE2F, E2F, nE2F, IkBaNFkB, nIkBaNFkB, IkBa, nIkBa*	extra intermediate term to account for IκBα disruption of NF-κB:E2F1 binding, inferred by competition, required to drive cytoplasmic localisation

Table 6.1 NF-κB:E2F-1 mathematical model Mk.II evolutionary steps: A Difference in average EGFP-E2F-1 t½ between nuclear and cytoplasmic compartments **B** EGFP-E2F-1 ablation of IκBα and IκBε transcription **C** Cytoplasmic E2F-1 related inhibition of IKK activity **D** Disruption of the NFkB:E2F-1 complexes by IκBα.

The model equations that were altered as a result of these evolutionary steps are shown in Table 6.2.

$$\frac{d}{dt}E2F(t) = -ki2\times E2F(t) + ke2\times nE2F(t) - kg3\times E2F(t) + kd3\times(NF\kappa B:E2F)(t) - ka3\times E2F(t)\times NF\kappa B(t) + kd7b\times(NF\kappa B:E2F)(t)\times I\kappa B\alpha(t) \quad (3)$$

$$\frac{d}{dt}nE2F(t) = +ki2\times kv\times E2F(t) - ke2\times kv\times nE2F(t) - kg4\times nE2F(t) + kd7\times(nNF\kappa B:nE2F)(t) - ka7\times nE2F(t)\times nNF\kappa B(t) + kd7b\times(nNF\kappa B:nE2F)(t)\times nI\kappa B\alpha(t) \quad (4)$$

$$\frac{d}{dt}tI\kappa B\alpha(t) = kiscpt1\times 0\times\frac{nNF\kappa B:nE2F^h(t)}{nNF\kappa B:nE2F^h(t)+k^h} + kiscpt1\times\frac{nNF\kappa B^h(t)}{nNF\kappa B^h(t)+k^h} - kg5\times tI\kappa B\alpha(t) \quad (5)$$

$$\frac{d}{dt}I\kappa B\alpha(t) = kd1\times(I\kappa B\alpha:NF\kappa B)(t) - ka1\times I\kappa B\alpha(t)\times NF\kappa B(t) + ktrl1\times tI\kappa B\alpha(t) - kg6\times I\kappa B\alpha(t) - ki3\times I\kappa B\alpha(t) + ke3\times nI\kappa B\alpha(t) - kc1\times IKK(t)\times I\kappa B\alpha(t) - kd7b\times(NF\kappa B:E2F)(t)\times I\kappa B\alpha(t) \quad (6)$$

$$\frac{d}{dt}nI\kappa B\alpha(t) = kd6\times(nI\kappa B\alpha:nNF\kappa B)(t) - ka6\times nI\kappa B\alpha(t)\times nNF\kappa B(t) - kg7\times nI\kappa B\alpha(t) + ki3\times kv\times I\kappa B\alpha(t) + ke3\times kv\times nI\kappa B\alpha(t) - kd7b\times(nNF\kappa B:nE2F)(t)\times nI\kappa B\alpha(t) \quad (7)$$

$$\frac{d}{dt}IKK(t) = TR\times kact1\times IKKn(t) - kinact1\times\frac{kact2+E2F^2(t)+(NF\kappa B:E2F)^2(t)}{kact2}\times IKK(t) \quad (9)$$

$$\frac{d}{dt}IKKi(t) = kinact1\times\frac{kact2+E2F^2(t)+(NF\kappa B:E2F)^2(t)}{kact2}\times IKK(t) - kpd\times\frac{kiA20}{kiA20+TR\times A20(t)}\times IKKi(t) \quad (10)$$

$$\frac{d}{dt}tA20(t) = kiscpt2\times 0\times\frac{nNF\kappa B:nE2F^h(t)}{nNF\kappa B:nE2F^h(t)+k^h} + kiscpt2\times\frac{nNF\kappa B^h(t)}{nNF\kappa B^h(t)+k^h} - kg11\times tA20(t) \quad (11)$$

$$\frac{d}{dt}(NF\kappa B:E2F)(t) = ka3\times E2F(t)\times NF\kappa B(t) - kd3\times(NF\kappa B:E2F)(t) - ki4\times(NF\kappa B:E2F)(t) + ke4\times(nNF\kappa B:nE2F)(t) - kg13\times(NF\kappa B:E2F)(t) - kd7b\times(nNF\kappa B:nE2F)(t)\times nI\kappa B\alpha(t) \quad (17)$$

$$\frac{d}{dt}(nNF\kappa B:nE2F)(t) = ka7\times nE2F(t)\times nNF\kappa B(t) - kd7\times(nNF\kappa B:nE2F)(t) + ki4\times kv\times(NF\kappa B:E2F)(t) - ke4\times kv\times(nNF\kappa B:nE2F)(t) - kg14\times(nNF\kappa B:nE2F)(t) - kd7b\times(nNF\kappa B:E2F)(t)\times nI\kappa B\alpha(t) \quad (18)$$

$$\frac{d}{dt}(I\kappa B\alpha:NF\kappa B)(t) = ka1\times I\kappa B\alpha(t)\times NF\kappa B(t) - kd1\times(I\kappa B\alpha:NF\kappa B)(t) - kg1\times(I\kappa B\alpha:NF\kappa B)(t) + ke6\times(nI\kappa B\alpha:nNF\kappa B)(t) - kc2\times IKK(t)\times(I\kappa B\alpha:NF\kappa B)(t) + kd7b\times(NF\kappa B:E2F)(t)\times I\kappa B\alpha(t) \quad (21)$$

$$\frac{d}{dt}(nI\kappa B\alpha:nNF\kappa B)(t) = ka6\times nI\kappa B\alpha(t)\times nNF\kappa B(t) - kd6\times(nI\kappa B\alpha\circ nNF\kappa B)(t) - ke6\times kv\times(nI\kappa B\alpha\circ nNF\kappa B)(t) - kg2\times(nI\kappa B\alpha:nNF\kappa B)(t) + kd7b\times(nNF\kappa B:nE2F)(t)\times nI\kappa B\alpha(t) \quad (22)$$

Table 6.2 Reactions affected by the evolution of the NF-κB:E2F-1 model MkII: Showing ODEs from the MkI model that have been altered as a result of evolutionary steps (alterations shown in red).

6.4 Suspended oscillations revisited

Previously, the initial NF-κB:E2F-1 mathematical model was tested through prediction of suspended nucleo-cytoplasmic oscillations in p65-dsRedXP when co-transfected with a plasmid expressing EGFP-E2F-1 and stimulated with TNFα (Figure 5.12). It is now possible to revisit this work, firstly to show that the Mk.II mathematical model is capable of similar predictions, albeit through differing mechanisms (Figure 6.8). Here it is shown that the suspension time (equivalent to the second peak of maximum steady-state localisation, MNL2) is proportional to the degradation time of cytoplasmic EGFP-E2F-1, giving strong correlation (R^2=0.972) which the model is able to reproduce. Interestingly, the MkII model also reproduces the lengthening of NF-κB MNL time with increase in initial E2F-1 level.

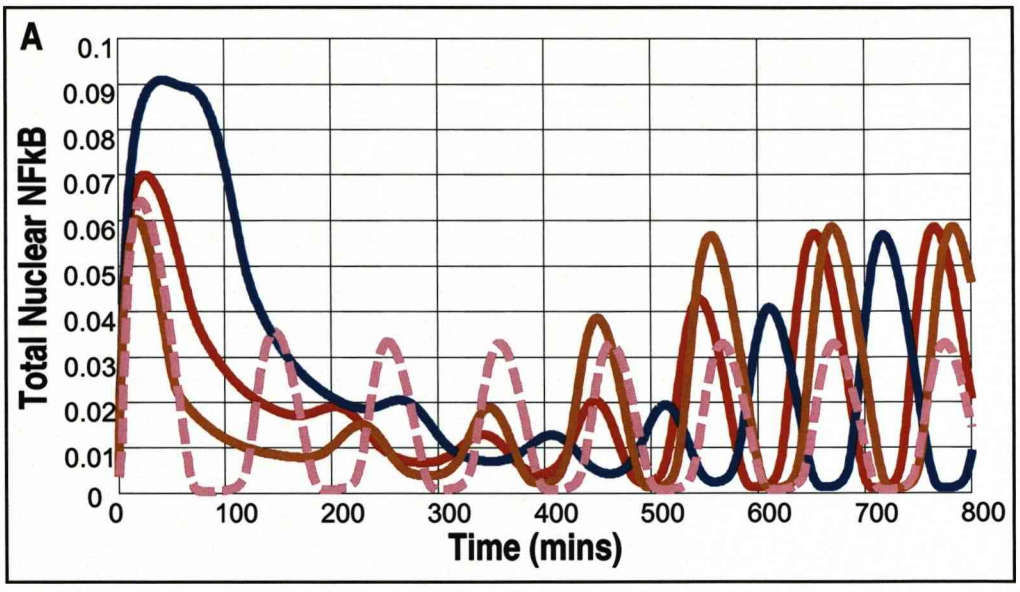
A
Total Nuclear NFkB
0.1
0.09
0.08
0.07
0.06
0.05
0.04
0.03
0.02
0.01
0
0
100
200
300
400
500
600
700
800
Time (mins)

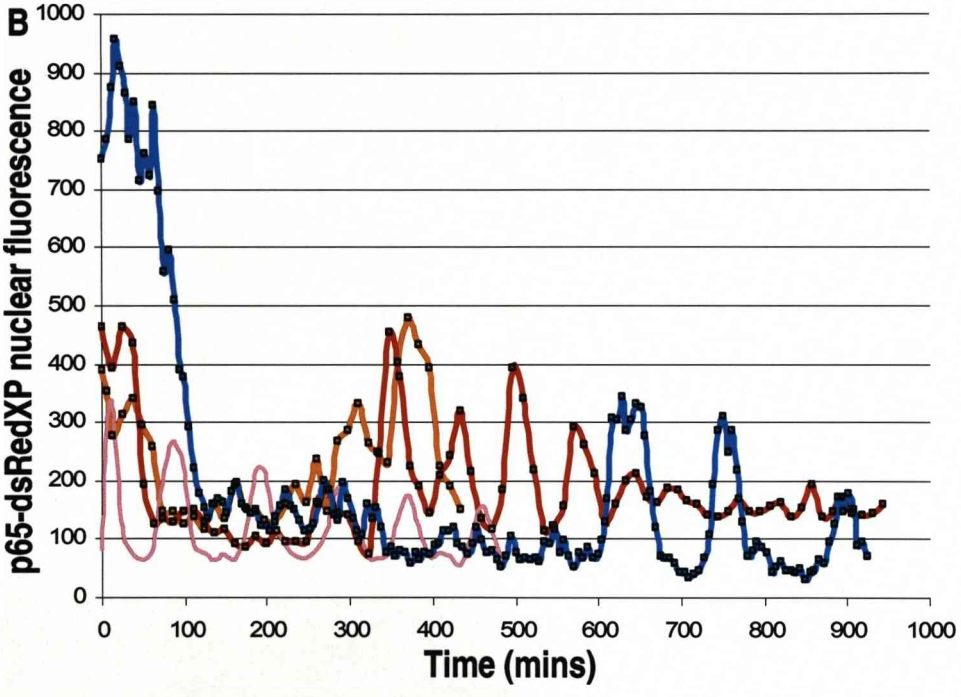
B
p65-dsRedXP nuclear fluorescence
1000
900
800
700
600
500
400
300
200
100
0
0
100
200
300
400
500
600
700
800
900
1000
Time (mins)

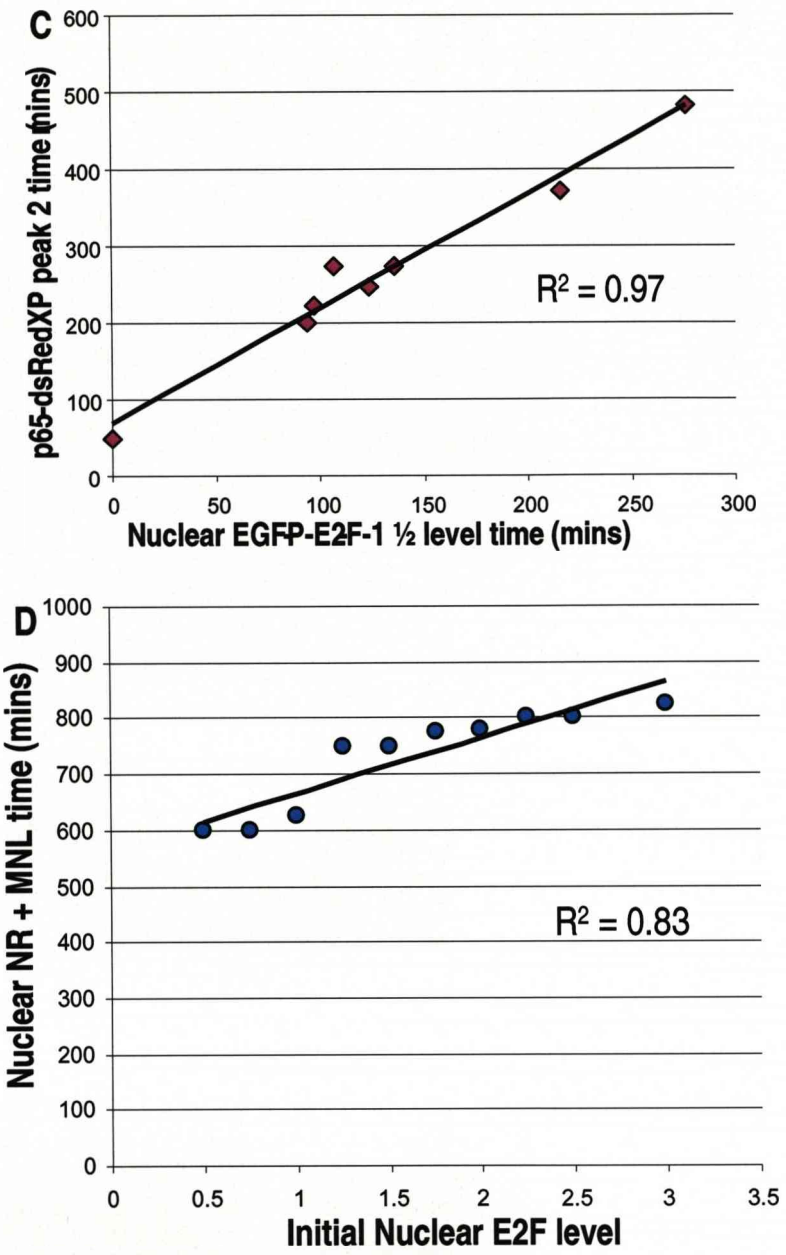

Figure 6.8 Proportional relationship between E2F-1 degradation and suspension of nucleo-cytoplasmic oscillations in p65-dsRedXP: A Model plots showing stimulated time courses with different initial levels of *E2F*; 0 (pink dashed line), 0.05 (orange line), 0.1(red line), 0.2 (blue line). Model predicts suspension time is proportional to *E2F* degradation time. **B** Experimental data showing SK-N-AS cells showing different nucleo-cytoplasmic suspension times for different estimated degradation times (t½) of EGFP-E2F-1; orange- 136 minutes, red- 217 minutes, blue- 277 minutes. Pink line shows p65-dsRedXP dynamics from cell with negligible detectable level of EGFP-E2F-1. **C** Showing strong correlation between EGFP-E2F-1t½ time and p65-dsRedXP MNL2 time (R^2=0.972). Chart representative of 10 cells. **D** The model is able to reproduce high correlation (R^2=0.83) between initial level of E2F and corresponding suspension time of oscillations, calculated at sum of the Nuclear Retention time and the post-peak 1 Maximum Nuclear Localisation time.

6.5 Discussion – Variability in NF-κB dynamics

To summarise at this point, the Mk.II mathematical model accurately predicts the suspension of nucleo-cytoplasmic oscillations, albeit through a different mechanism to the initial model (described in Section 5.4) Figure 6.9 shows the relationship between degradation of cytoplasmic *E2F* and the rise in IKK activity affecting the overall dynamics of nuclear *NFkB*. Progressive activation of IKK leads to nucleo-cytoplasmic oscillations in *NFkB*, which approach a steady-state.

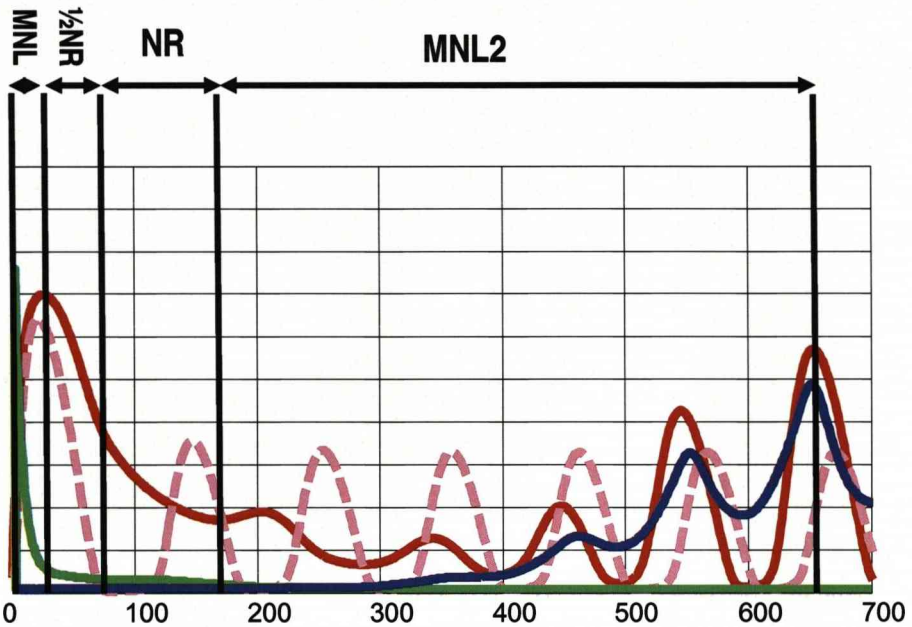

Figure 6.9 The NF-κB:E2F-1 mathematical model Mk.II: Showing degradation of cytoplasmic *E2F* (green line) and resultant rise in IKK activity (purple line), leading to nucleo-cytoplasmic oscillations in *NFkB* (red line) in response to TNFα stimulation. Pink dashed line shows "normal" NF-κB oscillations, generated with *E2F* set to zero.

The Mk.II model suggests a dual role for E2F-1 in control of the NF-κB system. Firstly, interaction with IKK may delay the first peak of nuclear localisation (MNL) expected with TNFα stimulation in the absence of exogenous E2F-1 to occur within 30 minutes (Section 1.3.3). Secondly, direct interaction between E2F-1 and the NF-κB dimer (p65:p50) may delay translocation back to cytoplasmic state (NR), expected in the absence of exogenous E2F-1 to occur within 50 minutes (Section 1.3.3).

This suggests an interesting competitive effect between nuclear sequestration by E2F-1 which is periodically expressed throughout the cell cycle and cytoplasmic

sequestration by IκBα which is constitutively produced, allowing a second conceptual model to be drawn (Figure 7.3) Intuitively one would expect a population of cells stimulated with TNFα to show consequential variability in the dynamics of the first peak of p65-dsRedXP nuclear occupancy dependant on the level of endogenous E2F-1 coincident with stimulation time. Figure 6.10 shows first peak dynamics for a population of SK-N-AS cells transfected with a plasmid vector expressing p65-dsRedXP alone. From the point of stimulation, it can be seen that MNL time varies between 15-45 minutes and that NR time can vary between 40-120 minutes.

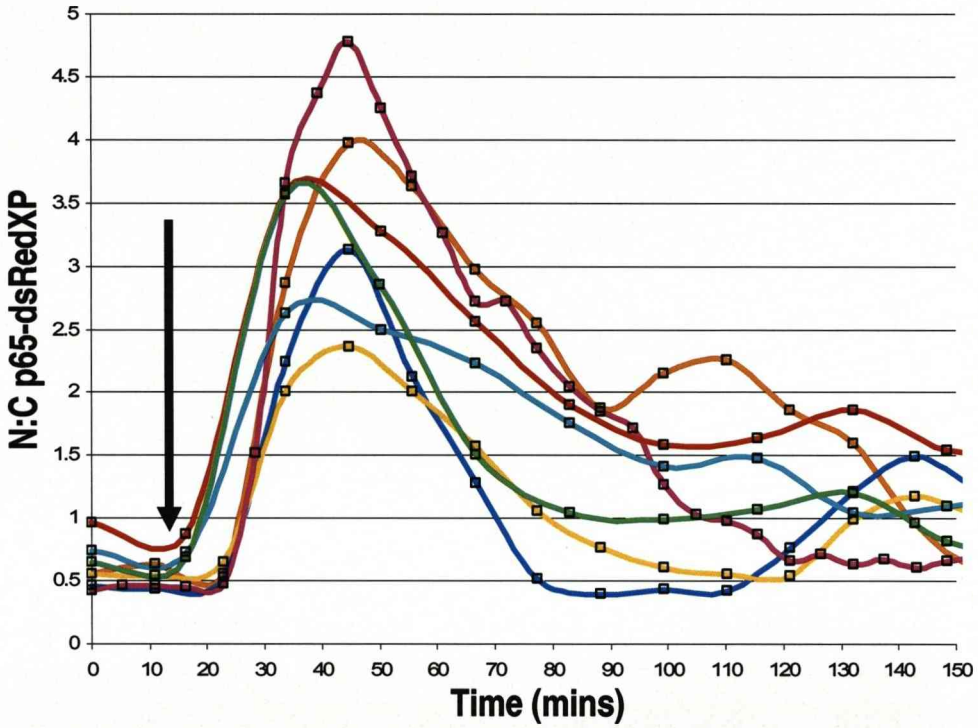

Figure 6.10 Variability in p65-dsRedXP dynamics in SK-N-AS cells: Showing variability in both MNL time and NR time of p65-dsRedXP from point of stimulation (black arrow), in cells with similar expression levels of p65-dsRedXP.

In order to properly characterise this variability as an effect of E2F-1 it was decided to examine the relationship between endogenous E2F-1 and p65:p50. To do this the physiological profile of E2F-1 must be considered, placing interaction between E2F-1 and the NF-κB system within an endogenous context, that of inflammatory response at the G1/S checkpoint of the mammalian cell cycle.

Chapter 7 –

NF-κB:E2F-1 - The Cell Cycle Context

7.1 Introduction and rationale

At this stage we have conceptual and mathematical models of the NF-κB:E2F-1 system based on exogenous studies. Work on the exogenous system has suggested E2F-1 provides a source of variability to NF-κB signalling (Figure 5.9 and 6.8). In this chapter we will begin to expand the context of the NF-κB:E2F-1 system to the cell cycle. Work on the endogenous system was hoped to both support exogenous studies and provide a more physiologically significant model for the NF-κB:E2F-1 system at G1/S.

Despite this shift of focus, attempts were made to link exogenous expression of p65-dsRedXP and EGFP-E2F-1 to cell cycle events, yielding interesting results. Figure 7.1 shows the fluorescence dynamics of representative SK-N-AS cell stimulated at t0 with TNFα before and after Mitosis. Nucleo-cytoplasmic oscillations in the parent cell can clearly be seen, which lead to predominant nuclear localisation immediately prior to the start of Mitosis. Fluorescence traces from the two daughter cells are first observable 10 hours after this point, and the two daughter cells show different NR dynamics dependant on the comparative levels of p65-dsRedXP to EGFP-E2F-1 at the time of the first peak (consistent with Section 5.5).

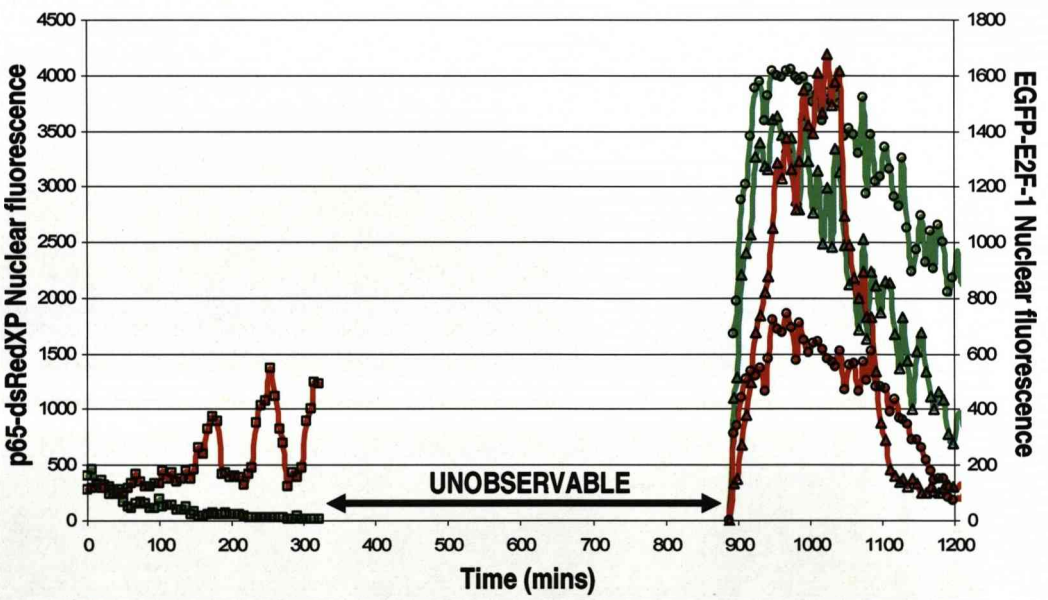

Figure 7.1 Imaging parent and daughter cells: Showing a representative SK-N-AS cell expressing EGFP-E2F-1 and p65-dsRedXP in the presence of TNFα. Cell shows oscillations in p65-dsRedXP and takes a nuclear localisation prior to the start of Mitosis. Daughter cells imaged from point of first observable fluorescence.

7.2 Conceptual and experimental models for cell cycle studies

In order to investigate the relationship between endogenous E2F-1 and NF-κB signalling dynamics it is necessary to develop an experimental model for cell cycle synchronisation so as to obtain populations of cells with different levels of E2F-1. Double Thymidine block is a common method to obtain late G1 synchronisation of HeLa cells ((Whitfield *et al.* 2000; Whitfield *et al.* 2002), described in detail in Section 2.2.2.3) This was chosen as a suitable synchronisation model to extend the SK-N-AS exogenous work as HeLa cells display similar NF-κB dynamics to SK-N-AS cells in response to TNFα (Nelson *et al.* 2004). The Double Thymidine Block protocol was found to give highly effective synchronisation in HeLa cells (Figure 7.2) and was easily adapted for different experimental procedures, as outlined below.

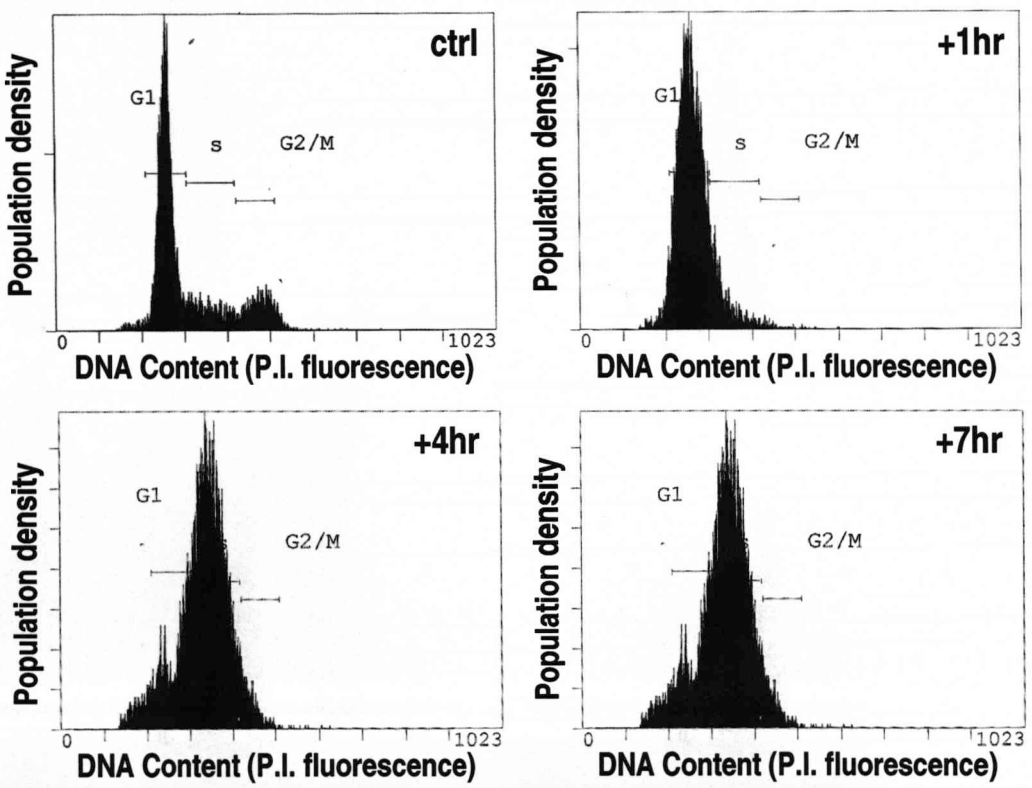

Figure 7.2 Flow Cytometric DNA Analysis of Thymidine synchronisation model: Showing populations of HeLa cells assessed for DNA content at various stages after release from Double Thymidine Block synchronisation. The data indicate a gradual increase in DNA content at increasing times from release, concurrent with cell cycle progression and hence effective synchronisation.

Application of the experimental synchronisation model to characterisation of the relationship between endogenous E2F-1 and the NF-κB system requires a new conceptual model to be drawn (Figure 7.3).

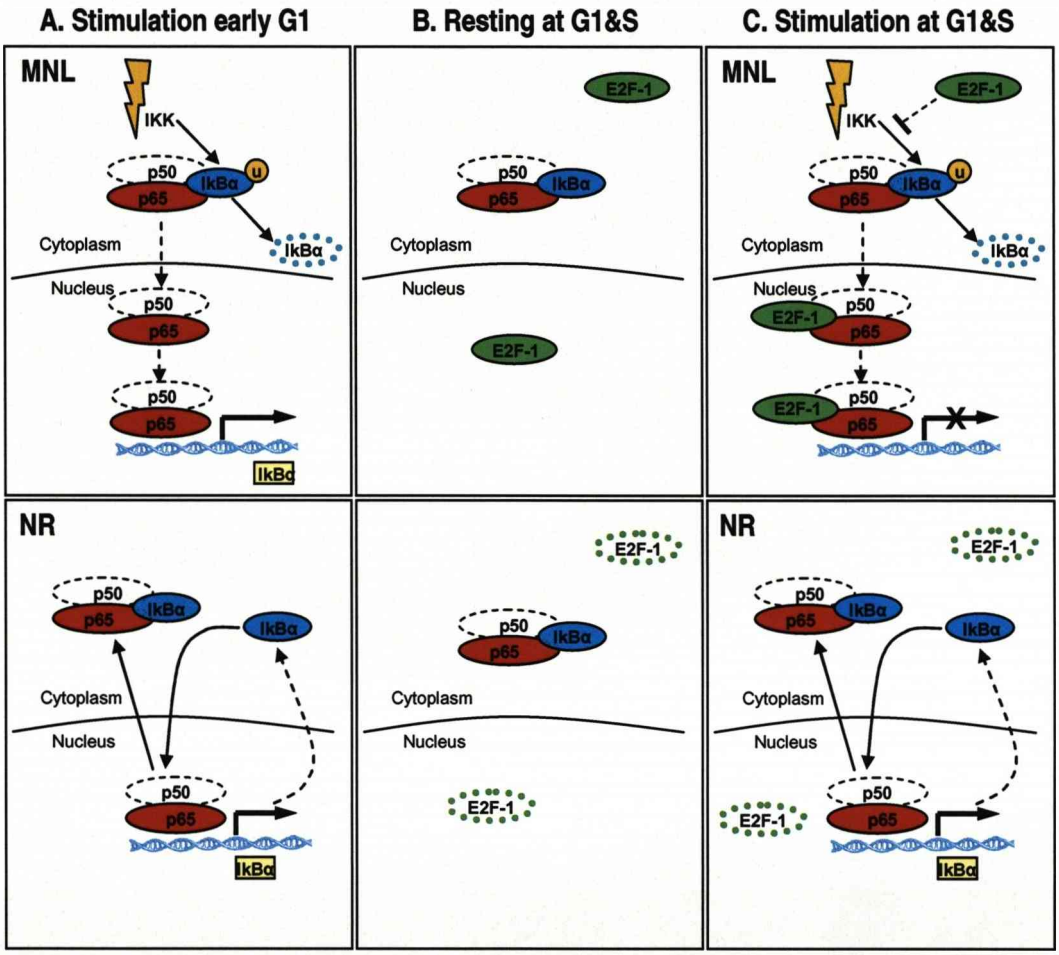

Figure 7.3 Conceptual "catch" model: NF-κB response at different cell cycle stages: A Showing a NF-κB response with E2F-1 at low level, similar to 90% cell cycle, giving MNL time of 30 minutes and NR time of 50 minutes. **B** Resting equilibrium at G1/S phase, giving NF-κB a predominantly cytoplasmic state whilst E2F-1 remains predominantly nuclear. **C** An NF-KB response at G1/S, giving MNL and NR times longer than A due to inhibition of IKK by cytoplasmic E2F-1 and sequestration of p65:p50 by nuclear E2F-1.

The conceptual "catch" model for NF-κB response at G1/S suggests that association between E2F-1 and the p65:p50 NF-κB dimer may not occur in unstimulated "resting" conditions. This is due to constitutive production of IκBα compared to periodic

production of E2F-1 throughout the cell cycle and a steady-state cytoplasmic localisation of the IκBα:NF-κB complex in resting conditions, in contrast to E2F-1 which is periodically expressed and takes a predominantly nuclear localisation. As such there is predicted to be a clear difference between endogenous and exogenous resting phenotypes, due to exogenous expression of p65-dsRedXP and EGFP-E2F-1 both increasing the amount of free NF-κB in the cell and creating an excess of E2F-1 relative to IκBα.

The situation changes with the addition of TNFα. With NF-κB held in the cytoplasm by IκBα, stimulation leads to the translocation of NF-κB into the nucleus. If this coincides with a cell cycle phase at which the level of E2F-1 is low (such as G2 phase), the Maximum Nuclear Localisation (MNL) time and Nuclear Retention (NR) time of NF-κB is predicted to be short compared to a response coinciding with high E2F-1 levels at G1/S. Figuratively, E2F-1 is able to "catch" the NF-κB dimer and sequester it in the nucleus.

Concurrent to the development if this new conceptual model, Thymidine synchronisation was tested for the ability to generate a cell cycle profile for E2F-1 and E2F-4 equivalent to the current view held in the literature (shown in Figure 7.4, reviewed in (Tsantoulis *et al.* 2005)). Figure 7.4 shows a delay in the peak of endogenous E2F-4 protein compared to E2F-1. E2F-1 is shown to rise to a peak at 2 hours after release from Thymidine block, giving a G1/S timing consistent with FACS data shown in Figure 7.3.

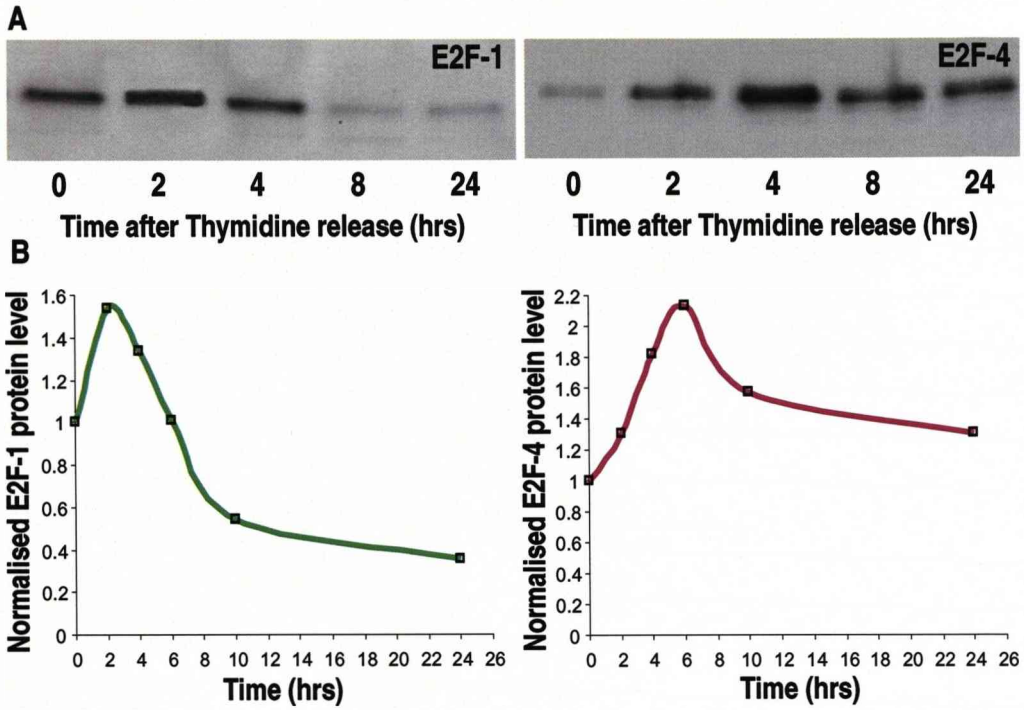

Figure 7.4 E2F profiles achieved through Thymidine synchronisation: A Showing synchronised populations of Hela cells sampled at intervals after release and probed for E2F-1 or E2F-4 via Immuno-blot. **B** Showing quantification of the blots in A, normalised to Cyclophilin A levels. The profiles show a peak of E2F-1 at 2 hours after release from Thymidine block.

.

A physiological profile for E2F-1 allowed us to derive an experimental model from the conceptual model with which to test conceptual hypotheses in Figure 7.3 (Figure 7.5). Following the 72-hour Double Thymidine Block synchronisation protocol (Section 2.2.2.3), HeLa cells are released from arrest (at a time designated T0) re-entering the cell cycle synchronised in late G1 phase. Taking into account the ~30 minute delay between TNFα stimulation and total nuclear localisation in non-synchronised cells (Section 1.3.3), cells were stimulated with TNFα 30 minutes prior to points of interest in the cell cycle, thus providing a suitable experimental model for comparing NF-κB dynamics coincident with different endogenous levels of E2F-1.

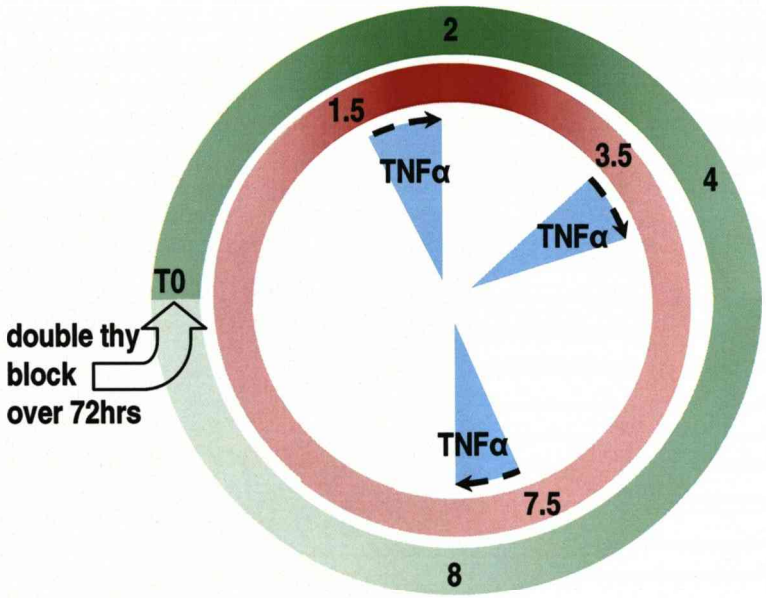

Figure 7.5 Experimental model: NF-κB response at different cell cycle stages: Upon release from Thymidine block (see text for details) cellular populations are lysed at points in the cell cycle with different levels of E2F-1 (green line), 2 hours (peak), 4 and 8 hours. NF-κB stimulation to coincide with these time points (red line) optionally occurs 30 minutes prior to lysis.

7.3 Endogenous localisation and binding of E2F-1 and NF-κB

Figure 7.6 shows Immuno-CytoChemistry data for populations of HeLa cells fixed at 2hours, 4hours and 8 hours after release from Thymidine. All dishes were stimulated with TNFα 30 minutes prior to fixation and were stained for both E2F-1 and p65 Immuno-fluorescence. It is clear in both stimulated and non-stimulated samples that a higher proportion of cells have high levels of E2F-1 nuclear fluorescence at 2 hours than at 4 or 8 hours. This result concurs with the peak of E2F-1 protein at G1/S (Section 1.2.3, Figure 7.4). Interestingly, staining for p65 revealed a higher proportion of cells with high N:C fluorescence in stimulated samples coinciding with the peak of E2F-1 at 2 hours, compared to 4 hours and 8 hours. This result supports the theory that E2F-1 acts to sequester NF-κB in the nucleus in a proportional manner (Section 4.7). Both synchronised and non-synchronised non-stimulated samples showed a predominant cytoplasmic localisation for p65 as assumed by the conceptual model.

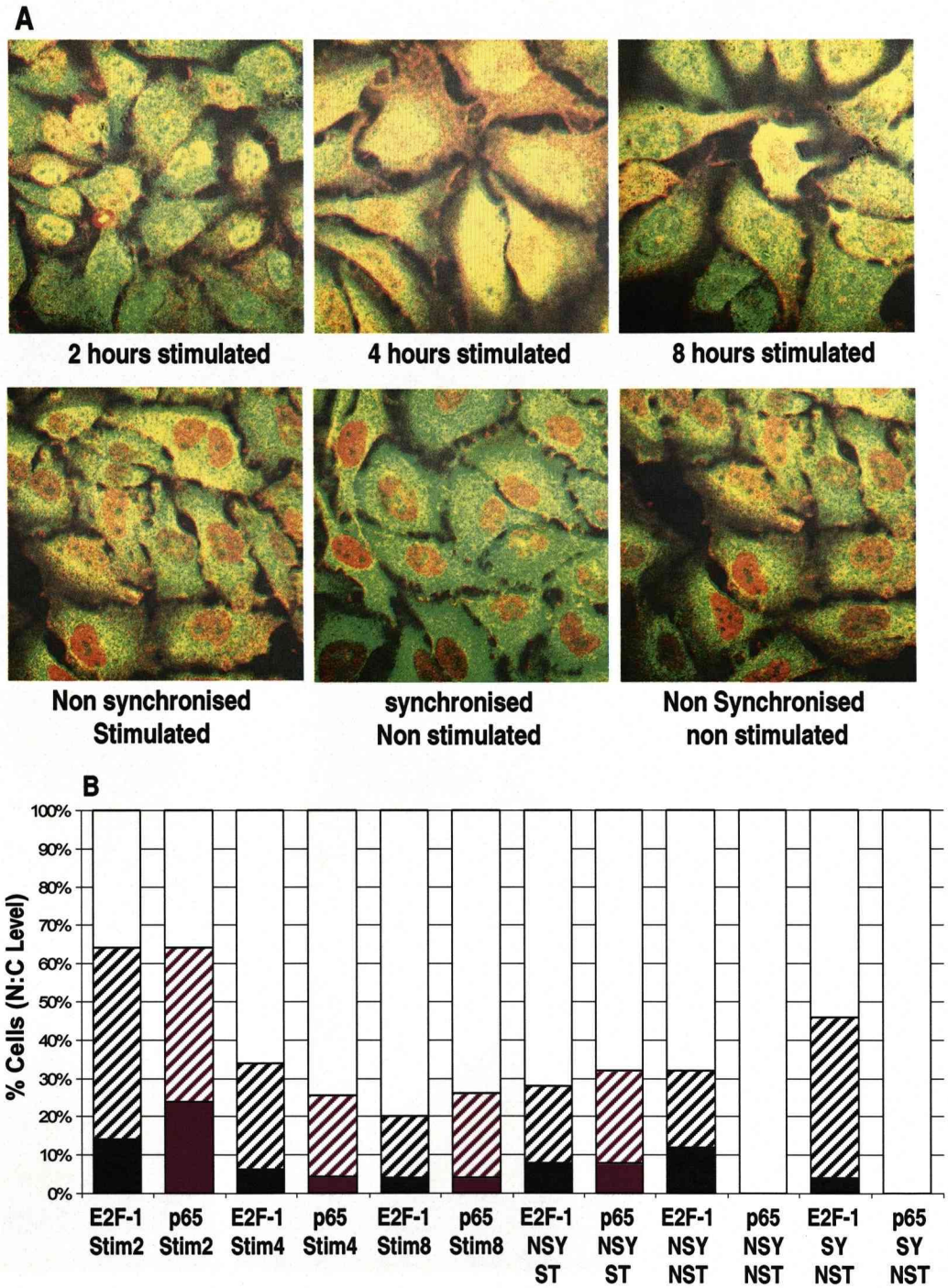

Figure 7.6 Immuno-cytochemistry to assess p65 and E2F-1 co-localisation in HeLa cells: A Showing populations of HeLa cells treated as indicated, showing red immuno-fluorescence (E2F-1) and green immuno-fluorescence (p65). **B** Quantification of cellular populations indicated in A. Black bars indicate staining for E2F-1, red bars indicate staining for p65, stimulation to coincide with cell cycle time points as indicated. Controls used include non-synchronised, stimulated (NSY ST); non-synchronised, non-stimulated (NSY NST); and synchronised, non-stimulated (SY NST); Solid colour indicates N:C Ratio >2, broken colour >1, no colour <1. Data sets involve 50+ cells per condition.

Interestingly, these data suggest a cell cycle dependant change in localisation for E2F-1. This is coincident with a change in the NF-κB response, with a TNFα response timed 8 hours after G1/S resulting in a smaller degree of nuclear p65-dsRedXP compared to a response timed at G1/S, but comparable to non-synchronised samples. These data support the G1/S "catch" model (Figure 7.3), suggesting that a response timed at G1/S, when E2F is predominantly nuclear, results in fast nuclear translocation (due to uninhibited IKK) and nuclear sequestration of NF-κB (NMR short, NR long). However, as E2F moves to take a cytoplasmic localisation, a response is less likely to illicit translocation due to inhibition of IKK by E2F-1, resulting in a long NMR time and a short NR time due to E2F no longer being localised to affect sequestration. Variability in MNL and NR times is investigated further is Section 7.6.

Analysis of endogenous binding between E2F-1 and NF-κB proved difficult as the peak of E2F-1 lasts for approximately 10% of the HeLa cell cycle coincident with the G1/S phase transition. As has been highlighted above, competition for binding of NF-κB between IκBα and E2F-1 depends on the comparative level of E2F-1 and IκBα. Endogenously, with E2F-1 at low levels for ~90% of the cell cycle, p65 is sequestered in the cytoplasm by IκBα, whilst E2F-1 is predominantly nuclear (Similar to Figure 3.2). Intuitively stimulation with TNFα prior to G1/S phase was expected to give the best opportunity for measurement of endogenous binding.

To assess binding of E2F-1 to the NF-κB in a cell cycle context, Co-immunoprecipitation was performed on synchronised HeLa cells (Figure 7.7) using a similar model as for ICC. Unfortunately, evidence for binding between endogenous p50 and E2F-1 was difficult to obtain due to the presence of a non-specific IgG band at 50kDa. (Consequently, it is difficult to interpret 50kDa bands present in protein pull-downs of E2F-1 taken at T0, 2hours and 2hours+TNFα after release from Thymidine as representative of p50, although endogenous Co-immunoprecipitation was shown between E2F-1 and p50 in SK-N-AS cells (Section 4.4) as well as in previous work (Kundu *et al.* 1997). Similar samples were probed for p65 and yielded surprising results. A clear band of ~50kDa was observed, (in addition to the expected 65kDa band) in synchronised control samples probed for p65. Interestingly, this band appears

in E2F-1 pull-down samples probed for p65 although the 65kDa band is absent.

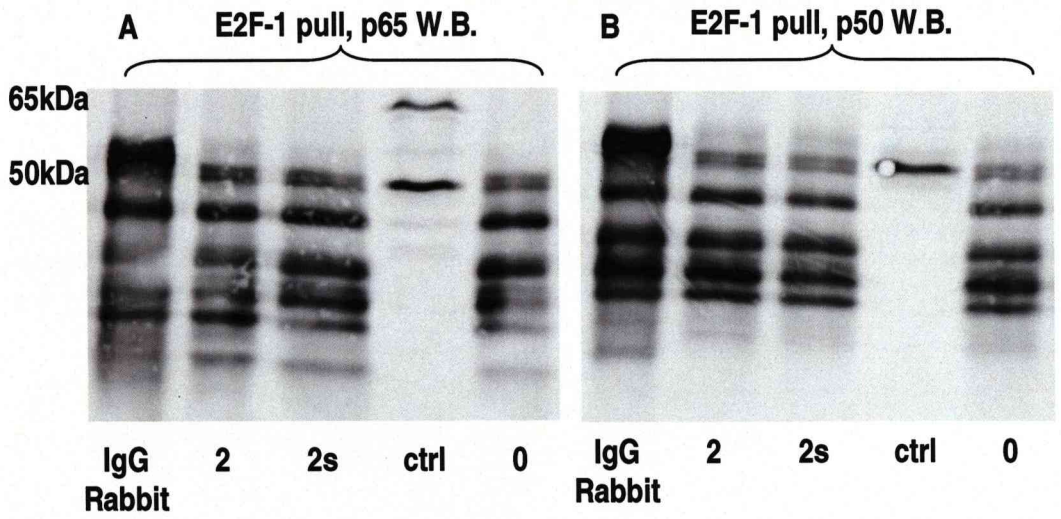

Figure 7.7 Co-ImmunoPrecipitation in synchronised HeLa cells: A Showing possible cleavage of p65 **B** Showing a band at 50kDa in all pull-downs consistent with both p50 control and non specific IgG

The next aim was to investigate the apparent processing of p65 in HeLa cells over a broader time scale. Synchronised cell populations were stimulated and then lysed at 0, 2, 4 and 8 hours after release from Thymidine. An immunoblot probed for p65 yielded further evidence of p65 processing (Figure 7.8).

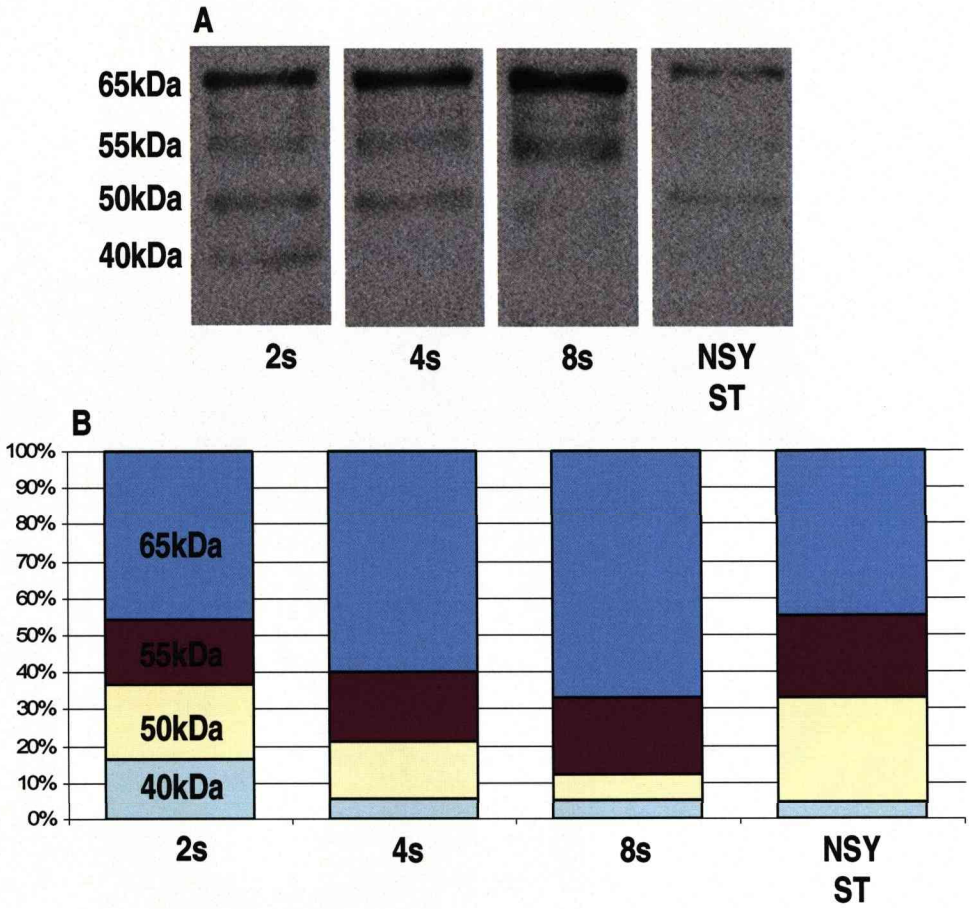

Figure 7.8 Assessment of p65 cleavage in synchronised, stimulated cells: A Showing populations of HeLa cells stimulated prior to G1/S (2s) showing 4 bands for p65 (65, 55, 50 and 40 kDa) compared to different combinations of these bands in 4s 8s and non-synchronised, stimulated samples. Intensity of bands in all lanes summed up to similar totals. **B** Analysis of bands in A normalised to cyclophilin A

7.4 Transcriptional studies revisited

Exogenous studies predict that whilst sequestered by E2F-1 in the nucleus, NF-κB transcriptional activity is directed away from the IκBα and IκBε promoters (Section 6.2), contributing to delay in subsequent nucleo-cytoplasmic oscillations. These data suggest the hypothesis that an NF-κB response occurring after the peak of E2F-1 in the cell cycle would lead to differential transcription of IκB proteins. To investigate this hypothesis, Quantitative PCR was performed on samples prepared using similar methods to those used for the ICC work above (Figure 7.9). These data clearly show

an increased production of both IκBα and IκBε following the peak of E2F-1 at 4 hours and a further increase to 8 hours.

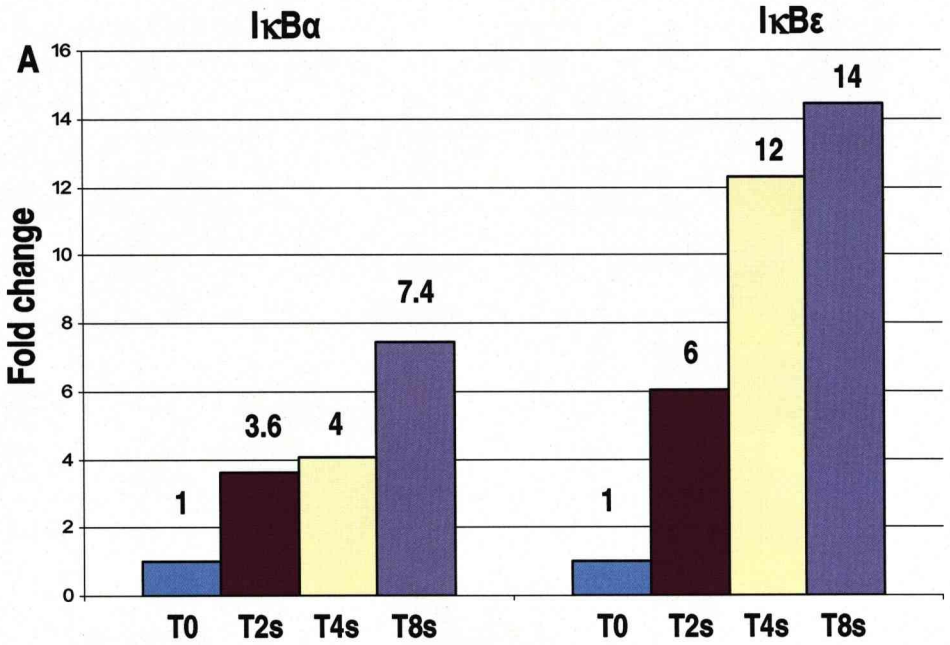

Figure 7.9 IκB Levels associated with NF-κB response at different cell cycle stages: Showing Fold induction of IκBα and IκBε from populations of HeLa cells stimulated prior to G1/S (2s) giving lower IκB transcript levels than later time points. Single replicate.

To investigate the reciprocal effect of NF-κB on E2F-1 related transcription, preliminary work used the exogenous experimental model. Populations of HeLa cells were transfected with plasmid vectors expressing p65-dsRedXP and EGFP-E2F-1, EGFP-E2F-1 or empty vectors. Quantitative PCR was performed on these samples to assess the relative levels of the E2F-1 transcript (Figure 7.10). The results show a clear induction of E2F-1 transcription (~47 fold) in cells expressing EGFP-E2F-1 confirming work done using the exogenous experimental model (Chapters 4 and 5) allow for E2F auto-transcription to be taken into account. Interestingly, cells co-expressing p65-dsRedXP show a partial decrease (~20%) in E2F-1 transcription (Figure 7.10 A). Other preliminary work supports a theory of NF-κB inhibition of E2F-1 mediation transcription. Populations of SK-N-AS cells transfected in a similar manner were assessed for their ability to transactivate the Cyclin E promoter of a CycE-luc luciferase reporter vector (Figure 7.10 B). The results show a clear induction of Cyclin E transcription (~25 fold)

in cells expressing EGFP-E2F-1 and an empty-Red vector which is significantly reduced (~50%) in cells co-expressing EGFP-E2F-1 and p65-dsRedXP. Moreover cells co-expressing EGFP-E2F-1 and empty-Red stimulated with TNFα over a 6 hour period show a significant reduction in Cyclin-E luciferase activity (~30%) giving evidence that the endogenous NF-κB system is able to inhibit the transcriptional effect of exogenous E2F-1 expression.

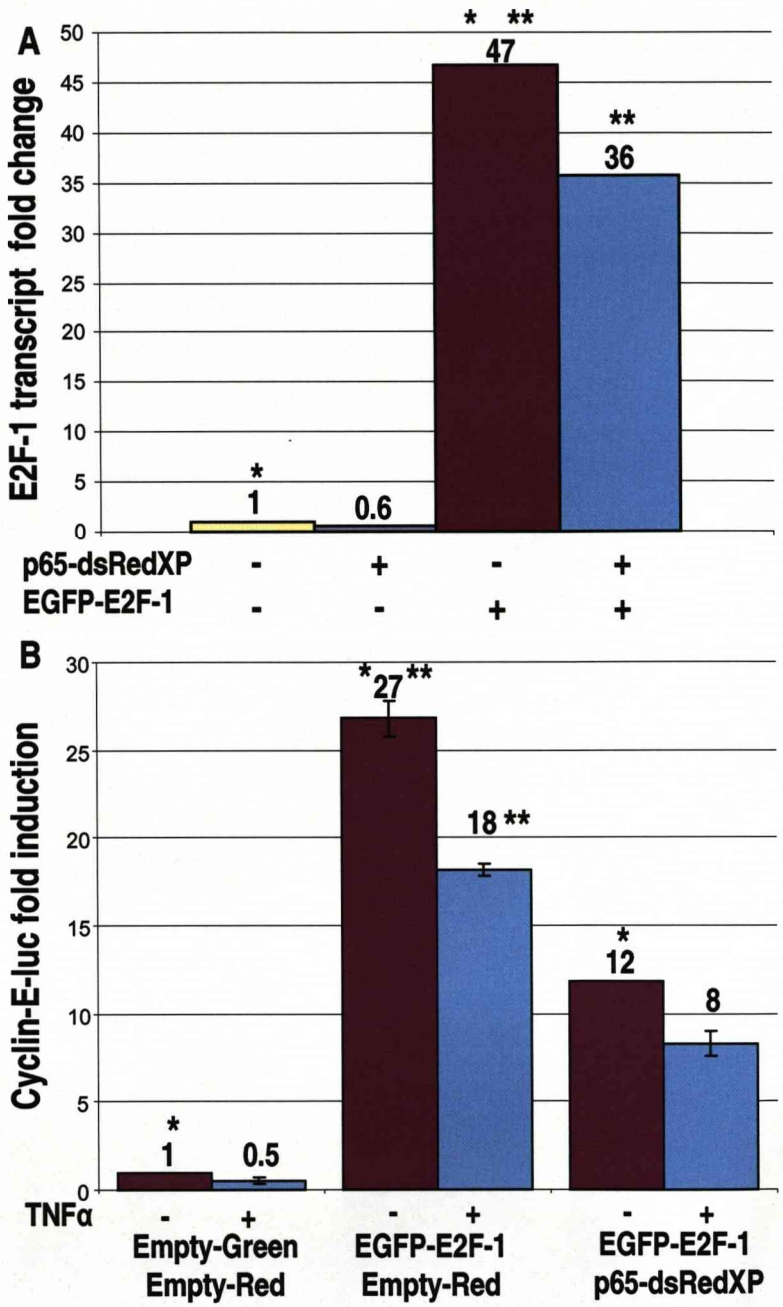

Figure 7.10 Transcriptional studies on cell cycle genes in exogenous system: A Quantitative PCR results Showing significant fold increase in E2F-1 transcript levels resultant from EGFP-E2F-1 expression (*) which are significant decreased by co-expression of p65-dsRedXP (**) **B** Showing luciferase reporter assay using Cyclin-E-luciferase reporter. Expression of EGFP-E2F-1 causes significant fold induction in Cyclin E transcription (*) which is significantly decreased by both TNFα stimulation (**) and co-expression of p65-dsRedXP (*).

7.5 Apoptosis revisited

It was previously shown that exogenous expression of p65-dsRedXP significantly decreased cell death associated with exogenous E2F expression (Section 4.6). Transcription studies (Figure 7.10) suggest a possible explanation might be that physical interaction between E2F-1 and NF-κB is blocking E2F-1-mediated transcription of genes required to move into S-Phase (E2F-1, Cyclin E), thereby inhibiting cell death caused by premature S-phase entry through exogenous expression of E2F-1 (Johnson *et al.* 1993; Qin *et al.* 1994). It was subsequently possible to consider the effect of TNFα stimulation in such cases. Figure 7.11 shows populations of SK-N-AS cells derived from imaging experiments involving expression of EGFP-E2F-1 in combination with either p65-dsRedXP or an empty-Red vector as indicated. The presence of TNFα stimulation is also indicated. Consistent with previous work (Section 4.6), the number of transfected cells at the start of imaging was calculated, and compared to the number of these cells that remained healthy after a 12-hour period. The percentage of cell death was compared across populations of at least 50 cells.

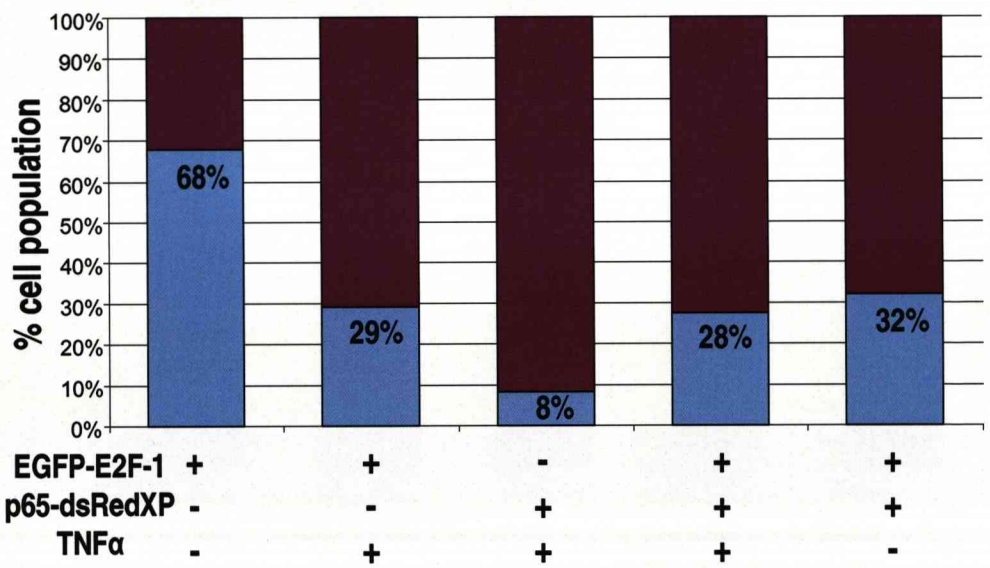

Figure 7.11 E2F-1 related Apoptosis (II): Populations of SK-N-AS cells assessed for cell death over 12 hours period by live cell imaging. Showing 68% cell death due to EGFP-E2F-1 which is decreased by both p65-dsRedXP (28%) and TNFα stimulation (29%). Red section of bar represents proportion of live cells, blue represents proportion of dead cells.

Commenting on these results, it may be observed that TNFα has a clear effect on the level of apoptosis related to exogenous E2F-1 expression, reducing cell death by

nearly 40%. This result is comparable with the effect of co-expression with p65-dsRedXP and suggests the endogenous NF-κB system is just as efficient at blocking E2F-1 related apoptosis and the exogenous system. Interestingly, p65-dsRedXP co-expression in addition to TNFα stimulation has little cumulative effect on the level of cell death implying a threshold of efficiency for NF-κB in blocking E2F-1-mediated cell death.

7.6 Variability in NF-κB dynamics revisited

Previously we addressed the question of variability in the dynamics on the first peak of p65-dsRedXP nuclear occupancy after stimulation with TNFα in SK-N-AS cells (Section 6.5). It was hypothesised that E2F-1 may have a dual role as a source of this variability. Firstly, E2F-1 extended the Maximum Nuclear Localisation (MNL) time after TNFα stimulation and the degradation of IκBα was slowed (Section 6.2) potentially through inhibition of IKK. Secondly, evidence was presented that E2F-1 interacted with the NF-κB complex (Section 4.4), sequestering it in the nucleus and silencing transcription of IκBα and IκBε (Section 6.2) which are necessary for NF-κB secondment to the cytoplasm, thereby effecting the p65-dsRedXP Nuclear Retention (NR) time. Concurrently, both MNL and NR times have been shown to be proportional to E2F-1 half-life in the exogenous system (Sections 5.5 and 6.4). Addressing variability in NF-κB dynamics in the endogenous system required further use of the synchronisation model (Figures 7.5 and 7.6).

A non-synchronised population of HeLa cells expressing transiently expressed p65-dsRedXP was imaged over a long time course (Figure 7.12, movie M7.12). The cells were stimulated with TNFα and assessed for their initial peak dynamics. The resultant data set showed high variability in MNL and NR times in response to TNFα, similar to identical experiments carried out in SK-N-AS cells. Interestingly, cells which divide within 9 hours from the point of stimulation show different p65-dsRedXP dynamics than cells which do not divide during the 15 hour time course. In this case, although the cells are "synchronous" in terms of their stimulation time, they are at different stages in the cell cycle when stimulus occurs. The cells 8 hours away from division, intuitively close to M-phase when E2F-1 levels are low, give an MNL time of ~40 minutes and a NR

time of ~20 minutes. The cells which are at least 15 hours away from division, intuitively closer to S-phase where levels of E2F-1 are higher, give an MNL time of ~80 minutes and a NR time of ~60 minutes. This leads to the conclusion that NF-κB responses coincident with different phases of the cell cycle give different NF-κB dynamics.

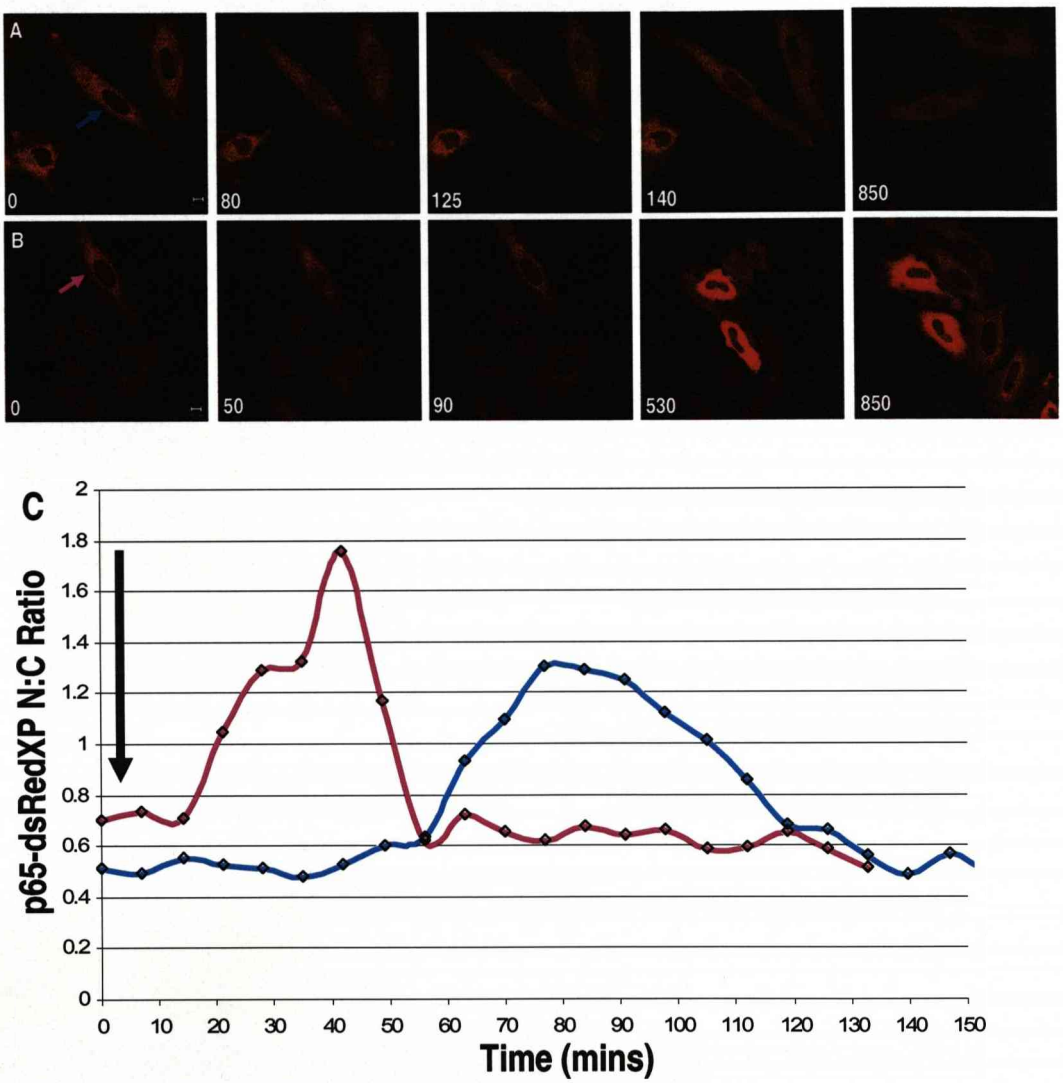

Figure 7.12 Variability in NF-κB dynamics in non-synchronised HeLa cells: A showing MNL time of 80 minutes and NR time of 60 minutes in cells at least 15 hours from Mitosis **B** showing MNL time of 40 minutes and NR time of 20 minutes in cells 8 hours from Mitosis **C** Analysis of representative cells in A and B

To further investigate this hypothesis, a population of HeLa cells expressing p65-dsRedXP was synchronised and released from synchronisation 2 hours before the expected peak of endogenous E2F-1. Live cell imaging proceeded with TNFα

stimulation occurring 30 minutes prior to the expected peak. Figure 7.13 (movie M7.13) shows the first peak dynamics of a typical cell, with MNL time of ~30 minutes, and an NR time of ~60minutes.

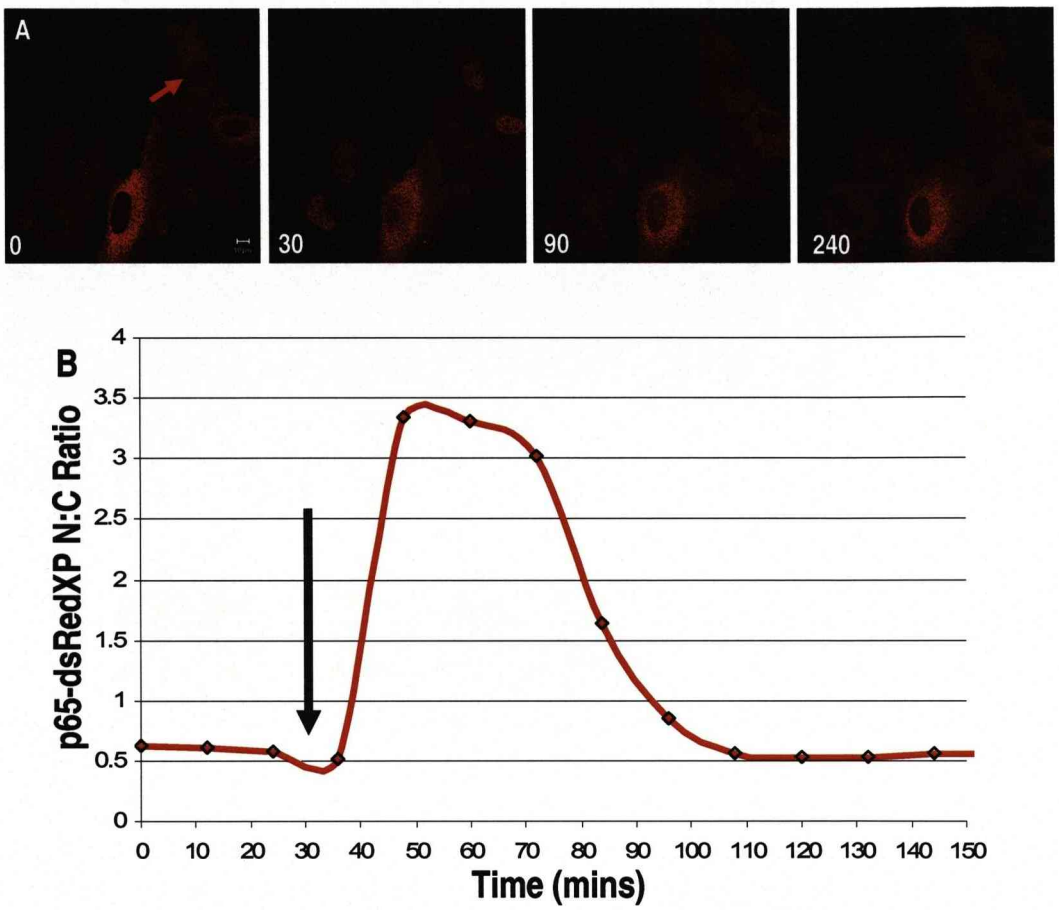

Figure 7.13 NF-κB dynamics in synchronised HeLa cells stimulated prior to G1/S: Showing MNL time of 30 minutes and NR time of 60 minutes

Most interestingly, when considering the non-synchronous and synchronous populations side-by-side it is possible to observe a high variability in the NF-κB dynamics of non-synchronous cells compared to a high degree of consistency in cells stimulated to coincide with G1/S and the peak of endogenous E2F-1 (Figure 7.14). By synchronising the cells in terms of cell cycle phase in addition to stimulation time the variability in the endogenous system has been reduced. This evidence concurs with the theory that TNFα-mediated NF-κB dynamics change with respect to the level of endogenous E2F-1.

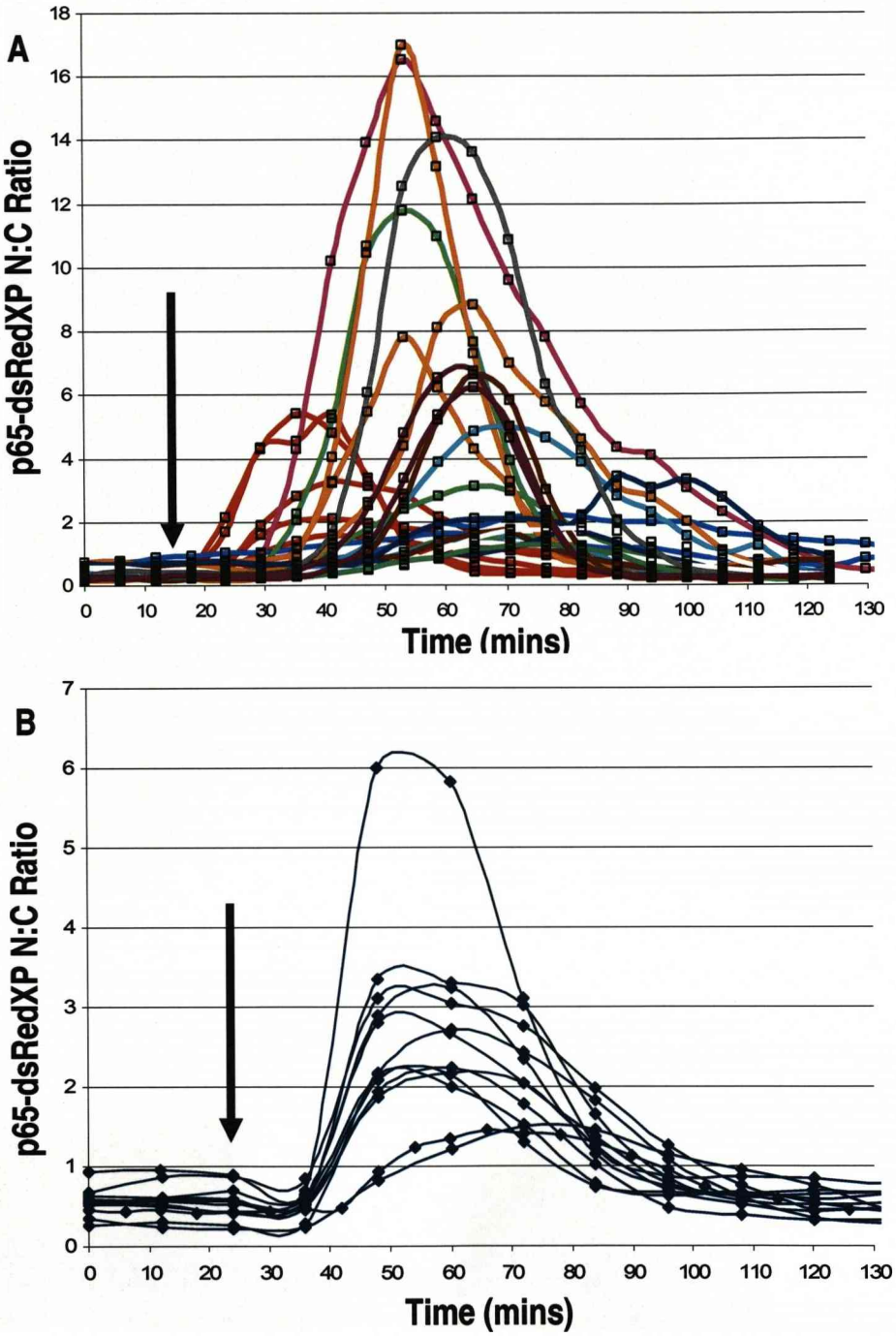

Figure 7.14 Variability in NF-κB dynamics in synchronised and non-synchronised HeLa cells: A Showing high degree of variability in NF-κB dynamics of stimulated, non-synchronous cells. **B** Showing high degree of consistency in NF-κB dynamics of stimulated, synchronous cells.

7.7 Discussion

In the work described in this chapter the aim was to place previous exogenous work into the context of the endogenous Cell Cycle system. Initially a conceptual model was developed for response at G1/S (Figure 7.3) together with an experimental model involving synchronisation with which to test it (Figure 7.5). To parallel exogenous work, evidence was obtained to support the presence of endogenous co-localisation of p65 and E2F-1 (Figure 7.6), showing a more prevalent nuclear co-localisation across a cellular population stimulated prior to G1/S than at later times in the cell cycle. Although binding between endogenous p65 and E2F-1 in Hela cells proved difficult to reproduce due to technical reasons (Figure 7.7), endogenous binding in SK-N-AS cells was previously shown (Section 4.4). Transcriptional studies focussed on the transcription of IκB proteins due to NF-κB stimulation in the endogenous system, seen to increase as level of E2F-1 decreases (Figure 7.9) concurrent with (Section 6.2). Further transcription work used an exogenous model to make preliminary investigations into the effect of NFκB on E2F-1-mediated transcription (Figure 7.10). These results showed an NF-κB-mediated inhibition of E2F-1 transcription which was hypothesised to be the cause of a decrease in apoptosis linked to exogenous E2F-1 expression (Figure 7.11). Finally, the issue of variability in NF-κB dynamics was re-addressed in the endogenous system (Figures 7.12, 7.13, 7.14), leading to the conclusion that E2F-1 was indeed a source of variability affecting both MNL and NR timings observed for the NF-κB response. This presents the intriguing hypothesis that NF-κB dynamics and transcription profiles resulting from an inflammatory response might vary dependant on cell cycle phase.

Chapter 8 -
General Discussion

8.1 Overall reflection on project

8.1.1 General comments

The broad aim of this project was to take a combined experimental and theoretical approach to characterising interaction between two intra-cellular signalling systems. In order to achieve these aims, it was necessary to consider precisely the requirements of a mathematical Systems Biology approach in this case, and to select biological and experimental model systems accordingly. As such, this project has tackled two common Systems Biology questions, "Why do I need a mathematical model?" – to make predictions of a system that is too complex to suggest intuitive predictions, and "What does a mathematical model need?" – model systems able to experimentally resolve predictions within an appropriate context.

8.1.2 Reflection on Thesis aims

This project aimed to apply a Mathematical Systems Biology approach to investigate the interaction between the NF-κB system and the mammalian cell cycle at G1/S ("The E2F system"). Initial work, however, was arguably reductionist in nature, characterising protein:protein interactions between E2F-1, p65 and p50 through FRET and Co-ImmunoPrecipitation studies (Section 4.4). Indeed it has been claimed that "*successful integration on a systems level must be built on successful reduction*", although "*reduction alone is far from sufficient*" (Noble 2006). Concurrently, interaction data was necessary to support subsequent live cell imaging work, on which the foundation for a conceptual model was based (Section 4.5).

The overall outcome of this investigation has been an increased understanding of the relationship between NF-κB and a cell cycle regulator, E2F-1. Evidence is provided that suggests the NF-κB:E2F-1 interaction to be a mechanism which allows E2F-1 to take temporal control of the immune response. The implications of these data may be considered across multiple contexts.

8.2 The NF-κB context

8.2.1 Results in perspective

This project began with work towards a conceptual model for E2F-1 interaction with the NF-κB system. The model took into account physical interactions between E2F-1, p65 and p50 (Section 4.4). A functional effect of these interactions was observed to be a temporary silencing of NF-κB oscillations by direct sequestration of the NF-κB complex in the nucleus. Whilst bound, the NF-κB:E2F complex was suggested to be transcriptionally inactive at IκB promoters, thereby lengthening NF-κB nuclear retention time (Sections 5.5 and 6.2). Through further investigation, a second interaction was characterised between E2F-1 and the NF-κB system which suggested inhibition of IKK activity, leading to a delay in NF-κB maximum nuclear localisation time in response to TNFα stimulation, proportional to the level of cytoplasmic E2F-1 in the cell (Section 6.2). Considered together, these relationships gave evidence for the role of E2F-1 as temporal coordinator of the NF-κB response, with high correlation between EGFP-E2F-1 half life and p65 dynamic timings (Section 5.5). This hypothesis was supported using an endogenous model to observe variability in NF-κB dynamics coincident with TNFα stimulation prior to different cell cycle stages (Sections 7.3 and 7.6).

The endogenous model also provided evidence that E2F-1 may change its predominant localisation in a cell cycle dependent manner (Figure 7.6). Intuitively, this suggests that NF-κB dynamics in response to TNFα may vary depending on cell cycle phase, due not only to the periodic expression of E2F-1, but also due to changes in localisation of E2F-1 (Figure 8.1). Examining this prediction, we may suggest that a TNFα response coinciding with G1/S, when E2F-1 is at it's peak level and predominantly nuclear, may result in a maximum nuclear localisation timing comparable with cells in which E2F-1 levels are low (or the observed average from non synchronous cells), as there is comparatively little cytoplasmic E2F-1 present to inhibit IKK. However, the nuclear retention time associated with stimulation at G1/S is predicted to be elongated due to nuclear sequestration of NF-κB by nuclear E2F-1. Complimentarily, stimulation during S-phase, when E2F-1 is both depleted in level and predominantly cytoplasmic (the cytoplasmic fraction having been shown to have a

longer half-life (Figure 6.3)) is predicted to result in an elongated MNL time due to the inhibition of IKK activity by E2F-1 leading to the prolonged stability of the IκBα:NF-κB complex. Assuming that NF-κB is only freed to translocate to the nucleus upon degradation of cytoplasmic E2F-1 and IKK-mediated phosphorylation of IκBα, the NR time of NF-κB in S-phase is predicted to be short due to the low level of nuclear E2F-1. These predictions, illustrated in Figure 8.1, are supported by the variability observed in NF-κB dynamics compared to stimulation timed to coincide with G1/S (Section 6.5), and further complimentary work is planned (Section 8.2.2).

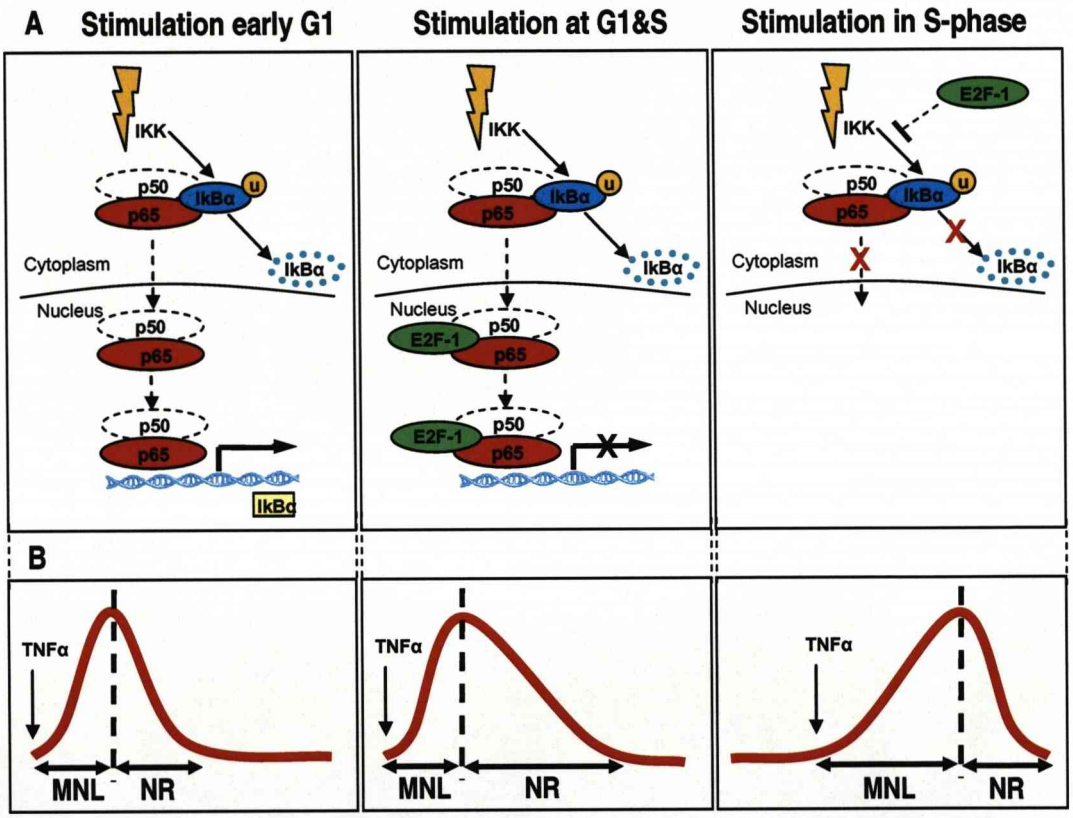

Figure 8.1 Conceptual "Catch" model Mk.II for NF-κB:E2F-1 interaction: A Showing mechanisms controlling NF-κB dynamics. Stimulation in early G1 phase, when levels of E2F-1 are low, leads to "normal" NF-κB response (outlined in Section 1.3.1). Stimulation at G1/S, when levels of E2F-1 are both high and predominantly nuclear, results in nuclear sequestration of the NF-κB complex. Stimulation in S-phase, when E2F-1 is predominantly cytoplasmic, results in a delayed response due to inhibition of IKK activity. **B** Showing the effects of these mechanisms on the dynamics of NF-κB (see text for details).

The NF-κB:E2F mathematical models played important roles in the development of these theories. Predictions were made for the proportional lengthening of both NR and MNL times, which were verified experimentally (Sections 5.5 and 6.4). Crucially, the models demonstrated that an initial assumption regarding IκBα transcription, whilst incorrect at least in part, fitted observed data (Section 5.6), thereby leading experimentation towards the effect of E2F-1 on the stability of IκBα. In fitting the IKK:E2F-1 relationship a model made a prediction for a difference in degradation rates between nuclear and cytoplasmic E2F-1 species, which has since been shown to be the case (Section 6.3). From a Systems Biology perspective, this study makes a contribution towards the eventual goal of linking the NF-κB system to the G1/S system, as illustrated in Figure 8.2. .

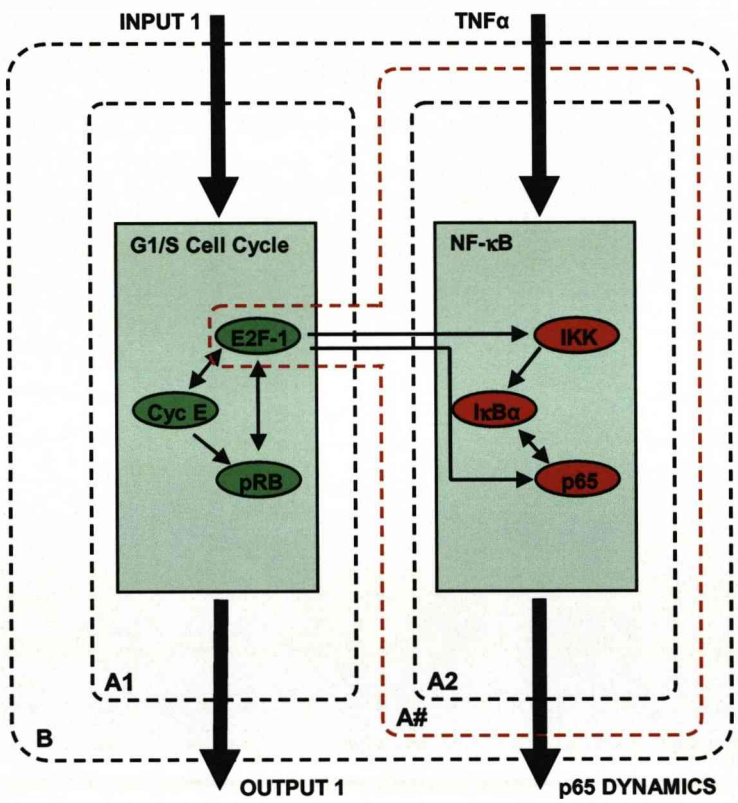

Figure 8.2 Review of steps taken towards coupling the NF-κB and G1/S linked systems: A1 and **A2** Showing models defined for NF-κB and, hypothetically, for G1/S progression. system A1 has a unique input, TNFα stimulation, and output, p65-dsRedXP dynamics. **A#** Model A2 is expanded to include interaction between protein 'p65' (system A2, NF-κB) and protein 'E2F-1' (system A1, G1/S). Interaction between p65 and E2F-1 may now be considered within the context of system A2 (NF-κB). **B** Expansion of A# to encompass system A1 (G1/S progression).

8.2.2 Future work

Previously, we began with a well defined model for The NF-κB system ("A-type", Figure 8.2). This has now been extended to include multiple interactions with E2F-1 (as a "A#-type" model). With a view to continuing the coupling procedure, and expanding the context of this model, we have a choice of how to proceed. Firstly, we may consider linking this A#-type model to an A-type cell cycle model providing a suitable physiological profile for endogenous E2F-1. However, experimentation in a cell cycle context will require the development of new experimental model systems (considered in Section 8.5). Secondly, within the NF-κB context, future development of the A#-type model may proceed by considering interactions between NF-κB and other cell cycle proteins from the G1/S system.

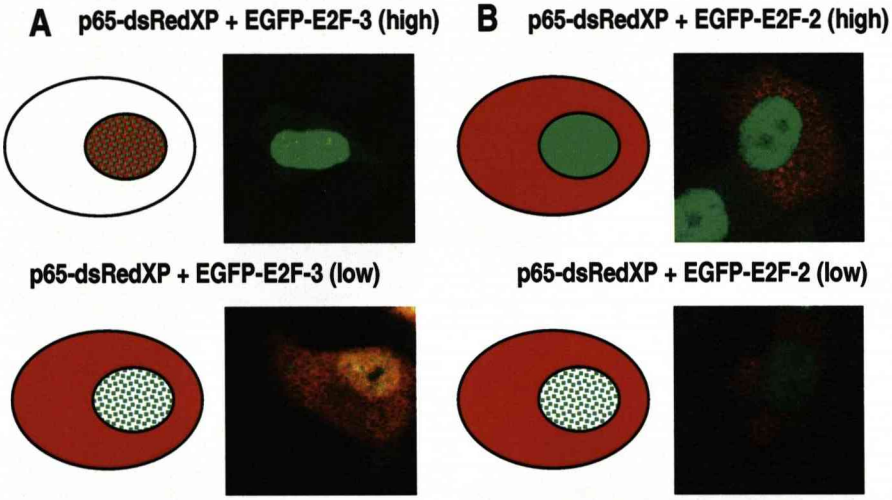

Figure 8.3 Localisation of transiently expressed p65 with E2F-2 and E2F-3 fluorescent reporter proteins: Showing SK-N-AS cells transfected with plasmid vectors expressing combinations of fluorescent fusion proteins. **A** The effects of high and low levels of EGFP-E2F-3 on p65-dsRedXP localisation, suggesting a dynamic relationship and nuclear sequestration similar to the effect of EGFP-E2F-1 on p65-dsRedXP. **B** The effects of high and low levels of EGFP-E2F-2 on p65-dsRedXP localisation (no change).

Figure 8.3 shows preliminary work investigating the effect of expression of EGFP-E2F-2 and EGFP-E2F-3 on p65-dsRedXP localisation. Interestingly, nuclear co-localisation between EGFP-E2F-1 and p65-dsRedXP appears to be common to EGFP-E2F-3 but not to EGFP-E2F-2. Although there is a high degree of structural and functional similarity between E2F-1, 2 and 3, E2F-2 has also been shown to have distinct roles

(Opavsky *et al.* 2007; Infante *et al.* 2008) Characterisation of these observations provides an obvious and interesting area for future investigation.

To further investigate the predictions made for different NF-κB dynamic profiles resulting from stimulation coincident with different stages of the cell cycle (Figure 8.1), further live cell imaging experiments are required to complement the data set shown in Figure 6.5, involving stimulation at time points later than the G1/S checkpoint. It may also be possible to repeat these experiments using stably transfected cell lines, although this is dependent on their susceptibility to synchronisation.

Throughout the course of this study, several live cell imaging experiments were carried out in an attempt to observe the dynamics of IκBα-AmCyan in the presence of EGFP-E2F-1 and p65-dsRedXP. However, due to spectral overlap between EGFP and AmCyam fluorescence, a certain degree of "spill-over" was detected between fluorescence channels. This made it difficult to make definite interpretations regarding the dynamics of EGFP-E2F-1 or IκBα-AmCyan when expressed together, although it looks likely from initial data that exogenous E2F-1 expression does abate apoptosis habitually associated with exogenous IκBα expression. These difficulties were reconciled by imaging EGFP-E2F-1 and p65-dsRedXP from a triple transfection with a plasmid vector expressing IκBα-AmCyan which was not observed. We therefore assumed that exogenous IκBα was present in such experiments through the observation of a predominantly cytoplasmic localisation for p65-dsRedXP prior to TNFα stimulation (considered as 1.3.3). Further development of the experimental model to allow observation of all three of these proteins is desirable.

To provide insight into the effects of E2F-1 on NF-κB transcription, a generic reporter construct (NF-luc) was used in luciferase reporter assays (Section 4.5). The artificial nature of this construct, which contains a 5x NF-κB consensus sequence, makes the development of more accurate reporters on NF-κB transcription desirable, such as the creation of Bacterial Artificial Chromosome (BAC) constructs containing large promoter regions for NF-κB target genes. Concurrent with this approach, future studies may include further Q-PCR work involving an expanded set of NF-κB target genes.

The majority of this project involved work in an exogenous system, requiring a significant amount of subsequent work in the endogenous system to ensure the observed effects were physiologically "real" and not simply artefacts of transient

transfection or ectopic expression. The move into an endogenous system required a change of cell line from SK-N-AS to HeLa which were able to be synchronised by Double Thymidine Block (Section 7.2). The development of a (synchronisable) cell line with stably integrated p65-dsRedXP and EGFP-E2F-1 provides perhaps the most beneficial direction for future development of the experimental model system.

8.3 The cell cycle context

8.3.1 Results in perspective

Although the primary focus of this work was the NF-κB system, the data gathered provided novel observations regarding NF-κB interaction with E2F-1 in a cell cycle context. Most strikingly, it was shown that exogenous E2F-1 expression caused apoptosis in transfected cells but that co-expression of p65-dsRedXP is enough to rescue a proportion of these cells from cell death (Sections 4.6 and 7.5). Similarly, death caused by expression of EGFP-E2F-1 alone, was partially abated by TNFα stimulation, suggesting that endogenous NF-κB activation blocked EGFP-E2F-1 related apoptosis. Initial transcriptional studies suggest a possible mechanism for this effect, with EGFP-E2F-1-mediated expression of both E2F-1 and Cyclin E impaired by co-expression of p65-dsRedXP, possibly abating premature S-phase entry habitually associated with E2F-1 related apoptosis (Section 7.4). As such, a more comprehensive study of transcriptional activity associated with the NF-κB:E2F-1 complex is desirable, possibly utilising Chromatin-ImmunoPrecipitation (ChIP) at E2F-1 and NF-κB responsive promoters. Complimentarily, in the near future it is intended to begin a collaboration working towards predicting a structure for the NF-κB:E2F-1 complex.

In addition, evidence was provided for differential degradation of E2F-1 in different cellular compartments (Section 6.3). Initial work characterising the localisation of E2F-1 have shown both exogenous and endogenous protein to take a predominantly nuclear localisation (Sections 4.2 and 7.3), however the localisation of endogenous E2F-1 has been observed to change, to predominantly cytoplasmic, as the cell proceeds into S-phase away from the G1/S checkpoint (Figure 7.3). Although exogenous, GFP-tagged, E2F-1 has not been seen to consistently change localisation when ectopically expressed alone, initial work involving SK-N-AS cells co-expressing E2F-1 and Cyclin

E fluorescent fusion proteins does show variation in the localisation of exogenous E2F-1(Figure 8.4). This preliminary work supports the idea of interaction with Cyclin E as a mechanism influencing the localisation of E2F-1, which has been previously hypothesised in theoretical studies (Baguley *et al.* 2005).

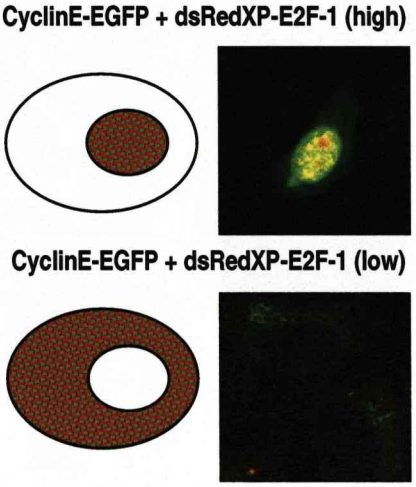

Figure 8.4 Localisation of transiently expressed E2F-1 and Cyclin E fluorescent reporter proteins: Showing SK-N-AS cells transfected with plasmid vectors expressing combinations of fluorescent fusion proteins. The effects of CyclinE-GFP on high and low levels of EGFP-E2F-1 localisation, consistent wih a dynamic relationship.

8.3.2 Future work

Within a cell cycle context, there is considerable opportunity for live cell imaging experiments applied to the characterisation of cell cycle events, such as the use of fluorescent cell cycle markers of restriction point transition (Sakaue-Sawano *et al.* 2008) in cancer cell lines, or a live cell imaging approach to investigating the nucleo-cytoplasmic shuttling of Cyclin complexes (Jackman *et al.* 2002). Indeed, arguably the biggest priority for future work is characterisation of the potential oscillatory relationship between Cyclin E and E2F-1, which may be investigated using a similar systems-level approach to that applied in this study.

Within the context of NF-κB interaction with the cell cycle, preliminary results suggest further evidence for oscillatory behaviour of EGFP-E2F-1, in this case upon ectopic co-expression of p50 precursor protein p105 in unstimulated conditions (Figure 8.5, movie

M8.5). This observation may suggest a role for the NF-κB system in regulating the nuclear occupancy of E2F-1 in certain situations.

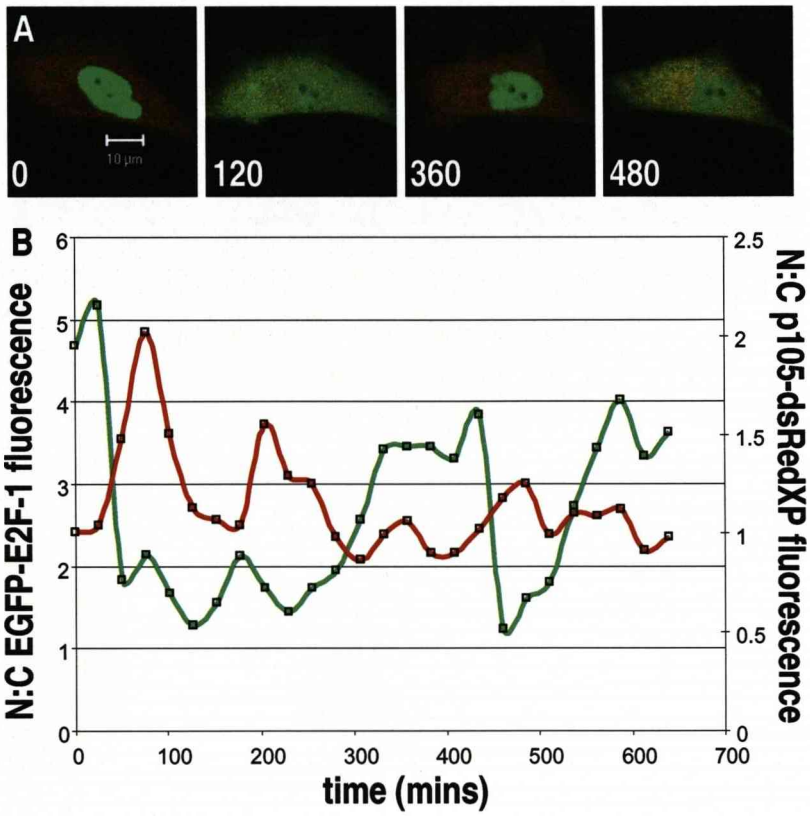

Figure 8.5 Localisation of transiently expressed E2F-1 and p105 fluorescent reporter proteins: Showing SK-N-AS cells transfected with plasmid vectors expressing EGFP-E2F-1 and p105-dsRedXP. A time course showing oscillatory behaviour in EGFP-E2F-1 in unstimulated conditions.

The development of experimental models for cell cycle studies has already begun, such as the procurement of knock-out MEF cell lines for E2F proteins (Wu *et al.* 2001), and the design of cloning strategies for expression vectors involving cell cycle proteins under endogenous promoters. These approaches may be combined in the future with emergent time-lapse FRET techniques involving expression vectors with photo-convertible fluorophores, allowing FRET to be assessed in real time at various cell cycle stages.

8.3.3 The Systems Biology of the cell cycle

Consideration of the characterisation of the NF-κB:E2F-1 interaction alongside initial work in a cell cycle context provides an impetus for the coupling of the NF-κB:E2F model with an A or A#-type model for cell cycle progression to form a "B-type" model (recalling definitions from Figure 8.2) for NF-κB interaction with E2F-1 within the context of G1/S progression.

There have been many Systems Biology approaches to modelling cell cycle progression. Current modelling approaches vary in level of abstraction from the entire mammalian cell cycle (Basse *et al.* 2003) to G1/S progression (Qu *et al.* 2003; Novak *et al.* 2004; Haberichter *et al.* 2007) to a consideration of feedback loops involving E2F-1 at G1/S (Baguley *et al.* 2005; Yao *et al.* 2008). These approaches are often carefully abstracted from complex conceptual models (Kohn 1999; Calzone *et al.* 2008), the circuitry of which may hide "*a central cell-cycle engine*" (Novak *et al.* 2004). The importance of a carefully drawn conceptual model is clear in the literature, but so too is the need for a justifiable rationale for taking the interdisciplinary approach, with modelling approaches used to suggest "gaps" in the current view of a system (Haberichter *et al.* 2007). It has even been argued that the complexities of cancer can only be fully understood through Systems Biology approaches (Hornberg *et al.* 2006).

The creation of a cell cycle model for coupling to the NF-κB model has the immediate advantage that a more realistic profile for E2F-1 can be generated. This would provide a suitable physiological context with which to investigate the predictions made for the role of E2F-1 in coordinating the dynamics of an NF-κB response (Figure 8.1).

8.5 G1/S Response context – Physiological perspective

The balance model for response at G1/S previously hypothesised for both the p53 and NF-κB systems (Sections 1.2.5.2 and 1.3.4) is generalised in Figure 8.6. We may now consider the similarities between p53 and NF-κB related mechanisms controlling temporary arrest of the cell cycle.

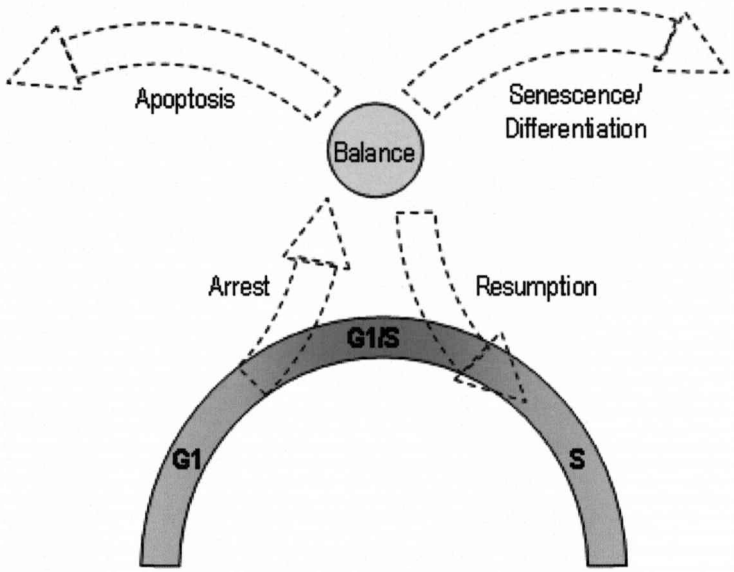

Figure 8.6 G1/S "Balance" model: Showing the processes involved in temporary arrest at G1/S, involving arrest of the cell cycle, a period of balance whereby cell fate decisions are coordinated. The outcome may be apoptosis, senescence, differentiation or the resumption of proliferation.

Both p53 and NF-κB may transactivate p21 to initiate cell cycle arrest (el-Deiry *et al.* 1993; Hinata *et al.* 2003), and Cyclin D1 to encourage proliferation (Spitkovsky *et al.* 1995; Guttridge *et al.* 1999), placing both systems in a G1/S context. Resumption of the cell cycle is dependent on a period of balance during which cell fate decisions are made. Both p53 and NF-κB have strong links to apoptosis (Kucharczak *et al.* 2003; Braithwaite *et al.* 2006), differentiation (Feng *et al.* 1999; Stiewe 2007) and senescence (Shay *et al.* 1991; Helenius *et al.* 1996), reviewed futher in (Mathon *et al.* 2001). However, for these processes to be coordinated within a G1/S context, one would expect temporal regulation by G1/S proteins in order to appropriately govern cell fate decisions prior to S-phase.

Accordingly, p53 has been previously shown to interact directly with E2F-1. E2F-1 binds to p53 at a region which overlaps the p53 NES thereby retaining active p53 in the nucleus (O'Connor *et al.* 1995; Hsieh *et al.* 2002). This binding is overturned by p53-

mediated transcription of inhibitor MDM2, which leads to the export of p53 to the cytoplasm whilst stabilising E2F-1 (Zhang *et al.* 2005) and by increasing levels of Cyclin A, which competes with p53 for binding to E2F-1 ending E2F-related transcription (Peeper *et al.* 1995; Hsieh *et al.* 2002). This story is startlingly similar to the story presented in this work, NF-κB binds directly to E2F-1 and is retained in the nucleus (Sections 4.3 and 5.5), subsequent translocation to the cytoplasm is dependant on the transcription of inhibitor IκBα (Section 7.4) and proportional to E2F-1 degradation (Section 6.4). Both balance models therefore intuitively lead not only to resumption of the cell cycle but also a re-set steady state for both p53 and NF-κB systems.

The interactions between G1/S proteins and p53 or G1/S proteins and NF-κB, that contribute to cell cycle suspension, balance and resumption of the cell cycle have been previously described (Sections 1.2.5.1 and 1.3.4) and are summarised in detail in Figures 8.7, 8.8 and 8.9 respectively.

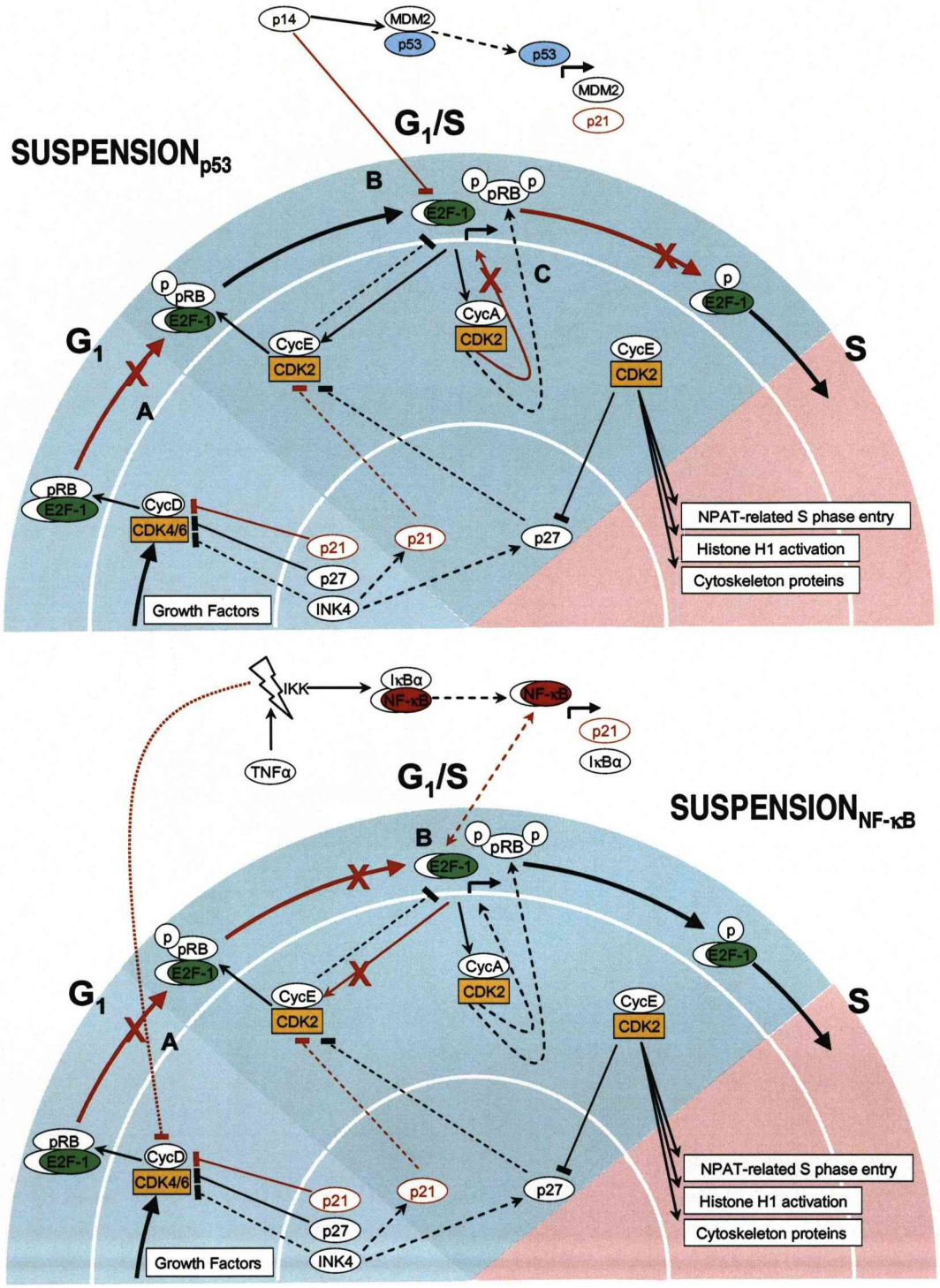

Figure 8.7 G1/S Balance model – cell cycle suspension mechanisms for p53 and NF-κB: SUSPENSION (p53) Showing p53-mediated induction of p21, CDKI for CDK4, inhibition of E2F-1 by p53 activator p14 and direct binding between E2F-1 and p53 at a region which prevents re-associated between pRB and E2F-1 and S-phase entry. See text for details. **SUSPENSION (NF-κB)** Showing NF-κB-mediated induction of p21, IKK inhibition of CDK4, and binding between NF-κB and E2F-1 which inhibits E2F-1-mediated transcription of E2F-1 and Cyclin E, as shown in this study. See text for details. Solid black lines represent direct processes, dotted lines represent

indirect and delayed processes. An arrowhead represents positive regulation, a flat-head line represents repression. Large arrows mark the transition between cell cycle stages. Red lines represent mechanisms contributing to cell cycle arrest.

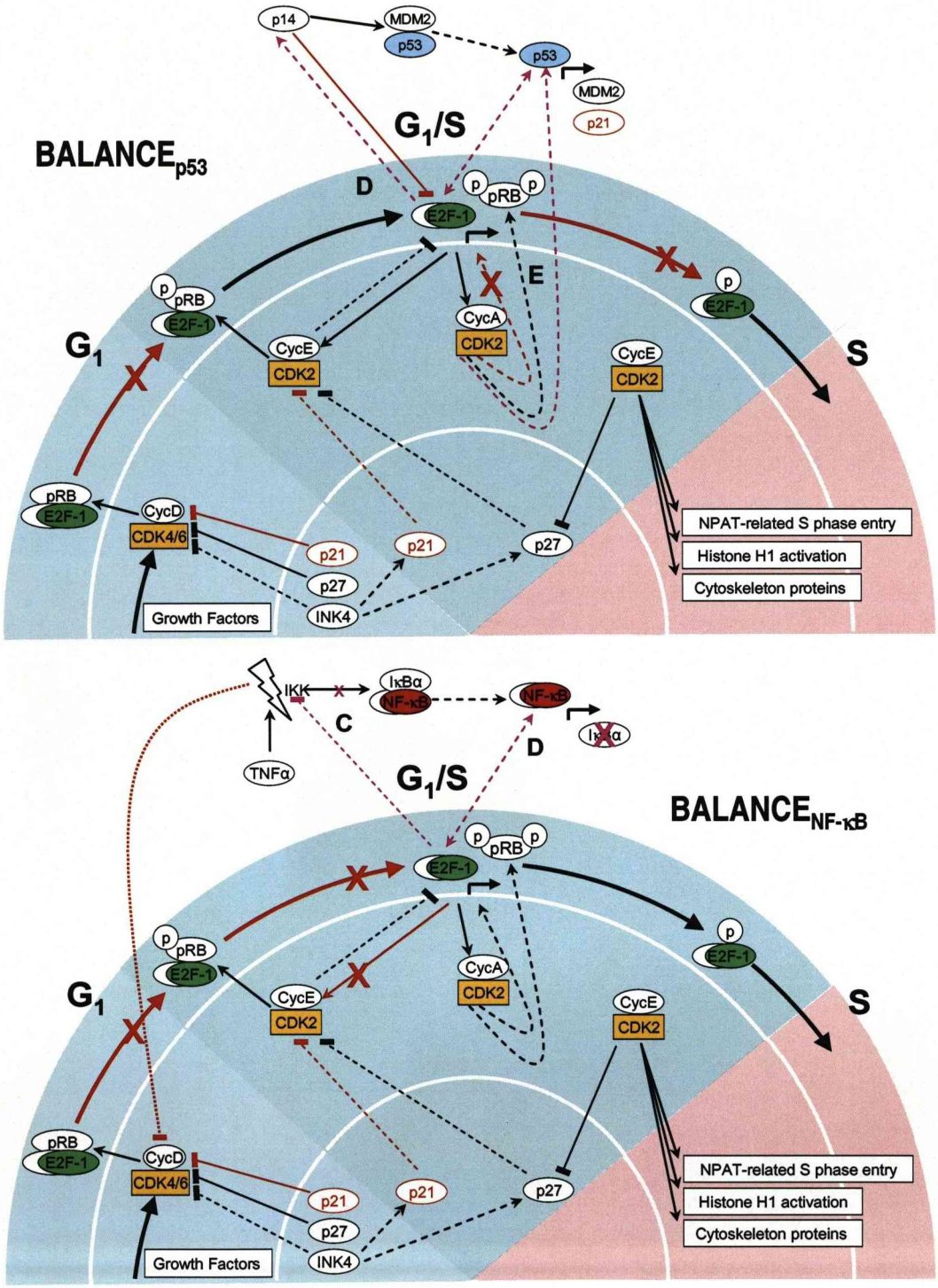

Figure 8.8 G1/S Balance model – G1/S-mediated co-ordination of p53 and NF-κB signalling: BALANCE (p53) Showing E2F-1-mediated induction of p14, activator of p53 and the direct binding of E2F-1 to p53 at a region which overlaps the p53 NES, which is overturned by Cyclin A phosphorylation, a target gene of E2F-1. See text for details. **BALANCE (NF-κB)** Showing E2F-1-mediated inhibition of IKK and NF-κB-mediated transcription of IκB proteins, as shown in this study. See text for details.

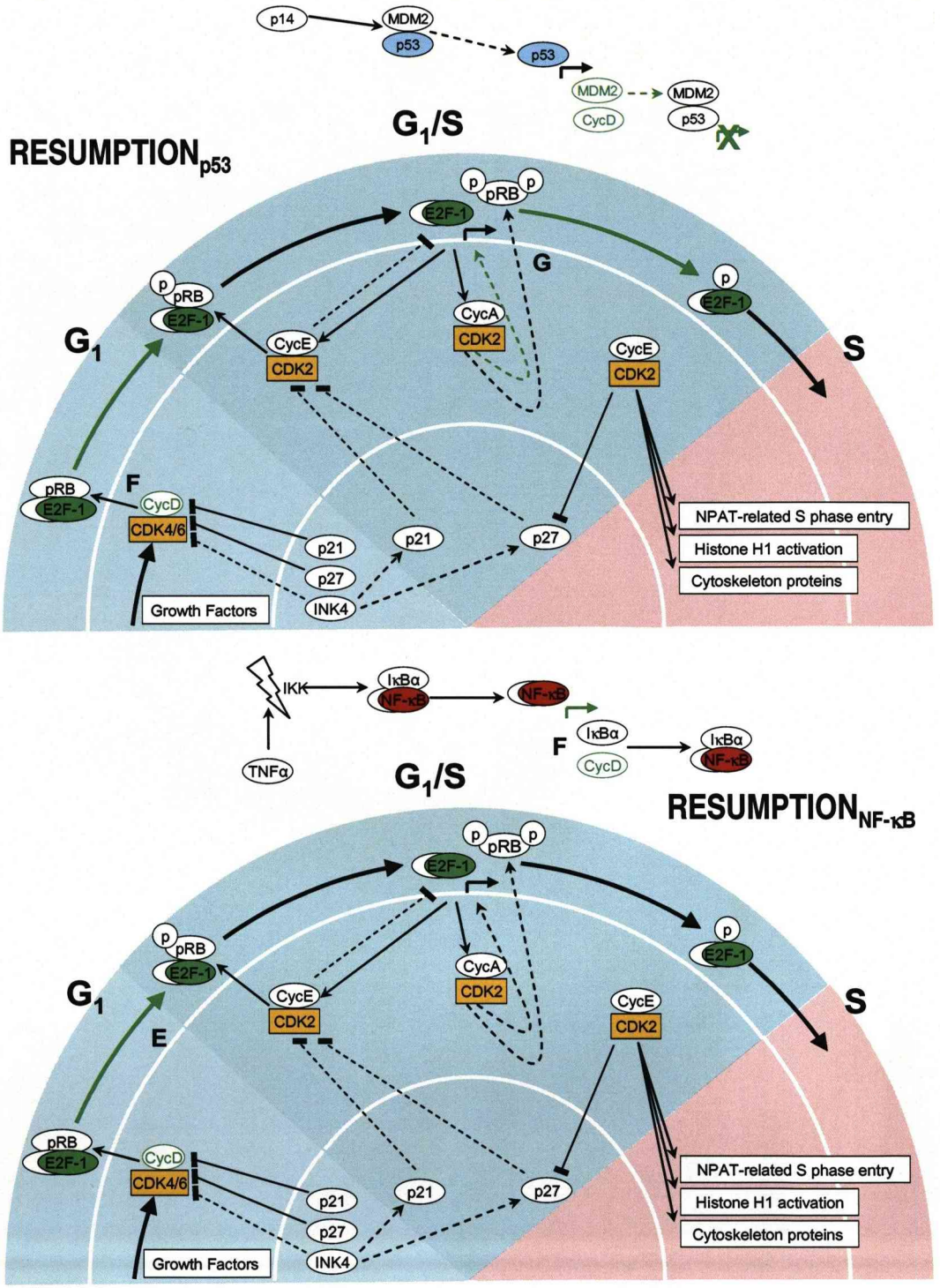

Figure 8.9 G1/S Balance Model – cell cycle resumption mechanisms for p53 and NF-κB: RESUMPTION (p53) Showing p53-mediated transcription of Cyclin D, and MDM2 which releases p53 from binding to E2F-1, whilst stabilising E2F-1. E2F-1 can then be targeted for phosphorylation by Cyclins A and E. The p53 system is "reset" to a dormant state. See text for details. **RESUMPTION (NF-κB)** Showing transcription of Cyclin D, and, as shown in this study, transcription of IκBα at a point at which NF-κB is unbound from E2F-1. The NF-κB system is "reset" to a dormant state. See text for details.

The development of live cell imaging techniques for cell cycle studies may also provide the opportunity to investigate the relationship between localisation of Cyclin A, p53 and E2F-1 outlined above. Indeed, the balance model provides arguably the most intriguing area for future investigation, given the mechanistic similarities between p53 and NF-κB responses within a G1/S context, and published interaction between the p53 and NF-κB systems (Webster *et al.* 1999; Chang 2002; Furuya *et al.* 2007) considered further in (Tergaonkar *et al.* 2007). Complementarily to the development of these models, the concept of temporary delay at G1/S is implicit in the current views of both p53 and NF-κB systems (Braithwaite *et al.* 2006; Perkins *et al.* 2006; Maddika *et al.* 2007) with recent studies characterising an NF-κB-mediated "short-term cell cycle block" (Penzo *et al.* 2009) and a similar model for p53 (Toettcher *et al.* 2009). The work presented is therefore believed to concur fully with the current view of NF-κB immune response G1/S and allows logical comparisons to be drawn with p53-mediated DNA damage response at G1/S.

Considering the NF-κB:E2F-1 interactions within the context of G1/S balance, we propose that the cell may act to give an inflammatory response "priority" prior to beginning DNA synthesis. However, during S-phase, when DNA synthesis must take the priority, the inflammatory response may be either delayed or abated. Interactions of this type provide an interesting paradigm in Systems Biology, i.e. cross-talk between two systems which results in a differential "switch" between systems - as one system is "switched on" the other is "switched off". In contrast to what we expect when linking such signalling systems, interactions such as these may actually lead to a reduction in complexity.

8.6 Final Comment – The importance of metaphor

It can be argued that metaphors are essential to Systems Biology as the process of abstraction involves the definition of systems analogous to physiological context. However, metaphor serves a further purpose in aiding understanding, particularly when comparing similar processes with shared properties (Noble 2006). For example, as highlighted in Chapter 1, oscillatory processes have been seen to span periods of time from fractions of a second/minutes (Calcium) to minutes/hours (NF-κB, p53, segmentation clock) to hours/days (circadian clock and cell cycle). We considered the possibility that interactions between these dynamic processes may well link together like the cogs in a clockwork mechanism. The clock metaphor is well established for circadian rhythms (Pittendrigh 1957; Dunlap 1999) and the cell cycle (Sherr 1996; Morgan 1997), in which oscillatory behaviour is generated by multiple levels of feedback, controlling phase transition. The strength of the clock metaphor in these cases is that key events are "timed" by the use of oscillations (considered in detail in (Rensing *et al.* 2001)).

I propose that the clockwork metaphor may be taken a step further to consider the Balance model characterised in this work (Figure 8.5) in similar terms, i.e. as an integral component of the cell cycle clock. The control of the "pace" of proliferation through a restriction point may well be analogous to the way in which an escapement mechanism controls the pace of a pendulum. This analogy has been considered previously, albeit for different mechanisms, in bacteria (Holtzendorff *et al.* 2004).

Denis Noble, pioneer of work modelling ion wave patterns across the human heart (DiFrancesco *et al.* 1985; Noble 2006), has recently underlined the importance of such metaphors to highlighting the principles of Systems Biology (Noble 2006). Noble chooses to compare collaboration and subtlety in protein interaction to musical orchestration, as an answer to the question of complexity arising from a relative small genome (the "*organ of 30,000 pipes*"), an analogy we have recently sought to apply to single cell model systems (Ankers *et al.* 2008), and others have compared to oscillatory patterns of gene activation (Sun *et al.* 2008). "*Different, even competing metaphors*", Noble claims, "*can illuminate different aspects of the same situation*", but are merely "*ladders to understanding ... Once you have climbed them, you can throw them away*".

Chapter 9 -
References

Ainbinder, E., M. Revach, O. Wolstein, S. Moshonov, N. Diamant and R. Dikstein (2002). "Mechanism of rapid transcriptional induction of tumor necrosis factor alpha-responsive genes by NF-kappaB." Mol Cell Biol **22**(18): 6354-62.

Albanese, C., K. Wu, M. D'Amico, C. Jarrett, D. Joyce, J. Hughes, J. Hulit, T. Sakamaki, M. Fu, A. Ben-Ze'ev, J. F. Bromberg, C. Lamberti, U. Verma, R. B. Gaynor, S. W. Byers and R. G. Pestell (2003). "IKKalpha regulates mitogenic signaling through transcriptional induction of cyclin D1 via Tcf." Mol Biol Cell **14**(2): 585-99.

Angus, S. P., D. A. Solomon, L. Kuschel, R. F. Hennigan and E. S. Knudsen (2003). "Retinoblastoma tumor suppressor: analyses of dynamic behavior in living cells reveal multiple modes of regulation." Mol Cell Biol **23**(22): 8172-88.

Ankers, J. M., D. G. Spiller, M. R. White and C. V. Harper (2008). "Spatio-temporal protein dynamics in single living cells." Curr Opin Biotechnol **19**(4): 375-80.

Ashall, L., C. A. Horton, D. E. Nelson, P. Paszek, C. V. Harper, K. Sillitoe, S. Ryan, D. G. Spiller, J. F. Unitt, D. S. Broomhead, D. B. Kell, D. A. Rand, V. See and W. M.R.H. (2009). "Oscillation synchronisation and downstream gene expression regulated by feedback loops in the NF-κB system." Science (In press).

Assoian, R. K. (1997). "Anchorage-dependent cell cycle progression." Journal of Cell Biology **136**(1): 1-4.

Attwooll, C., E. Lazzerini Denchi and K. Helin (2004). "The E2F family: specific functions and overlapping interests." Embo J **23**(24): 4709-16.

Aulehla, A., W. Wiegraebe, V. Baubet, M. B. Wahl, C. Deng, M. Taketo, M. Lewandoski and O. Pourquie (2008). "A beta-catenin gradient links the clock and wavefront systems in mouse embryo segmentation." Nat Cell Biol **10**(2): 186-93.

Baeuerle, P. A. and D. Baltimore (1988). "Activation of DNA-binding activity in an apparently cytoplasmic precursor of the NF-kappa B transcription factor." Cell **53**(2): 211-7.

Bagchi, S., P. Raychaudhuri and J. R. Nevins (1990). "Adenovirus E1A proteins can dissociate heteromeric complexes involving the E2F transcription factor: a novel mechanism for E1A trans-activation." Cell **62**(4): 659-69.

Baguley, B. C. and E. Marshall (2005). "Do negative feedback oscillations drive variations in the length of the tumor cell division cycle?" Oncol Res **15**(6): 291-4.

Balsalobre, A., F. Damiola and U. Schibler (1998). "A serum shock induces circadian gene expression in mammalian tissue culture cells." Cell **93**(6): 929-37.

Barre, B. and N. D. Perkins (2007). "A cell cycle regulatory network controlling NF-kappaB subunit activity and function." Embo J **26**(23): 4841-55.

Bartkova, J., J. Lukas, M. Strauss and J. Bartek (1998). "Cyclin D3: requirement for G1/S transition and high abundance in quiescent tissues suggest a dual role in proliferation and differentiation." Oncogene **17**(8): 1027-37.

Basak, S., H. Kim, J. D. Kearns, V. Tergaonkar, E. O'Dea, S. L. Werner, C. A. Benedict, C. F. Ware, G. Ghosh, I. M. Verma and A. Hoffmann (2007). "A fourth IkappaB protein within the NF-kappaB signaling module." Cell **128**(2): 369-81.

Basse, B., B. C. Baguley, E. S. Marshall, W. R. Joseph, B. van Brunt, G. Wake and D. J. Wall (2003). "A mathematical model for analysis of the cell cycle in cell lines derived from human tumors." J Math Biol **47**(4): 295-312.

Bean, J. M., E. D. Siggia and F. R. Cross (2006). "Coherence and timing of cell cycle start examined at single-cell resolution." Mol Cell **21**(1): 3-14.

Berridge, M. J. (1990). "Calcium oscillations." J Biol Chem **265**(17): 9583-6.

Bjursell, G. and P. Reichard (1973). "Effects of thymidine on deoxyribonucleoside triphosphate pools and deoxyribonucleic acid synthesis in Chinese hamster ovary cells." J Biol Chem **248**(11): 3904-9.

Bracken, A. P., M. Ciro, A. Cocito and K. Helin (2004). "E2F target genes: unraveling the biology." Trends Biochem Sci **29**(8): 409-17.

Braithwaite, A. W., G. Del Sal and X. Lu (2006). "Some p53-binding proteins that can function as arbiters of life and death." Cell Death Differ **13**(6): 984-93.

Cai, L., C. K. Dalal and M. B. Elowitz (2008). "Frequency-modulated nuclear localization bursts coordinate gene regulation." Nature **455**(7212): 485-90.

Calzone, L., A. Gelay, A. Zinovyev, F. Radvanyi and E. Barillot (2008). "A comprehensive modular map of molecular interactions in RB/E2F pathway." Mol Syst Biol **4**: 173.

Campanero, M. R. and E. K. Flemington (1997). "Regulation of E2F through ubiquitin-proteasome-dependent degradation: stabilization by the pRB tumor suppressor protein." Proc Natl Acad Sci U S A **94**(6): 2221-6.

Carey, L. B., J. K. Leatherwood and B. Futcher (2008). "Huxley's revenge: cell-cycle entry, positive feedback, and the G1 cyclins." Mol Cell **31**(3): 307-8.

Carnero, A. and G. J. Hannon (1998). "The INK4 family of CDK inhibitors." Curr Top Microbiol Immunol **227**: 43-55.

Cartwright, P. and K. Helin (2000). "Nucleocytoplasmic shuttling of transcription factors." Cell Mol Life Sci **57**(8-9): 1193-206.

Chang, N. S. (2002). "The non-ankyrin C terminus of Ikappa Balpha physically interacts with p53 in vivo and dissociates in response to apoptotic stress, hypoxia, DNA damage, and transforming growth factor-beta 1-mediated growth suppression." J Biol Chem **277**(12): 10323-31.

Chen, J., J. Lin and A. J. Levine (1995). "Regulation of transcription functions of the p53 tumor suppressor by the mdm-2 oncogene." Mol Med **1**(2): 142-52.

Chen, Y. Q., L. L. Sengchanthalangsy, A. Hackett and G. Ghosh (2000). "NF-kappaB p65 (RelA) homodimer uses distinct mechanisms to recognize DNA targets." Structure **8**(4): 419-28.

Colburn, T. and G. Shute (2007). "Abstraction in computer science." Minds and Machines **17**(2): 169-184.

Collins, C. J. and J. M. Sedivy (2003). "Involvement of the INK4a/Arf gene locus in senescence." Aging Cell **2**(3): 145-50.

Cuthbertson, K. S. and P. H. Cobbold (1985). "Phorbol ester and sperm activate mouse oocytes by inducing sustained oscillations in cell Ca2+." Nature **316**(6028): 541-2.

DeGregori, J., G. Leone, A. Miron, L. Jakoi and J. R. Nevins (1997). "Distinct roles for E2F proteins in cell growth control and apoptosis." Proc Natl Acad Sci U S A **94**(14): 7245-50.

DiFrancesco, D. and D. Noble (1985). "A model of cardiac electrical activity incorporating ionic pumps and concentration changes." Philos Trans R Soc Lond B Biol Sci **307**(1133): 353-98.

Dimri, G. P., K. Itahana, M. Acosta and J. Campisi (2000). "Regulation of a senescence checkpoint response by the E2F1 transcription factor and p14(ARF) tumor suppressor." Mol Cell Biol **20**(1): 273-85.

Dolmetsch, R. E., R. S. Lewis, C. C. Goodnow and J. I. Healy (1997). "Differential activation of transcription factors induced by Ca2+ response amplitude and duration." Nature **386**(6627): 855-8.

Dolmetsch, R. E., K. Xu and R. S. Lewis (1998). "Calcium oscillations increase the efficiency and specificity of gene expression." Nature **392**(6679): 933-6.

Doonan, J. H. and G. Kitsios (2009). "Functional Evolution of Cyclin-Dependent Kinases." Mol Biotechnol.

Dunlap, J. C. (1999). "Molecular bases for circadian clocks." Cell **96**(2): 271-90.

Dyson, N. (1998). "The regulation of E2F by pRB-family proteins." Genes Dev **12**(15): 2245-62.

el-Deiry, W. S., T. Tokino, V. E. Velculescu, D. B. Levy, R. Parsons, J. M. Trent, D. Lin, W. E. Mercer, K. W. Kinzler and B. Vogelstein (1993). "WAF1, a potential mediator of p53 tumor suppression." Cell **75**(4): 817-25.

Elowitz, M. B., A. J. Levine, E. D. Siggia and P. S. Swain (2002). "Stochastic gene expression in a single cell." Science **297**(5584): 1183-6.

Fall, C. P., Marland, E. S., Wagner, J. M. and Tyson, J. J. (2002). Computational Cell Biology, Springer.

Feng, Z. and A. G. Porter (1999). "NF-kappaB/Rel proteins are required for neuronal differentiation of SH-SY5Y neuroblastoma cells." J Biol Chem **274**(43): 30341-4.

Floridi, L. (2008). "The method of levels of abstraction." Minds and Machines **18**(3): 303-329.

Friedman, P. N., X. Chen, J. Bargonetti and C. Prives (1993). "The p53 protein is an unusually shaped tetramer that binds directly to DNA." Proc Natl Acad Sci U S A **90**(8): 3319-23.

Furuya, K., T. Ozaki, T. Hanamoto, M. Hosoda, S. Hayashi, P. A. Barker, K. Takano, M. Matsumoto and A. Nakagawara (2007). "Stabilization of p73 by nuclear IkappaB kinase-alpha mediates cisplatin-induced apoptosis." J Biol Chem **282**(25): 18365-78.

Galbiati, L., R. Mendoza-Maldonado, M. I. Gutierrez and M. Giacca (2005). "Regulation of E2F-1 after DNA damage by p300-mediated acetylation and ubiquitination." Cell Cycle **4**(7): 930-9.

Gatz, S. A. and L. Wiesmuller (2006). "p53 in recombination and repair." Cell Death Differ **13**(6): 1003-16.

Geva-Zatorsky, N., N. Rosenfeld, S. Itzkovitz, R. Milo, A. Sigal, E. Dekel, T. Yarnitzky, Y. Liron, P. Polak, G. Lahav and U. Alon (2006). "Oscillations and variability in the p53 system." Mol Syst Biol **2**: 2006 0033.

Grynkiewicz, G., M. Poenie and R. Y. Tsien (1985). "A new generation of Ca2+ indicators with greatly improved fluorescence properties." J Biol Chem **260**(6): 3440-50.

Guttridge, D. C., C. Albanese, J. Y. Reuther, R. G. Pestell and A. S. Baldwin, Jr. (1999). "NF-kappaB controls cell growth and differentiation through transcriptional regulation of cyclin D1." Mol Cell Biol **19**(8): 5785-99.

Haberichter, T., B. Madge, R. A. Christopher, N. Yoshioka, A. Dhiman, R. Miller, R. Gendelman, S. V. Aksenov, I. G. Khalil and S. F. Dowdy (2007). "A systems biology dynamical model of mammalian G1 cell cycle progression." Mol Syst Biol **3**: 84.

Hamstra, D. A., M. S. Bhojani, L. B. Griffin, B. Laxman, B. D. Ross and A. Rehemtulla (2006). "Real-time evaluation of p53 oscillatory behavior in vivo using bioluminescent imaging." Cancer Res **66**(15): 7482-9.

Harhaj, E. W. and S. C. Sun (1999). "Regulation of RelA subcellular localization by a putative nuclear export signal and p50." Mol Cell Biol **19**(10): 7088-95.

Harper, J. W., S. J. Elledge, K. Keyomarsi, B. Dynlacht, L. H. Tsai, P. Zhang, S. Dobrowolski, C. Bai, L. Connell-Crowley, E. Swindell and et al. (1995). "Inhibition of cyclin-dependent kinases by p21." Mol Biol Cell **6**(4): 387-400.

Hartwell, L. H. and T. A. Weinert (1989). "Checkpoints: controls that ensure the order of cell cycle events." Science **246**(4930): 629-34.

Hayflick, L. (1965). "The Limited In Vitro Lifetime Of Human Diploid Cell Strains." Exp Cell Res **37**: 614-36.

Helenius, M., M. Hanninen, S. K. Lehtinen and A. Salminen (1996). "Changes associated with aging and replicative senescence in the regulation of transcription factor nuclear factor-kappa B." Biochem J **318 (Pt 2)**: 603-8.

Hinata, K., A. M. Gervin, Y. Jennifer Zhang and P. A. Khavari (2003). "Divergent gene regulation and growth effects by NF-kappa B in epithelial and mesenchymal cells of human skin." Oncogene **22**(13): 1955-64.

Hodgkin, A. L. and A. F. Huxley (1952). "A quantitative description of membrane current and its application to conduction and excitation in nerve." J Physiol **117**(4): 500-44.

Hoffmann, A., A. Levchenko, M. L. Scott and D. Baltimore (2002). "The IkappaB-NF-kappaB signaling module: temporal control and selective gene activation." Science **298**(5596): 1241-5.

Hofmann, F., F. Martelli, D. M. Livingston and Z. Wang (1996). "The retinoblastoma gene product protects E2F-1 from degradation by the ubiquitin-proteasome pathway." Genes Dev **10**(23): 2949-59.

Holtzendorff, J., D. Hung, P. Brende, A. Reisenauer, P. H. Viollier, H. H. McAdams and L. Shapiro (2004). "Oscillating global regulators control the genetic circuit driving a bacterial cell cycle." Science **304**(5673): 983-7.

Hornberg, J. J., F. J. Bruggeman, H. V. Westerhoff and J. Lankelma (2006). "Cancer: A systems biology disease." Biosystems **83**(2-3): 81-90.

Hsiao, K. M., S. L. McMahon and P. J. Farnham (1994). "Multiple DNA elements are required for the growth regulation of the mouse E2F1 promoter." Genes Dev **8**(13): 1526-37.

Hsieh, J. K., D. Yap, D. J. O'Connor, V. Fogal, L. Fallis, F. Chan, S. Zhong and X. Lu (2002). "Novel function of the cyclin A binding site of E2F in regulating p53-induced apoptosis in response to DNA damage." Mol Cell Biol **22**(1): 78-93.

Huang, T. T., N. Kudo, M. Yoshida and S. Miyamoto (2000). "A nuclear export signal in the N-terminal regulatory domain of IkappaBalpha controls cytoplasmic localization of inactive NF-kappaB/IkappaBalpha complexes." Proc Natl Acad Sci U S A **97**(3): 1014-9.

Huxford, T., D. B. Huang, S. Malek and G. Ghosh (1998). "The crystal structure of the IkappaBalpha/NF-kappaB complex reveals mechanisms of NF-kappaB inactivation." Cell **95**(6): 759-70.

Iaquinta, P. J. and J. A. Lees (2007). "Life and death decisions by the E2F transcription factors." Curr Opin Cell Biol **19**(6): 649-57.

Infante, A., U. Laresgoiti, J. Fernandez-Rueda, A. Fullaondo, J. Galan, R. Diaz-Uriarte, M. Malumbres, S. J. Field and A. M. Zubiaga (2008). "E2F2 represses cell cycle regulators to maintain quiescence." Cell Cycle **7**(24).

Ishida, S., E. Huang, H. Zuzan, R. Spang, G. Leone, M. West and J. R. Nevins (2001). "Role for E2F in control of both DNA replication and mitotic functions as revealed from DNA microarray analysis." Molecular and Cellular Biology **21**(14): 4684-4699.

Jackman, M., Y. Kubota, N. den Elzen, A. Hagting and J. Pines (2002). "Cyclin A- and cyclin E-Cdk complexes shuttle between the nucleus and the cytoplasm." Mol Biol Cell **13**(3): 1030-45.

Jacobs, M. D. and S. C. Harrison (1998). "Structure of an IkappaBalpha/NF-kappaB complex." Cell **95**(6): 749-58.

Jameson, D., K. Garwood, C. Garwood, T. Booth, P. Alper, S. G. Oliver and N. W. Paton (2008). "Data capture in bioinformatics: requirements and experiences with Pedro." BMC Bioinformatics **9**: 183.

Johnson, C., D. Van Antwerp and T. J. Hope (1999). "An N-terminal nuclear export signal is required for the nucleocytoplasmic shuttling of IkappaBalpha." Embo J **18**(23): 6682-93.

Johnson, D. G., J. K. Schwarz, W. D. Cress and J. R. Nevins (1993). "Expression of transcription factor E2F1 induces quiescent cells to enter S phase." Nature **365**(6444): 349-52.

Karpova, T. S., C. T. Baumann, L. He, X. Wu, A. Grammer, P. Lipsky, G. L. Hager and J. G. McNally (2003). "Fluorescence resonance energy transfer from cyan to yellow fluorescent protein detected by acceptor photobleaching using confocal microscopy and a single laser." J Microsc **209**(Pt 1): 56-70.

Kearns, J. D., S. Basak, S. L. Werner, C. S. Huang and A. Hoffmann (2006). "IkappaBepsilon provides negative feedback to control NF-kappaB oscillations, signaling dynamics, and inflammatory gene expression." J Cell Biol **173**(5): 659-64.

Kerszberg, M. (2004). "Noise, delays, robustness, canalization and all that." Curr Opin Genet Dev **14**(4): 440-5.

Ko, C. H. and J. S. Takahashi (2006). "Molecular components of the mammalian circadian clock." Hum Mol Genet **15 Spec No 2**: R271-7.

Kohn, K. W. (1999). "Molecular interaction map of the mammalian cell cycle control and DNA repair systems." Mol Biol Cell **10**(8): 2703-34.

Kohn, K. W., M. I. Aladjem, J. N. Weinstein and Y. Pommier (2006). "Molecular interaction maps of bioregulatory networks: a general rubric for systems biology." Mol Biol Cell **17**(1): 1-13.

Kovesdi, I., R. Reichel and J. R. Nevins (1986). "Identification of a cellular transcription factor involved in E1A trans-activation." Cell **45**(2): 219-28.

Kucharczak, J., M. J. Simmons, Y. Fan and C. Gelinas (2003). "To be, or not to be: NF-kappaB is the answer--role of Rel/NF-kappaB in the regulation of apoptosis." Oncogene **22**(56): 8961-82.

Kufe, D. W., E. M. Egan, A. Rosowsky, W. Ensminger and E. Frei, 3rd (1980). "Thymidine arrest and synchrony of cellular growth in vivo." Cancer Treat Rep **64**(12): 1307-17.

Kundu, M., M. Guermah, R. G. Roeder, S. Amini and K. Khalili (1997). "Interaction between cell cycle regulator, E2F-1, and NF-kappaB mediates repression of HIV-1 gene transcription." J Biol Chem **272**(47): 29468-74.

Kwak, Y. T., R. Li, C. R. Becerra, D. Tripathy, E. P. Frenkel and U. N. Verma (2005). "IkappaB kinase alpha regulates subcellular distribution and turnover of cyclin D1 by phosphorylation." J Biol Chem **280**(40): 33945-52.

Lahav, G., N. Rosenfeld, A. Sigal, N. Geva-Zatorsky, A. J. Levine, M. B. Elowitz and U. Alon (2004). "Dynamics of the p53-Mdm2 feedback loop in individual cells." Nat Genet **36**(2): 147-50.

Lamberti, C., K. M. Lin, Y. Yamamoto, U. Verma, I. M. Verma, S. Byers and R. B. Gaynor (2001). "Regulation of beta-catenin function by the IkappaB kinases." J Biol Chem **276**(45): 42276-86.

Lauper, N., A. R. Beck, S. Cariou, L. Richman, K. Hofmann, W. Reith, J. M. Slingerland and B. Amati (1998). "Cyclin E2: a novel CDK2 partner in the late G1 and S phases of the mammalian cell cycle." Oncogene **17**(20): 2637-43.

Lee, E. G., D. L. Boone, S. Chai, S. L. Libby, M. Chien, J. P. Lodolce and A. Ma (2000). "Failure to regulate TNF-induced NF-kappaB and cell death responses in A20-deficient mice." Science **289**(5488): 2350-4.

Levins, R. (1966). "The strategy of model building in population biology." American Scientist **54**: 421-431.

Li, J., S. H. Joo and M. D. Tsai (2003). "An NF-kappaB-specific inhibitor, IkappaBalpha, binds to and inhibits cyclin-dependent kinase 4." Biochemistry **42**(46): 13476-83.

Li, W., J. Llopis, M. Whitney, G. Zlokarnik and R. Y. Tsien (1998). "Cell-permeant caged InsP3 ester shows that Ca2+ spike frequency can optimize gene expression." Nature **392**(6679): 936-41.

Lim, C. A., F. Yao, J. J. Wong, J. George, H. Xu, K. P. Chiu, W. K. Sung, L. Lipovich, V. B. Vega, J. Chen, A. Shahab, X. D. Zhao, M. Hibberd, C. L. Wei, B. Lim, H. H. Ng, Y. Ruan and K. C. Chin (2007). "Genome-wide mapping of RELA(p65) binding identifies E2F1 as a transcriptional activator recruited by NF-kappaB upon TLR4 activation." Mol Cell **27**(4): 622-35.

Lipniacki, T., P. Paszek, A. R. Brasier, B. A. Luxon and M. Kimmel (2005). "Stochastic regulation in early immune response." Biophys J.

Lipniacki, T., P. Paszek, A. Marciniak-Czochra, A. R. Brasier and M. Kimmel (2006). "Transcriptional stochasticity in gene expression." J Theor Biol **238**(2): 348-67.

Lipniacki, T., K. Puszynski, P. Paszek, A. R. Brasier and M. Kimmel (2007). "Single TNFalpha trimers mediating NF-kappaB activation: stochastic robustness of NF-kappaB signaling." BMC Bioinformatics **8**: 376.

Lotka, A. J. (1925). "Elements of physical biology." Baltimore: 460 p.

Maddika, S., S. R. Ande, S. Panigrahi, T. Paranjothy, K. Weglarczyk, A. Zuse, M. Eshraghi, K. D. Manda, E. Wiechec and M. Los (2007). "Cell survival, cell death and cell cycle pathways are interconnected: implications for cancer therapy." Drug Resist Updat **10**(1-2): 13-29.

Magae, J., C. L. Wu, S. Illenye, E. Harlow and N. H. Heintz (1996). "Nuclear localization of DP and E2F transcription factors by heterodimeric partners and retinoblastoma protein family members." J Cell Sci **109 (Pt 7)**: 1717-26.

Malek, S., Y. Chen, T. Huxford and G. Ghosh (2001). "IkappaBbeta, but not IkappaBalpha, functions as a classical cytoplasmic inhibitor of NF-kappaB dimers by masking both NF-kappaB nuclear localization sequences in resting cells." J Biol Chem **276**(48): 45225-35.

Malek, S., D. B. Huang, T. Huxford, S. Ghosh and G. Ghosh (2003). "X-ray crystal structure of an IkappaBbeta x NF-kappaB p65 homodimer complex." J Biol Chem **278**(25): 23094-100.

Martelli, F., T. Hamilton, D. P. Silver, N. E. Sharpless, N. Bardeesy, M. Rokas, R. A. DePinho, D. M. Livingston and S. R. Grossman (2001). "p19ARF targets certain E2F species for degradation." Proc Natl Acad Sci U S A **98**(8): 4455-60.

Mathon, N. F. and A. C. Lloyd (2001). "Cell senescence and cancer." Nat Rev Cancer **1**(3): 203-13.

Milo, R., S. Shen-Orr, S. Itzkovitz, N. Kashtan, D. Chklovskii and U. Alon (2002). "Network motifs: simple building blocks of complex networks." Science **298**(5594): 824-7.

Miyamoto, S., M. Maki, M. J. Schmitt, M. Hatanaka and I. M. Verma (1994). "Tumor necrosis factor alpha-induced phosphorylation of I kappa B alpha is a signal for its degradation but not dissociation from NF-kappa B." Proc Natl Acad Sci U S A **91**(26): 12740-4.

Morgan, D. O. (1997). "Cyclin-dependent kinases: engines, clocks, and microprocessors." Annu Rev Cell Dev Biol **13**: 261-91.

Muller, H., M. C. Moroni, E. Vigo, B. O. Petersen, J. Bartek and K. Helin (1997). "Induction of S-phase entry by E2F transcription factors depends on their nuclear localization." Mol Cell Biol **17**(9): 5508-20.

Murphy, M., M. G. Stinnakre, C. Senamaud-Beaufort, N. J. Winston, C. Sweeney, M. Kubelka, M. Carrington, C. Brechot and J. Sobczak-Thepot (1997). "Delayed early embryonic lethality following disruption of the murine cyclin A2 gene." Nat Genet **15**(1): 83-6.

Nelson, D. E., A. E. Ihekwaba, M. Elliott, J. R. Johnson, C. A. Gibney, B. E. Foreman, G. Nelson, V. See, C. A. Horton, D. G. Spiller, S. W. Edwards, H. P. McDowell, J. F. Unitt, E. Sullivan, R. Grimley, N. Benson, D. Broomhead, D. B. Kell and M. R. White (2004). "Oscillations in NF-kappaB signaling control the dynamics of gene expression." Science **306**(5696): 704-8.

Nelson, G., L. Paraoan, D. G. Spiller, G. J. Wilde, M. A. Browne, P. K. Djali, J. F. Unitt, E. Sullivan, E. Floettmann and M. R. White (2002). "Multi-parameter analysis of the kinetics of NF-kappaB signalling and transcription in single living cells." J Cell Sci **115**(Pt 6): 1137-48.

Nelson, G., G. J. Wilde, D. G. Spiller, S. M. Kennedy, D. W. Ray, E. Sullivan, J. F. Unitt and M. R. White (2003). "NF-kappaB signalling is inhibited by glucocorticoid receptor and STAT6 via distinct mechanisms." J Cell Sci **116**(Pt 12): 2495-503.

Nelson, M. T., H. Cheng, M. Rubart, L. F. Santana, A. D. Bonev, H. J. Knot and W. J. Lederer (1995). "Relaxation of arterial smooth muscle by calcium sparks." Science **270**(5236): 633-7.

Noble, D. (2006). The music of life: biology beyond the genome. Oxford, Oxford University Press.

Noble, D. (2006). "Systems biology and the heart." Biosystems **83**(2-3): 75-80.

Novak, B. and J. J. Tyson (2004). "A model for restriction point control of the mammalian cell cycle." J Theor Biol **230**(4): 563-79.

O'Connor, D. J., E. W. Lam, S. Griffin, S. Zhong, L. C. Leighton, S. A. Burbidge and X. Lu (1995). "Physical and functional interactions between p53 and cell cycle co-operating transcription factors, E2F1 and DP1." Embo J **14**(24): 6184-92.

Ohtsubo, M., A. M. Theodoras, J. Schumacher, J. M. Roberts and M. Pagano (1995). "Human Cyclin-E, a Nuclear-Protein Essential for the G(1)-to-S Phase-Transition." Molecular and Cellular Biology **15**(5): 2612-2624.

Opavsky, R., S. Y. Tsai, M. Guimond, A. Arora, J. Opavska, B. Becknell, M. Kaufmann, N. A. Walton, J. A. Stephens, S. A. Fernandez, N. Muthusamy, D. W. Felsher, P. Porcu, M. A. Caligiuri and G. Leone (2007). "Specific tumor suppressor function for E2F2 in Myc-induced T cell lymphomagenesis." Proc Natl Acad Sci U S A **104**(39): 15400-5.

Pardee, A. B. (1974). "A restriction point for control of normal animal cell proliferation." Proc Natl Acad Sci U S A **71**(4): 1286-90.

Peeper, D. S., P. Keblusek, K. Helin, M. Toebes, A. J. van der Eb and A. Zantema (1995). "Phosphorylation of a specific cdk site in E2F-1 affects its electrophoretic mobility and promotes pRB-binding in vitro." Oncogene **10**(1): 39-48.

Pellegata, N. S., R. J. Antoniono, J. L. Redpath and E. J. Stanbridge (1996). "DNA damage and p53-mediated cell cycle arrest: a reevaluation." Proc Natl Acad Sci U S A **93**(26): 15209-14.

Penzo, M., P. E. Massa, E. Olivotto, F. Bianchi, R. M. Borzi, A. Hanidu, X. Li, J. Li and K. B. Marcu (2009). "Sustained NF-kappaB activation produces a short-term cell proliferation block in conjunction with repressing effectors of cell cycle progression controlled by E2F or FoxM1." J Cell Physiol **218**(1): 215-27.

Perkins, N. D. and T. D. Gilmore (2006). "Good cop, bad cop: the different faces of NF-kappaB." Cell Death Differ **13**(5): 759-72.

Phair, R. D. and T. Misteli (2001). "Kinetic modelling approaches to in vivo imaging." Nat Rev Mol Cell Biol **2**(12): 898-907.

Phillips, A. C., M. K. Ernst, S. Bates, N. R. Rice and K. H. Vousden (1999). "E2F-1 potentiates cell death by blocking antiapoptotic signaling pathways." Mol Cell **4**(5): 771-81.

Pittendrigh, C. S. B., V.G. (1957). An Oscillator Model for Biological Clocks. Rhythmic and Synthetic Processes in Growth. D. Rudnick. Princeton, NJ, Princeton Universtiy Press: 75-109.

Polyak, K., M. H. Lee, H. Erdjument-Bromage, A. Koff, J. M. Roberts, P. Tempst and J. Massague (1994). "Cloning of p27Kip1, a cyclin-dependent kinase inhibitor and a potential mediator of extracellular antimitogenic signals." Cell **78**(1): 59-66.

Price, B. D., L. Hughes-Davies and S. J. Park (1995). "Cdk2 kinase phosphorylates serine 315 of human p53 in vitro." Oncogene **11**(1): 73-80.

Prives, C. and P. A. Hall (1999). "The p53 pathway." J Pathol **187**(1): 112-26.

Qin, X. Q., D. M. Livingston, W. G. Kaelin, Jr. and P. D. Adams (1994). "Deregulated transcription factor E2F-1 expression leads to S-phase entry

and p53-mediated apoptosis." Proc Natl Acad Sci U S A **91**(23): 10918-22.

Qu, Z., J. N. Weiss and W. R. MacLellan (2003). "Regulation of the mammalian cell cycle: a model of the G1-to-S transition." Am J Physiol Cell Physiol **284**(2): C349-64.

Reis, T. and B. A. Edgar (2004). "Negative regulation of dE2F1 by cyclin-dependent kinases controls cell cycle timing." Cell **117**(2): 253-64.

Rensing, L., U. Meyer-Grahle and P. Ruoff (2001). "Biological timing and the clock metaphor: oscillatory and hourglass mechanisms." Chronobiol Int **18**(3): 329-69.

Ridgway, E. B. and A. C. Durham (1976). "Oscillations of calcium ion concentrations in Physarum polycephalum." J Cell Biol **69**(1): 223-6.

Sakaguchi, K., H. Sakamoto, M. S. Lewis, C. W. Anderson, J. W. Erickson, E. Appella and D. Xie (1997). "Phosphorylation of serine 392 stabilizes the tetramer formation of tumor suppressor protein p53." Biochemistry **36**(33): 10117-24.

Sakaue-Sawano, A., H. Kurokawa, T. Morimura, A. Hanyu, H. Hama, H. Osawa, S. Kashiwagi, K. Fukami, T. Miyata, H. Miyoshi, T. Imamura, M. Ogawa, H. Masai and A. Miyawaki (2008). "Visualizing spatiotemporal dynamics of multicellular cell-cycle progression." Cell **132**(3): 487-98.

Sauer, U., M. Heinemann and N. Zamboni (2007). "Genetics. Getting closer to the whole picture." Science **316**(5824): 550-1.

Schauvliege, R., J. Vanrobaeys, P. Schotte and R. Beyaert (2002). "Caspase-11 gene expression in response to lipopolysaccharide and interferon-gamma requires nuclear factor-kappa B and signal transducer and activator of transcription (STAT) 1." J Biol Chem **277**(44): 41624-30.

Schultz, T. F. and S. A. Kay (2003). "Circadian clocks in daily and seasonal control of development." Science **301**(5631): 326-8.

Schulze, A., K. Zerfass, D. Spitkovsky, S. Middendorp, J. Berges, K. Helin, P. Jansen-Durr and B. Henglein (1995). "Cell cycle regulation of the cyclin A gene promoter is mediated by a variant E2F site." Proc Natl Acad Sci U S A **92**(24): 11264-8.

Shakhov, A. N., D. V. Kuprash, M. M. Azizov, C. V. Jongeneel and S. A. Nedospasov (1990). "Structural analysis of the rabbit TNF locus, containing the genes encoding TNF-beta (lymphotoxin) and TNF-alpha (tumor necrosis factor)." Gene **95**(2): 215-21.

Shay, J. W., O. M. Pereira-Smith and W. E. Wright (1991). "A role for both RB and p53 in the regulation of human cellular senescence." Exp Cell Res **196**(1): 33-9.

Shen, H., G. Nelson, D. E. Nelson, S. Kennedy, D. G. Spiller, T. Griffiths, N. Paton, S. G. Oliver, M. R. White and D. B. Kell (2006). "Automated tracking of gene expression in individual cells and cell compartments." J R Soc Interface **3**(11): 787-94.

Sherr, C. J. (1996). "Cancer cell cycles." Science **274**(5293): 1672-7.

Sherr, C. J., A. Diehl, D. E. Quelle, F. Zindy and M. F. Roussel (1997). "Cyclin D-dependent kinases during G1 phase progression." European Journal of Cell Biology **72**: 4-4.

Shimojo, H., T. Ohtsuka and R. Kageyama (2008). "Oscillations in notch signaling regulate maintenance of neural progenitors." Neuron **58**(1): 52-64.

Skotheim, J. M., S. Di Talia, E. D. Siggia and F. R. Cross (2008). "Positive feedback of G1 cyclins ensures coherent cell cycle entry." Nature **454**(7202): 291-6.

Spencer, M. and J. E. Tanner (2008). "Lotka-Volterra competition models for sessile organisms." Ecology **89**(4): 1134-1143.

Spitkovsky, D., P. Steiner, R. V. Gopalkrishnan, M. Eilers and P. Jansen-Durr (1995). "The role of p53 in coordinated regulation of cyclin D1 and p21 gene expression by the adenovirus E1A and E1B oncogenes." Oncogene **10**(12): 2421-5.

Stanelle, J., T. Stiewe, C. C. Theseling, M. Peter and B. M. Putzer (2002). "Gene expression changes in response to E2F1 activation." Nucleic Acids Research **30**(8): 1859-1867.

Stiewe, T. (2007). "The p53 family in differentiation and tumorigenesis." Nat Rev Cancer **7**(3): 165-8.

Sun, L., G. Yang, M. Zaidi and J. Iqbal (2008). "TNF-induced gene expression oscillates in time." Biochem Biophys Res Commun **371**(4): 900-5.

Sung, M. H. and R. Simon (2004). "In silico simulation of inhibitor drug effects on nuclear factor-kappaB pathway dynamics." Mol Pharmacol **66**(1): 70-5.

Takahashi, Y., J. B. Rayman and B. D. Dynlacht (2000). "Analysis of promoter binding by the E2F and pRB families in vivo: distinct E2F proteins mediate activation and repression." Genes Dev **14**(7): 804-16.

Tanaka, H., H. Arakawa, T. Yamaguchi, K. Shiraishi, S. Fukuda, K. Matsui, Y. Takei and Y. Nakamura (2000). "A ribonucleotide reductase gene involved in a p53-dependent cell-cycle checkpoint for DNA damage." Nature **404**(6773): 42-9.

Tergaonkar, V. and N. D. Perkins (2007). "p53 and NF-kappaB crosstalk: IKKalpha tips the balance." Mol Cell **26**(2): 158-9.

Ting, A. Y. and D. Endy (2002). "Signal transduction. Decoding NF-kappaB signaling." Science **298**(5596): 1189-90.

Toettcher, J. E., A. Loewer, G. J. Ostheimer, M. B. Yaffe, B. Tidor and G. Lahav (2009). "Distinct mechanisms act in concert to mediate cell cycle arrest." Proc Natl Acad Sci U S A.

Trimarchi, J. M. and J. A. Lees (2002). "Sibling rivalry in the E2F family." Nat Rev Mol Cell Biol **3**(1): 11-20.

Tsai, T. Y., Y. S. Choi, W. Ma, J. R. Pomerening, C. Tang and J. E. Ferrell, Jr. (2008). "Robust, tunable biological oscillations from interlinked positive and negative feedback loops." Science **321**(5885): 126-9.

Tsantoulis, P. K. and V. G. Gorgoulis (2005). "Involvement of E2F transcription factor family in cancer." Eur J Cancer **41**(16): 2403-14.

Tu, Z., S. Prajapati, K. J. Park, N. J. Kelly, Y. Yamamoto and R. B. Gaynor (2006). "IKK alpha regulates estrogen-induced cell cycle progression by modulating E2F1 expression." J Biol Chem **281**(10): 6699-706.

Turner, S. and J. A. Sherratt (2002). "Intercellular adhesion and cancer invasion: A discrete simulation using the extended Potts model." Journal of Theoretical Biology **216**(1): 85-100.

van den Heuvel, S. and N. J. Dyson (2008). "Conserved functions of the pRB and E2F families." Nat Rev Mol Cell Biol **9**(9): 713-24.

Verona, R., K. Moberg, S. Estes, M. Starz, J. P. Vernon and J. A. Lees (1997). "E2F activity is regulated by cell cycle-dependent changes in subcellular localization." Mol Cell Biol **17**(12): 7268-82.

Volterra, V. (1926). "Fluctuations in the abundance of a species considered mathematically." Nature **118**: 558-560.

Webster, G. A. and N. D. Perkins (1999). "Transcriptional cross talk between NF-kappaB and p53." Mol Cell Biol **19**(5): 3485-95.

Wells, J., K. E. Boyd, C. J. Fry, S. M. Bartley and P. J. Farnham (2000). "Target gene specificity of E2F and pocket protein family members in living cells." Mol Cell Biol **20**(16): 5797-807.

Welsh, D. K., S. H. Yoo, A. C. Liu, J. S. Takahashi and S. A. Kay (2004). "Bioluminescence imaging of individual fibroblasts reveals persistent, independently phased circadian rhythms of clock gene expression." Curr Biol **14**(24): 2289-95.

Werner, S. L., J. D. Kearns, V. Zadorozhnaya, C. Lynch, E. O'Dea, M. P. Boldin, A. Ma, D. Baltimore and A. Hoffmann (2008). "Encoding NF-kappaB temporal control in response to TNF: distinct roles for the negative regulators IkappaBalpha and A20." Genes Dev **22**(15): 2093-101.

White, M. R., J. Morse, Z. A. Boniszewski, C. R. Mundy, M. A. Brady and D. J. Chiswell (1990). Technique **2**: 194-201.

Whitfield, M. L., G. Sherlock, A. J. Saldanha, J. I. Murray, C. A. Ball, K. E. Alexander, J. C. Matese, C. M. Perou, M. M. Hurt, P. O. Brown and D. Botstein (2002). "Identification of genes periodically expressed in the human cell cycle and their expression in tumors." Mol Biol Cell **13**(6): 1977-2000.

Whitfield, M. L., L. X. Zheng, A. Baldwin, T. Ohta, M. M. Hurt and W. F. Marzluff (2000). "Stem-loop binding protein, the protein that binds the 3' end of histone mRNA, is cell cycle regulated by both translational and posttranslational mechanisms." Mol Cell Biol **20**(12): 4188-98.

Woods, N. M., K. S. Cuthbertson and P. H. Cobbold (1986). "Repetitive transient rises in cytoplasmic free calcium in hormone-stimulated hepatocytes." Nature **319**(6054): 600-2.

Wright, C. (1983). Frege's Conception of Numbers as Objects. Aberdeen, Aberdeen University Press.

Wu, C. L., L. R. Zukerberg, C. Ngwu, E. Harlow and J. A. Lees (1995). "In vivo association of E2F and DP family proteins." Mol Cell Biol **15**(5): 2536-46.

Wu, L., C. Timmers, B. Maiti, H. I. Saavedra, L. Sang, G. T. Chong, F. Nuckolls, P. Giangrande, F. A. Wright, S. J. Field, M. E. Greenberg, S. Orkin, J. R. Nevins, M. L. Robinson and G. Leone (2001). "The E2F1-3 transcription factors are essential for cellular proliferation." Nature **414**(6862): 457-62.

Yao, G., T. J. Lee, S. Mori, J. R. Nevins and L. You (2008). "A bistable Rb-E2F switch underlies the restriction point." Nat Cell Biol **10**(4): 476-82.

Yoshiura, S., T. Ohtsuka, Y. Takenaka, H. Nagahara, K. Yoshikawa and R. Kageyama (2007). "Ultradian oscillations of Stat, Smad, and Hes1 expression in response to serum." Proc Natl Acad Sci U S A **104**(27): 11292-7.

Young, A. P., R. Nagarajan and G. D. Longmore (2003). "Mechanisms of transcriptional regulation by Rb-E2F segregate by biological pathway." Oncogene **22**(46): 7209-17.

Zhang, Z., H. Wang, M. Li, E. R. Rayburn, S. Agrawal and R. Zhang (2005). "Stabilization of E2F1 protein by MDM2 through the E2F1 ubiquitination pathway." Oncogene **24**(48): 7238-47.

Zhong, H., M. J. May, E. Jimi and S. Ghosh (2002). "The phosphorylation status of nuclear NF-kappa B determines its association with CBP/p300 or HDAC-1." Mol Cell **9**(3): 625-36.

Appendix 1

A1.1 Complete plots for NF-κB:E2F-1 model Mk.I

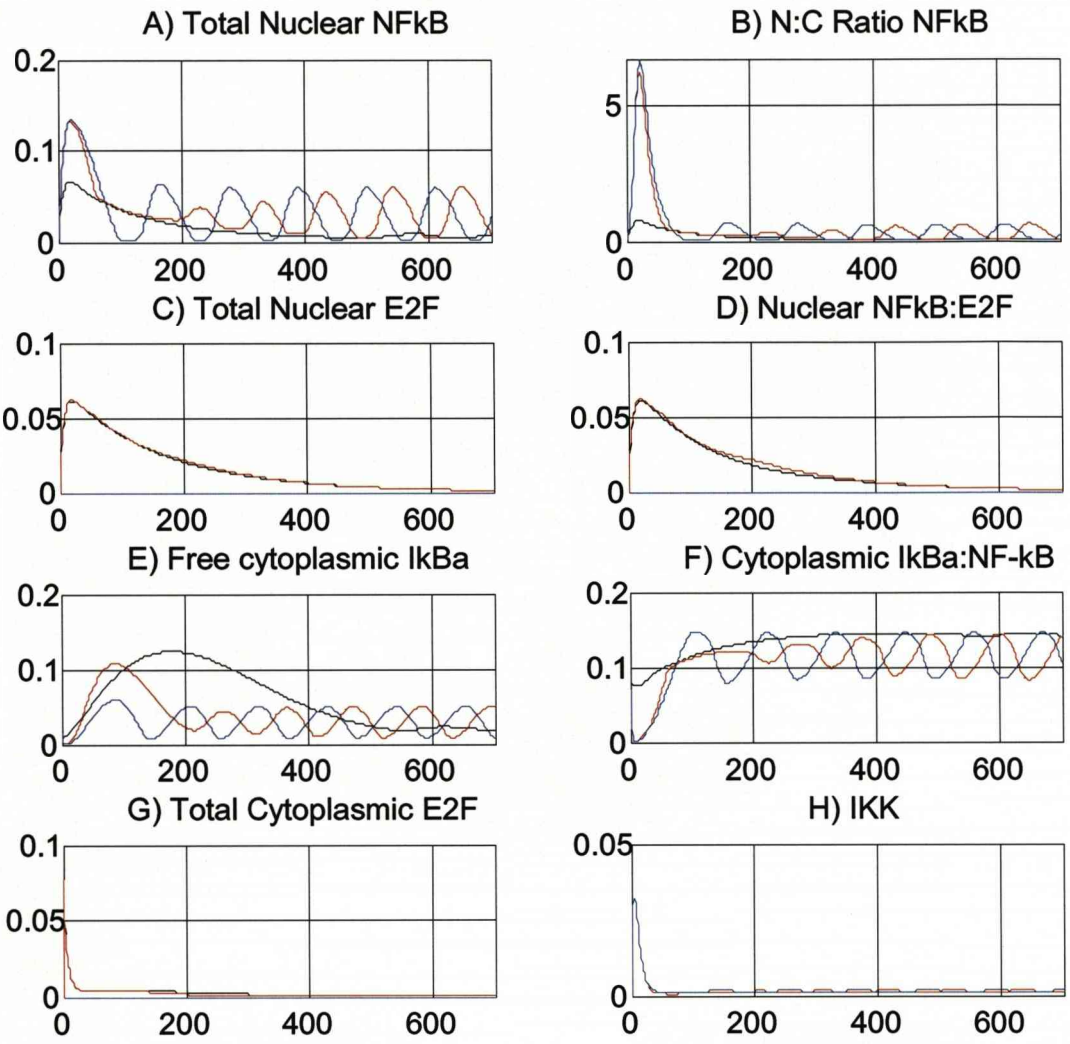

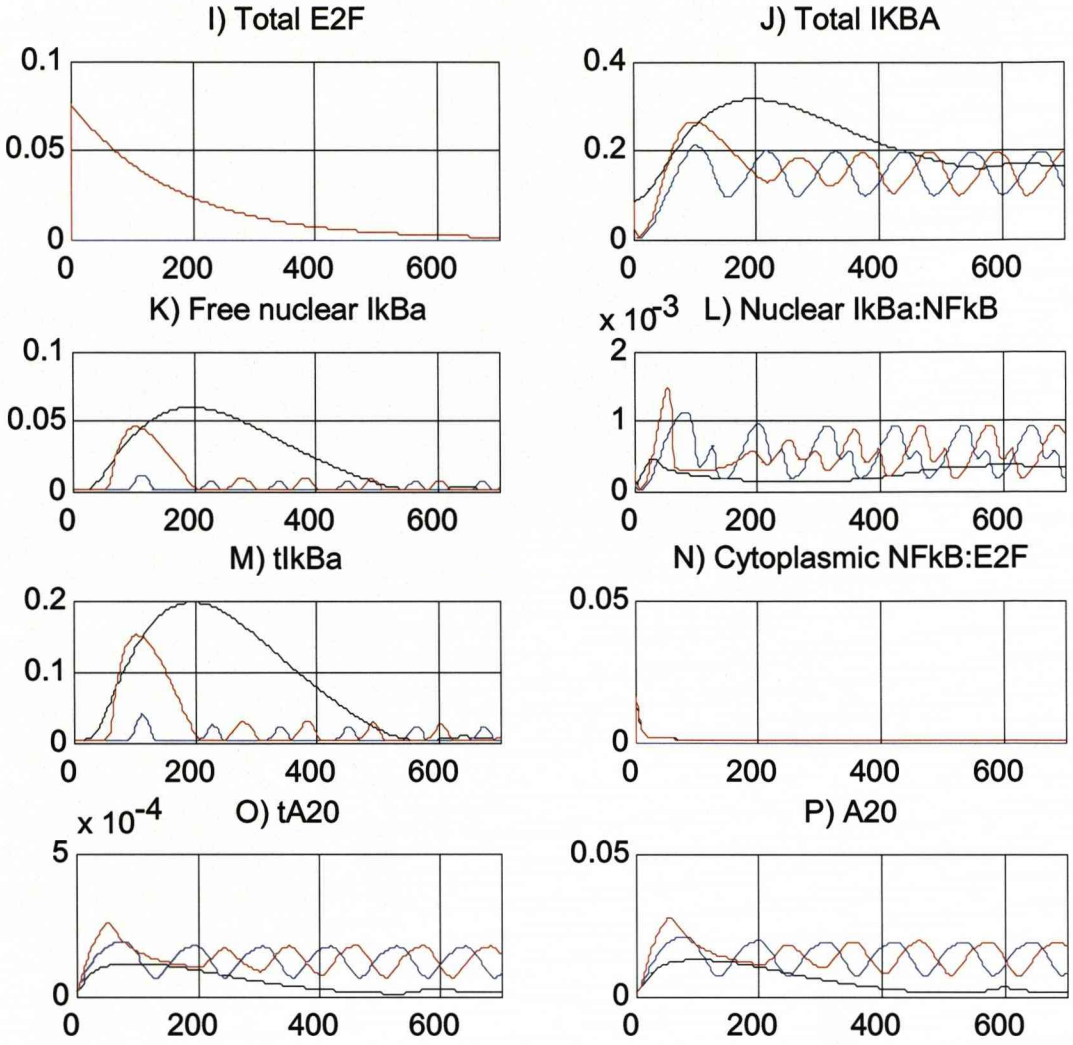

Figure A.1 Model plots for species in the NF-κB:E2F-1 model Mk.I: Showing traces representing exogenous expression of p65 with TNFα stimulation (blue line), exogenous expression of p65 and E2F-1 without TNFα stimulation (black line) and exogenous expression of p65 and E2F-1 with TNFα stimulation (red line).

A1.2 Complete plots for NF-κB:E2F-1 model Mk.II

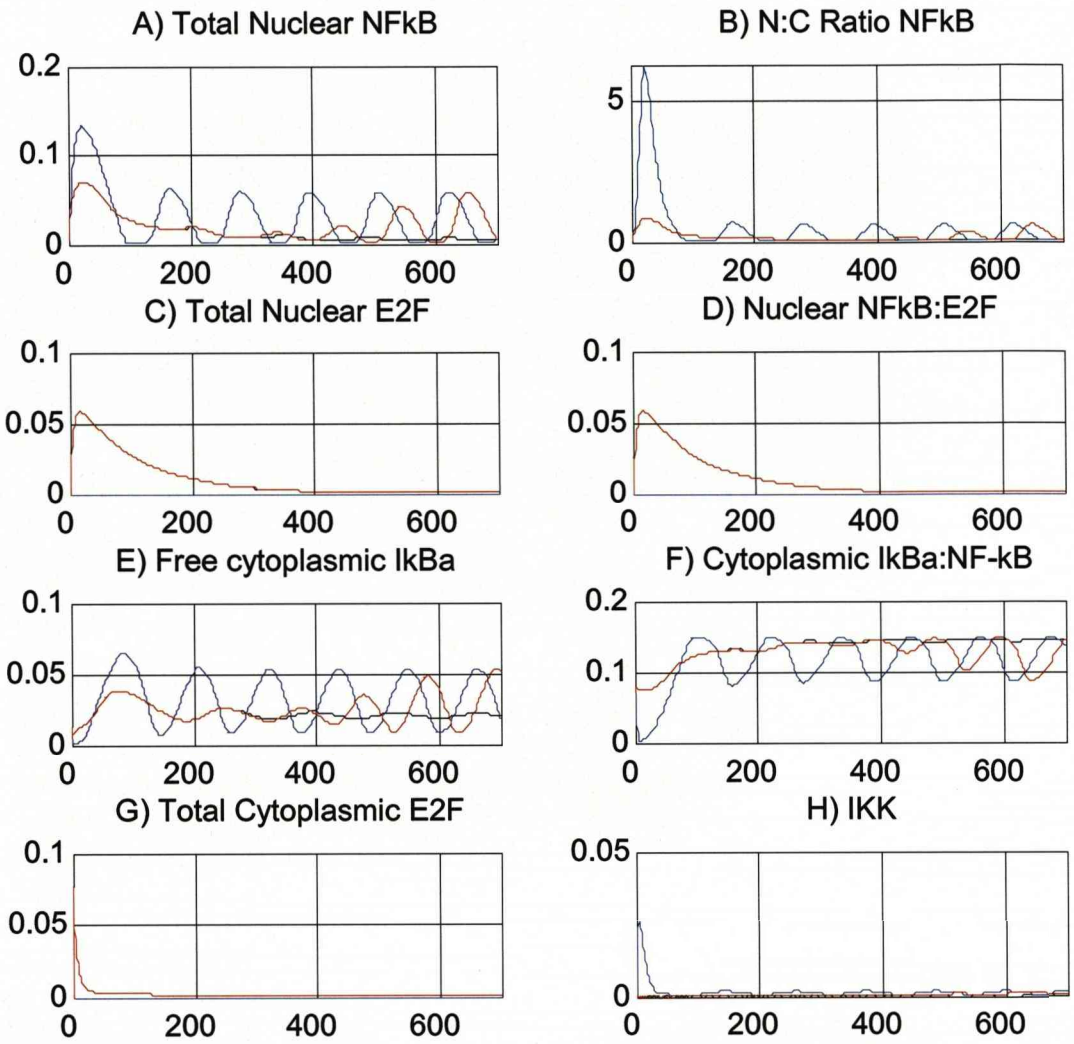

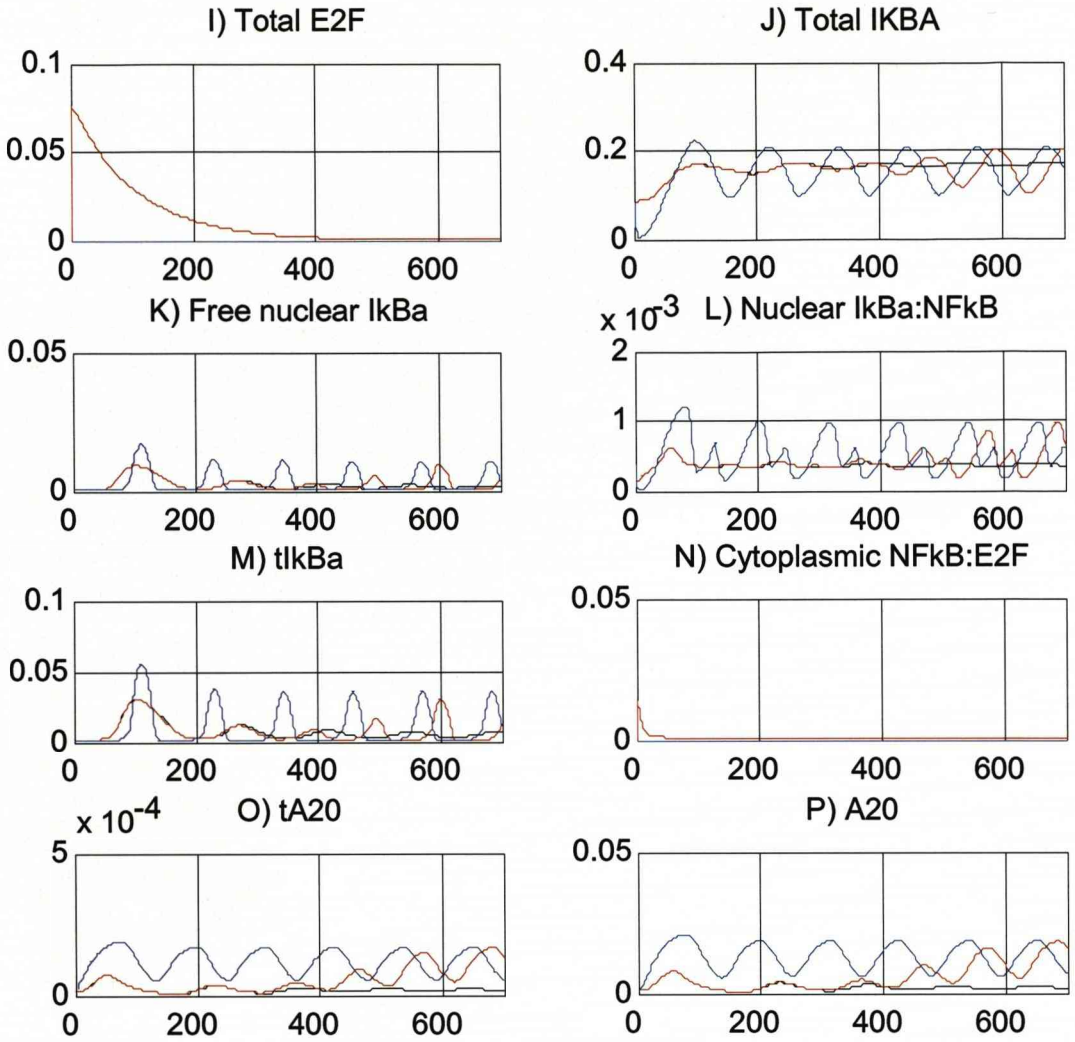

Figure A.2 Model plots for species in the NF-κB:E2F-1 model Mk.II: Showing traces representing exogenous expression of p65 with TNFα stimulation (blue line), exogenous expression of p65 and E2F-1 without TNFα stimulation (black line) and exogenous expression of p65 and E2F-1 with TNFα stimulation (red line).